ORAL

3D image analysis of endocytosed nanoparticles: towards optimisation of drug delivery for regenerative medicine

A De Grazia [1, 2], ND Evans [2], MRR De Planque [1]

[1] *Electronics and Computer Science and* [2] *Institute for Developmental Sciences, University of Southampton, Southampton SO17 1BJ, United Kingdom.*

INTRODUCTION: Flow cytometry is the prominent high-throughput single-cell characterisation technique, detecting whether individual cells flowing sequentially through a capillary are labelled by a particular fluorescent marker. However, conventional cytometry does not yield information about the subcellular location of labels, while imaging adaptations do not compare with high-numerical aperture (NA) microscopy. Here we aimed to improve the throughput of fluorescence microscopy to enable subcellular characterisation of cell populations. We present a scalable platform to image thousands of cells in predefined array sites, compatible with (semi)automated imaging workflows, and show initial data on nanoparticle association and uptake, informing systematic drug delivery studies.

METHODS: We fabricated a microfluidic device able to array ~15,000 cells by soft lithography. A hydrodynamic flow of 10 µL/min guides cells through a serpentine channel into 4.8 µm-high trap pockets positioned along the main channel [1].

Red fluorescent silica nanoparticles were incubated with whole blood and DiI-loaded polymeric nanoparticles (PMs) with the cancer cell line MG63 to study membrane association and intracellular distribution of the particles and the DiI molecule. Cells were microfluidically arrayed and imaged.

Z-stack imaging, i.e. taking images at different focal distances, also enabled 3D analysis, with an image processing workflow involving ImageJ and Matlab.

RESULTS: Not all the white blood cells internalized the 500 nm silica nanoparticles.

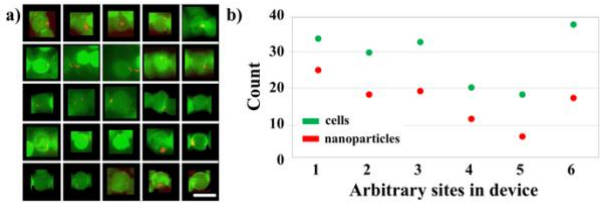

Fig. 1: a) Twenty-five images of single white blood cells stained with anti-CD45 (green) which internalised silica red fluorescent nanoparticles (scale bar: 10 µm); b) Comparison between number of cells and number of nanoparticles in different sites of the array for 200 analysed cells.

Fig. 1a shows the morphology of different white blood cells with endocytosed red silica nanoparticles in arbitrary sites in the device. The membrane staining with anti-CD45 (in green) clarifies that the nanoparticles are inside the cells and in the cytoplasm. *Fig. 1b* shows the number of nanoparticles imaged in the volume of the cells using z-stacks with a 63x oil immersion objective (NA=1.4). Out of ~200 cells, approximately 50% of the cells contained a single nanoparticle.

For the MG63 cells exposed to self-assembled PMs loaded with lipophilic DiI molecules, a punctate pattern of fluorescence was observed suggesting compartmentalisation in endosomes. *Fig. 2a* shows a high-resolution microscopy image of arrayed cells. Z-stack imaging facilitated characterisation of the stained organelles by volume and fluorescence intensity (*Fig. 2b*).

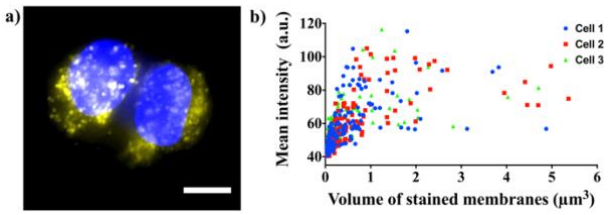

Fig. 2: a) Fluorescence of arrayed MG63 cells showing nuclei in blue and DiI in yellow (scale bar: 5 µm); b) Scatter plot showing volume and intensity of membranes stained with DiI in which 110 ± 31 objects per cell were imaged (n=3), potentially corresponding to endosomes.

DISCUSSION & CONCLUSIONS: The use of a microfluidic device able to array thousands of cells and to image these with high-NA objectives, will give population-level insight in nanoparticle interactions. For example, it is possible to evaluate plasma membrane association and the efficiency of nanoparticle endocytosis. This is promising for regenerative medicine studies where we aim at targeting stem cells from bone marrow with drugs to trigger differentiation signalling.

REFERENCES: [1] Chung *et al.* (2011) *Anal. Chem.* **83**:7044-7052.

A 3D *ex vivo* model for testing nerve guidance conduits using high throughput light-sheet microscopy

M Behbehani[1], F Claeyssens[1], JW Haycock[1]

[1]*Department of Materials Science and Engineering, The University of Sheffield, UK*

INTRODUCTION: Nerve guidance conduits (NGCs) are used to promote peripheral nerve regeneration in short gap injuries. However, they are not suitable for injuries >3cm in humans. NGC scaffolds with internal alignment through microfibres could provide additional outgrowth guidance to enhance nerve regeneration. However, this has not yet been optimised. In this study, we designed a novel *in vitro* NGC testing model using dorsal root ganglia (DRG). This model was used for high throughput screening of a number of NGC design variables such as fibre diameter, packing density and surface modification. This 3D model enables a reduction of downstream *in vivo* nerve injury models by allowing direct comparisons of NGC designs in a more physiologically relevant environment compared to commonly conducted evaluations on flat scaffold materials[1].

METHODS: Aligned polycaprolactone (PCL) fibres were electrospun to 1, 5, 8, 10 and 13 µm diameters. 6 mm long poly(ethylene glycol) (PEG) NGCs with an internal diameter of 1.1 mm were fabricated by microstereolithography. Fibres were inserted inside NGCs. Samples were surface-modified by air plasma and modification confirmed by XPS. Embryonic day 12 chick DRGs were placed on the upper surface of the fibre-filled conduits and cultured for 7 days. Immunocytochemistry was performed and light-sheet and confocal microscopy used to visualise and measure neurite and SC outgrowth from the proximal DRG body towards the distal end of the 6 mm tube (Figure 1).

RESULTS: Air plasma deposited fibre scaffolds supported DRG outgrowth significantly greater than non-modified fibres. The average maximum outgrowth on plasma-deposited scaffolds measured between 1.3 and 3.1 mm dependant on the fibre diameter, where 10 µm fibres performed best after 7 days of culture (Figure 1). Data obtained by confocal microscopy showed overall longer outgrowth rates than those imaged by light-sheet microscopy but was less accurate. In contrast, light-sheet microscopy revealed significant differences in outgrowth lengths by providing analytical image data through the entire sample and at all positions along regenerating ganglia.

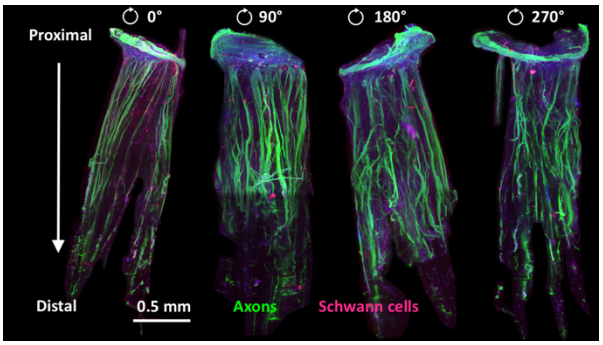

Fig. 1: Light-sheet microscopy images of chick DRG outgrowth along air-plasma modified PCL fibre scaffolds (10 µm) contained within PEG NGCs using a 3D DRG in vitro model. After 7 days of culture, Schwann cells and axons were labelled for S100β (red) and βIII tubulin (green), respectively. Sample images were captured at 90 ° aspects (0, 90, 180 and 270° from left to right). Arrow indicates outgrowth direction from the proximal DRG body towards the distal end. Scale bar = 0.5 mm.

DISCUSSION & CONCLUSIONS: There is a large gap between the evaluation approaches of new NGC scaffold designs. These are usually based on flat scaffold surfaces *in vitro* or on complex NGC structures *in vivo*. With the current dogma surrounding animal testing and the pitfalls of current 2D *in vitro* tests that lack the key aspects of the cells native 3D environment, this 3D DRG model is of high relevance to the research community to greatly improve current *in vitro* testing models. The present study highlighted the importance of aligned fibre diameter and surface modification of PCL fibres in successfully supporting nerve repair in internal NGC scaffolds. Light-sheet microscopy was found to be a more rigorous imaging technique compared with identical samples imaged by confocal microscopy, and consequently enabled high throughput imaging and sample position control.

REFERENCES: [1] Behbehani et al. (2018), *Int J Bioprint*, 4(1):123.

ACKNOWLEDGEMENTS: We are grateful to the EPSRC (UK) for the funding.

A highly programmable and non-invasive biomaterial to aid wound healing

V Llopis-Hernandez[1], F Warren[1], M Salmeron-Sanchez[2], MJ Dalby[1]

[1] Centre for Cell Engineering, University of Glasgow, Glasgow, UK [2] School of Engineering, University of Glasgow, Glasgow, UK

INTRODUCTION: We are working towards an effective, safe therapeutic solution in the management of complex (partial and full thickness) wounds. Non-healing ulcers, among other problems, can lead to infection and disability and current wound management protocols are not satisfactory. Wound healing is promoted by a number of growth factors (GFs) including platelet-derived GF-BB (PDGF-BB). Current GF products have a large associated cost and potential adverse effects (e.g. PDGF containing Regranex® warns not to use more than 3 times due to health warnings such as death secondary to malignancy). Appropriate interactions of GFs with the extracellular matrix are critical to regulation of signalling and effectiveness. Our approach utilizes poly(ethyl acrylate) (PEA) that promotes self-organization of fibronectin (FN) into biological nanonetworks, unravelling the FN molecule to reveal cell adhesive and GF binding domains. We have previously showed successfully effectiveness of this system to deliver BMP-2 for bone regeneration[1]. Further, a new approach is the inclusion of cytokines that are critical to wound healing, making use of the FNI1-5 domain that has been demonstrated to bind and efficiently present cytokines/chemokines [2]. Here, we engineer advanced wound healing microenvironment facilitating the exposure of FNIII12-14 to bind PDGF-BB in close apposition to the integrin binding FNIII9-10 domain as well as FNI1-5 exposure to promote the binding of CXC family chemokines (*Fig. 1*).

METHODS: Human fibronectin from plasma, recombinant PDGF-BB, CXCL11 and CXC12 protein were used to develop the system. L929 and hTERT fibroblasts and human adult foreskin keratinocytes were used to evaluate the biological activity of the construct. Atomic force microscopy, ELISA (PDGF-BB, CXCL11) and CXCL12, wound healing assays (fibroblasts, keratinocytes and co-cultures), qPCR (keratin 14, involucrin, p63, basonuclin1 and 2), flow cytometry (CD49f, CD71), in-cell western (keratin 14) and immunofluorescence (fibroblast and keratinocyte co-culture) were used to characterise cell migration and maturation. Image J was used to quantify cell migration.

RESULTS: The FN nanonetworks sequester PDGF-BB at very low concentration (100 ng/ml) compared to clinical GF containing products. The biological activity of the system with PDGF-BB and CXCL11 and CXCL12 chemokines has been evaluated *in vitro* using fibroblasts (L929 and hTERT) to correlate enhanced cellular migration to the wound site with the synergistic presentation of GFs and chemokines using wound healing assays. Significant increase in both fibroblast and keratinocyte migration as well as keratinocyte maturation has been demonstrated *in vitro (Fig. 2)*.

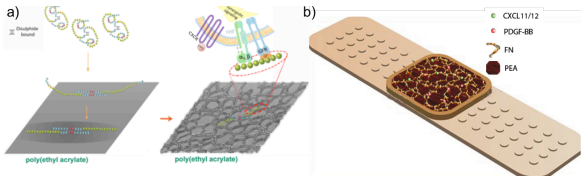

Fig. 1: a) Biological diagram of the GF/chemokine presentation in the developed system b) Sketch of the future implantation of the system in clinics in a bandage form

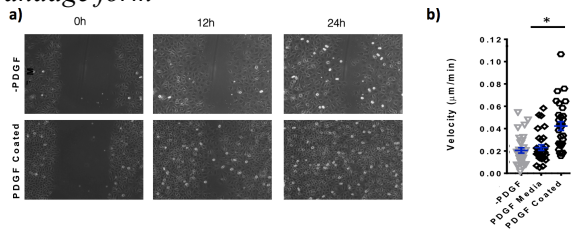

Fig. 2: a) Fibroblast wound healing assay b) Human primary keratinocytes velocities after 40h $p<0.5$

DISCUSSION & CONCLUSIONS: The accelerated cell migration coupled to ultra-low dose PDGF-BB delivery will provide cost effective, safe, enhanced would closure.

REFERENCES: [1] V. Llopis-Hernandez, M. Cantini, C. González-García, Z.A. Cheng, J. Yang, P.M. Tsimbouri, A.J. García, M.J. Dalby, M. Salmerón-Sánchez (2016) Material-driven fibronectin assembly for high-efficiency presentation of growth factors Science Advances 2, 8 [2] F. Tortelli, M. Pisano, P.S. Briquez, M.M. Martino, J.A. Hubbell (2013) Fibronectin Binding Modulates CXCL11 Activity and Facilitates Wound Healing Plos One 8, 10

ACKNOWLEDGEMENTS: We acknowledge MRC grant MR/L022710/1 and EPSRC grant EP/P001114/1. We thank Carol-Anne Smith for her technical assistance.

A tissue engineered muscle capable of regeneration following injury

JW Fleming[1], AJ Capel[1], DJ Player[1], A Stolzing[2], MP Lewis[1]

[1]School of Sport, Exercise & Health Sciences, Loughborough University. [2] Wolfson School of Mechanical, Electrical and Manufacturing Engineering, Loughborough University

INTRODUCTION: The process of skeletal muscle wound healing is a complex, temporally regulated process which allows muscle to regenerate fully functional tissue following a wounding insult. However, in some cases, such as wounds seen in military trauma, muscle wounds fail to fully regenerate, leading to fibrosis and/or heterotopic ossification [1]. Our understanding of the healing process to date has relied heavily upon animal models; however inter-species differences, technical challenges and difficulties with reproducibility are holding back our understanding of the cellular and molecular mechanisms that regulate the healing process. Previous reports have shown some regeneration of tissue engineered muscle [2], therefore the aim of this work is to use a tissue engineered model of skeletal muscle, which is composed of extracellular matrix components found in skeletal muscle, to simulate regeneration and so produce a platform which can be used for the study of skeletal muscle regeneration.

METHODS: The mouse muscle progenitor cell line, C2C12s, were incorporated into a type I collagen/Matrigel^{TM} hydrogel and cultured for 14 days to produce a tissue engineered muscle containing aligned, contractile myofibers. These constructs were then treated with 12% $BaCl_2$ (w/w) solution (50ul/ml culture medium) for 6 hrs to simulate a wounding insult. Constructs were then regenerated over 14 days, in growth media (20% FBS in DMEM, 4 days) and differentiation media (2% HS in DMEM, 10 days). Cellular morphology, macroscopic deformation, gene expression and force generation were analysed during recovery.

RESULTS: Addition of $BaCl_2$ caused substantial loss of myofibers (fig 1a) from constructs and reduced force output to 14% of control (fig 1b), without causing a reduction in total nuclei number (data not shown). Following 4 days myofiber number had regenerated to levels not significantly below control (83%) and force output had also recovered to control levels (fig 1b). Following a further 10 days of recovery force generation had increased to 2.5 fold that of control (fig 1b), but no increase of myotube number was observed over 4 days post injury. Upregulation of inflammatory genes IL-6 (10 fold) and MCP-1 (6 fold, data not shown) was also observed at 0 HR and 4 days following injury in line with *in vivo* observations [3]

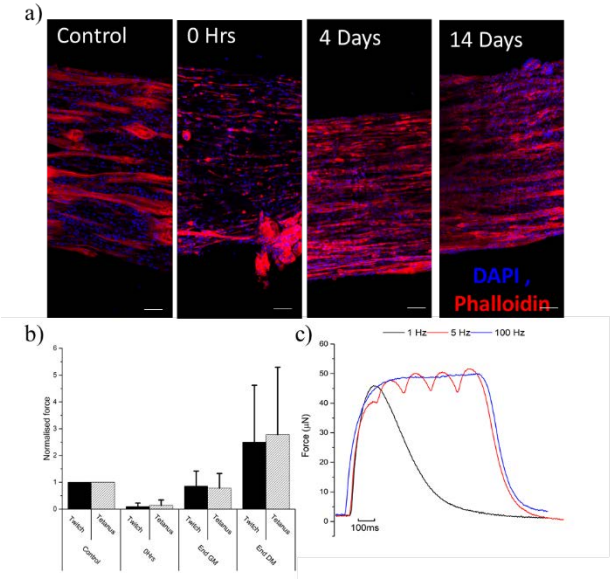

Fig. 1: (a) 40x confocal fluorescence micrographs of C2C12 tissue engineered muscle. Scale bar = 100µm (b) Force generation normalised to control. Black – Twitch (1 Hz), Grey – Tetanus (100Hz) (c) Representative control force traces from C2C12 tissue engineered muscle.

DISCUSSION & CONCLUSIONS: We have shown in previous work that $BaCl_2$ treatment of 2D C2C12 and human muscle cultures do not support total regeneration following injury. Neither does the supplementation of basement membrane (BM) proteins in 2D support full regeneration. Furthermore, type I collagen only hydrogels do not support regeneration (unpublished data). However, the combination of a 3D environment and BM proteins in the form of Matrigel^{TM} produces a system which is capable of regenerating myofibers and contractile function following an injurious insult. We see this model forming the basis of future work, using human muscle precursor cells, studying muscular disorders which have disrupted regeneration e.g. severe traumatic injuries and muscular dystrophies.

REFERENCES: [1]Järvinen TA, Järvinen M & Kalimo H (2013) *Muscles. Ligaments Tendons J. 3: 337–45* [2] Juhas, M *et al* (2014). *Proc Natl Acad Sci U S A, 111*(15), 5508–5513. [3]Muñoz-Cánoves, P., & Serrano, A. L. (2015). *Trends in Endocrinology and Metabolism*, *26*(9), 449–450.

Anti-inflammatory and chondroprotective effects of mesenchymal stem cell-derived extracellular vesicles in inflammatory arthritis

AG Kay[1], R Morgan[2], M Platt[3], P Roach[3], N Forsyth[4], O Kehoe[2]

[1]Biology Department, University of York, Wentworth Way, York, UK [2]Keele University, ISTM at RJAH Orthopaedic Hospital, Oswestry, Shropshire, UK [3]Loughborough University, Chemistry Department, Loughborough, UK [4]Keele University, ISTM, Guy Hilton Research Centre, Keele University, Staffordshire, UK

INTRODUCTION: Rheumatoid arthritis (RA) is a debilitating and painful disorder affecting more than 690,000 people in the UK, with 12,000 new cases diagnosed annually[1]. There is no cure for RA. Novel biological therapies have revolutionised the management of RA. However, up to 30% of RA patients fail to respond to currently available biological therapeutics and 50% of those prescribed the treatment discontinue use after 2 years. It is therefore vital to develop a new, effective therapy for RA. Mesenchymal stem cells (MSCs) possess anti-inflammatory and immunosuppressive properties that may be exploited therapeutically[2]. MSCs function in immunomodulation predominantly through paracrine mechanisms, via growth factors, cytokines, chemokines and extracellular vesicles (EVs) which can all be readily detected in MSC conditioned medium (CM-MSC)[3]. EVs are a heterogeneous group of small membrane vesicles with key roles in cell-to-cell communications, cell signalling and immune response modulation[4]. The aim of this pilot project was to investigate whether mesenchymal stem cell derived EVs exhibit anti-inflammatory functional properties in an experimental inflammatory arthritis model.

METHODS: EVs were isolated from bone marrow CM-MSC by ultracentrifugation. Identification of EVs was achieved using a flow cytometric analysis (MACSPlex human exosome detection kit, Miltenyi). Tunable Resistive Pulse Sensing Technology from IZON Science was used to measure the size of isolated EVs. AIA was induced in pre-immunised animals by intra-articular injection of methylated BSA and EVs were injected intra-articularly 1 day post arthritis induction. Control animals were injected EV-depleted medium.

RESULTS: The positive confirmation of tetraspanin proteins CD9, CD63, CD81 was achieved by flow cytometry. The size of isolated vesicles ranged from 159 to 290 nm and the mean size and standard deviation was 198.0 ± 44.7nm.

Analysis of knee diameter as a measure of swelling showed significant reductions both 2 and 3 days post-induction of arthritis compared to control injected animals (Figure 1A). EV-treated mice revealed a significant reduction in cartilage depletion and arthritis index, representing overall disease severity, compared to control-treated mice at day 3 (Figure 1B).

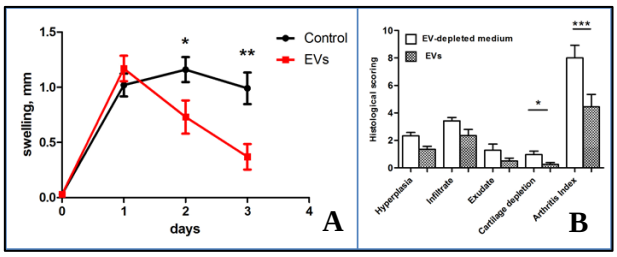

*Fig1. (A) Reduction in knee diameter (swelling) of AIA mice following EV treatment (n=10 per group, **p<0.01, independent samples t-test, error bars = SEM). (B) Reductions in the histopathological symptoms of AIA, including cartilage depletion and arthritis index. Arthritic index is the sum of all observations (n=10, *p<0.05, ***p<0.001, Mann-Whitney U test, error bars=SEM).*

DISCUSSION & CONCLUSIONS: The results demonstrate a clear beneficial effect via injection of EVs into the inflamed joint. Further studies are required to identify the molecular properties of EVs responsible for their therapeutic effects.

REFERENCES: [1]NICE Clinical Guideline **79** (2013) *Rheumatoid arthritis. The management of rheumatoid arthritis in adults*;1-36. [2]F. Djouad et al. (2009) *Nat Rev Rheumatol* **5**:392-399.[3] A.I Caplan and J.E Dennis (2006) *J.Cell Biochem.* **98**:1076-1084. [4]C.Théry et al. (2009) *Nat Rev Immunol*.**9**(8):581-93.

ACKNOWLEDGEMENTS: Research was funded by the RJAH Orthopaedic Hospital Charity and the Institute of Orthopaedics, Oswestry.

Bilayer biomembrane for regeneration of tendon synovial sheath

A Imere[1], JKF Wong[2], M Domingos[3], SH Cartmell[1]

[1] School of Materials, The University of Manchester, UK [2] Plastic Surgery Research, Institute of Inflammation and Repair, The University of Manchester, UK [3] School of Mechanical, Aerospace and Civil Engineering, The University of Manchester, UK

INTRODUCTION: A large number of people suffer from tendon injury, which can result in rupture[1]. Current clinical treatments – based mainly on different suture repair methods[1] – can provide appropriate outcomes in terms of tendon healing but can be complicated by adhesion formations[2] as result of disruption of tendon synovial sheath. Hence, there is the need for development of novel anti-adhesion systems able to restore tendon gliding ability. One of the most promising approaches is introducing a biomembrane that acts as a physical barrier for adhesion-forming cells while regenerating tendon synovial sheath[3]. Here, we propose to combine electrospinning technique and cell-laden hydrogels to produce a bilayer biomembrane for regeneration of synovial sheath and prevention of adhesion formation after tendon repair. The aim of this work was to perform preliminary studies to investigate the mechanical properties of poly(ε-caprolactone) (PCL) electrospun meshes and evaluate cell viability after encapsulation in a self-assembling peptide hydrogel (SAPH).

METHODS: PCL meshes were prepared by electrospinning 10% w/v solution of PCL (M_n 50,000) dissolved in 1,1,1,3,3,3,-hexafluoro-2-propanol at 1 ml/h flow rate, 20kV high voltage and 20 cm needle-collector distance for 1 h. Samples were imaged using Scanning Electron Microscopy (SEM) and fibre diameter analysed using ImageJ. Tensile testing of PCL meshes (n=7) was performed using an Instron 3344 equipped with a 10 N load cell at strain rate of 10 mm/min.

3T3 cells were encapsulated in PGD-α1 SAPH (2×10^6 cells/ml of hydrogel) and cell-laden SAPH constructs were produced using the 3D Discovery printer. Cell viability was assessed via LIVE/DEAD staining at 1 hour, 1, 3 and 7 days after printing.

RESULTS: The spinning process produced PCL electrospun meshes with thin fibres (Mean = 0.254 µm), as shown in Fig. 1A, and high mechanical properties in terms of E and UTS (Fig. 1B).

Analysis of cell-laden constructs revealed that high structural integrity, reproducibility and geometrical and dimensional accuracy can be obtained with the utilized 'bottom-up' approach. Moreover, good cell viability and proliferation was detected through the 7 day-observation period (Fig. 1C).

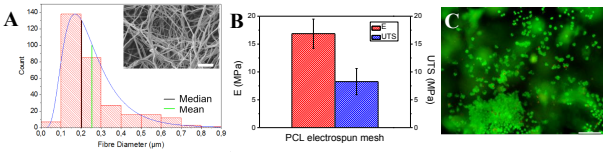

Fig. 1: A) Distribution of fibre diameters and SEM image of PCL electrospun mesh (Scale bar 5 µm). B) E and UTS of PCL meshes. C) Cell viability after 7 days in PGD-α1 SAPH (Scale bar 100 µm).

PCL electrospun mesh and cell-laden SAPH constructs can be combined as shown in Fig. 2 to create a bilayer biomembrane that, wrapped around the tendon, can restore tendon lubrication and prevent adhesion formation.

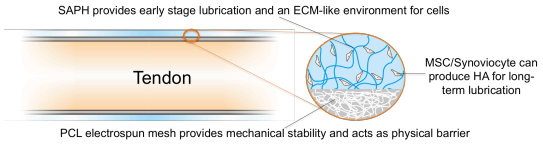

Fig. 2: Schematic of proposed bilayer biomembrane (ECM: extracellular matrix, MSC: mesenchymal stem cell, HA: hyaluronic acid).

DISCUSSION & CONCLUSIONS: The thin fibres and high mechanical properties of the PCL electrospun meshes suggest that a physical barrier with good mechanical stability and structural integrity can be achieved in the proposed biomembrane model. Moreover, the 3D bioprinting process allows great control over the spatial distribution of the hydrogel phase without being detrimental to cell viability. This approach is very versatile as it has the potential to be applied to several hydrogel systems (e.g. BiogelX) to create the adequate ECM-like environment for sustained cell growth, proliferation and production of HA.

REFERENCES: [1]Rawson, S. *et al. Muscles. Ligaments Tendons J.* **3,** 220–228 (2013). [2]Wong, J. K. F. *et al. Am. J. Pathol.* **175,** 1938–1951 (2009). [3]Khanna, A. *et al. Br. Medial Bull.* **90,** 85–109 (2009).

ACKNOWLEDGEMENTS: The authors thank EPSRC and MRC for financial support (grant no. EP/L014904/1).

Bisphosphonates prevent the formation and re-epithelialisation of the oral mucosa *in vitro* in 3D

G Bullock[1], CA Miller[2], A McKechnie[3], V Hearnden[1]

[1] *Kroto Research Institute, Materials Science and Engineering, University of Sheffield, UK.* [2] *School of Clinical Dentistry, University of Sheffield, UK.* [3] *Faculty of Medicine and Health, University of Leeds, UK.*

INTRODUCTION: Bisphosphonate-related osteonecrosis of the jaw (BRONJ) is a disease found in patients taking bisphosphonates (BPs), a group of drugs widely used to treat osteoporosis and bone metastases. BRONJ often follows dental surgery, and presents as exposed, necrotic sections of the jaw where the overlying soft tissue fails to heal. This study aims to investigate the effects of BPs on the oral mucosa in a 3D to gain greater understanding of the role of the soft tissues in BRONJ in order to develop future treatment strategies.

METHODS: Human oral fibroblasts and keratinocytes were cultured onto de-cellularised dermis for 3 days to create a 3D oral mucosa model, before lifting to air liquid interface (ALI) [1]. Models were then cultured at ALI for up to 14 days to allow keratinocytes to form a stratified epithelium. Models were also selectively seeded with keratinocytes in a 3D wound healing model. Models were dosed with pamidronic or zoledronic acid, two BPs most likely to cause BRONJ, at different stages of epithelial stratification. Resazurin assays were used to assess the viability of cells within the oral mucosa, with histology used to monitor wound healing. The effect of BPs on these three dimensional models as well as in 2D cell monolayers was measured to determine the effect of BPs on soft tissue viability.

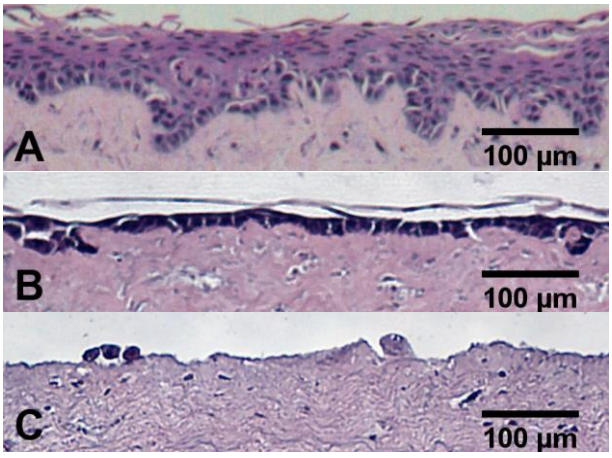

Fig. 1: Haematoxylin and eosin stained sections of oral mucosa model treated for with (A) control medium, (B) 1 µM zoledronic acid or (C) 30 µM zoledronic acid at ALI.

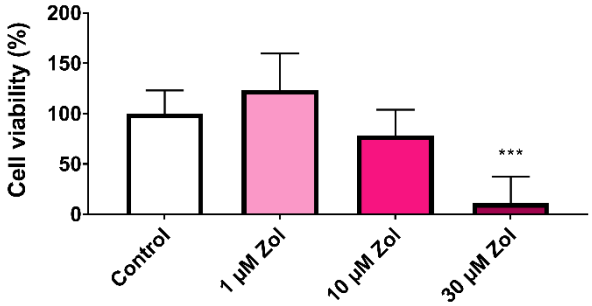

*Fig. 2: Day 14 cell viability of oral mucosa models when treated with zoledronic acid 7 days after culturing at ALI, measured with a resazurin assay. N=3. Error bars = SD. Significance against control indicated by ***P≤0.001.*

RESULTS: Tissue comparable to native oral mucosa was cultured, with histology showing a stratified squamous epithelium. Clinically relevant concentrations of BPs significantly reduced cell viability in 2D over 72 hours. 3D models were more resilient, with no toxicity apparent before 7 days treatment. BPs prevented the stratification of the epithelium when single layer epithelia was treated, however, when established, stratified epithelia were treated epithelium thickness was reduced (*Fig. 1*) and cell viability reduced in a dose dependant manner (*Fig. 2*). BPs negatively affected re-epithelialisation in the 3D wound healing model.

DISCUSSION & CONCLUSIONS: Here we have used a 3D model to investigate the effects of two BPs, clinically relevant to BRONJ, on the epithelium of the oral mucosa to gain further understanding of the effect of BPs on the soft tissues affected in BRONJ. This study demonstrated that our tissue engineered oral mucosa can model both the effects of BPs on healthy epithelia as well as on oral mucosa wound healing, which are both important in the development and resolution of BRONJ. Future work will further develop this model to examine potential treatment strategies.

REFERENCES: [1]Colley, Hearnden, Jones et al. (2011) *Br J Cancer*, 105:1582-92

ACKNOWLEDGEMENTS: The authors would like to thank the EPSRC for funding this research.

Developing tissue-engineered nerve constructs containing aligned endothelial cells to accelerate nerve regeneration

P Muangsanit[1, 3], A Lloyd[2], J Phillips[1, 3]
[1] *Biomaterials and Tissue Engineering, Eastman Dental Institute, University College London, UK*
[2] *MRC Laboratory for Molecular Cell Biology, University College London, UK*
[3] *UCL Centre for Nerve Engineering, University College London, UK*

INTRODUCTION: Blood vessels have been shown to serve as tracks for Schwann cells to migrate along and thus promote axonal regeneration following peripheral nerve injury [1]. In this study the aim was to develop a tissue-engineered construct, using self-aligned endothelial cells within a collagen gel for use in nerve tissue engineering.

METHODS: HUVECs (Human Umbilical Vein Endothelial Cells) were grown in culture. All gels were prepared using Type I rat tail collagen. Collagen gels containing 4×10^6 cells/ml HUVECs were cast in rectangular moulds and tethered at each end [2]. Length of time in culture to achieve optimal endothelial tube formation was examined. To determine the effectiveness of the constructs to support and guide Schwann cell alignment and neuronal growth, a co-culture was established by seeding Schwann cells and neurons onto the surface of the cellular collagen gels.

RESULTS: Endothelial cells formed aligned tubes optimally after 4 days of culture in tethered gels (*Figure 1*). Schwann cells migrated further along HUVEC gels compared with control Schwann cell gels. Furthermore, long straight neurites were detected growing along the HUVEC alignment axis (*Figure 2*).

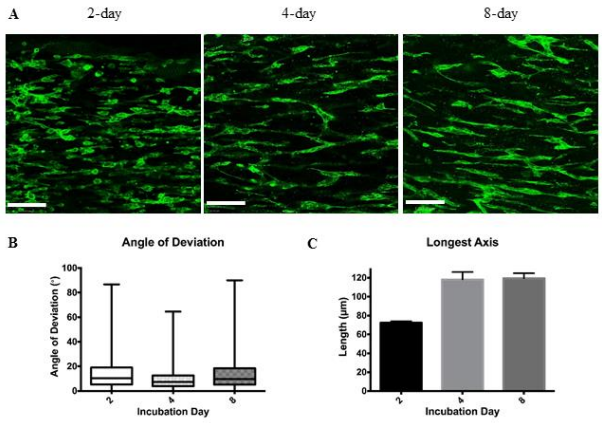

Fig. 1: Self-alignment of HUVECs and formation of tube-like structures within tethered collagen gels. Confocal micrographs show aligned HUVECs forming vascular networks after 2, 4 and 8 days in culture (A). Angle of deviation between HUVEC/tube alignment and the longitudinal axis of the gel (B). Boxes show interquartile range and median values, whiskers indicate maximum and minimum angles (n=3 gels). The lengths of tube-like structures (C) were compared in 2-day, 4-day and 8-day cultured gels. Graphs show mean value ± SEM. (n=3 gels). Scale bars = 120 µm.

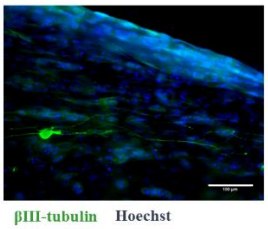

Fig. 2: Elongated neurite regeneration along the longitudinal axis of the gel. Scale bar = 100 µm.

DISCUSSION & CONCLUSIONS: This work demonstrated that the formation of tube-like structures using HUVECs in collagen gels can be achieved in 4 days of culture. Furthermore, the aligned HUVECs supported Schwann cell migration and neuronal growth *in vitro,* suggesting they could be good candidates to test *in vivo*.

REFERENCES: [1] Cattin, A.L., et al., *Macrophage-Induced Blood Vessels Guide Schwann Cell-Mediated Regeneration of Peripheral Nerves.* Cell, 2015. 162(5): p. 1127-39. [2] Georgiou, M., et al., *Engineered neural tissue for peripheral nerve repair.* Biomaterials, 2013. 34(30): p. 7335-43.

ACKNOWLEDGEMENTS: The authors are grateful for the support of a Royal Thai Government Scholarship.

Development of 3D vascularised tumours *in vitro* using self-assembling peptide hydrogels

H Clough[1,2], A Miller[1,2], O Tsigkou[3]

[1]*School of Chemical Engineering & Analytical Sciences, University of Manchester, UK,* [2]*Manchester Institute of Biotechnology, University of Manchester, UK,* [3]*School of Materials, University of Manchester, UK*

INTRODUCTION: The tumour microenvironment (TME) is a diverse interplay between cancer cells, vasculature, extracellular matrix (ECM) and other cell types, providing external barriers to chemotherapeutic drugs [1]. Three-dimensional (3D) *in vitro* models can bridge the gap between two-dimensional (2D) and animal models, providing realistic responses to drugs by mimicking features of the TME. Self-assembling peptide hydrogels (SAPH), using ionic-complementary peptides, are promising due to their chemical definition, ability to spontaneously self-assemble into 3D fibrillar scaffolds, biocompatibility and tunable mechanical properties, thus mimicking ECM [3]. This study aims to develop 3D vascularised multicellular cancer spheroids that mimic many features of the *in vivo* TME *in vitro* using SAPH. As a first attempt laminin was incorporated within the SAPH and the effect on endothelial and tumour cell viability, growth and organisation was assessed.

METHODS: PeptiGel-Alpha1 and PeptiGel-Alpha2 SAPHs were sourced from PeptiGelDesign Ltd. Oscillatory rheometry was used to measure the stiffness of SAPHs using frequency sweeps between 0.1 – 10 Hz at a strain of 0.2%. Fourier transform infrared (FTIR) spectroscopy was used to determine the presence of β-sheet structures within the hydrogels. MCF-7 breast adenocarcinoma cells and human umbilical vein endothelial cells (HUVECs) were cultured on laminin (5, 25 and 50 µg/mL) up to 7 days. MCF-7 cells were encapsulated within SAPH enriched with laminin for up to 14 days and their viability was monitored with LIVE/DEAD assay. The ability of the SAPH to support tube formation was assessed with high-throughput screening and time-lapse microscopy. Actin organisation and cell-cell contact were assessed though phalloidin staining and E-cadherin immunostaining.

RESULTS: The presence of laminin within SAPH was found not to affect the mechanical properties of the gels. FTIR analysis confirmed that β-sheet formation within the SAPHs was not affected by the presence of laminin. HUVECs and MCF-7 cells were viable when cultured on laminin. Moreover, fluorescent microscopy on the 50 µg/mL laminin TCP revealed the organisation of the MCF-7 cells in an altered morphology resembling that of polarised acini. Cell polarisation and cell-cell interactions in the structures revealed by actin and E-cadherin staining will be presented.

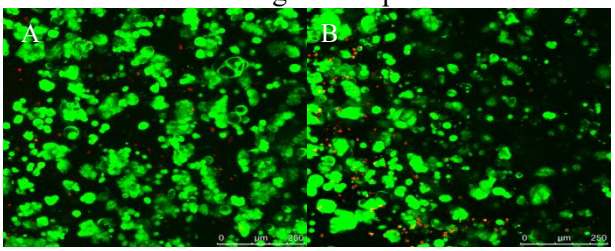

Figure 1. LIVE/DEAD of MCF-7 breast adenocarcinoma cells encapsulated within PeptiGel-Alpha1 (A) and PeptiGel-Alpha1 + 50µg/mL laminin (B) after 7 days.

LIVE/DEAD staining confirmed that MCF-7 cells encapsulated within SAPH maintained a high viability up to 14 days (Figure 1). Laminin incorporation within the SAPHs was used to determine the parameters required to stimulate vessel-like tubule formation. Data on tubule number, length, density and branch points will also be presented.

DISCUSSION & CONCLUSIONS: This work demonstrates the potential of SAPHs to support MCF-7 and HUVEC cell encapsulation and growth. Incorporating ECM proteins opens up the modulation of key features of the TME and provides cell binding motifs found *in vivo*.

REFERENCES: [1] Junttila, M. R. & de Sauvage, F. J. *Nature* **501,** 346–354 (2013). [2] Zanoni, M., Piccinini, F. & Arienti, C. *et al. Sci Rep.* **6,** 19103 (2016). [3] Gough, J. E., Saiani, A. & Miller, A. *Bioinspired, Biomim. Nanobiomaterials* **1,** 4–12 (2012).

ACKNOWLEDGEMENTS: H Clough would like to thank the EPSRC-MRC CDT for Regenerative Medicine for financial support.

This template was modified with kind permission from eCM Journal.

Engineering soft tissues: learning from nature

N Mehrban[1], DN Woolfson[2], SF Badylak[3], MA Birchall[1]

[1]*UCL Ear Institute, University College London, London, UK,* [2]*School of Chemistry, University of Bristol, Bristol, UK,* [3]*McGowan Institute for Regenerative Medicine, University of Pittsburgh, Pittsburgh, USA*

INTRODUCTION: When tissue is damaged, either through disease or trauma, surgery attempts to ease patient discomfort typically by adopting a repair approach. Whilst surgery has some limits (primarily issues with complete functional restoration) tissue engineering offers a means of not only repairing the tissue but also total replacement. For this to occur it is essential that the scaffold used supports and guides cell behaviour while integrating with surrounding healthy tissue at the wound site.

METHODS: Peptides were synthesised using standard solid-phase synthesis protocols, purified by reversed-phase HPLC and their masses confirmed by mass spectrometry. Peptide functionalisation was achieved through standard click chemistry. The resulting gels were seeded with murine neural cells, adipocytes and tenocytes and tested for attachment, migration, proliferation and differentiation. Scaffold stiffness was assessed through rheometry.

All experiments with decellularised tissue were conducted by Crapo et al.[3] and Wolf et al.[4]. Briefly, porcine bladder was mechanically and enzymatically decellularised and the resulting extracellular matrix (ECM) was lyophilised. Lyophilised ECM was either kept whole or milled and reconstituted as a pH-neutralised hydrogel. Scaffold were then seeded with 3T3 fibroblasts and C2C12 myoblasts for viability assessment.

RESULTS: Soft tissue scaffolds were formed via peptide synthesis (Figure 1A and 1B) or through decellularisation methods (Figure 1C and 1D). All scaffolds supported cell attachment, migration and proliferation. Some functional differentiation was also observed. Preliminary data shows that some of these materials may be mass produced using 3D printing technology.

DISCUSSION & CONCLUSIONS: Here two distinct types of scaffolds are presented towards soft tissue engineering; *de novo* peptide-based materials which can be chemically and physically tuned to match tissue type[1,2] and, decellularised materials that can be modified to suit patient-specific geometries.[3,4] Both materials are based on exploiting nature's designs, either by using existing architecture or through understanding design rules to develop a new class of materials.

The resulting scaffolds allow better control of overall geometry, cell attachment, migration and differentiation[5] as well as scaffold stiffness[6] for better integration with healthy native tissue and towards full functional restoration.

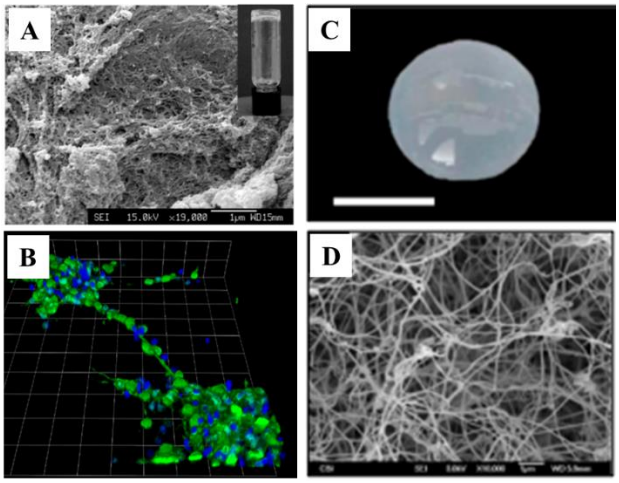

Fig. 1: Fibrous scaffolds to support cell proliferation were formed through peptide synthesis (A and B) or through decellularisation techniques (C and D). All images taken from previously published text [2-5].

REFERENCES: [1] E.F. Banwell, E.S. Abelardo, D.J. Adams et al. (2009) *Nat. Mat.* **8**:596-600. [2] N. Mehrban, E. Abelardo, A. Wasmuth et al. (2014) *Adv. Health. Mat.* **3**:1387-91. [3] P.M. Crapo, T.W. Gilbert, S.F. Badylak (2011) *Biomat.* **32**:3233-43. [4] M.T. Wolf, K.A. Daly, E.P. Brennan-Pierce et al. (2012) *Biomat.* **33**:7028-38. [5] N. Mehrban, B. Zhu, F. Tamagnini et al. (2015) *ACS Biomat. Sci. Eng.* **1**:431-39. [6] D.E. Discher, D.J. Mooney, P.W. Zandstra (2009) *Science* **324**:1673-7.

ACKNOWLEDGEMENTS: All work presented reflect collaborations with the Woolfson Group (University of Bristol), Song Group (Cardiff University), Randall Group (University of Exeter), Bowen Group (Open University) and the Badylak Group (University of Pittsburgh).

Frequency-dependent control of pluripotent stem cell differentiation through charge-balanced electrical stimulation.

CJ Bullock[1, 2], T Kisby[1, 2] K Kostarelos[1], C Bussy[1]

[1]*Nanomedicine Laboratory, School of Health Sciences, Faculty of Biology, Medicine and Health, University of Manchester, UK.*

[2]*EPSRC-MRC Centre for Doctoral Training in Regenerative Medicine, University of Manchester, UK.*

INTRODUCTION: Endogenous bioelectic signalling is highly involved in embryonic development as well as in cellular morphogenesis, proliferation, migration and patterning in tissue repair [1]. Coincidentally, these are also the natural behaviours that researchers are most interested in replicating for use in tissue engineering and regenerative medicine applications. Based on these processes, we hypothesised that electrical stimulation could be used as an instructive cue for directing mouse embryonic stem cell differentiation.

METHODS: In order to test this hypothesis, a biocompatible graphene-based cell culture substrate with a high degree of capacitive charge injection was developed. This approach enabled electrical charge to be delivered evenly across samples without the release of faradaic species and associated pH changes that have been shown to affect stem cell differentiation [2]. E14-2TGA Mouse Embryonic Stem cells were formed into embryoid bodies and charge-balanced sinusoidal potential waveforms were then applied. Following stimulation, embryoid bodies were placed into three different media to push their differentiation towards each of the three embryonic germ lineages or under conditions that either maintained pluripotency or a 'neutral' differentiation media that did not contain any cytokines. All cells were then allowed to differentiate for 5 days. After this time, a 8 colour flow cytometry panel was used to assess the viability and lineage commitment of the cells relative to non-stimulated cells. This approach enables the co-expression of seven different lineage commitment markers to be quantified in each individual cell, enabling robust analysis of heterogenous cell populations.

RESULTS: Electrical stimulation had no significant impact on cell viability over any of the conditions tested. Stimulation of 1 Hz significantly decreased the percentage of cell double positive for pluripotency markers SOX2 and SSEA1 compared to non-stimulated controls (***Fig.1 A***), suggesting that this stimulation regime enhanced the differentiation of the cells. In contrast, 0.2 Hz and 10 Hz stimulation did not appear to affect pluripotency marker expression. However, 0.2 Hz stimulation did significantly increase the population of cells positive for early mesoderm marker CD31 (Pecam1) coupled with a significant decrease in the cell population double positive for early ectoderm markers Nestin and Notch1 (***Fig.1 B***), suggesting that 0.2 Hz electrical stimulation may be able to push differentiating stem cells towards a mesodermal cell fate over the ectodermal lineage. Applying 10 Hz stimulation on cells had no significant impact, demonstrating the importance of frequency.

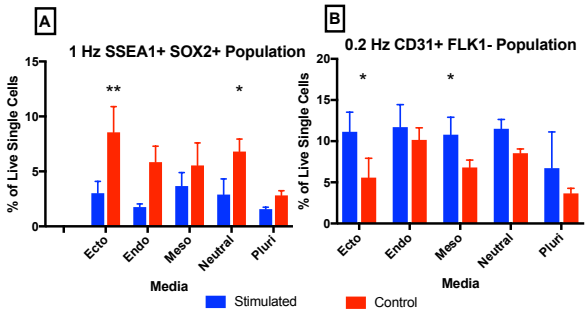

Fig. 1: *A/ Impact of 1Hz stimulation on SSEA1+ SOX2+ Cell population. B/ Impact of 0.2 Hz stimulation on CD31+ FLK1- population.*

CONCLUSIONS: Here, we have systematically probed the impact of charge-balanced electrical stimulation on pluripotent stem cell differentiation. We have shown the importance of stimulation frequency. In particular, low frequency stimulation appears to be able to push embryonic stem stems to assume a mesodermal fate ahead of ectoderm.

REFERENCES: [1] Levin M. et al (2017) *Endogenous Bioelectric Signalling Networks: Exploiting Voltage Gradients for Control of Growth and Form*. Annu. Rev. Biomed. Eng. 19: 353–87. [2] Balint R. et al (2013) *Electrical Stimulation Enhanced Mesenchymal Stem Cell Gene Expression for Orthopaedic Tissue Repair*. J. Biomater. Tissue Eng. 3(2): 212-221.

ACKNOWLEDGEMENTS: Prof JA Garrido and the University of Manchester Flow Cytometry and Genomic Technology Facilities.

Generating fibroblast-derived 3D native scaffolds to examine the role of the extracellular matrix in oral cancer progression

AL Harding[1], DW Lambert[1], HE Colley[1]

[1]*Ibio research group, School of Clinical Dentistry, Sheffield University, UK*

INTRODUCTION: Interaction of cells with the surrounding extracellular matrix (ECM) is the foundation that regulates tissue homeostasis. During cancer progression regulation is determined by interactions between tumour cells, stromal cells (fibroblasts and leukocytes) and other components of the microenvironment such as the ECM. The ECM is predominantly deposited by cancer associated fibroblasts (CAF) and plays a key role in cancer progression. Although considerable evidence exists demonstrating a role for CAF in oral squamous cell carcinoma (OSCC), little is known about their influence on ECM: tumour interactions. The aim of this research was to generate novel tissue-engineered 3D constructs using normal oral fibroblast (NOF)- and CAF derived ECM, as native scaffolds to accurately model tumour:ECM interactions in OSCC progression.

METHODS: Utilising a transwell technique, culture conditions were optimised to stimulate NOF- and CAF-derived ECM deposition. Full thickness epithelium models were produced by culturing normal (FNB6) or OSCC (H357) cell lines seeded onto ECM scaffolds at an air to liquid interface for 10-14 days. Key epithelial and fibroblast markers were characterised by immunohistochemistry (Ki67, AE1/3, COLIV, COL1A1, Vimentin (VIM), E-cadherin, Integrin-β4 and αSMA) and immunoblotting (αSMA, FN1-EDA, VCAN, COL1A1, LAM, and VIM). Collagen linearisation, width and elongation in NOF- and CAF-derived matrices were analysed using second harmonic generation microscopy (SHGM). Atomic force microscopy (AFM) and live-cell fluorescence imaging microscopy (LFIM) determined ECM biomechanics and the complex behavioural interplay of cancer cells in these ECM scaffolds respectively.

RESULTS: NOF stimulated to produce ECM, over a four-week culture period, generated an organised matrix with an average thickness of ~200 µm compared to CAFs which produced a thicker (350 µm), highly irregular ECM. Immunoblotting of the matrices revealed a significantly different protein deposition of CAF matrices compared to NOF matrices. SHGM revealed collagen width, length, and linearisation as statistically different in CAF-derived matrices than NOF-derived matrices (Figure 1). Addition of FNB6 and H357 cells generated a stratified epithelial layer histologically resembling normal and cancerous tissue *ex vivo* (Figure 2). Further immunohistochemical analysis revealed differential expression of ECM proteins and evidence of CAF-mediated tumour progression. AFM determined the micromechanical properties of the ECM and alterations of tissue stiffness, in disease progression. LFIM provided information on the migration rates and invasion of cancer cells within these models.

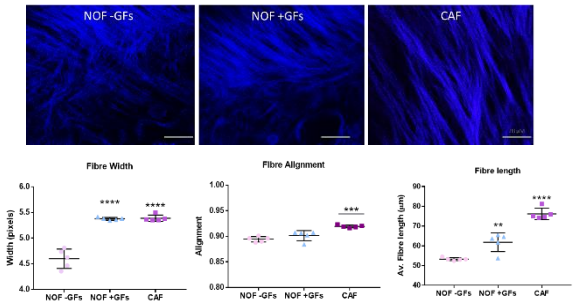

Fig. 1: Images of second harmonic generation of collagen fibres in matrices. Graphs depict changes in collagen fibre width, alignment and length. Statistical significance was confirmed by one-way ANOVA. All experiments N=3, n=3.

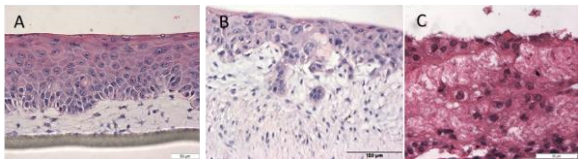

Fig. 2: H&E staining of fibroblast-derived matrices depicting disease progression. FNB6 on NOF matrix (A), FNB6 on CAF matrix (B), and H357 on CAF matrix (C).

DISCUSSION & CONCLUSIONS: Using tissue-engineering techniques it is possible to model fibroblast-mediated ECM deposition providing a novel, physiologically relevant *in vitro* tool for the study of OSCC progression.

ACKNOWLEDGEMENTS: I would like to generously thank Professor Keith Hunter for his ethical approval pertaining to the collection of tumour tissue. As well as Dr R Bolt and Dr H Colley for the collection and ethics pertaining to the collection of healthy oral mucosa.

Genome engineering in hydrogel to control cell behaviour: a method for modulating human-induced pluripotent stem cell-derived cardiomyocytes.

V Alageswaran[1], S Kalra[2], Y Yang[1], V George[1],

[1]*ISTM, Guy Hilton Research Centre, Keele University.* [2]*CBTRC, QMC, University of Nottingham*

INTRODUCTION: Recent years have seen a flood of protocols that show differentiation of human-induced pluripotent stem cells (hiPSCs) into cardiomyocytes (hiPSC-CMs) using defined conditions with growth factors or small molecules. However, inefficiency of sub-type specificity coupled with immaturity of hiPSC-CMs somewhat disqualifies them from being representative of the adult human heart. In an attempt to understand and regulate these properties of hiPSC-CMs, this study employs a genome engineering tool called dLITE (**d**Cas9 **C**RISPR **L**ight-inducible **T**ranscriptional **E**ffectors). dLITE allows endogenous activation and repression of target genes by modulating gene enhancers in the presence of blue light. Therefore, by controlling developmental genes involved in hiPSC-CM differentiation and maturation, we hypothesise a genetic model for controlling stem cell differentiation into bonafide cardiomyocytes, which can be enhanced in a hydrogel microenvironment.

METHODS: dLITE consists of the photoactivator plasmids - dCas9-CIB1 and CRY2-VP64 which are responsive to only blue light (~470nm) (termed as dLITE1.0), its target dictated by a humanized gRNA. An advanced dLITE system was engineered by replacing the VP64 activator domain with an improved activator called VPR (VP64-P53-Rta) by sub-cloning (termed as dLITE2.0). To address efficiency of dLITE delivery across a range of cell types, hiPSCs were tested alongside primary cells - human foreskin fibroblasts (HFFs) and the immortalized human embryonic kidney cells HEK293 cells. An assay for checking functional gRNA targeting was also developed by cloning gene enhancers upstream of a NanoLuc® luciferase reporter.

RESULTS: By creating the next generation of dLITE components (dLITE2.0), the first of its kind, we identified the optimal conditions required to activate dLITE2.0 in terms of frequency of light pulse (0.13Hz) over a duration of exposure to the cells (24 hours being optimal) to achieve a response above control values (~2 fold increase in light-responsive GFP sensitivity when stimulated with 0.13Hz) in HEKs. The spatial influence of light stimulation on the dLITE2.0 system was assessed by observing the light-responsive GFP sensitivity in transfected cells at various spatial proximities to the light source. Light-responsive dLITE sensitivity drops ~6.5 fold from a height of 28mm and drops ~1.2 fold from a distance of 63.75mm laterally from the light source, suggesting a radial zone of dLITE sensitivity from point of optical stimulation. To achieve optimal sequential transfection of multiple dLITE components in a range of cell types, different methods of delivery of optogenetic plasmids were assessed. An engineered approach combining hydrogel (0.1% gelatin Type B) with genetic plasmids enhanced delivery substantially to produce ~23%-30% increase in transfection efficiency in HEKs as well as in HFFs. Genes responsible for cardiomyocyte differentiation and maturation including PIM1, MESP1, TNNI1, TNNI3, KCNJ2 and IRX4 were screened for optimal gRNA sensitivity using an in-cell NanoLuc® reporter assay that allows us to determine target specificity and to then facilitate endogenous upregulation in hiPSCs/hiPSC-CMs.

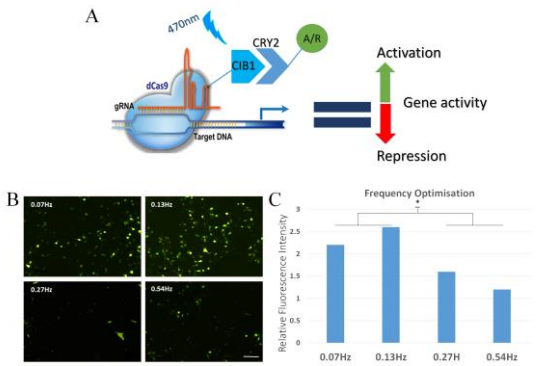

Fig. 1: (A) Mechanism of dLITE (B) Light-responsive GFP fluorescence in HEK293 cells transfected with dLITE2.0 at various frequencies of optical stimulation (Scale bar 100µm) (C) Quantitative estimation of GFP fluorescence using plate reader.

DISCUSSION & CONCLUSIONS: With the optimization of the new dCas9 CRISPR optogenetic system in a biomaterial and by exploiting its unique features, efforts are now underway to target differentiation of hiPSCs and improve maturation of hiPSC-CMs using optogenetics, without resorting to growth factors or small molecules.

ACKNOWLEDGEMENTS: This project is funded by the Keele ACORN studentship.

In vivo MRI cell tracking of autologous mesenchymal stem cells in an ovine osteochondral defect model.

H. Markides [1], K. J. Newall [2], H. Rudorf [3], L. Blokpoel Ferreras [4], J. E. Dixon [4], R. H. Morris [5], M. Graves[6], J. Kaggie[6], F. Henson [2,3], A. J.El Haj [1*]

1. Institute of Science and Technology in Medicine, Keele University. 2. Department of Surgery, University of Cambridge. 3. Department of Veterinary Medicine, University of Cambridge. 4. Centre for Biomolecular Sciences, The University of Nottingham. 5. School of Science and Technology, Nottingham Trent University, Nottingham, UK. 6. Department of Radiology, University of Cambridge.

INTRODUCTION: Osteochondral injuries represent a significant clinical problem requiring novel cell-based therapies to restore function of the damaged joint. Pre-clinical studies are fundamental in translating such therapies, however, technologies to non-invasively assess *in vivo* cell fate are currently limited. We investigate the potential of a MRI and SPION (superparamagnetic iron oxide nanoparticle) based technique to monitor cell delivery and cellular bio-distribution in vivo. Furthermore, we define a protocol to successfully label ovine MSCs with Nanomag, a novel cell-penetrating peptide (P218R) using a technique known as GET (Glycosaminoglycan-binding enhanced transduction) (1). The suitability of this system in tracking stem cell homing to the site of injury is explored in an acute and chronic osteochondral injury model over 7 days.

METHODS: Autologous ovine MSCs were isolated, expanded and labelled overnight with Nanomag; a 250nm dextran coated SPION with the aid of the cell-penetrating peptide, P218R. *In vitro* and *ex vivo* MRI detection thresholds were determined prior to *in vivo* studies. Cell viability, proliferation and differentiation potential pre and post Nanomag labelling were further evaluated. A single 8mm diameter osteochondral defect was created in the medial femoral condyle in the left knee joint of each sheep with the contralateral joint serving as the control. $10x10^6$ Nanomag labelled-MSCs (P3) were subsequently labelled with a fluorescent lipophilic dye (DII) and delivered by intra-articular injection at either 1 week or 4.5 weeks post defect creation. Sheep were then sacrificed 7 days post implantation and immediately MR imaged using an ESAOTE 0.2T scanner and validated using a Siemens 3T MRI scanner. Joints were then processed for histology.

RESULTS: *In vitro* and *ex vivo* MRI data demonstrated significant increase in MRI contrast as a result of P218R:Nanomag uptake. Cell viability, proliferation and differentiation capabilities were not affected by Nanomag-labelling. Images revealed evidence of implanted cells within the synovial joint of the injured leg of the chronic model only with no signs of cell localisation to the defect site in either model (figure 1). This was validated histologically determining the location of implanted cells in the synovium. Evidence of engulfment of Nanomag-labelled cells by leukocytes is observed in the injured legs of the chronic model only. Finally, serum CRP (c-reactive protein) levels were measured by ELISA with no obvious increase in CRP levels observed as a result of P21-8R:Nanomag delivery.

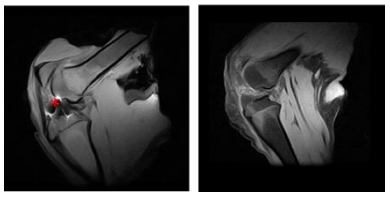

Fig 1: Cross sectional MRI images of the knee joints 7 days' post cell delivery in the (i) chronic and (ii) acute injury models. T_1 MRI scans obtained using a 0.25T Escote MRI scanner. Red star indicates the presence of SPIONs

DISCUSSION & CONCLUSIONS: This study clearly demonstrates the potential of Nanomag and P218R as an effective means of imaging and tracking cells in an ovine osteochondral defect model. This protocol has great implications in the clinical translation of a wide range of stem cell based therapies.

REFERENCES:

1. Dixon JE, Osman G, Morris GE, Markides H, Rotherham M, Bayoussef Z, et al. Highly efficient delivery of functional cargoes by the synergistic effect of GAG binding motifs and cell-penetrating peptides.

Investigating the use of autologous fat derived cells to stimulate regeneration in the pelvic floor

E Mironska[1,2], S Roman[1], C Chapple[2], S MacNeil[1]

[1] *Kroto Research Institute, Department of Materials Science and Engineering, University of Sheffield, UK.* [2] *Royal Hallamshire Hospital, Sheffield, UK*

INTRODUCTION: Synthetic, transvaginal mesh made of polypropylene (PPL) has been the mainstay of pelvic organ prolapse surgery for many years. However, it is now recognised that this material can lead to severe complications such as pain, infection and even erosion through patient's native tissues. Thousands of women worldwide have been affected by the adverse consequences of transvaginally implanted PPL mesh, resulting in the award of multi-billion-dollar settlements by several mesh manufacturers. Consequently, many products have been withdrawn from the market entirely. Therefore, there is an urgent need for new materials for use within the pelvic floor. Our group has previously developed poly-L-lactic acid (PLA) scaffolds with different fibre orientations to meet the specific biomechanical requirements of the pelvic floor[1]. These scaffolds maintained mechanical integrity, compared to PPL meshes, over 90 days following implantation using a rabbit model[2]. It was shown that PLA scaffolds integrated well into host tissues with constructive remodelling (referred to as an M2 response), cell infiltration and neovascularization.

METHODS: We have since refined the scaffold design to incorporate 'tunnels' into which a cell population can be placed. This has been achieved by co-spinning a 10% PLA bi-layer over Teflon strips. These Teflon strips are later removed, leaving a patent 'fat tunnel' in place (Figure 1). Co-spinning enables our scaffolds to be composed of both random and aligned fibres. Adipose derived mesenchymal stem cells (ADMSCs) have been shown to promote angiogenesis and reduce inflammation while promoting tissue regeneration. However, they are time consuming and labour intensive to culture. Using donated human fat, we can have isolated three distinct cell populations; Expanded ADMSCs, stromal vascular fraction (SVF) and 'nanofat'. The SVF is a cell rich pellet containing ADMSCs and other progenitor cells. 'Nanofat' is fat which has been mechanically processed only, without enzymatic digestion or incubation[3].

RESULTS: We report that all three cell populations (ADMSCs, SVF and nanofat) have improved metabolic activity and collagen production in vitro when seeded within PLA scaffolds.

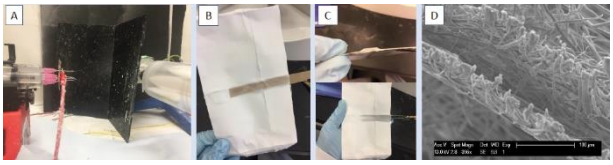

Fig. 1: (A) Electrospinning rig (B) Teflon removal from PLA scaffold (C) Cross section of tunnel (top) and demonstration of tunnel patency and strength with forceps (bottom) (D) SEM image showing cross section of the PLA tunnel.

DISCUSSION & CONCLUSIONS: Any new material proposed for use within the pelvic floor is, quite correctly, going to be under intense scrutiny to demonstrate a superior safety record to PPL mesh. We report the first steps to achieving a material which can be combined with patients' cells for implantation into the pelvic floor in one single operation. Nanofat is an exciting prospect for a simple, user friendly method of obtaining a useful cell population from fat that could stimulate tissue regeneration. Further work is needed to fully characterise nanofat and evaluate each cell populations performance within a bioreactor whilst undergoing uniaxial distension.

REFERENCES:

1. Roman, S,Mangir N, Bissoli J,et al. J BiomaterAppl. 2016;30(10):1578-88. 2. Roman S, Urbánková I, Callewaert G, et al. J Urol. 2016;196(1):261-9. 3. Tonnard, P., Verpaele, A., Peeters, G, et al. Plast Reconstr Surg. 2013;132(4), 1017-26.

ACKNOWLEDGEMENTS: This work was funded by a grant from the Urology Foundation.

This template was modified with kind permission from eCM Journal.

Near-human tissue-engineered, dynamic model of the large airways

R Sbordoni[1], N Mehrban[1], G Wayne[2], S Hopkins[2], G Dal Negro[2], MA Birchall[1]

[1]*Ear Institute, University College London, London, United Kingdom.*[2]*GlaxoSmithKline Medicines Research Centre, Stevenage, United Kingdom.*

INTRODUCTION: The use of animal models in biomedical research and drug discovery comes with a series of limitations, including issues of reproducibility, consistency amongst models [1], and ethical concerns. Alternatives to animal models are needed and tissue engineering could provide valid tools to address this challenge.

Tissue-engineering can be adopted as a tool for developing realistic *in vitro* models to corroborate or substitute the use of current animal models [2]. One method of developing biomimetic tissue-engineered models is by seeding cells on decellularised biological scaffolds, which can provide cues for cell proliferation and differentiation [3].

The aim of this project is to develop a miniaturised tissue-engineered *in vitro* model of the human medium and large bronchi by seeding human bronchial epithelial cells on decellularised biological scaffolds placed in a dynamic bioreactor, which simulates mechanical stress during respiration.

METHODS: The ideal scaffold source will be identified through comparisons of chemical, ultrastructural, and biomechanical properties of decellularised upper airways of human and animal provenience. Tissue will be decellularised with a vacuum-assisted chemical-enzymatic protocol [4] and sterilised via gamma irradiation. Epithelial cells will be isolated from human bronchial biopsies and seeded on the decellularised scaffolds; their phenotype will be assessed through immuno-histochemical stainings of FOX-J1, MUC5AC, P63, Ki67, ZO-1 markers. The seeded scaffold will be placed in a bespoke dynamic bioreactor.

RESULTS: Porcine tracheas, upper bronchi and lower bronchi were successfully decellularised. Histological analysis of fibroblasts seedings on sections of decellularised porcine lower tracheas indicate good cell attachment and proliferation (fig. 1A, 1B). A prototype of the dynamic bioreactor has been developed to study cell behaviour in an environment approaching human respiration (fig. 1C).

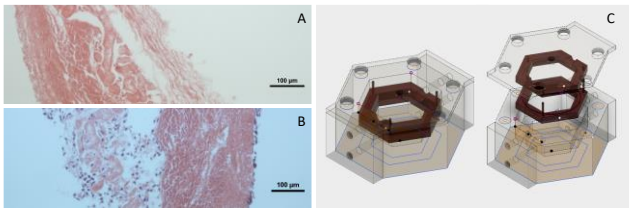

Fig. 1. A: decellularised mucosal tract of porcine lower trachea (H&E staining). B: recellularisation with 3T3 fibroblasts, day 15 (H&E staining). C: bioreactor prototype, closed (left) and opened (right).

DISCUSSION & CONCLUSIONS: Tissue engineering approaches based on the decellularisation of biological tissue can be adopted for the development of *in vitro* models of the upper respiratory airways. Tissue-engineered models could then be used for drug testing and as platforms to study the physiology of airway epithelium, such as extracellular matrix-cell interactions. Preliminary data shows that this is possible using decellularised scaffolds. Furthermore, bespoke bioreactors will provide appropriate physical stimuli allowing the assessment of mechanical stress effects on cells in a biomimetic environment. This model has huge potential for industrial and academic applications.

REFERENCES: [1] van der Worp, HB, Howells, DW et al (2010) *Plos Med* **7**(3): e1000245. [2] Nichols, JE., Niles, JA et al (2014) *Exp Biol Med* **239**(9): 1135-1169. [3] Rana, D., Zreiqat, H., et al (2015) *J Tissue Eng Regen Med* **11**(4): 942-965. [4] Lange, P., Greco, K., et al (2015) *J Tissue Eng Regen Med* **11**(3): 800-811.

ACKNOWLEDGEMENTS: This work was funded jointly by the London Interdisciplinary Doctoral Programme, GlaxoSmithKline, and the BBSRC.

DISCLAIMER: All animal studies were ethically reviewed and carried out in accordance with Animals (Scientific Procedures) Act 1986 and the GSK Policy on the Care, Welfare and Treatment of Animals. Human biological samples within this study are sourced ethically and their research use is in accord with the terms of the informed consents under an IRB/EC approved protocol.

New designs of polymeric microparticles for regenerative medicine: Examining the influence of topographically-textured microparticles on mesenchymal stem cell fate

Mahetab Amer[1], Marta Alvarez-Paino[1], Kevin Shakesheff[1], David Needham[1,2], Morgan Alexander[1], Cameron Alexander[1] and Felicity Rose[1]

[1]*School of Pharmacy, University of Nottingham, Nottingham, UK* [2]*Department of Mechanical Engineering and Material Science, Duke University, Durham, North Carolina, USA*

INTRODUCTION: Microparticles have numerous applications in tissue engineering and cell therapy, such as drug and biologic carriers for cell production and transplantation. Material properties, such as topography, are capable of influencing cell behaviour[1]. Assessing the influence of varying microparticle surface topography on stem cell behaviour is critical for their use as cell delivery systems in regenerative medicine applications.

METHODS: Textured PLA microparticles were produced using fusidic acid that phase separates from the polymer into spherical microdomains during loss of solvent from an oil-in-water emulsion. The fusidic acid then itself dissolves leaving the textured surfaces shown in Fig 2A. By varying emulsion settings, microparticles of two key dimpled morphologies were produced: dimpled, termed 'golf ball'-like, and those which had undergone such surface changes that they were no longer spherical, termed 'boulder'-shaped. To investigate the influence of microparticle topography on cell response, a planar cell culture system was developed by heat sintering them into discs (Figure 1A). The influence of topographical features on the attachment, proliferation and morphology of primary human mesenchymal stem cell (hMSCs; 2 donors) was investigated. Early and late markers of osteogenesis were assessed after culturing cells in basal (in the absence of osteo-inductive supplements) and osteo-inductive media to identify the effects of microparticle topography on osteogenic differentiation of hMSCs.

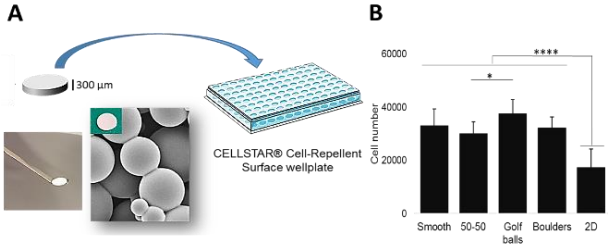

*Figure 1: (A) Preparation of 2.5D cell culture systems. (B) Attachment of hMSCs on the 2.5D systems, measured using PrestoBlue, 4 hours post-seeding (n≥6; 2 donors & 4 independent experiments; *p<0.05, ****p<0.001).*

RESULTS: In comparison to dimpled 'golf ball' topographies alone, a 50/50 mixture of smooth and golf-ball topographies resulted in significantly lower hMSC attachment on 2.5D substrates (Fig. 1B). Cell morphologies were influenced by the different topographies, with cells spreading on smooth surfaces and adopting more rounded morphologies on golf ball and boulder-like ones (Fig. 2A). In the absence of osteo-inductive supplements, cells cultured on microparticles with golf ball-like topographies exhibited notably increased expression of osteocalcin after 14 days in culture relative to smooth microparticles (Fig. 2B).

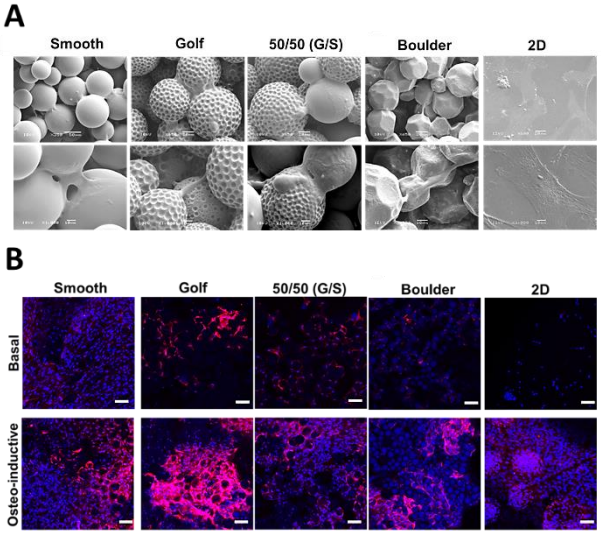

Figure 2: (A) SEM images of hMSCs attached to surfaces of 2.5D culture systems 4 hours post-seeding. (B) Osteocalcin (red) and nuclear (blue) staining of hMSCs on 2.5D topographical discs 14 days post-seeding, cultured in either basal or osteo-inductive media. (Scale bar=100 µm)

DISCUSSION & CONCLUSIONS: Topographically-textured microparticles of varying microscale features were used to investigate stem cell adhesion and subsequent differentiation. This study demonstrates the sensitivity of hMSC attachment, spreading and differentiation to microparticles' surface topography. It highlights the importance of tailoring topographical design of microparticles and provides the opportunity to control stem cell fate for bone tissue engineering by inducing osteogenesis without the use of exogenous osteo-inductive factors.

REFERENCES: [1] HV Unadkat *et al.* (2011) *PNAS* 108 (40) 16565-16570

Porosity of poly(glycerol sebacate urethane) scaffolds controls angiogenic response and tissue ingrowth *in vivo*

A. Samourides[1], L. Browning[1], B. Chen[1,2], V. Hearnden[1]

[1] *Department of Materials Science and Engineering, University of Sheffield, Sheffield, S3 7HQ*

[2] *School of Mechanical and Aerospace Engineering, Queen's University Belfast, Belfast, BT9 5AH*

INTRODUCTION: Soft tissue reconstruction and replacement requires novel synthetic materials which can support new tissue growth and blood vessel infiltration. Poly(glycerol sebacate urethane) (PGSU) is a soft, elastomeric material which is biocompatible, biodegradable, has mechanical properties which are comparable to native soft tissues and which can be fabricated into 3D structures [1]. In this study we investigate the biological response to PGSU scaffolds using a simple *in vivo* assay, to examine how pore size affected tissue infiltration and blood vessel in-growth.

METHODS: PGSU porous scaffolds were fabricated with varying pore sizes (small-12µm, medium-28µm and large-110µm) using freeze drying. These scaffolds were compared to non-porous films fabricated from PGSU as a control. The ability of scaffolds to support tissue and blood vessel ingrowth was assessed using the *ex ovo* chick chorioallantoic membrane (CAM) assay. PGSU samples were implanted onto the surface of the CAM on day 7 and the increase in the number of blood vessels growing towards the samples between days 7 and 13 was measured.

RESULTS:

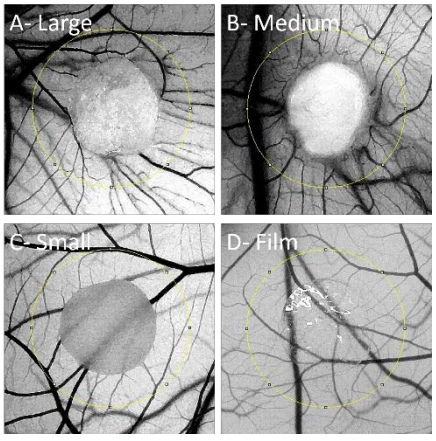

Fig. 1: Representative greyscale images of PGSU scaffolds and films on the CAM angiogenesis assay following 6 days of incubation. Films were non-porous while scaffolds had average pore sizes of: small-12µm, medium-28µm and large-110µm.

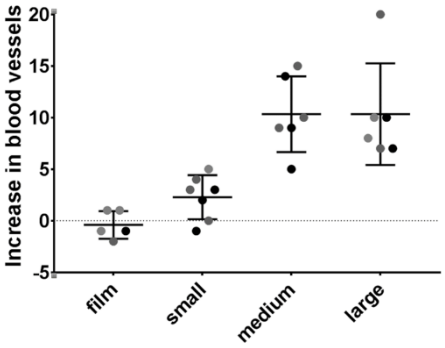

Figure 2. Quantification of the increase in the number of new blood vessels growing towards PGSU samples from day 7 to day 13. Mean ± s.d. N=5

Medium pore size PGSU scaffolds (28µm pores) were able to support rapid tissue ingrowth and blood vessel ingrowth with no further stimuli in the *ex ovo* CAM assay (Fig. 1&2). Scaffolds with larger pores (110µm) showed a similar increase in blood vessels growing towards the scaffolds however blood vessels within the scaffold were leaky and disorganised compared to the vessels found within medium pore size scaffolds. Small pore size scaffolds (12µm) and PGSU films did not induce an angiogenic response (Fig. 1&2).

DISCUSSION & CONCLUSIONS: In conclusion this study demonstrates the importance of controlling pore size when fabricating implantable materials. This study also demonstrates that PGSU has potential as a material for soft tissue reconstruction as it supports rapid tissue ingrowth and vascularization following implantation.

REFERENCES: [1]M. Frydrych, & B. Chen, Fabrication, structure and properties of three-dimensional biodegradable poly(glycerol sebacate urethane) scaffolds, Polymer, 122 p159-168 (2017)

ACKNOWLEDGEMENTS: Thank you to Naside Mangir for the support with the CAM assay. Thanks to the University of Sheffield for financially supporting this research.

Remote control of cell signalling using tagged magnetic nanoparticles for neuronal cell differentiation- emerging cell therapies for Parkinsons disease

M Rotherham[1], T Nahar[1], T Goodman[1], T Hopkins[2], A Studd[3], ND Telling[1], M Gates[1], AJ El Haj[1]

[1]Institute for Science and Technology in Medicine, Keele University, UK, [2]Robert Jones and Agnes Hunt Orthopaedic and District Hospital NHS Trust, UK, [3]University of Nottingham, UK

INTRODUCTION: Signalling pathways such as Wnt and Trek signalling are important controllers of cell fate and regulators of neuronal development[1]. There is therefore great interest in developing signalling modulators for treating neurodegenerative disease. Cell surface receptors that initiate signalling and neural progenitor differentiation pathways can be targeted using ligand functionalised magnetic nanoparticles (MNP). This allows remote mechano-stimulation of receptors using externally applied magnetic fields for subsequent activation of differentiation pathways[2] or induction of directional neurite outgrowth[3]. The aim of this research was to investigate the effects of remote activation of the Wnt receptor Frizzled and Trek1 K+ channels on the neuronal differentiation of neuroprogenitor cells.

METHODS: Target receptor expression was assessed in SH-SY5Y and neural progenitor cells using rtPCR. 250nm MNP were coated with peptides or antibodies allowing MNP tagging to Frizzled/Trek receptors. Remote MNP-receptor complex stimulation was performed in 1h-3h sessions using alternating magnetic field gradients provided by a magnetic force bioreactor. Downstream signalling activity was assessed by monitoring β-catenin mobilisation and TCF/LEF responsive gene expression using a luciferase reporter. Neuronal differentiation marker expression was also determined in vitro and in an *ex vivo* embryonic rat slice model to assess the effects of remote signalling activation on neuronal differentiation of injected progenitor cells.

RESULTS: Basal expression of Frizzled1, 2 and Trek1 was confirmed in SH-SY5Y cells and fluctuated during RA/BDNF induced neural differentiation. β-catenin mobilisation and TCF/LEF luciferase reporter activity both increased over 24h in response to Frizzled targeted MNP and magnetic field stimulation. Short-term fluctuations in expression of stress-response genes NF-κB and COX2 were also observed in response to MNP induced receptor activation. Expression of dopaminergic markers DAT and TH was augmented by MNP *in vitro* and maintained in *ex vivo* rat brain slices when SH-SY5Y cells were cultured in differentiation media and treated with MNP and magnetic stimulation.

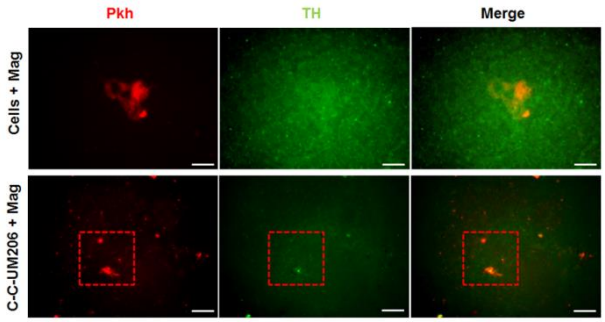

Fig. 1: Dopaminergic marker TH expression (green) in injected and magnetically stimulated SH-SY5Y cells 7 days post-injection. Cells were tagged with Wnt targeted MNP (C-C-UM206) and injected into the striatal-nigral pathway in embryonic rat brain slices cultured ex vivo. Cells are shown by Pkh (red) staining. Scale bar represents 50μm.

DISCUSSION & CONCLUSIONS: Our results demonstrate that remote activation of Wnt signalling pathways can be achieved in neuronal precursor cells using tagged magnetic particles and external magnetic fields. This remote activation approach can then be used to stimulate and augment precursor cell differentiation towards the neuronal lineage. This technique may offer a novel therapeutic strategy for treating neuro-degenerative diseases such as Parkinsons disease.

REFERENCES: [1]M. Joksimovic and R. Awatramani (2014) *J Molecular Cell Biology* **6** (1):27–33. [2]M. Rotherham et al (2018) *Nanomedicine: Nanotechnology, Biology and Medicine* **14** (1):173-184. [3]G.D. Borasio et al (1989) *Neuron* **2** (1):1087-1096.

ACKNOWLEDGEMENTS: We gratefully acknowledge MICA Biosystems who provided the magnetic force bioreactor and the European Union's Horizon 2020 research and innovation programme (grant agreement no. 686841) who funded this research.

RGD-containing fibrillin-1 fragments: an initiator protein for anterior cruciate ligament repair and regeneration?

ZL Smith[1], D Kumar[1], SA Cain[2] Y Ashraf Kharaz[3], E Comerford[3], JE Gough[1]

[1] School of Materials, University of Manchester, U.K. [2] School of Biological Sciences, University of Manchester, U.K. [3] Institute of Ageing and Chronic Disease, University of Liverpool, U.K.

INTRODUCTION: Anterior cruciate ligament (ACL) ruptures/tears are the most common sports injuries, costing Germany ~€133.3 million annually[1]. Gold standard treatments currently include autografting of patellar tendon or hamstring[2]. Loosening of screws at the bone tunnel site and a mismatch in tensile properties at the interface between the autograft and the bone tunnel site have contributed to failure and subsequent re-intervention[3]. Synthetic alternatives have been explored, but limited cellular integration due to lack of biological receptors has often resulted in failure[4]. We propose a novel, poly-e-caprolactone (PCL) construct (mimicking native ACL topography), biofunctionalised with an RGD-containing Fibrillin-1 fragment (termed PF-8) to accelerate and guide matrix deposition with suitable mechanical properties for the repair and regeneration of ACL tissue.

METHODS: PCL (15% w/v) was electrospun onto a rotating collector to acquire aligned fibres (3.42 ± 1.11 µm) and mounted onto glass coverslips (12mm^2). A set of constructs were plasma treated (air, 1 min) only and another sample group were further treated with PF-8 (10 ng on surface at 4 ºC, overnight).

Histidine-tag (using 0.2M Glycine for quenching) staining was performed and blocked using 2% fish skin gelatin (FSG). Constructs were stained with anti-his mouse primary (1:400 in 2% FSG; overnight, 4ºC) and goat anti-mouse 568nm secondary (1:800 in 2% FSG; 2 hrs, RT), before imaging (Nikon Eclipse 50i). PF-8 concentration was lifted to 250ng to enable detection.

Canine Anterior cruciate ligamentocytes (cACLs; passages 2-5) were seeded (60,000 cells/construct) and cultured for between 4 hours and 7 days. Live/Dead was performed using ethidium homodimer/calecin AM and incubated (20 mins, 37ºC) before washing and imaging. Metabolic assay was performed using resazurin salt solution (1:8000 dilution for stock, 1:10 in media) and incubated (2 hrs, 37ºC). Extracellular matrix staining (cell nucleus, Fibronectin, Collagen 1A1 and Fibrillin) was quenched/permeabilised (0.2M glycine/0.5% triton-x-100) and stained using 2% FSG and 1:400 dilutions of all primary and secondary antibodies (as before).

RESULTS: Histidine-tag immunofluorescent staining of protein at 5 µg/ml showed successful adsorption of PF-8 to the construct. Live/Dead images appeared to show that PF-8 exposed cells exhibited elongated, native morphologies with greater cellular dispersion at earlier time points when compared to constructs without protein. Metabolic assays showed that cACLs on plasma treated constructs containing PF-8 had elevated metabolic activity at both 4 hours ($p<0.05$) and 7 days ($p<0.01$) when compared to the negative controls.

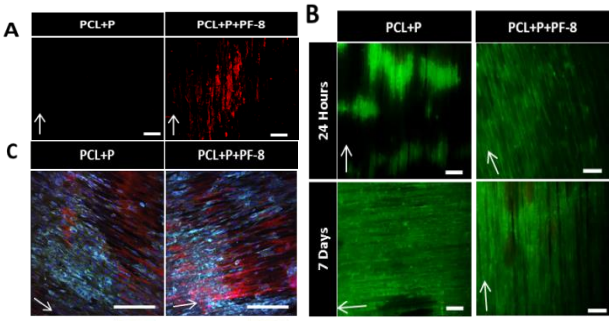

***Fig. 1**: **A** PF-8 protein. **B** cACLs on PF-8 functionalised constructs (A, B scale bar 100 µm). **C** ECM proteins at 28 days on PF-8 coated constructs (scale bar 250 µm).*

DISCUSSION & CONCLUSIONS: Increased cellular viability, uniform alignment and mature ECM production may well indicate that RGD-containing Fibrillin-1 fragment, PF-8, may be the ideal initiator protein to biofunctionalise ACL regenerative constructs. Further experimentation into this area may reveal the ability of PF-8 to initiate Elastin production in cACLs and subsequent deposition, rendering the construct a promising platform for ACL repair and regeneration.

REFERENCES: [1]Bierbaum M *et al.* (2017) *Health Econ Rev* **7**:8. [2] Kraeutler M *et al.* (2013) *Am. J. Sports. Med.* **41**(10):2439-2448. [3] MARS Group *et al.* (2010) *Am. J. Sports. Med.* 38(10):1979-1986. [4] Chen B *et al.* (2016) *Scientific Reports.* **6**:25940.

ACKNOWLEDGEMENTS: Acknowledgement of funding from EPSRC, MRC, UKRMP.

Rho kinase inhibitor supports unlimited, feeder-free, expansion of Sus scrofa domesticus airway stem cells for regenerative medicine research

TP Dale[1], EL Borg D'Anastasi[1], W Al Tameemi[1], NR Forsyth[1]

[1]*Institute for Science and Technology in Medicine, Keele University, Guy Hilton Research Centre, Thornburrow Drive, ST4 7QB, UK.*

INTRODUCTION: Chronic diseases including asthma and COPD are highly prevalent with no curative treatments, thus respiratory disorders such as these represent a significant target for regenerative medicine therapies. Nevertheless, progress remains slow due to the difficulty in isolating and culturing primary airway cells in sufficient numbers. The reliable isolation and culture of airway cells from an animal source would be a valuable research tool; to date the majority of research performed has been carried out using rodent cells. We describe a system for the isolation and long-term culture of porcine cells isolated from the airways of Sus scrofa domesticus, supported by the addition of the Rho kinase inhibitor (RI) Y-27632. The reliable, long-term culture of porcine airway cells is a valuable step forward, improving greatly the number of cells available and, due to significant differences between rodent and human airways, biological relevance.

METHODS: Porcine lungs were obtained within hours of animal death; airways were dissected from lung parenchymal tissue, washed in antibiotics and antimycotics and digested overnight at 4°C in 1 mg/mL protease XIV, 0.005% trypsin and 10 ng/mL DNAse I in F12:DMEM (1:1). Airway sections were opened along the lumen and cells scraped off with a sterile scalpel and transferred to HBSS before being plated on collagen coated tissue culture plastic in 4 different media formulations (A: 4% FBS epithelial, B: commercial serum free 1, C: 10% FBS epithelial and D: commercial serum free 2) in the presence or absence of RI Y-27632 (10 µg/mL). Cell recovery was compared by colony and cell counts; cell phenotype was determined by immunofluorescence to vimentin (fibroblast), pan-cytokeratin, E-cadherin, p63, β tubulin and mucin 5AC (epithelial); functionality of expanded cells was established using air-liquid interface and organoid models and interleukin-8 (IL-8) production in the presence of lipopolysaccharide (LPS).

RESULTS: Cells with an epithelial morphology were recovered in all media, with greater numbers in medium A and C compared to commercial media B and D. In all cases recovered cell numbers were increased by supplementation with Y-27632, significantly so in A (2.6-fold increase, $p \leq 0.0001$) and C (12-fold increase, $p \leq 0.0001$). Long term expansion of cells was only possible in medium C supplemented with Y-27632 where at the time of writing cells had undergone more than 30 passages (120 population doublings). In the absence of Y-27632 epithelial cells ceased proliferating and adopted a senescent morphology after fewer than 10 passages (Figure 1).

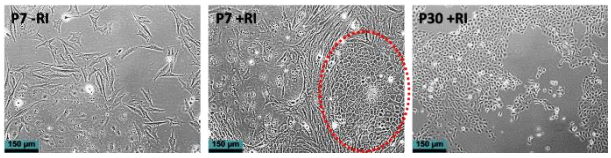

Fig. 1: Porcine airway cells. Left: Passage 7 cells undergoing senescence. Centre: Passage 7 cells with RI supplementation containing proliferative epithelial colonies. Right: Passage 30 cells with RI supplementation, a uniform proliferative, epithelial population.

Immunophenotyping of primary cultures indicated homogeneous pan-cytokeratin and a robust population of airway epithelial cells in all conditions; this was maintained in expanded cells and accompanied by expression of E-cadherin and p63, the airway basal cell marker. LPS exposure induced significant secretion of IL-8 at all concentrations. Differentiation models have demonstrated the presence of both ciliated and mucous producing cells confirming the potency for mucociliary differentiation.

DISCUSSION & CONCLUSIONS: Through the optimisation of culture medium formulation and the use of RI we have developed a strategy for the successful isolation and unlimited expansion of airway cells from a readily available animal source with greater availability and biological relevance than current heavily relied-on rodent tissue sources. We are currently translating this strategy to the culture of human cells to enable the study of cell function in both asthma and COPD models.

ACKNOWLEDGEMENTS: We would like to acknowledge the Royal Society, North Staffordshire Medical Institute, UHNM Charity, and EPSRC CDT Regenerative Medicine for providing funding for this study.

Ru (II) complexes and two-photon photodynamic therapy for treatment of human melanoma

Ahtasham Raza[1], Stuart Archer[2], Julia A. Weinstein[2], Sheila MacNeil[1], James A. Thomas[2] and John W. Haycock[1]

[1] *Department of Materials Science & Engineering*, [2]*Department of Chemistry*, *The University of Sheffield, Sheffield, S3 7HQ, U.K.*

INTRODUCTION: Photodynamic therapy (PDT) requires the use of light to activate a photosensitizer (PS) that generates reactive oxygen species (ROS) to treat cancers[1-3]. Whilst a number of PDT drugs have reached clinical trial, there are only a few successful commercial examples[4]. A major limitation of this particular therapy is (1) non-specific binding of the drugs to non-cancer cells and (2) the relatively poor limit of penetration of visible light into the target tissue.

Aim: Our aim was to tackle both problems by using Ru(II) complexes that bind to specific sequences and structures of DNA (in the quadruplex form) within cancer cells[5] and to use two-photon excitation of these PS modalities with a highly selective targeted laser focus to improve irradiance penetration within deeper tissues.

METHODS: A di-nuclear Ru-Ru TAP was synthesised where the two cores of $Ru(TAP)_2$ were coupled via the tpphz bridge. The compound cellular localization, cytotoxicity and photo-toxicity was investigated in melanoma C8161 cell line using a 405±20nm LED light (Thor Lamp™). The 2-photon photo-toxicity of the complex was then studied in human melanoma spheroid models using Ti-sapphire laser equipped with Zeiss confocal microscopy.

RESULTS: Ru-Ru TAP compound is water-soluble, and accumulates within the nucleus and mitochondria of cells. We report on efficient photo-toxicity properties (LD 50 values = 49.2, 33.9 and 31.6 µM for 6, 12 and 18 J/cm^2 at 405 ± 20 nm, respectively) with no cytotoxicity in human melanoma cells in absence of light. The complex was also studied using two-photon activation in human melanoma cells in 2D culture and in a human melanoma 3D spheroid. Ru-Ru TAP dosage and a two-photon activation profile were established (wavelength and power) by assessing the phototoxic effect using time-sequenced fluorescence imaging. The results showed a large two-photon cross-section of Ru-Ru TAP compound that absorbed maximally at 900nm with a highly efficient phototoxic PS activity. This was observed even under conditions of very low two-photon activation power (20mW) and exposure time of 10min for cultured melanoma cells. In 3D spheroids dosed with Ru-Ru TAP and exposed to two-photon excitation (900nm at 60mW power and continuous laser exposure at every 10 µm optical slices for 30min) there was obliteration of the tumour masss.

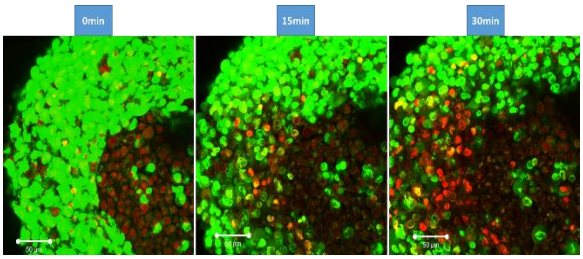

Fig. 1: Two-photon photo-toxicity of Ru-Ru TAP on spheroid. Human melanoma spheroids cultured for 10 days. The spheroids were then allowed to settle on a 35mm plate overnight and incubated with Ru-Ru TAP (100uM), propidium iodide (500nM) and Syto-9 (2µM) in SFM for 24 hours. Spheroids were irradiated with a 900nm laser (60mW) using a continuous z-stack scan (10µM apart) for 30 min. Followed by live and dead cell scan through the whole spheroid (before and after every 15 min irradiance). The z-stack data were then compressed in single projection using Zeiss LSM Image browser. Observe the obliteration of spheroid with increasing 2-photon irradiance time (Scale bar = 50 µm).

CONCLUSIONS: In conclusion, this data supports the potential of Ru-Ru TAP compounds in combination with two-photon photodynamic therapy to be a powerful approach for tagetted and effective therapeutic treatment of cutaneous melanoma.

REFERENCES: [1]Celli, J. P. *et al. Chem Rev.* 110, 2795-2838, (2010). [2]Abrahamse, H.*et al.* Biochem. J. 473 (2016). [3]Dolmans, D. *et al*. Nature Reviews Cancer. 3(5), pp.380-387, (2003). [4]Van Straten, D. et al. Cancers. 9(2) (2017). [5]Martin R. G. et al. Nature Chem. 1(8), pp 662-627, (2009).

ACKNOWLEDGEMENTS: We thank the EPSRC (UK) for funding AR and SA.

SIRT1 activation in ESC derived prechondrocytes promotes cartilage ECM expression

CA Smith[1], M Dvir-Ginzberg[2], SJ Kimber[1]

[1] University of Manchester, UK. [2] HUJI, Israel.

INTRODUCTION: Regulation of genes and transcription factors by epigenetic factors is essential for successful differentiation. SIRT1, is a histone deacytalase enzyme, able to bind and deacetylate the main chondrogenic factor SOX9 (Bhurmann *et al*, 2014). Indeed, osteoarthritic and dedifferentiating primary chondrocytes display decreased SIRT1 protein expression. The aim of this study is to identify the role and activity of SIRT1 during the differentiation of human pluripotent stem cells hPSCs to chondrocytes and its impact of extracellular matrix expression.

METHODS: hPSCs were differentiated to prechondrogenic cells using a 2D 14-day defined differentiation protocol (Oldershaw *et al*, 2010). At 14-days, cells were pelleted and cultured for an additional 14-day period in 3D pellet culture, with SIRT1 activator or inhibitors. Additionally, TC28a2 immortalized juvenile chondrocytes were cultured in pellet culture, with SIRT1 activator SRT1720 or inhibitor EX527. QRT-PCR and Protein expression was used to assess chondrogenic output. ChIP-PCR was used to determine chromatin binding of SIRT1 under different conditions. Histological assessment was run to determine the structure of the pellets.

RESULTS: Result show no beneficial effect of activation or inhibition of SIRT1 during the 2D chondrogenesis stage with no change to COL2A1 or ACAN gene expression. During 3D culture inhibition of SIRT1 caused no significant change in gene expression compared to control. Activation of SIRT1 led to significant increases in SOX5, ARID5B and ACAN, with significant decreases in COL1A1 and RUNX2 gene expression (Fig 1). Activation of TC28a2 cells with SIRT1 activator only led to an increase in ECM gene expression in 3D not 2D, in particular SOX5 and ACAN. This was supported by western blot analysis of ACAN which showed a 3.5-fold increase in activated cells. Overexpression of SIRT1 in TC28a2 cells did not result in an increase of ECM gene expression

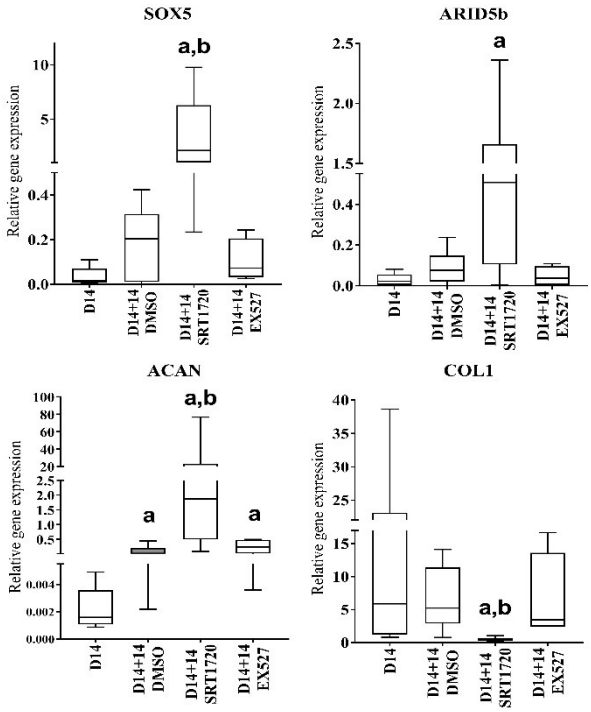

Fig. 1: Gene expression analysis of hPSC derived chondrocytes treated with SIRT1 activator SRT1720 or inhibitor EX527. Data displayed as 2^dCT with standard error. a, statistical significance (p≤0.05) in comparison to day 14 cells. b, statistical significance (p≤0.05) in comparison to DMSO vehicle control.

DISCUSSION & CONCLUSIONS: The results of this study indicate that SIRT1 expression and activity are important to PSC derived chondrocyte development, by being involved with a protein complex required for the transcription of chondrogenic genes.

REFERENCES: [1] Bhurmann et al (1991) *JBC* 289.32: 22048-22062. [2] Oldershaw et al (2010) *Nat Biotechnol* 28.11:1187.

ACKNOWLEDGEMENTS: The authors wish to thank Dr Louise Reynard and her lab for access to TC28a2 cell line.

Supercritical carbon dioxide decellularization optimization

R Loczenski[1], C Alexander[1], SM Howdle[2], LJ White[1]

[1] School of Pharmacy, [2] School of Chemistry; University of Nottingham, UK

INTRODUCTION: Organ transplantation comes with many risks, such as organ rejection, lifelong immune suppression, and drastically reduced life expectancy. Using an extracellular matrix (ECM) derived scaffold to engineer a new personalised organ is a promising alternative that can minimize these risks due to the biochemical and biophysical properties of the ECM [1]. Current decellularization methods used to generate ECM scaffolds utilize a combination of chemical and biological agents that disrupt the ECM architecture and surface structure and may leave residual detergents and toxicity behind [2]. Herein, supercritical carbon dioxide was investigated for its decellularization efficacy as a non-toxic and safe alternative.

METHODS: Pig liver (1g), stored at -20°C before use, was exposed to supercritical carbon dioxide ($scCO_2$) in a 20 ml autoclave at ~2900 psi and 37°C for varying durations within a batch system. Residual DNA content was used as a metric of decellularization. DNA concentration (ng/ml) was determined using the Quant-iT Pico Green (Invitrogen) assay kit and normalized to dry tissue weight. A 1.5% (w/v) agarose gel, stained with ethidium bromide, was used to assess DNA size. Histology was performed to evaluate morphological changes. Statistical analysis was done via PRISM (GraphPad). Results deemed significant if $p<0.05$.

RESULTS: $scCO_2$ exposure influenced DNA removal in a time dependent manner. Five hours (300 minutes) was the minimum time required to facilitate significant DNA removal from the tissue ($p < 0.01$). DNA content was further reduced following exposure to $scCO_2$ for 3 days (4320 minutes; $p < 0.0001$; *Figure 1A*). After 3 days exposure to $scCO_2$, the tissue was pale and discoloured compared to the colour prior to $scCO_2$ treatment (*Figure 1B*). Compared to the control, both $scCO_2$ and detergent-based decellularization method successfully reduced DNA content ($p < 0.0005$, $p < 0.0001$; respectively; *Figure 1C*). Residual DNA content after 3 days in $scCO_2$ was similar to the residual DNA content of the detergent-based decellularization method ($p > 0.05$; *Figure 1C*). However, macroscopic differences were evident between tissue decellularization using the two methods.

The detergent- based method resulted in a white and clear extracellular matrix scaffold (*Figure 1D*), whereas tissue from the $scCO_2$ method remained opaque (*Figure 1B*).

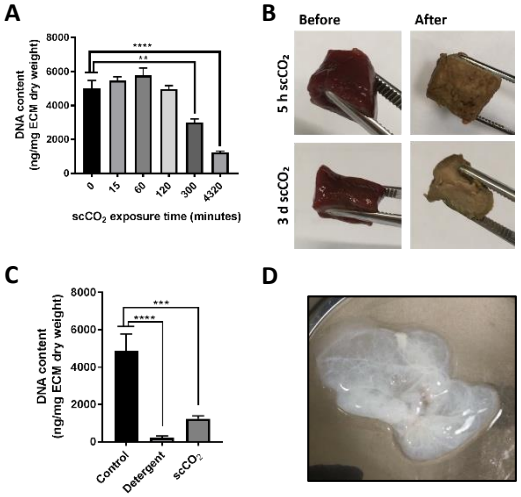

Figure 1. *Effect of $scCO_2$ exposure time on DNA removal of pig liver* ***(A)*** *DNA content (up to 3 days)* **(B)** *Respective image before and after $scCO_2$ exposure.* ***(C)*** *Comparison of $scCO_2$ decellularization to standard detergent treatment.* ***(D)*** *Respective image of porcine liver after detergent decellularization. All data are mean +/- SD (n = 3). Significance is indicated by ** p < 0.01,*** p < 0.0005, **** p < 0.0001.*

DISCUSSION & CONCLUSIONS: The preliminary results herein demonstrate that $scCO_2$ has decellularization capabilities, as determined by the extent of DNA removal. Future studies will investigate the full potential of $scCO_2$ in combination with low concentrations of $scCO_2$ soluble additives to further improve the level of DNA removal. The use of $scCO_2$ presents a novel approach to decellularize with reduced toxicity.

REFERENCES: [1] Badylak, S. F., & Gilbert, T. W. (2008). Immune Response to Biologic Scaffold Materials. Seminars in Immunology, 20(2), 109–116. [2] White, L. J., et al. (2017). The impact of detergents on the tissue decellularization process: a ToF-SIMS study. Acta Biomaterialia, 50, 207–219.

ACKNOWLEDGEMENTS: This work was supported by the University of Nottingham and the EPSRC Centre for Innovative Manufacturing and Regenerative Medicine.

TURBOTALK + POSTER

Bioengineering the structure of the human intestine mucosa

NJ Darling[1], SA Przyborski[1,2]

[1] *Department of Biosciences, Durham University, Durham, UK* [2] *Reprocell Europe, Sedgefield, UK*

INTRODUCTION: Investigations into intestinal epithelial function require the use of *in vivo* animal models or *ex vivo* human tissue samples. To reduce animal usage, several cell culture-based transport models have been developed, the gold standard of which is the Caco-2 monolayer, a simple monolayer of enterocyte cells[1,2]. However, such *in vitro* models have many limitations including the absence of extracellular matrix, the lack of communication between different cell types and differences in protein expression and activity to the *in vivo* intestine resulting in difficulties in extrapolating data from transport studies to the human situation.

We have developed an *in vitro* model that incorporates multiple cell types in a 3D microenvironment to recapitulate native intestine architecture. We hypothesise that this improved structure will lead to an enhanced function of the epithelial cells. This will improve the predictive accuracy of *in vitro* assays by recapitulating the behaviour of the native tissue.

METHODS: Human dermal fibroblasts (HDFn) were seeded into Alvetex® Scaffold inserts and cultured for 14 days to allow for extracellular matrix proteins to be deposited into the scaffold, creating a foundation to support the culture of the epithelial cells. Caco-2 intestinal epithelial cells were then seeded on top of the fibroblast construct and were cultured for a further 21 days allowing epithelial differentiation to occur.

Tissue construct morphology was analysed using histology (H&E staining), transmission electron microscopy and immunofluorescence.

RESULTS: Co-culture of fibroblasts and Caco-2 cells results in the formation of a highly polarised monolayer of differentiated enterocytes, evidenced by a transition in cell shape to columnar epithelium, in conjunction with the formation of a microvilli brush border and junctional proteins between cells.

The presence of a basement membrane is observed at the interface between the epithelial cells and supporting stromal fibroblasts. A rich extracellular matrix is formed in the stromal compartment, with significant evidence of collagen deposition.

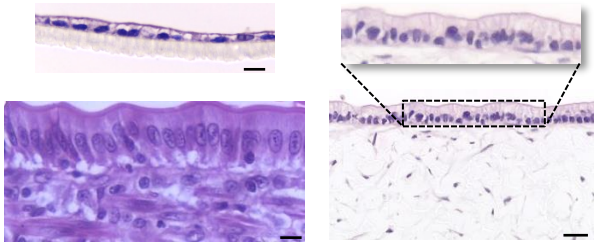

Fig. 1: H&E staining of Caco-2 cells cultured for 21 days on Transwell® inserts (left, top) and on top of fibroblasts cultured for 14 days prior to Caco-2 cell seeding (right). H&E staining of human small intestinal tissue (left, bottom). Scale bar: 50 µm.

DISCUSSION & CONCLUSIONS: The 3D intestinal mucosa construct more accurately resembles the architecture of the inner layer of the intestine than previous *in vitro* models.

Further characterisation of the model will examine the functional properties. This will be done by analysing junctional proteins and measuring the transepithelial electrical resistance (TEER) of the epithelium which in the Caco-2 monolayer, is much greater than that of the *in vivo* intestinal epithelium. TEER in combination with lucifer yellow transport assays will provide information on the barrier formation and strength of the model and drug absorption studies will also be carried out to determine how similar epithelial transport is to the Caco-2 monolayer and the human intestine. Preliminary data indicates that TEER values of the mucosal model are decreased to values closer to *in vivo* conditions.

The model is also being further developed to incorporate goblet-like cells and immune cells and will be adapted to simulate inflammatory pathologies of the intestinal mucosa.

REFERENCES: [1] I.J. Hidalgo, T.J. Raub and R.T. Borchardt (1989) *Gastroenterology* **96:**736-49. [2] A.R. Hilgers, R.A. Conradi and P.S. Burton (1989) *Pharm. Res.* **7(9):**902-10.

ACKNOWLEDGEMENTS: The authors would like to thank the NC3Rs for funding this project and Reprocell Europe for providing human tissue samples.

Characterisation and *in vivo* assessment of physical guidance cues in nerve guidance conduits

J Field[1], A Harding[1], JW Haycock[2], F Claeyssens[2], F Boissonade[1]

[1] *School of Clinical Dentistry, University of Sheffield, United Kingdom*
[2] *Department of Materials Science and Engineering, University of Sheffield, United Kingdom*

INTRODUCTION: There is a clinical need for improved treatments for peripheral nerve injury to overcome the disadvantages associated with autograft repairs. Nerve guidance conduits (NGCs) can be used as an alternative treatment, however current commercial NGCs have simple designs and are only successful in short distance nerve gaps, up to around 20 mm [1]. It has been shown that aligned structures such as grooves and fibres can have a beneficial effect on the growth of nerve cells *in vitro*. Here, conduits were fabricated containing intraluminal guidance cues in the form of either internal microgrooves or aligned microfibres. Both were investigated *in vivo* to assess the influence of each type of guidance structure on peripheral nerve regeneration.

METHODS: Polycaprolactone (PCL) was functionalised with methacrylate groups to produce photocurable polycaprolactone-methacrylate (PCL-MA). This was used to fabricate NGCs via microstereolithography with a 405 nm laser and a digital micromirror device; plain tubes and tubes containing internal microgrooves were both produced (Fig. 1A,B). Aligned PCL microfibers were electrospun (Fig. 1C) and inserted into the plain tubes to act as intraluminal guidance structures (Fig. 1D). The individual components and combined constructs were analysed via scanning electron microscopy, helium pycnometry and micro-computed tomography.

Conduit performance was assessed in an *in vivo* nerve injury model in thy-1-YFP mice with inherently fluorescent axons. The NGCs were used to repair a 3 mm injury of the common fibular nerve and regeneration was assessed via confocal imaging to determine the effectiveness of each conduit type in promoting nerve regeneration over a 3 week recovery period.

RESULTS: PCL fibres with diameters ranging from 2–16 µm were electrospun to a high degree of alignment and inserted into the plain PCL-MA tubes. Fibre packing density was quantified to give a percentage fill of the conduit lumen and conduits were created with packing densities ranging from 10 to 50%. PCL-MA conduits were also produced with aligned microgrooves along the internal wall, with no material occluding the luminal area.

In vivo regeneration through the microgrooved and fibre-filled NGCs was quantitively assessed via the counting and tracing of fluorescent axons across the injury site and results were compared to empty conduit controls and graft repairs. Axons were seen to traverse the 3 mm nerve gap in each conduit type.

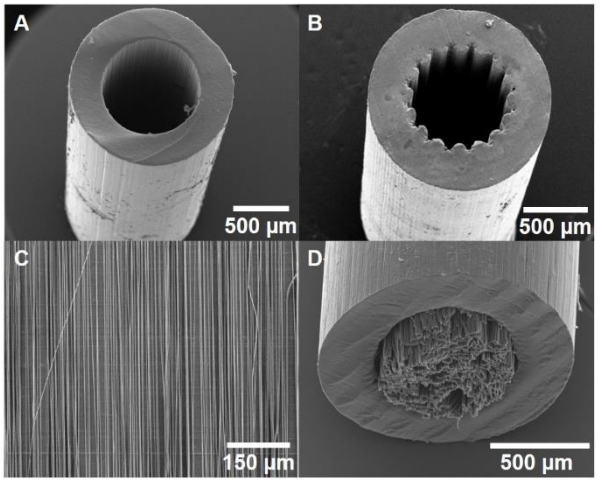

Figure 1: SEM images: plain conduit (A), grooved conduit (B), electrospun fibres (C) and fibre-filled conduit (D).

DISCUSSION & CONCLUSIONS: Advanced NGCs containing intraluminal guidance structures have shown potential for promoting nerve regeneration *in vivo*. The thy-1-YFP mouse model allows us to compare the effect of different guidance structures within NGCs by visualising whole nerve explants and imaging fluorescent axons without the need for destructive processing and analysis techniques.

REFERENCES: [1] J.H. Bell & J.W. Haycock (2012) *Tissue Eng Part B Rev* **18,** 116–128.

ACKNOWLEDGEMENTS: The authors would like to thank the EPSRC and the University of Sheffield, Faculty of Medicine, Dentistry and Health for funding this research.

Chondrogenic differentiation of human embryonic stem cells can be enhanced with the application of a Wnt platform

NC Foster[1], SJ Kimber[2], AE El Haj[1]

[1] *Institute of Science and Technology in Medicine, Faculty of Health, Keele University, Staffordshire.* [2] *Faculty of Biology, Medicine and Health, University of Manchester, Manchester.*

INTRODUCTION: Over time, cartilage damage and degradation can lead to the onset of osteoarthritis (OA), which poses a great financial burden to healthcare providers and seriously compromises patients' quality of life. Current gold standard treatments rarely give long-term relief; thus there is a need for tissue-engineered alternatives. Immobilised Wnt3a can induce asymmetrical cell division in pluripotent stem cells [1,2]. Human embryonic stem cells (hESC) can yield large numbers of chondroprogenitors [3]. However, the risk of residual pluripotent cells with the potential to form teratomas, presents a barrier to their clinical application. Use of a Wnt platform [2] as a substrate for differentiation, with the addition of an acellular hydrogel, may result in a cartilaginous construct with a more homogenous population of chondroprogenitors.

METHODS: A 14-day directed differentiation protocol (DDP) [3] was initiated on hESC. On d4, cells were split and transferred to Wnt-modified [4] polycaprolactone (PCL) discs. On d6, acellular fibrin gels were placed on top of cells and the DDP was completed. Gene expression analysis, DNA assay, sulphated GAG (sGAG) assay and immunocytochemistry (ICC) were carried out on d9 and d12 samples. Alamar Blue assay was carried out throughout the incubation period in order to estimate levels of proliferation. For control samples, bound Wnt ligands were inactivated with dithiothreitol (DTT) before cells were seeded onto polymers.

RESULTS: Cells remaining on Wnt-modified polymer discs at d15 retained pluripotency (fig. 1) while those on inactive controls did not. Proliferation was significantly higher in all d12 cells compared to d8 and cells on Wnt-modified polymers had significantly higher levels of proliferation on d6 compared to inactive controls (fig. 2). DNA content (fig. 3B) was significantly higher in the Wnt-modified group by d12, indicating higher levels of cell migration. No significant difference in levels of sGAG was observed (fig. 3A). Wnt-modified groups had significantly higher levels of collagen type II and significantly lower levels of collagen type X (fig. 4), indicating that they were more chondrogenic and less hypertrophic. There was no significant difference in levels of ACAN, COL1, OCT4 and SOX9 (data not shown).

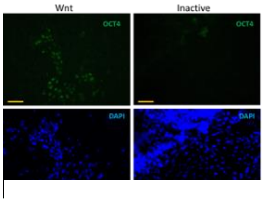

Fig. 1: Cells remaining on Wnt-modified polymer at d15 retained greater pluripotency

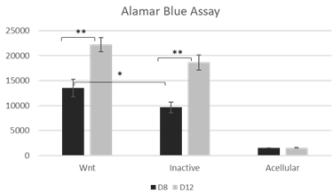

Fig. 2: Wnt-modified groups showed significantly higher rates of proliferation on d8. Proliferation significantly higher in both groups on d12 compared to d8

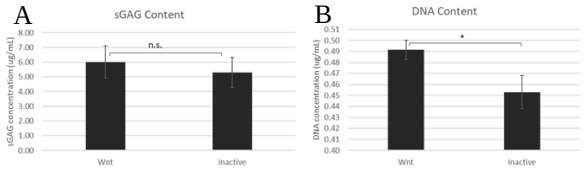

Fig.3: DMMB and PicoGreen assay of d12 constructs A) sGAG not significantly different B) DNA content significantly higher in constructs cultured on Wnt-modified polymer

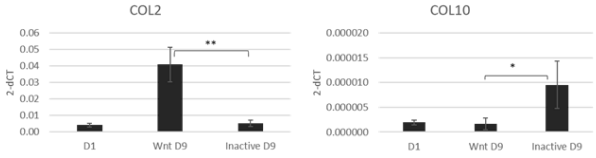

Figure 4: Gene expression analysis of d9 constructs. COL2 significantly higher (A) and COL10 significantly lower (B) in constructs cultured on Wnt-modified polymer. Expression relative to GAPDH

DISCUSSION & CONCLUSIONS: Use of the Wnt platform, in combination with the DDP, yielded hydrogels with enhanced chondrogenic potential. Further refinement of the protocol will hopefully produce more mature tissue-engineered cartilaginous constructs.

REFERENCES: [1] S.J. Habib, et al (2013) *Science* **339**: 1445–1448 [2] M. Lowndes, et al (2016) *Stem Cell Reports* **7**: 126-137 [3] R. Oldershaw, et al (2010) *Nat Biotechnol* **28**: 1187-1196

ACKNOWLEDGEMENTS: The authors would like to thank the UKRMP Hub for funding.

Fusidic-acid loaded polycaprolactone/chitosan electrospun scaffolds for wound healing applications

K Thakur[1, 2], B Singh[1], OP Katare[1], FRAJ Rose[2]

[1]*University Institute of Pharmaceutical Sciences, Panjab University, Chandigarh, India*
[2]*Division of Regenerative Medicine and Cellular Therapies, School of Pharmacy, Centre for Biomolecular Sciences, University of Nottingham, Nottingham, UK*

INTRODUCTION: Nanofibrous scaffolds produced by electrospinning are reported here as potential candidates for wound healing applications. This is attributed to their structure that mimics the extracellular matrix. Additionally, antibiotics can be loaded into the scaffolds to prevent infection and therefore promote tissue regeneration *via* drug delivery.

METHODS: In the current study, polycaprolcatone (PCL) and chitosan (CS) were blended and processed employing electrospinning to obtain nanofibrous scaffolds with desired physicochemical properties for wound healing. PCL is one of the most used polymers to engineer tissue scaffolds because of its biocompatibility, biodegradability and mechanical properties. CS is a natural cationic polymer that promotes cell adhesion, proliferation and differentiation. Fusidic acid (FA) was incorporated into the nanofibrous scaffolds as an antibiotic used to treat topical infections and the resulting scaffolds were characterized for their physicochemical properties such as morphology, fibre diameter and mechanical strength. The biological properties of the scaffolds were evaluated by seeding with fibroblasts cells. The morphology and viability of the cells on scaffolds were examined employing Scanning electron microscopy (SEM) and the Presto Blue assay, respectively.

RESULTS: PCL/CS electrospun nanofibrous scaffolds were successfully developed *via* electrospinning for controlled release of fusidic acid. PCL (12-20%)/Chitosan (5%) solution with 3:1 composition was selected and electrospun to form a nanofibrous scaffold. The structural and physico-chemical characterization of the scaffolds confirmed incorporation of the drug molecule. The SEM images showed that the fiber diameters were in the range of 240-1190 nm with a smooth morphology. The drug release study indicated a burst release of FA from the scaffolds in the initial phase followed by a prolonged release. The Presto Blue assay showed that the developed drug-loaded nanofibrous scaffolds have good cytocompatibility, indicating that these scaffolds may be suitable for use as an antibacterial dressing for wound healing.

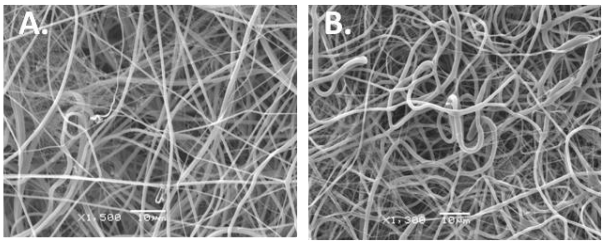

Fig. 1: SEM images of PCL/CS electrospun scaffolds (A) Blank scaffolds (without drug) (B) FA-loaded scaffolds

Table 1: The mean fibre diameter with and without FA (µm ± SD)

PCL (w/w, %)	Blank Scaffolds	FA-loaded scaffolds
12	0.24 ± 0.10	0.42 ± 0.12
15	0.55 ± 0.19	0.99 ± 0.30
20	0.99 ± 0.30	1.19 ± 0.29

DISCUSSION & CONCLUSIONS: In the current study, antibiotic-loaded electrospun PCL/CS scaffolds were prepared. The nanofibrous scaffold possessed fibres with a smooth morphology which were biodegradable and biocompatible. The fibres also demonstrated a sustained delivery of FA to control the infection at the wound site. The study showed the possibility of incorporating a natural polymer into a hydrophobic synthetic polymer matrix in addition to anitibiotic loading by a single step electrospinning process to produce a promising wound dressing material.

REFERENCES: [1]X. Liu, L.H. Neilsen, S.N. Klodzinska, et al (2018) *Eur J Pharm Biopharm* **123**:42-49. [2]K.T. Shalumon, K.H. Anulekha, K.P. Chennazhi, et al (2011) *Int J Biol Macromol* **48(4)**: 571-576. [3]A. Mickova, M. Buzgo, O. Benada et al (2012) *Biomacromolecules* **13**: 952-962.

ACKNOWLEDGEMENTS: The authors acknowledge the financial support by Commonwealth Scholarship Commission, UK (awarded to K Thakur) and University of Nottingham.

Mechanical loading of murine bioengineered skeletal muscle mimics the transcriptional & epigenetic response of human skeletal muscle after exercise

DC Turner[1], RA Seaborne[1,2], CE Stewart[2], MF Murphy[2], JC Jarvis[2], NRW Martin[3], AP Sharples[1]

[1] *Inst. for Science & Technology in Medicine, Keele University, Staffordshire, UK.*

[2] *Research Inst. for Sport & Exercise Sciences, Liverpool John Moores University, Liverpool, UK.*

[3] *School of Sport Exercise & Health Sciences, Loughborough University, Loughborough, UK.*

INTRODUCTION: Recent investigations from our lab have characterised the genome-wide epigenetic (DNA methylation) and gene expression changes in skeletal muscle (SkM) following anabolic (resistance) exercise (RE) in humans [1]. We aimed to create 3D bioengineered SkM that mimicked the *in-vivo* response to anabolic exercise using bioreactor systems *in-vitro*. The ultimate aim, to provide a suitable replacement for *in-vivo* human exercise interventions that would enable deeper investigation into the molecular mechanisms of adaptation to exercise and importantly, the impaired anabolic responses we observe after physical activity in ageing (termed anabolic resistance). A phenomenon that is strongly associated with the progression of sarcopenia.

METHODS: Our previous data has identified the most significantly and/or frequently altered genes at the transcript and epigenetic level in human SkM after both acute (5 quadriceps exercises × 4 sets × 10 reps) and chronic RE (5 quadriceps exercises × 4 sets × 10 reps/3 days per wk for 7 wks, evoking an average 6.5% increase in lower limb lean mass [1]). In the present study, gene expression (qRT-PCR) and DNA methylation (Methyl II PCR Assay) analysis of the same genes was assessed in 3D bioengineered SkM following mechanical loading in bioreactors (Fig. 1) in attempt to identify any similar changes to those already identified in human muscle tissue following RE. 3D SkM bioengineered from a mouse cell line (Fig. 1a, b) was loaded for 5 intervals × 4 sets × 10 reps (at 0.4 mm/s with 90 s rest between sets) at 10% stretch (1.2 mm) at 37°C/5% CO_2 (Fig. 1c). RNA was isolated after 30 minutes of loading. Finally, 4 weeks of chronic electrical stimulation in rats (5 sets × 10 reps, frequency of 100 Hz, once a day for 4 weeks) *in-vivo* using implanted electrical stimulators was undertaken, evoking an average 15% increase in muscle weight. This also allowed the same genes analysed in loaded 3D murine bioengineered muscle to be compared across species in various models of anabolic exercise.

RESULTS: UBR5 and ODF2 significantly ($P \leq 0.05$) increased in loaded 3D SkM (Fig. 2). Importantly, no significant differences within any gene were observed between loaded 3D SkM & after RE exercise in human/rat tissue *in-vivo* ($P > 0.05$). Preliminary DNA methylation analyses on the most elevated transcript across all sample sets, UBR5, demonstrated hypomethylation in 3D muscle loading, similar to that previously identified after acute and chronic RE in human tissue [1].

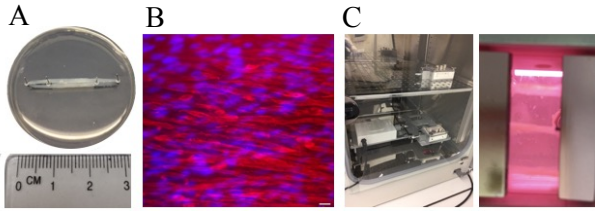

*Fig. 1: **(A)** Image of C2C12 3D muscle **(B)** Stained 3D myotubes (red = Desmin, blue = Nuclei, scale = 20 µm) **(C)** Bioreactor for loading in incubator.*

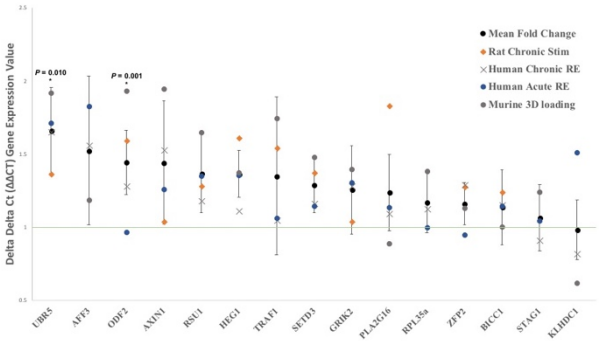

Fig. 2: Comparative gene expression in 3D loading, acute & chronic resistance exercise (RE) in human tissue & electrical stimulation (stim) in rat tissue.

DISCUSSION & CONCLUSIONS: Loaded 3D muscle displayed similar changes to human and rat tissue in response to acute and chronic exercise. DNA methylation of all genes will be completed for the current data set to further confirm that epigenetic responses to exercise in bioengineered muscle are similar to human muscle tissue. Longer term, we will develop the first aged human bioengineered SkM and use this system to investigate mechanisms of 'anabolic resistance' to loading in sarcopenia.

REFERENCES: [1] R.A Seaborne, A.P Sharples, et al (2018) *Scientific Reports (Nature)* **8**:1898.

This template was modified with kind permission from eCM Journal.

Nervous tissue restoration following traumatic brain injury by coral skeleton-based implants

Orly Eva Weiss[1], Roni Mina Hendler[1], Eyal Aviv Canji[1], Tzachy Morad[1], Danny Baranes[1]

[1] *Department of Molecular Biology, Ariel University, Israel*

INTRODUCTION: Traumatic brain injury (TBI) is a major cause of mortality and disability in the world and has no cure. The capacity of the brain to be self-restored is limited, thus identifying tissue engineering-based means that could enhance the regeneration of the brain tissue in the wound and recover functionality is a major challenge[1]. One promising strategy is grafting scaffolds that can enhance cell invasion into the wound. The aragonite skeleton of corals is a useful scaffold for testing this strategy, being supportive for neural cells in culture[2].

METHODS: A quantitative penetrating TBI model developed in our lab was used to perform injuries in 2 months-old mice. A precise volume of cortical tissue ($2mm^3$, in this case) at specific coordinates was removed by a microdrill attached to a stereotactic system. Coral skeleton grains (<40µm) were mixed with collagen and polymerized to get coralline and collagen-based hydrogels, which were implanted into the site of injury. Implanted mice's cognitive functionality and anxiety levels were evaluated two weeks and one-month post-implantation by Morris Water Maze and Open Field tests, respectively. A month post-implantation, mice were sacrificed and thick sections containing the whole wound area were stained immunofluorescently to specific neural markers. Confocal microscope was used to take tissue micrographs, which were then analysed by ImageJ software.

RESULTS: We found that implantation of scaffolds made of aragonite crystalline skeleton of corals into cortical TBI wounds in mice, caused histological and functional recoveries. Two weeks to one month following implantation, wounds were filled with cells in their open void volume, as well as around and within the implants. Implanted wounds, by contrast to non-implanted, contained astrocytes (expressing glial fibrillary acidic protein), neuronal processes (mainly neurofilament M expressing axons), neural precursors (nestin positive) and synaptic connections (expressing SV2 and GluR1) (Fig.1). Open Field tests showed that implanted TBI mice performed more than two-folds better than non-implanted TBI mice, in terms of walking velocity and time in center of the field. These results suggest that the implant caused a reduction in TBI-generated anxiety. Morris Water Maze test showed an improvement in memory skills among implanted mice, in comparison to injured but non-implanted ones.

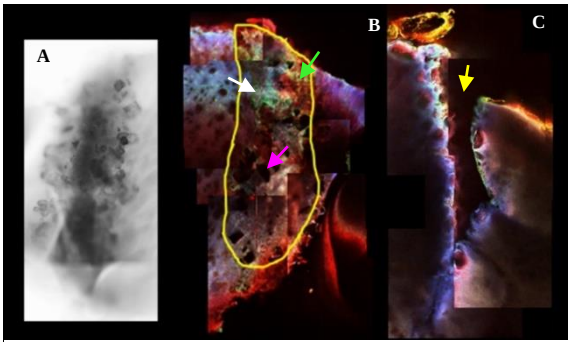

Picture 1: Coralline and collagen-based implant induces formation of pre-synaptic and postsynaptic sites in TBI wound. **(A)** Site of an implanted TBI, Bright Field. **(B)** The site of injury shown in panel A, the yellow line shows the areas of contact of the tissue with the implant. White arrow – SV2 positive staining on the implant's surface, green arrow – GluR1 positive staining. **(C)** A site of TBI wound with no scaffold implanted. Scale: 500µm

DISCUSSION & CONCLUSIONS: The results demonstrate that using coralline-based scaffolds to repair TBI injuries in the nervous system is an approach of great therapeutic potential. This scaffold can be applicable to other types of brain damages, such as those caused by neurodegenerative diseases.

REFERENCES:

1. Alvis-Miranda, H., Castellar-Leones, S. M. & Moscote-Salazar, L. R. Decompressive Craniectomy and Traumatic Brain Injury: A Review. *Bull. Emerg. Trauma* **1,** 60–68 (2013).
2. Peretz, H., Talpalar, A. E., Vago, R. & Baranes, D. Superior survival and durability of neurons and astrocytes on 3-dimensional aragonite biomatrices. *Tissue Eng.* **13,** 461–472 (2007).

Optimisation of photoresponsive hydrogels to enable in situ analysis of cellular responses to reversible stiffness modulation

D Richards[1], LS Wong[2], J Swift[3], SM Richardson[1]

[1] *Division of Cell Matrix Biology and Regenerative Medicine*, [2] *Manchester Institute of Biotechnology*, [3] *Wellcome Trust Centre for Cell-Matrix Research*, *University of Manchester, UK.*

INTRODUCTION: Matrix stiffness is a potent regulator of cellular properties and behaviors[1]; however, commonly used static stiffness models do not reflect the dynamic nature of cell-matrix interactions caused by continued remodelling during processes such as development, ageing and fibrosis. Mesenchymal stem cells (MSCs) in particular have been shown to maintain a 'mechanical memory' capable of promoting pro-fibrotic phenotypes following exposure to pathologically stiff matrices.[2] Therefore, in order to further understand the mechanisms and physiological relevance of these cellular responses, we have developed a photoresponsive hydrogel for the photoswitchable manipulation of primary human MSCs.[3] To advance the physiological relevance of this system, the current study describes the successful incorporation of acrylic acid N-hydroxysuccinimide ester (NHS) to enable covalent fibronectin (Fn) attachment and cellular adhesion to the hydrogel network, as well as development of a cytocompatible irradiation scheme to stimulate stiffness modulation.

METHODS: Hydrogels were prepared and analysed as previously reported[3], with or without the inclusion of 1µl NHS (1mg/ml in DMSO) prior to polymerisation. Briefly, storage and loss modulus were measured during gelation. UV-vis absorbance spectra and atomic force microscopy measurements of Young's modulus were recorded before and after UV irradiation. MSC viability and morphology response on hydrogels with or without NHS and Fn coating, and following UV irradiation at different intensities, were analysed via LIVE/DEAD and DNA damage assays, and quantitative morphometric image analysis.

RESULTS: NHS inclusion did not detrimentally affect hydrogel gelation, cross-linker isomerisation, or photoswitchable stiffness properties (Fig. 1A). Furthermore, MSC viability and morphology response was maintained following NHS inclusion and covalent Fn attachment (Fig. 1B). UV intensity was optimised to maintain MSC viability during irradiation and did not detrimentally affect photoswitchable stiffness properties or modify MSC morphology response (Fig. 1C&D).

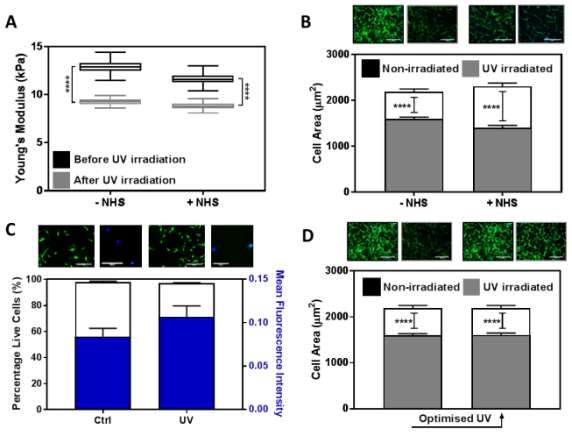

Fig. 1: (A) Young's modulus of hydrogels with or without NHS before and after UV irradiation. (B) MSC cytoplasmic area on non-irradiated or UV irradiated hydrogels with or without NHS. (C) Percentage live MSCs and DNA damage (nuclear foci) intensity before and after optimised UV irradiation. (D) MSC cytoplasmic area on non-irradiated or optimised UV irradiated hydrogels.

DISCUSSION & CONCLUSIONS: Covalent Fn attachment ensured direct cellular connection to the hydrogel network and conserved MSC morphology response, confirming cells are sensing hydrogel stiffness. Maintaining photoswitchable stiffness modulation with cytocompatible UV irradiation enables MSC exposure to reversible in situ stiffness modulation. The optimised photoresponsive hydrogel platform will now be used to study MSC response to stiffness modulation in real time, using time-lapse microscopy on fluorescently-tagged live cells and novel immortal YAP reporter MSC lines[4], in order to improve understanding of cell-matrix interaction during dynamic processes and the mechanotransduction mechanisms involved.

REFERENCES: [1] A. Engler et al (2006) *Cell* **126**:677-689. [2] C. X. Li et al (2017) *Nat. Mater.* **16**:379-389. [3] I. N. Lee et al (2018) *ACS Appl. Mater. Interfaces* **10**:7765-7776. [4] A. Torre et al (2018) *bioRxiv* **269225** [online preprint].

ACKNOWLEDGEMENTS: D Richards is supported by the EPSRC & MRC CDT in Regenerative Medicine (EP/L014904/1).

Prediction of clinical outcome following autologous chondrocyte implantation by magnetic resonance imaging

HS McCarthy[1,2], IW McCall[1], JM Williams[1,2], C Mennan[1,2], MN Dugard[1,2], JB Richardson[1,2], S Roberts[1,2]

RJAH Orthopaedic Hospital[1]; Keele University (ISTM)[2]

INTRODUCTION: The ability to predict long-term success of any surgical or clinical treatment is invaluable, particularly in clinical trials. We hypothesise that a better quality repair tissue at 12 months (12m) post- autologous chondrocyte implantation (ACI), resembling healthy, native articular cartilage, leads to an improved mid to long-term clinical outcome. We have examined data from patients who have received ACI for chondral/osteochondral defects of the knee, by assessing the quality of the repair tissue formed by both imaging and histology and compared it to clinical outcome in the short and longer term.

METHODS: All patients (n=163) recruited to this study have been investigated as part of an ethically approved project (REACT 09/H1203/90, granted by West Midlands National Research Ethics Service). Quality of repair tissue was assessed using either magnetic resonance imaging (MRI) at 11.5±1.4 months (n=91) and 39.2±18.5 (n=76) post-ACI, or histology at 16.3±11 months (n=102) post-ACI. MRIs were scored using the whole-organ MRI score (WORMS) and the magnetic resonance observation of cartilage repair tissue (MOCART) score, with additional assessments of the subchondral marrow and cysts. Histology of the repair tissue was assessed using the Oswestry cartilage score (OsScore) and the International Cartilage Repair Society (ICRS) II score. Patient-reported modified Lysholm scores, as a measure of knee function, were completed at baseline, at the time of biopsy and/or MRI, annually post-ACI and at the patients' latest clinical follow-up (minimum 2 years, mean of 8.5±3.7 years (range 2.0-17.8)).

RESULTS: The median baseline Lysholm score was 54 (range 21-83) and 12m post-ACI had significantly improved to 71 (range 21-100, $p<0.0001$). At the latest clinical follow-up however (mean 8.5yrs), the median Lysholm score had remained significantly higher than baseline ($p<0.035$) but reduced to 58 (range 17-100, $p<0.012$ vs 12m). At 12m, the median MOCART score was 70, significantly higher than at latest radiological follow-up (MOCART score 60 ($p=0.045$). The total MOCART score and 4 of the 9 individual parameters (degree of defect fill, surface and structure of the repair tissue, overall signal intensity) in addition to subchondral cysts were significantly associated with clinical outcome at 12m. Parameters including degree of defect fill, overall signal intensity and the surface of the repair tissue at 12 months also significantly correlated with longer term outcome. At latest radiological follow-up, the WORMS was significantly higher than baseline ($p=0.04$) and 12m ($p=0.05$). Total WORMS and individual parameters for the presence of cysts or effusion significantly correlated with clinical outcome at 12m. Thirty percent of repair tissue biopsies contained hyaline cartilage, 65% were fibrocartilage and 5% were fibrous tissue. Despite no correlation between either histological score with overall clinical outcome, the lack of hyaline cartilage or poor basal integration was associated with increased pain. Additionally, the presence of adhesions on MRI correlated with significantly better histology.

DISCUSSION & CONCLUSIONS: These results demonstrate a significant association between the MOCART score and some of its individual parameters with both short and longer-term clinical outcome in ACI-treated patients. This highlights the potential for MRIs to predict long-term clinical outcome following cartilage repair which may be particularly useful in clinical trials. Whereas the MOCART score assesses the complete graft, histology only examines a small discrete region and cannot assess parameters such as lateral integration, hypertrophy and subchondral cysts. However, the combined use of MRI with histology allows for a more complete assessment of repair tissue. The presence of cysts, effusion and adhesions and their relationship with both histology and clinical outcome requires further investigation. This may yield new insights into the mechanisms of cartilage repair and provide information to further understand pain-generating mechanisms not only in knees with focal cartilage defects, but also in OA.

ACKNOWLEDGEMENTS: We acknowledge the help of Dr Bernhard Tins for his assistance with the MRIs and funding from Arthritis Research UK (18480, 19429 and 21156), the MRC (MR/L010453/1) and the Institute of Orthopaedics.

synthetic photoreceptor engineering for optogenetic control of TGFβ signalling

P Humphreys[1,2], R Lucas[2], C Smith[1], S Kimber[1]

[1] *Division of Cell Matrix & Regenerative Medicine, University of Manchester, UK.*
[2] *Division of Neuroscience and Experimental Psychology, University of Manchester, UK.*

INTRODUCTION: The transforming growth factor-β (TGFβ) superfamily (including bone morphogenetic proteins – BMPs) are a family of signalling molecules crucial in chondrogenic differentiation. Current chondrogenic directed differentiation protocols (DDPs) of human pluripotent stem cells (hPSCs) rely upon timed supplementation of growth factors[1-3]. However, this may lead to poor differentiation reproducibly and quality because of batch-to-batch variation. Due to the essential role of the TGFβ-family during chondrogenesis, precise control of the signalling pathway may enable refinement of differentiation. This aim of this project is to utilise the novel technology of optogenetics to render the activation of the BMP-pathway light-sensitive[4-5]; enabling fine-tuning of signalling during chondrogenesis.

METHODS: Differentiation of MAN13 human embryonic stem cells (hESCs) towards chondrocytes was performed following an established protocol[1]. Differentiation was evaluated through RT-qPCR gene expression analysis of key chondrogenic markers. Optogenetic BMP-like receptors were generated through PCR and 'NeB HiFi Assembly' cloning and inserted into a doxycycline inducible vector. BMP transcriptional response element (BRE) reporter containing cell lines were transduced with optogenetic BMP-like receptors and SMAD1/5/8 transcriptional activity was measured through Nano-luciferase and GFP production.

RESULTS: An established chondrogenic DDP resulted in significant upregulation of chondrogenic-associated gene expression SOX9, SOX5 and COL2a1 after 14 days in 2D monolayer culture. Optogenetic BMP-like receptors were successfully generated and expressed by transduced cells through stimulation with doxycycline. Activation of optogenetic receptors with blue light resulted in GFP and Nano-luciferase production; indicating stimulation of the BRE reporter by transcriptionally active BMP-like SMAD1/5/8.

DISCUSSION & CONCLUSIONS: Findings shown here demonstrate the applicability of optogenetics for control of BMP signalling and a framework for future approaches. Light-stimulated dimerisation of Type I and II BMP-like receptors (*Fig 1*) appeared sufficient to stimulate SMAD1/5/8 activity and variable light dosage should enable fine-tuning of signal transduction. Incorporation of light-controlled BMP signalling in chondrogenic directed differentiation of hESCs may reveal rate-limiting steps and enable improvement of chondrogenic differentiation in the future.

REFERENCES: [1]Oldershaw, R. et al. (2010) Nature Biotechnology 28, 1187–1194. [2]Cheng, A. et al. (2018) Tissue Engineering Part A, epub1-11 [3]Cheng, A. et al. (2014). Stem Cells Translational Medicine 3, 1287–1294. [4]Sako, K. et al. (2016). Cell Reports 16, 866-877. [5]Grusch, M. et al. (2014). EMBO J 33, 1713-1726

ACKNOWLEDGEMENTS: Optogenetic BMP receptors were modified from 'Opto-mFGFR1_204' which was a gift from Harald Janovjak[5] (Addgene plasmid # 58745). BRE and lentiviral packaging vectors were kindly donated by Dr Stuart Cain. The authors would like to acknowledge the support of the EPSRC and MRC CDT in Regenerative Medicine.

Use of topography and ultralow dose growth factor delivery to enhance antimicrobial and osteogenic properties of 3D titanium implant materials.

Laila Damiati[1,2], Virginia Llopis-Hernández[1,2], Marcus Eales[3], Angela Nobbs[3], Bo Su[3], Richard Oreffo[4], Gordon Ramage[5], Peifeng Li[6], Penelope M. Tsimbouri[1,2], Manuel Salmeron-Sanchez[1,7], Matthew J. Dalby[1,2]

[1]Centre for the Cellular Microenvironment,[2]Institute of Molecular Cell and Systems Biology, University of Glasgow, Glasgow, UK; [3]Bristol Dental School, University of Bristol, Bristol, UK; [4]Bone and Joint Research Group, University of Southampton, Southampton, UK; [5]Institute of Infection Immunity and Inflammation, University of Glasgow, Glasgow, UK; [6]School of Engineering, University of Glasgow, UK; [7]Biomedical Engineering, University of Glasgow, Glasgow, UK.

INTRODUCTION: The Selective laser melting (SLM) technique provides a promising way to fabricate a micro-lattice structures[1]. This is interesting as 3D titanium (Ti) structures are growing in use in biomedical applications such as orthopaedic implants. However, infection is a problem with implants and engineering antimicrobial properties is desirable. We have thus developed antimicrobial, high aspect ratio, nanotopographies that can induce death of *Pseudomonas aeruginosa*[2]; however, this is at cost to osteogenesis from mesenchymal stem cells (MSCs). Thus, we have further developed a simple polymer system to help deliver osteogenesis on the antimicrobial features. Polyethylacrylate (PEA) can be applied, via plasma polymerization, as a very thin coating to 3D structures and it causes spontaneous unravelling of fibronectin (FN) upon contact. In the open conformation, FN can be decorated with ultra-low, but highly efficient doses of growth factors, such as BMP2[3]. We aim to combine these technologies to create 3D, antimicrobial yet osteogenic orthopaedic implant materials.

METHODS: Three Ti micro-lattice structures with different strut diameters were produced using the SLM technique (300, 600, 900 µm). Alkaline thermal processing (1h and 2h treatment) was used to produce nanowires on the 2D Ti and 3D Ti substrates. Plasma polymerisation was used to coat the substrate with PEA. Prior to Stro-1$^+$ hBM-MSC culture, the surfaces were coated with FN and BMP2 (Fig. 1). Physical and chemical characteristics were studies using SEM, AFM, WCA and XPS. Bone gene markers were tested using qPCR. *P. aeruginosa* was cultured on the substrates and the number of viable microbial cells was determined based on quantification of ATP.

RESULTS: The average maximum height of nanowires on 2D Ti was *Rt* ~ 400 and ~ 550 nm for 1h and 2h TiO_2 respectively. XPS showed the PEA coating partially covered the surfaces with short treatment times. Polymer coatings increased the hydrophobicity of Ti which increased the protein adsorption. On the other hand, FN decreased the hydrophobicity which improved the MSC adhesion. In 3D, the 2h TiO_2 topography showed a potential bactericidal effect on *P. aeruginosa* (Fig. 2-1*);* the same features in 2D showed by qPCR an improvement on bone gene expression. Further, the 3D Ti lattice with 900 µm struts has better MSC adhesion and growth (Fig. 2-2).

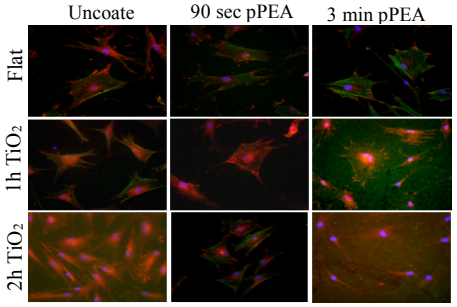

Fig. 1: *The focal adhesion of MSCs on different 2D Ti surfaces. Red: Vinculin, Green: Actin, and Blue: DAPI.*

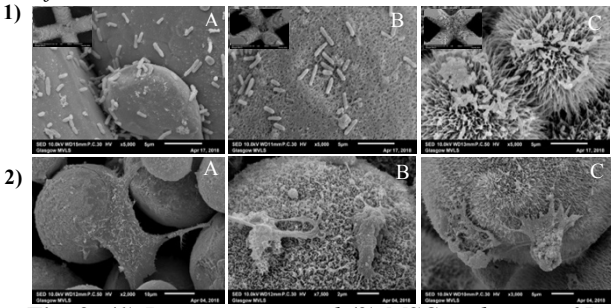

Fig. 2: (1) *P. aeruginosa and* ***(2)*** *MSCs culture on 3D Ti lattice (900 µm).* ***A.*** *Without nanowires,* ***B.*** *With 1h TiO_2 treatment and* ***C.*** *With 2h TiO_2 treatment.*

DISCUSSION & CONCLUSIONS:
We demonstrate the potential to fabricate 3D Ti implant materials with topographies that reduce microbial viability and polymer coatings that capture bone driving growth factors to enhance osteogenesis of MSCs *in vitro*.

REFERENCES:

[1]Do DK and Li P. *Virtual Phys Prototyp*, 2016.

[2]Tsimbouri *et al. Sci Rep,* 2016.

[3]Llopis-Hernández *et al. Science Advances,* 2016.

ACKNOWLEDGEMENTS: This project is supported by a studentship to LD from University of Jeddah, Jeddah- Saudi Arabia and EPSRC grant EP/K034898/1. We are grateful for the technical support of Carol-Anne Smith, Mark Ginty and Julia Wells.

POSTER

3D osteogenesis by nanovibrational stimulation of mesenchymal stem cells

PM Tsimbouri[1], PG Childs[2†], GD Pemberton[1†], J Yang[1], V Jayawarna[1], W Oripiriyakul[1], K Burgess[3], G Blackburn[3], D Thomas[4], P Campsie[2], MJP Biggs[4], ASG Curtis[1], M Salmeron-Sanchez[1], S Reid[2], MJ Dalby[1]

*[1]CeMi, University of Glasgow, UK. [2]SUPA, Strathclyde University, Glasgow, UK, [3]Glasgow Polyomics facility, University of Glasgow, UK. [4]Centre for Research in Medical Devices (*CÚRAM*), Ireland.*

INTRODUCTION: Mechanical stimulation has been explored as an avenue for regenerative medicine especially bone grafts, the most commonly transplanted tissue after blood. However, autologous grafts are in short supply, and can be associated with post operational complications. Tissue engineered bone graft would thus help meet this clinical demand in addition to providing a crucial missing stepping-stone from 2D to in vivo models in drug screening. Here we present a new nanovibrational (NV) bioreactor and demonstrate that vibration of nanoscale amplitude alone can differentiate a potential autologous cell source, mesenchymal stem cells (MSCs), into mineralised tissue in 3D.

METHODS: The NV bioreactor is a platform containing piezo actuators that generate and send nanovibrations at a frequency of 1 kHz with an amplitude of 30 nm ± 5 nm, into the cells. Human BM MSCs were seeded at 40,000cells/ml and stimulated for set time points. Cell differentiation was tested by QRT-PCR, Western blot and InCell western. MicroCT and von Kossa were used for mineralisation studies. Metabolomics were used to study metabolic changes associated to the osteogenic phenotype.

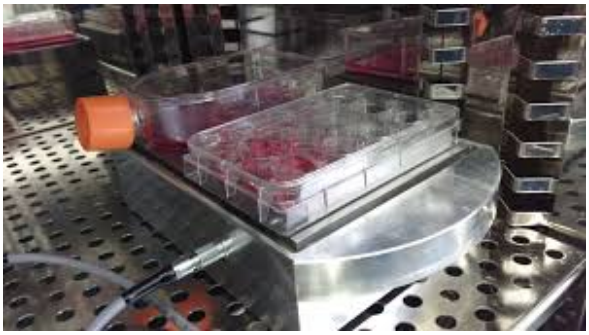

Fig. 1: Nanovibrational Bioreactor

RESULTS: Our previous work at the 2D level indicated that adhesion-based signalling, including signalling via ROCK, is important for nanovibration-induced MSC differentiation[1]. Here we show transient receptor potential (TRP) channels function as mechanosensors, and TRP channel activation occurs via cytoskeletal coupling leading to activation of major key pathways for stem cell differentiation. Metabolic analyses indicated the involvement of β-catenin and µCT confirmed mineral deposit formation in our 3D collagen gels[2] (Fig 2).

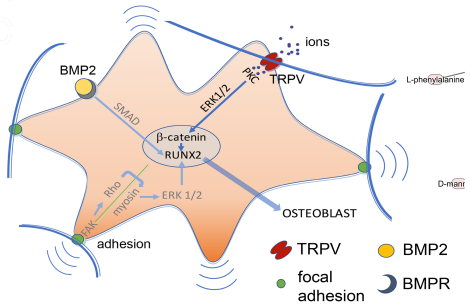

a)

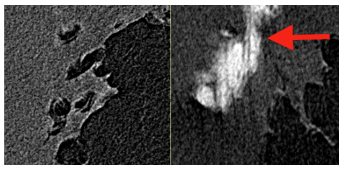

b) Control 3D NV 3D

Fig. 2 a) Schematic of osteogenesis models b) µCT mineral deposits

DISCUSSION & CONCLUSIONS: Nanovibrations alone can stimulate osteogenesis independently of other environmental factors, such as matrix rigidity. We show this by generating mineralised matrix from MSC seeded in collagen gels of very low stiffness. This is a novel and scalable method that can stimulate osteogenic differentiation, has potentially broad applications, and that would be compatible with 3D scaffolds.

REFERENCES: [1] Nikukar, H. *et al.* Osteogenesis of MSCs by nanoscale mechanotransduction. *ACS Nano,* **7**(3), 2758-2767 (2013). [2]Tsimbouri MP *et al.* Stimulation of 3D osteogenesis by mesenchymal stem cells using a nanovibrational bioreactor. *Nature Biomedical engineering* **1**, 758, (2017).

ACKNOWLEDGEMENTS: This work is funded by EPSRC and FABW.

3D skin model to investigate biocidal agents for infected burns

Beleid G[1], Shepherd J[2], Miller K[1], Le Maitre CL[1]
[1]*Sheffield Hallam University,* [2]*University of Sheffield.*

INTRODUCTION: Three dimensional skin models for clinical use to replace burned skin or to study skin biology, and treatment options for infection have been investigated[1]. However, these models have focused on primary skin cells which can be difficult to obtain and suffer from large patient variability. This study further developed a 3D skin model utilizing HaCaT cells and fibroblasts[2] which were seeded onto de epidermised dermis (DED). This model was then subjected to a controlled burn and infected with *Staphylococcus aureus* and effects of biocidal agents investigated.

METHODS: This study utilised commercially available cadaver skin from Euro skin to create DED. After removal of the epidermal layer, HaCaT and fibroblast cells were seeded onto the surface at a range of cell densities and culture conditions. Following thermal injury and infection with *S. aureus* as a bacterial biofilm, the effects of free radical generating antimicrobial strategies were investigated (H_2O_2, silver nitrate; 2-methyl-4-isothiazoline-3-one and medical grade manuka honey). The effect on cellular phenotype and toxicity of biocidal agents on mammalian and bacterial cells was determined.

RESULTS: Histological and immuno-histochemical analysis demonstrated that optimal growth conditions were seen in tissue engineered (TE) skin cultured in DMEM media containing 10% FBS together with 2ng/ml transforming growth factor alpha (TGF α). 3D skin was generated, which demonstrated keratinocyte (Cytokeratins 10 & 14) and fibroblast (S100A4) markers and underlying collagen type IV in the dermal layer (Figure 1). A decrease in *S. aureus* (SH1000) bacteria viability was observed in infected tissue-engineered skin models following biocide treatment (Figure 2). In addition, the zone of death of mammalian cells induced by biocides varied between agents with lowest toxicity seen following honey treatment.

DISCUSSION: Skin models cultured using DED scaffolds derived from Euro skin seeded with HaCaT and fibroblast cells were optimised in DMEM containing TGFα, demonstrating formation of a multi-layered 3D skin model. We have characterized this model using a combination of light microscopy and immunohistochemistry. Further, *S aureus* were able to colonize injured skin surfaces. In bacterial biofilms, there was marked inhibition of *S. aureus* (SH1000), growth with all biocides, whist toxicity to mammalian cells varied across biocidal agents (Figure 2).

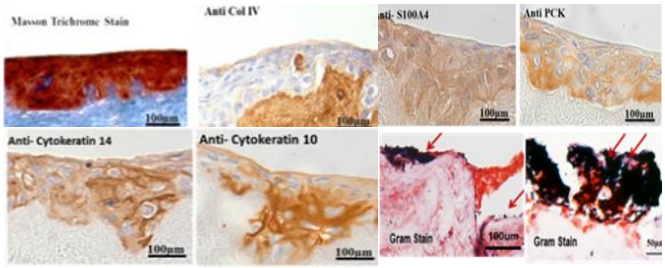

Fig. 1: Immunohistochemical staining of 3D TE skin. The sections were stained for Masson Trichrome, collagen IV, S100A4, Pan Cytokeratin (PCK), and Cytokeratin 10, 14.

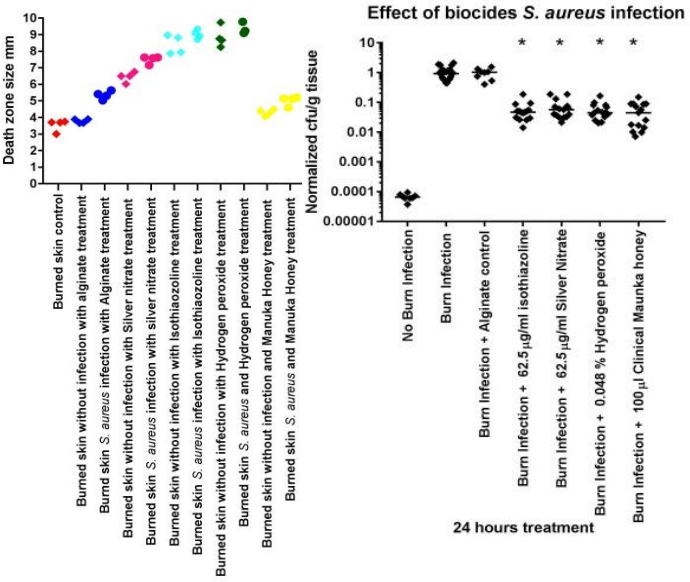

Fig. 2: Effect of biocidal agents on infected 3D skin models showing bacteria viability and death zone of skin following biocidal treatment. The biocidal effect was compared between burned infected controls and burned infected biocidal treated samples.

CONCLUSION: This study describes the development of a 3D skin model which can be utilized to develop and test biocidal agents and potential treatment methods for skin infections.

REFERENCES: 1. Deshpande, P., Ralston, D., & MacNeil, S. (2013). **Burns**, **39**(6), 1170-1177.
2. Maas-Szabowski N, Stärker A, Fusenig NE (2003). **J Cell Science 116**, 2937-2948

ACKNOWLEDGEMENTS: We thank the Libyan government for funding.

A collagen-based soft tissue barrier membrane with periosteal mesenchymal stem cell homing capability for bone defect repair

H Owston,
~~H Owston~~[1,2], K Moisley[1,2], G Tronci[3], P Giannoudis[2], S Russell[3] and E Jones[2]

[1]Institute of Medical and Biological Engineering, University of Leeds, UK. [2]Leeds Institute of Rheumatic and Musculoskeletal Medicine, University of Leeds, UK. [3]Nonwovens Research Group, School of Design, University of Leeds, UK

INTRODUCTION: Surgical interventions for critical size bone defect repair remains suboptimal. Current 'gold standard' autologous bone grafting risks inadequate graft containment and soft tissue invasion into the defect[1]. Here, a new regenerative strategy was explored, through bone graft containment using a barrier membrane wrapped around the defect site. The membrane is designed to prevent soft tissue ingrowth, whilst supporting periosteal regrowth, an important component to bone regeneration[2]. This study shows the development of a collagen-based barrier membrane that supports periosteal derived mesenchymal stem cell (P-MSC) growth.

METHODS: Barrier membranes were manufactured using free-surface electrospinning. Type I collagen was selected for P-MSC homing, whilst poly(ε-caprolactone) was employed as the fibre-forming polymer, ruling barrier membrane architecture. Varied membrane formulations, prepared in 1,1,1,3,3,3-Hexafluoro-2-propanol were assessed via scanning electron microscopy (SEM), gas flow porometry, and tensile testing. Together with Energy-dispersive X-ray spectroscopy (EDX) membrane collagen content was quantified using Picro Sirius Red (PSR). P-MSC attachment and proliferation was imaged using confocal microscopy in addition to barrier functionality using MINUSHEET® tissue carriers.

RESULTS: P-MSC-homing barrier membranes were successfully obtained with nonwoven nonaligned fibres. Introduction of collagen in the electrospinning mixture was correlated with a decrease in mean fibre diameter (*d*: 319 nm) and pore size (*p*: 0.2-0.6 μm), with respect to collagen-free membrane controls (*d*: 372 nm; *p*: 1-2 μm). Consequently, as the average MSC diameter is 20 μm, this provides convincing evidence of the creation of a MSC containment membrane[3].

SEM-EDX confirmed Nitrogen and therefore collagen fibre localisation. Following quantification using PSR, original collagen content was reduced by 50% after 24 hours (PBS, 37 °C), and maintained for 2 weeks, followed by a drop to 25% at week 3. The collagen-based membrane has a significantly higher elastic modulus compared to collagen-free control membranes.

P-MSCs grown onto collagen-based membranes showed cellular attachment and proliferation when imaged using confocal microscopy over 3 weeks. A modified transwell cell migration assay was developed to assess barrier functionality. In line with the matrix architecture, the collagen-based membrane proved to prevent cell migration (via confocal microscopy) in comparison to the migration facilitating positive control.

DISCUSSION & CONCLUSIONS: A non woven, collagen containing barrier membrane was produced that was shown to prevent MSC migration based on material architecture and functional testing results.

The aforementioned results obtained at molecular, cellular and macroscopic scales, highlight the applicability of this barrier membrane in a new 'hybrid graft' regenerative approach for the surgical treatment of critical size bone defects.

REFERENCES: [1] Dimitriou *et al.* (2012) *The role of barrier membranes for guided bone regeneration and restoration of large bone defects: current experimental and clinical evidence*. BMC Med. 10(81):1–24. [2] Chang & Knothe. (2012) *Concise review: the periosteum: tapping into a reservoir of clinically useful progenitor cells.* Stem Cells Transl Med. 1(1): 480–91. [3] Siegel *et al.(2013) Phenotype, donor age and gender affect function of human bone marrow-derived mesenchymal stromal cells*. BMC Med. 11(146): 1-20.

ACKNOWLEDGEMENTS: Acknowledgements to Katrina Moisley for membrane manufacture development.

The Engineering, Physical Sciences Research Council who provided funding through the Centre of Doctoral Training in Tissue Engineering and Regenerative Medicine programme at the University of Leeds.

A computational model of the human eye: a step towards defining cell spraying parameters to treat retinal diseases

M Nweze[1,3], T Baker[1], AG Limb[2], RJ Shipley[1,3]

[1]UCL Mechanical Engineering, [2]UCL Institute of Ophthalmology, [3]UCL Institute of Healthcare Engineering

INTRODUCTION: Millions of people suffer from retinal degenerative diseases. Despite recent progress in developing stem cell therapies for retinal diseases, methods for delivery are still subject of intense research. Aerosol technology is a promising technique that can spray cells evenly[1] across the retinal surface, promoting cell attachment and survival[2]. Optimizing cell spraying parameters (such as volume flow rate, air pressure and surface area covered) is costly to perform experimentally, thus creating the need for an alternative rapid and cost-effective technique. We use computational modelling as a tool to simulate stem cells delivery onto the inner retinal surface, hence define spraying parameters for aerosol systems.

METHODS: the experimental protocol consists of spraying a cellular scaffold (fibrin-derived hydrogel plus cells) onto the retina and stabilise the intraocular pressure as during vitrectomy. Hence, the computational setup consists of the geometry of the human eye (mimicked using a hemisphere with a diameter of 25 mm) and an injector with a diameter of 0.6 mm (setup summarised in Fig. 1).

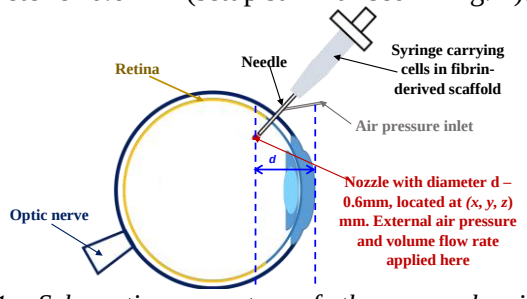

Fig.1: Schematic geometry of the eye, showing injector nozzle position, optic nerve and retina locations.

A mesh with an edge size of 0.2 mm is applied to the geometry using the finite element solver STAR-CCM+®. The material properties of the fibrin-derived hydrogel are determined using the rheometer DHR-3 (TA Instruments), and then imported into STAR-CCM+. We explore volume flow rates between 100 and 400 μLs^{-1}, with air pressures varying between 10 to 100 kPa. The spatial and temporal distribution of droplets are predicted.

RESULTS: The results demonstrate a strong dependence of spraying outputs on volume flow rate and pressure. The surface area covered by the spray system is dependent on the cone angle used for spraying as shown in Fig. 2. The outer cone angle used to spray the cell suspension can be used to control the surface area of the retina that is covered.

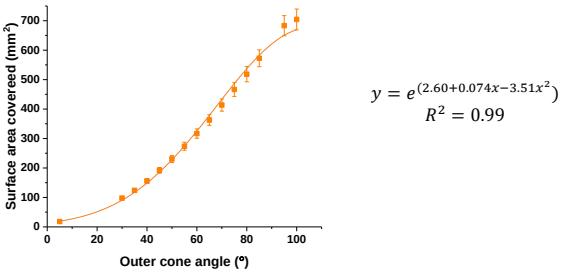

Fig.2: We present the surface area covering the inner retina for each spraying event as a function of the specified outer cone angle of sprayed cellular suspension (R^2=0.99).

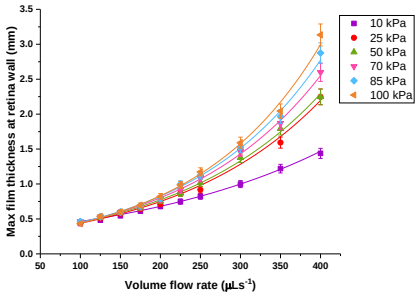

Fig.3: We present the maximum film thickness values for each spraying event as a function of volume flow rate and injector pressure (R^2=0.99).

These parameters could be used to predict operating parameters that enable a desired thickness on the retina to be achieved (see Fig 3). For example, the exponential relationship between maximum film thickness/mm (y) and volume flow rate/ μLs^{-1} (x) at 10 kPa is:

$$y = 0.30e^{0.004x}$$

DISCUSSION & CONCLUSIONS: This work indicates that simulation protocols may provide a platform to derive specific spraying parameters and could predict the required number of cells needed for each spraying event. Validation of these methods will require experimental testing *ex-vivo* and *in vivo* before they can be translated into the clinic and merits further investigations.

REFERENCES: [1]RE Maclaren et al (2006) Retinal Repair by Transplantation of Photoreceptor Precursors. Nature. 444:203-7. [2] A Roberts et al (2005) Aerosol delivery of mammalian cells for tissue engineering. *Biotechnol Bioeng* 91 (7)801-7.

A high-resolution 3D printed polymeric scaffold with micro-/nanoporous strut surfaces for osteogenic differentiation of human mesenchymal stem cells

A Prasopthum, KM.Shakesheff, J Yang [1]

[1] *Division of Regenerative Medicine and Cellular Therapies, School of Pharmacy, University of Nottingham, England*

INTRODUCTION: Stem cells are anchorage-dependent; therefore, modulation of early cell response including cell adhesion is prerequisite to gain subsequence desirable differentiation.[1] Surface topographies from micro- to nanoscale can direct cell responses.[2,3] Incorporating the surface features to the strut surfaces of 3D printed polymer scaffolds is challenging. It generally requires post-fabrication steps, i.e., chemical itching and lithography or use of sacrificial materials that increase complexity of the overall process and cost. Herein, we demonstrate a simple and quick technique based on 3D printing with polymer solution to fabricate 3D polymer scaffolds consisting of micro-struts with micro/nano pores. Adhesion, morphology, proliferation and osteogenic differentiation of human mesenchymal stem cells (MSCs) on the porous strut surfaces within 3D printed scaffolds were investigated compared to those with non-porous struts.

METHODS:

Scaffold fabrication by 3D printing of polymer solution: Scaffolds consisting of porous strands were 3D printed by deposition of homogeneous PCL/DCM solution that was agitated, which resulted in the formation of small bubbles. The scaffolds with non-porous strands were prepared with the same procedure excluding the agitation step. The polymer solutions were extruded through a 31G needle (diameter of 152 µm) using a 3D Discovery printer (RegenHU, Switzerlands).

Scaffold characterisation: SEM was used to characterise the topographies of printed strands and hMSC adhesion to the strand surfaces.

Stem cell culture: MSCs (5×10^5 cells) were seeded onto each scaffold ($1\times1\times0.5$ cm^3) and cultured in osteogenic differentiation medium. Initial cell morphology after 1 day attachment were observed by actin-vinculin staining. Cell proliferation and osteogenic differentiation were monitored over 4 weeks using a Picogreen® assay and an osteocalcin ELISA kit (Invitrogen), respectively.

RESULTS: Interconnected porous 3D scaffolds possessing micro-strands with porous surfaces (average pore size of 0.75 µm) were successfully created. MSCs exhibited smaller spreading area and slower proliferative rate up to 7 days. However, porous strand surface significantly enhanced osteocalcin production (as a marker of osteogenic differentiation) of MSCs at day 28.

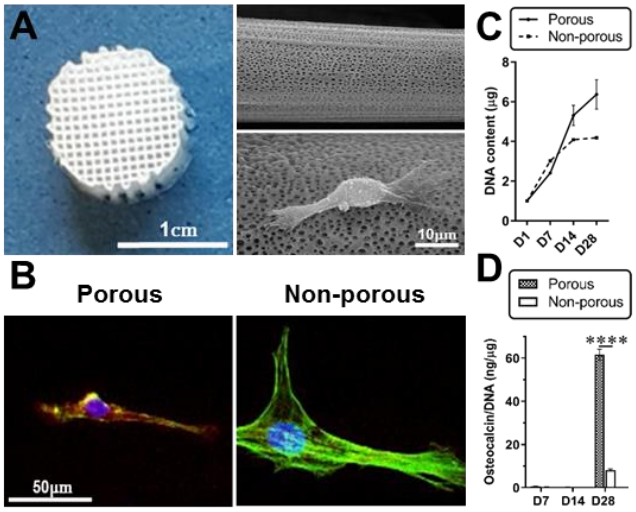

*Fig. 1: (A) A 3D printed PCL scaffold showing micro-strand consisting of porous surface and hMSC adhesion. (B) Actin (green) and vinculin (red) staining images showing initial adhesion at day 1 (C) MSC proliferation characterised by DNA content normalised to day 1. (D) Osteocalcin ELISA showing the amount of osteocalcin production (a marker of osteoblast) normalised to DNA content over 4 weeks. Statistically significant difference ($p<0.001$) is denoted by ****.*

DISCUSSION & CONCLUSIONS: Direct writing of agitated polymer solution ink can simply and rapidly create 3D scaffolds with porous strand surfaces. The porous strand surfaces directed initial attachment and promoted osteogenic differentiation of MSCs compared to those with non-porous surfaces. Our approach can potentially be used for a wide range of biomaterials to create desirable architectures with porous surfaces.

REFERENCES: [1]BD Boyan, et al (1996) *Biomaterials* **17**:137-46. [2]MJ Dalby et al (2007) *Nat Matter* **6**:997-1003. [3]D Khang, et al (2012) *Biomaterials* **33**:5997-6007.

ACKNOWLEDGEMENTS: DPST scholarship from the Royal Thai Government, NMRC for electron microscope facilities.

A mathematical model of cartilage regeneration after cell therapy mediated by growth factors

K Campbell[1,2], S Naire[1], JH Kuiper[2,3]

[1] School of Computing and Mathematics, Keele University, Keele, ST5 5BG, U.K. [2] Institute of Science and Technology in Medicine, Keele University, Keele, ST5 5BG, U.K. [3] Robert Jones and Agnes Hunt Orthopaedic & District Hospital NHS Trust, Oswestry, SY10 7AG, U.K.

INTRODUCTION: Autologous Chondrocyte Implantation (ACI) is the most commonly used cell-based therapy for treating chondral defects in joints, especially the knee. The procedure involves inserting chondrocytes, previously expanded in culture, into the defect region. The chondrocytes initiate the healing process by proliferating and depositing extracellular matrix (ECM), which allows them to further migrate in the defect until it is completely filled with new cartilage. Mesenchymal stem cells (MSCs) can be used instead of chondrocytes in this procedure with very similar long term results. It has been suggested that co-implanting a mix of the two cell types might improve short-term cartilage formation[1], but the long-term outcomes are unclear. Our aim is to use a mathematical model of cartilage repair[2] to investigate the effects of co-implanting MSCs and chondrocytes on cartilage formation.

METHODS: The key mechanisms involved in the regeneration process were simulated by modelling cell proliferation, migration and differentiation, nutrient diffusion and ECM synthesis at the defect site, both spatially and temporally. In addition, we modelled the interaction between MSCs and chondrocytes by including growth factors, such as FGF-1 and BMP-2, which are secreted by the cells and thought to influence proliferation and differentiation rates of the cells[1].

RESULTS: Our results indicate the implantation of any MSC and chondrocyte ratio improved the rate of healing within the first year when compared with ACI & mesenchymal stem cell implantation, potentially allowing the patient to become mobile sooner after surgery. The model presented gives us invaluable insight into potentially important advances in cell-based therapies[3].

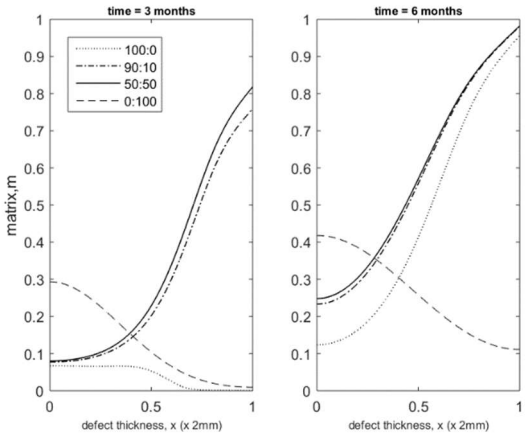

Fig. 1: Comparison of Extracellular Matrix levels for 100:0 (ASI, 100% Mesenchymal Stem Cells), 50:50 (50% Chondrocytes, 50% Mesenchymal Stem Cells), 90:10 (90% Mesenchymal Stem Cells, 10% Chondrocytes) & 0:100 (ACI, 100% Chondrocytes) at time 3 months and 6 months.

DISCUSSION & CONCLUSIONS: Our model enabled us to compare cartilage formation following various MSC and chondrocyte implantation ratios (Fig 1). Comparing our 90:10 and 50:50 co-implantation scenarios with our ACI and ASI results from previous work[2,3] shows that a mixture of MSCs and chondrocytes delivers the desired effect of increased matrix deposition, as hypothesised[1]. Matrix deposition takes place much earlier within the first 12 months of the procedure.

REFERENCES: [1]Wu, L., 2013. Mesenchymal stem cells as trophic mediators in cartilage regeneration. Ph.D. thesis. [2]Lutianov, M., Naire, S., Roberts, S., Kuiper, J.-H., 2011. A mathematical model of cartilage regeneration after cell therapy. Journal of Theoretical Biology 289, 136–150.[3] Campbell, K., Naire, S., Kuiper, J.H., 2017. A mathematical model of cartilage regeneration after cell therapy mediated by growth factors: Part 1 (To be submitted)

ACKNOWLEDGEMENTS: We would like to acknowledge Keele University for funding this work which forms a part of Kelly Campbell's PhD research.

A mathematical model to investigate the impact of seeded cell densities and distributions upon VEGF gradients and cell survival in engineered tissue

RH Coy[1,7], C O' Rourke[2,7], G Al-Badri[3,7], C Kayal[4,7], PJ Kingham[5], JB Phillips[6,7], RJ Shipley[4,7]

[1]CoMPLEX, UCL. [2]Eastman Dental Institute, UCL. [3]Dept. of Mathematics, UCL. [4]Mechanical Engineering, UCL. [5]Dept. of Integrative Medical Biology, Umeå University, Sweden. [6]School of Pharmacy, UCL. [7]UCL Centre for Nerve Engineering

INTRODUCTION: Vascularisation and cell survival are crucial for the success of engineered tissue. This is particularly true in the case of peripheral nerve repair, where vascularisation has been shown to guide and enhance neurite regrowth [1], as well as provide the nutrients required for survival of the implanted tissue. Gradients of vascular endothelial growth factor (VEGF) can encourage endothelial cell migration [2], and thereby enhance vascularisation. Here we use a mathematical model, parameterised against *in vitro* data, to investigate the impact of different seeded cell distributions and densities upon both cell survival and VEGF concentrations in the context of a nerve repair construct. This model allows us to quickly simulate different engineered tissue designs to inform future experimental choices.

METHODS: Schwann cell-like differentiated adipose-derived stem cells (dASCs) were seeded in plastic compressed collagen gels at varying densities and maintained with different external oxygen levels. After 24h, viability and VEGF concentration was measured using CellTiter-Glo (Promega) and VEGF ELISA respectively. Three coupled partial differential equations describe the interactions within the *in vitro* gel between viable cell density and oxygen and VEGF concentrations. The equations incorporate processes such as diffusion, cell death and VEGF secretion. The equations were solved over a geometry representative of a cell culture well using the Multiphysics software COMSOL, and fitted to the experimental data to derive new values for uncertain parameters. The model was then applied to a geometry representing a nerve repair construct to simulate the effects of different seeded cell densities and distributions.

RESULTS: Model simulations suggest that seeding the same number of cells in specific non-uniform distributions can achieve equal or increased numbers of viable cells after 24h as seeding them uniformly, whilst generating steeper and more spatially extensive gradients of VEGF. An example of this is shown in Fig. 1. Furthermore, the optimal spatial distribution of cells to maximise the number of viable cells after 24 hours is predicted to vary according to the initial total number of seeded cells.

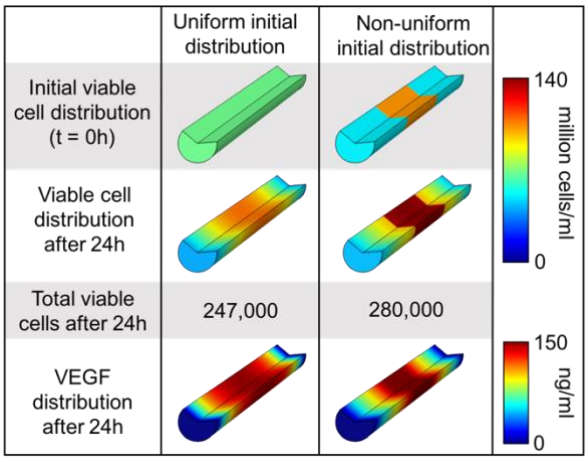

Fig. 1: Simulated viable cell and VEGF distributions after 24h in nerve repair constructs with uniform and non-uniform initial seeded cell distributions of 200,000 cells.

DISCUSSION & CONCLUSIONS: The model simulations suggest that varying the spatial distribution of cells could enhance the efficacy of engineered tissue by improving cell survival and through the generation of VEGF gradients required for vascularisation. The results also imply that choosing non-uniform seeded cell distributions could help to reduce the total number of cells required to achieve similar results, reducing future experimental and clinical costs. These model predictions can be tested *in vivo* and used to inform future experimental choices. Any further data collected can in turn be used to improve the model further. This flexible model can be applied to other tissue engineering scenarios, and has the potential to be expanded to incorporate the processes of neurite and vascular growth.

REFERENCES: [1]A Cattin, J Burden, L Van Emmenis et al (2015) *Cell* 162(5):1127-1139, [2]D Odedra, L Chiu, M Shoichet et al (2011) *Acta Biomaterialia* 7(8):3027-3035

ACKNOWLEDGEMENTS: This work was supported by EPSRC EP/N033493/1 and a doctoral training grant SP/08/004 from the British Heart Foundation to RC. RC is also supported through the UCL CoMPLEX doctoral training programme.

A novel piezoelectric composite to improve cell proliferation and collagen matrix production

B Tandon[1], A Kishor[1], E Stergiou[2], H Pearce[2], J J Blaker[1], H Khanbareh[2], S H Cartmell[1],

[1] *School of Materials, The University of Manchester, Manchester; UK,* [2]*The University of Bath, Bath, UK.*

INTRODUCTION:

Piezoelectric materials have gathered huge interest from tissue engineering community in the past few years (Tandon et al., 2018a; Tandon et al., 2018b). These materials have shown great promise in both static and dynamic conditions of cellular stimulation. Simply poling (a technique that induces the piezoelectric character by aligning the dipoles) the materials have shown to induce a positive cellular response in a variety of cell types (Tandon et al., 2018a). In this study, we analysed the effect of uncharged, positively and negatively charged surfaces of the piezoelectric particulate ceramic polymer matrix composite on cell response and tested the suitability of these materials for tissue engineering applications.

METHODS:

Piezoelectric composites were fabricated by randomly dispersing 15% (vol.) KNLN particles (average particle size 2.5 µm) in polydimethylsiloxane (PDMS) and curing it at 90°C under vacuum. The samples were poled using corona poling at 100°C. A voltage of 10kV was used for 1 hour and the samples were cooled to room temperature with the field on. L929 fibroblast cells were used to test the compatibility of composites manufactured and the effect of different types of surfaces on the cells was analysed.

RESULTS:

Table 1 Different piezoelectric characteristics of the composites synthesized.

Piezoelectric charge constant (d_{33})	3 pC/N
Dielectric constant	7
Dielectric loss	1%
Piezoelectric voltage constant (g_{33})	50 mV m/N

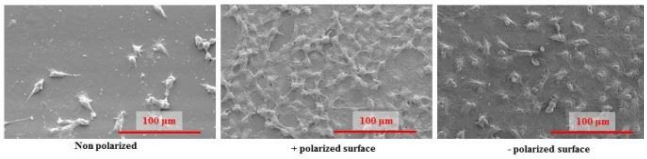

Figure 1 SEM images for L929 cells fixed on different surfaces of the composite materials at day 7.

The piezoelectric properties of the materials fabricated are listed in Table 1. The scanning electron microscopy (SEM) images of the fixed L929 cells on different surfaces of the piezoelectric composite material are shown in figure 1. Results obtained from resazurin reduction assay have been shown in figure 2.

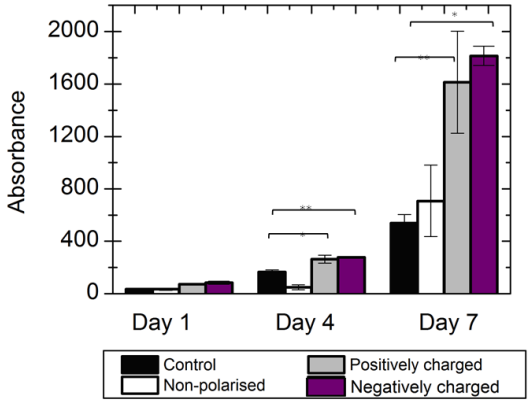

Figure 2 Cell viability after 1, 3 and 7 days measured via the Alamar Blue assay. Error bars indicate the standard deviation. *P <0.05 ; **P<0.005.

DISCUSSION & CONCLUSIONS: It was observed that L929 cells showed higher proliferation and viability on polarized surfaces (poled + and -) when compared to the non-polarized samples. However, there was no significant difference observed between + and – polarized samples. Similar results have been obtained in the past with piezoelectric polymers, ceramics and composites (reviewed in Tandon et al., 2018a). The cell culture in this experiment was performed in static conditions and it can be presumed that the piezoelectric effect has no major effect to play in such cases. In the past, the improved cellular response on polarised surfaces have been attributed to improved wettability of samples post polarization surfaces which could be possible reason supporting cell growth.

REFERENCES: Tandon B, Blaker JJ, Cartmell SH (2018a) Piezoelectric materials as stimulatory biomedical materials and scaffolds for bone repair. Acta Biomater.

Tandon B, Magaz A, Balint R, Blaker JJ, Cartmell SH (2018b) Electroactive biomaterials: Vehicles for controlled delivery of therapeutic agents for drug delivery and tissue regeneration. Adv. Drug Deliv. Rev.

ACKNOWLEDGEMENTS: The authors would like to thank the Commonwealth scholarship commission for their support.

Acoustically-stimulated microbubbles for bone fracture repair

AE Polydorou[1], S Ferri[1], D Angell[1], D Carugo[1], ND Evans[1]
[1]University of Southampton University Road, SO17 1BJ Southampton, United Kingdom

INTRODUCTION: 10% of bone fracture cases result in costly and debilitating conditions such as delayed or non-union, where the bone fails to heal properly. The aim of this project is to promote bone repair using gas-filled, lipid-coated microbubbles (MBs) or perfluorocarbon nanodroplets, which carry drugs and release them on exposure to ultrasound. One of the challenges faced is microbubble stability during storage, handling and administration, which significantly affects therapeutic performance *in-vivo*. We tested the hypotheses that firstly MB preparation is non-toxic to human cells and secondly, microbubbles' stability is affected by viscosity, temperature and dye-incorporation.

METHODS: To test cytotoxicity, MBs were fabricated using a 9:1 molar ratio of 1,2-distearoyl-sn-glycero-3-phosphocholine (DSPC) to polyoxyethylene(40) stearate (PEG40S) lipids, which were hydrated in PBS and sonicated to form a MB suspension. MG63 osteocarcinoma cells were treated with MBs at a range of concentrations between 6 x 10^7 and 6 x 10^5 MBs/mL. Following 72 hours incubation at 37°C and 5% CO_2, Alamar Blue® assay was carried out to quantify cell viability. The equivalent concentrations of lipid suspensions (LS) (not sonicated) were tested for the effect of free MB constituents (n=3, 3 repeats). To test stability, media with different viscosity (2-10 times greater than PBS) were prepared by hydrating the lipid films in solutions composed of different proportions of PBS, glycerol and propylene glycol. MBs were then stored at 4°C or incubated in a 37°C, 95% humidity and 5% CO_2 environment, and their stability was measured in terms of mean diameter and concentration over a period of 6 days. Finally, the effect of the incorporation of a lipophilic fluorescent dye, 1,1'-dioctadecyl-3,3,3',3'-tetramethylindocarbocyanine perchlorate (DiI), was determined as it enables MB tracking *in-vivo* and *in-vitro*. Molar ratios of Dil:MB in the range 1:4000-1:400 were tested.

RESULTS: Cytotoxicity tests revealed that increasing MB concentrations reduced cell viability overall, with the highest cell death measured upon incubation with 3x10^7 (1:2) MB/mL (41,800±4,100 vs 13,700±4500 relative fluorescence units; $p<0.001$). Incubation with LS caused a significantly more rapid reduction in cell viability compared to equivalent concentrations of MB suspension. This is evident as 1:5 dilution of LS (1.2x10^7 Lipids/ml), significantly reduced viability compared to 1.2x10^7 MBs/ml, ($p<0.05$). Stability tests revealed that temperature had a significant effect on MBs mean diameter. At 37°C, the diameter increased over two hours from 4.67±1.45 to 18.24±11.63 µm, while concentration decreased from 2.65x10^8 to 4x10^6 MBs/mL. In contrast, at 4°C, the mean diameter increased from 3.9±0.42 to 10.72±0.7 µm while the concentration decreased from 2x10^8 to 4x10^6 MBs/mL over six days. An increase in the viscosity (from 1.58 to 15.38 cP) led to smaller MBs, with mean diameter of 2.92±2.88 vs 3.66±2.89 µm (just after production) and 4.06±4.49 to 6.26±5.05 µm (after 1 day). Incorporation of the lipophilic dye, DiI, significantly affected MB size. The average diameter increased with increasing viscosity, from 4.99±3.8 to 5.48±2.99 µm, after production. Whereas, at day 6 the mean diameter increased from 13±11.82 to 17.94±14.74 µm with increasing DiI:MB ratio.

DISCUSSION & CONCLUSIONS: MBs are a safe drug delivery method and do not compromise cell viability after 72 hours incubation, when used below a concentration of 3x10^7 MBs/mL. Their stability is reduced with increasing storage temperature, however, it is enhanced by increasing the viscosity of the suspension medium. Incorporation of DiI into the lipid shell also decreased stability. To achieve therapeutic efficacy, future studies will focus on improving stability at different temperatures and labelling techniques that do not alter MB properties. Reducing the cytotoxic effect of free lipids will also be explored and drug encapsulation/release will be investigated.

ACKNOWLEDGEMENTS: We thank the EPSRC, the MRC and the Institute for Life Sciences, Southampton for funding. We also thank Dr Evans and Dr Carugo for their supervision and support.

Advanced polymeric nerve guide conduit modified with graphene oxide (GO) for peripheral nerve repair

Ying Lu *[1], Julie Gough [1]

1. *School of Materials, University of Manchester, Oxford Road, Manchester, M13 9PL*

Peripheral nerve injury (PNI) by trauma is an extremely common injury in daily life, more than half a million defect cases are reported annually around the word. Compared to clinical gold standard approach, autologous nerve grafting, nerve guide conduits serve as an alternative approach to repair PNI by providing temporary structural support at the defect site. In order to achieve a satisfactory regeneration outcome, it has been reported that intraluminal wall topographical cues, a grooved pattern, is a promising approach to enhance peripheral nerve regeneration via mimicking the native environment of the extracellular matrix (ECM). To improve storage time and mechanical properties, graphene oxide (GO) is introduced to play an anti-oxidant role during sterilization. Meanwhile, GO has also been reported to facilitate neural cell growth, proliferation and differentiation. The aim is to establish an advanced nerve conduit material, combining topographical cues, nano-scale features and other benefits of the addition of GO, to enhance nerve repair and regeneration.

An alginate-based encapsulation system for the delivery of therapeutic cells to the CNS

D Eleftheriadou[1], R Evans[2,3,4], AS Boyd[1,5], JC Knowles[2,4], VH Roberton[2,6] and JB Phillips[2,3]

[1]Division of Surgery and Interventional Science, University College London, London, UK. [2]Centre for Nerve Engineering, UCL, London, UK. [3]Department of Pharmacology, UCL School of Pharmacy, London, UK. [4]Biomaterials & Tissue Engineering, UCL Eastman Dental Institute, London, UK. [5]UCL Institute of Immunity and Transplantation, Royal Free Hospital, London, UK. [6]Biochemical Engineering, UCL Faculty of Engineering Science, London, UK.

INTRODUCTION: Cell therapy has emerged as a promising strategy for reducing brain dysfunction and modifying neurodegenerative disease progression. However, both pre-clinical and clinical evidence shows high rates of cell death after implantation, possibly due to the host immune response[1]. One of the most commonly employed immunoisolation technologies is encapsulation of cells in spherical microbeads made of polymers for local delivery[2]. Here we have developed a novel approach aimed at protecting therapeutic cells for long periods after implantation into the CNS.

METHODS: PC12 cells were used as a model cell line and encapsulated in hydrogel matrices. Alginate concentrations of 1.5% w/v and 2% w/v were tested, as well as composite formulations based on alginate and other natural polymers. The most suitable biomaterial was selected to form the core of microbeads for subsequent experiments. Finally, possible alginate microbead modifications were examined that could regulate cell survival, maintain phenotypic characteristics, and reduce adverse host cell responses. Physicochemical characterization was performed via stability testing, dynamic mechanical analysis, diffusion studies, and rheometry. Upon encapsulation, cell viability and metabolic activity were determined via live/dead staining and CellTiter-Glo® 3D assay. In vitro assays were used to replicate host cell responses to encapsulated cells and determine the efficiency of microbeads to act as a barrier.

RESULTS: New microbeads (mean size 2.33–1.29±0.1 mm) with dual functionality as smart delivery systems were developed and optimized. Hydrogel composition was found to influence degradation (stable up to 28 days), elastic modulus E' and nutrient diffusion. In addition, the physical properties of microbeads could be manipulated to comply with those of the native brain tissue, improving their biomechanical integration. Encapsulation of PC12 cells sustained their viability up to 75.2–85.9±2.4%. up to 7 days.

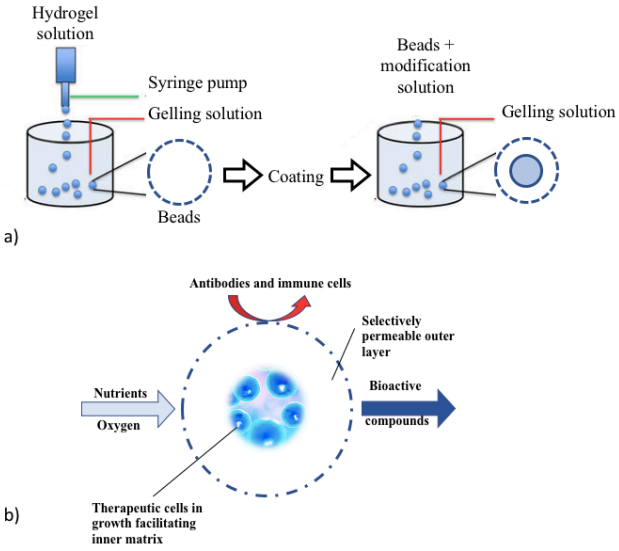

Fig. 1: Schematic representation of a) the methodology to generate capsules and b) the novel complex encapsulating system concept.

DISCUSSION & CONCLUSIONS: Encapsulation in alginate-based formulations designed for implantation into the brain has the potential to facilitate therapeutic cell survival and reduce detrimental host cell responses. Future work will further investigate the ability of selected material to improve the long-term viability of therapeutic cells.

REFERENCES:

[1]A. L. Piquet, K.Venkiteswaran, et al (2012) The immunological challenges of cell transplantation for the treatment of Parkinson's disease. *Brain Res. Bull*. **88**:320–331. [2] G.Orive, E.Santos, et al (2015) Cell encapsulation: technical and clinical advances. *Trends Pharmacol. Sci*. **36**:537–546.

ACKNOWLEDGEMENTS: This work was supported by funding from the Bodossaki Foundation, Greece.

An alveolar structural mimic: A tissue engineering approach for emphysema

A.Y. Kyoseva, Y. Yang, N.R. Forsyth

Guy Hilton Research Centre, Institute for Science and Technology in Medicine, Keele University, Thornburrow Drive, Stoke-on-Trent, ST4 7QB UK

INTRODUCTION: Respiratory diseases are the second highest cause of death in the UK and a huge economic burden to the NHS. The lung has a complex three- dimensional structure, and in this structure the connection of alveolar units to airways is necessary. Tissue engineering approaches represent an attractive potential for improving lung function. Our aim is to create an alveolar-like structure on a scaffold to replace damaged areas caused by respiratory diseases such as emphysema. With its highly porous structure and elasticity the commercially available gelatine sponge, Surgispon®, represents an ideal scaffold for an alveolar-like structure.

METHODS: Surgispon® mechanical stability was increased by crosslinking with 25% glutaraldehyde (GTA) vapour for 24 hours and pore size measured via mCT. Scaffolds were cleaned and sterilized before any cell culture work.

A549 human lung carcinoma epithelial cells and 35FL immortalised human lung fibroblasts were used for cell culture experiments under standard conditions (Akram et al., 2013). Cytotoxicity of any possible GTA on the scaffolds was investigated via alamarBlue cell viability assay. After cytotoxicity analysis, scaffolds were coated with either fibronectin (Biosera) and/or collagen type I, IV and solution from human fibroblast (Sigma-Aldrich). alamarBlue and DAPI stains were performed at days 7, 14 and 21.

RESULTS: Only crosslinked scaffolds survived incubation in media for longer than 7 days (Fig 1). Cytotoxicity testing showed that crosslinked scaffolds can support cell growth.

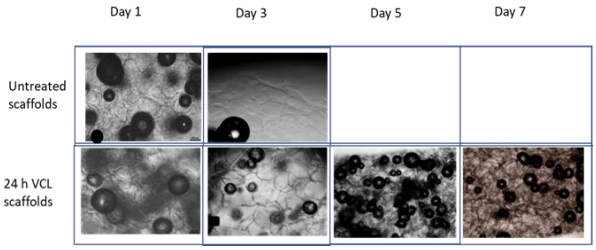

Fig. 1: Uncrosslinked scaffold vs 24h vapour crosslinked scaffold, incubated in cell culture media for 7 days.

Scaffold pores were determined to be 100-400 μm in diameter, measured via micro CT analysis establishing similarity to alveolar diameter.

AlamarBlue results indicated that there was significantly less A549 cell migration from scaffold to plate on collagen and fibronectin coated scaffolds than others on day 7 (Fig 2 and 3).

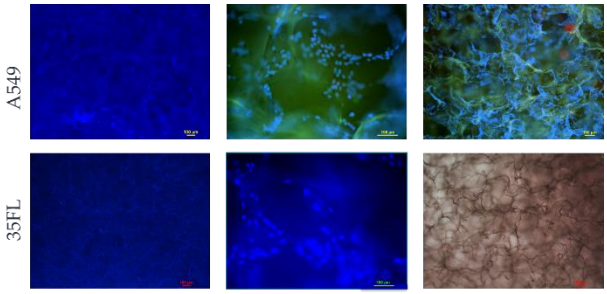

Fig. 2: A549 and 35FL cells after 7 days of cell culture on collagen and fibronectin. DAPI images.

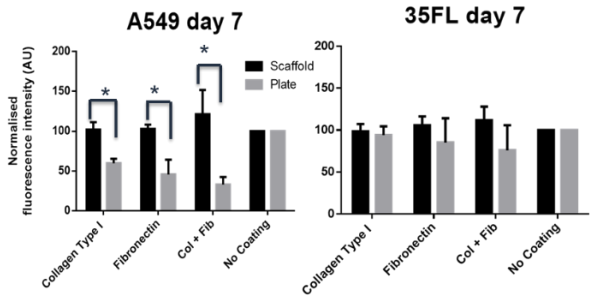

Fig. 3: Day 7 Alamar blue results of A549 and 35FL cell on coated and uncoated scaffolds.

No significant differences were seen across different collagen type coatings for 35FL.

DISCUSSION & CONCLUSIONS: Surgispon® requires cross linkage to maintain structure, and coating for 3D cell culture suitability. Collagen and fibronectin coatings increased cell stability on the scaffold. Overall, the interconnected porous structure of Surgispon® has great potential for 3D cell connectivity and could create an alveolar-like structure for lung cell study. We are currently exploring cross-linked Surgispon® suitability for culture of patient-matched type II pneumocyte and lung fibroblast cultures.

ACKNOWLEDGEMENTS: We acknowledge funding support from Royal Society, EPSRC Centre for Doctoral Training in Regenerative Medicine, North Staffordshire Medical Institute, and Keele University. This template was modified with kind permission from eCM Journal.

Anti-inflammatory properties of spinal cord derived hydrogel and dental mesenchymal stem cells

N Tatic[1], FRAJ Rose[1], A des Rieux[2], LJ White[1]

[1] *RMCT, School of Pharmacy, University of Nottingham, Nottingham, UK.* [2] *ADDB, Louvain Drug Research Institute, Brussels, Belgium*

INTRODUCTION: One of the consequences of spinal cord injury (SCI) is chronic inflammation, a phenomenon that hampers regeneration and is initiated by microglia [1]. We hypothesized that spinal cord extracellular matrix hydrogel (scECM) and mesenchymal stem cells from dental apical papilla (SCAP) can be used together in a strategy to reduce the inflammation in microglia cells. Previously, SCAP, easy to obtain from an adult immature tooth, have been tested in the context of SCI due to their neural embryogenetic origin [2]. Different ECM hydrogels have been shown to promote anti-inflammatory behavior of unstimulated macrophages [3], but they have not been tested on microglia cells. ECM hydrogels were tested in solubilised form [3], but our long term strategy is the delivery of cells embedded in scECM that forms a robust, solid hydrogel and remains at the sight of injection. Therefore, the objectives of this work were to i) determine if scECM hydrogel supports SCAP viability in 3D, ii) determine the optimal method of testing the influence of solid scECM on microglia cells and compare to the influence of solubilised form and iii) investigate anti-inflammatory potential of SCAP and scECM in combination.

METHODS: SCAP viability in scECM 8mg/mL (S8) (1x10^6 cells/mL of gel) was assessed after 7 days using a metabolic assay (PrestoBlue). S8 impact on untreated (M0) and LPS-treated microglia (M_{LPS}) was tested in two forms: i) robust, solid S8 on cell culture insert (pore size 1 µm) (indirect contact) and ii) solubilised S8 in medium (direct contact). Influence of SCAP and SCAP incorporated in S8 were tested indirectly. *Tnf*, *Arg1* and *Nos2* expression (RT-qPCR, Taqman primers and probes) and TNFα secretion (Invitrogen ELISA kit) in microglia (BV2 cells) was measured according to manufacturers' instructions. All experiments were performed in triplicates.

RESULTS: SCAP viability in S8 was 93.7% or higher throughout the experiment (data not shown). S8 in both of the forms showed no significant influence on TNFα secretion in M0 and M_{LPS} (data not shown). The addition of solid or solubilised S8 to M_{LPS} did not influence expression of tested genes. However, solubilised compared to solid S8 significantly increased *Nos2* expression (data not shown). SCAP decreased *Tnf* expression, but SCAP in S8 did not (Fig.1A). Both SCAP and SCAP incorporated in S8 decreased *Nos2*/*Arg1* ratio (Fig.1B).

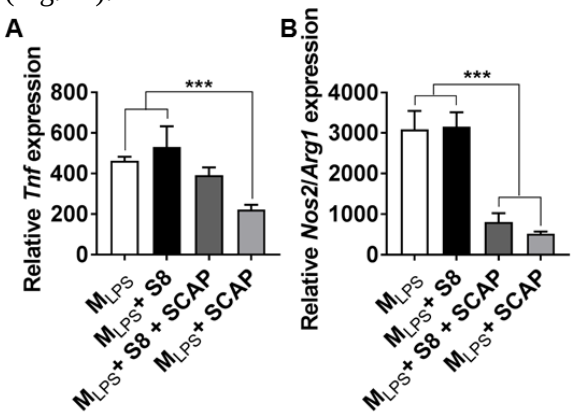

Fig. 1. SCAP and hydrogel influence on pro-inflammatory gene expression (A) and pro-/anti-inflammatory gene expression ratio (B).

DISCUSSION & CONCLUSIONS: S8 supported SCAP viability and from that perspective the two can be used in combination. S8 did not appear to induce or increase inflammation and so can be used in the context of SCI. Lack of the expected S8 influence on inflammatory gene expression may be due to ECM hydrogel origin, since it is anticipated that different ECM hydrogels will influence gene expression in a different way [3]. A further hypothesis is that ECM hydrogels might have different effect on microglia compared to macrophages. SCAP alone appeared to mitigate the inflammation seen in microglia cells, in accordance with literature [2]. However, SCAP in S8 were not as successful. These results are intriguing considering the impartial influence of S8. Therefore, the future research will explore new methods to investigate SACP and S8 interaction and cytokine diffusion in the inflammatory environment.

REFERENCES: [1] J. Gensel, B. Zang (2015) *Brain Res* 1619:1-11. [2] P. de Berdt et al (2018) *Cell Mol Life Sci*, pp 1-14. [3] J. Dziki (2016) *J Biomed Mater Res A*, 105:138-147.

ACKNOWLEDGEMENTS: This research was funded by Erasmus Mundus NanoFar.

Assessing the effects of substrate coating on cardiac stem cell aggregation

Bowen Xie[1,2*], Yixiang Wang[1,2*], Shuting Huang[1,2], Kun Chen[2], Ying Yang[1]
[1]*Institute of Science and Technology in Medicine, Keele University Stoker-on-Trent ST4 7QB, UK,*
[2]*School of Life Science. Guangzhou University, Guangzhou, China*

INTRODUCTION: Applications of cardiac stem cells (CSCs) therapy have been fully discussed, while better approaches on CSCs enrichment yet to be precise. Pluronic F127 is a type of copolymer that currently applied in biomaterial field as polymeric nonionic surfactant with high hydrophilicity. Cell adhesion in regular culture substrate relies on surface adhesive proteins. It has been reported that the expression patterns of surface adhesive proteins on stem cells and fibroblasts are different. In this study, we aim to investigate whether we can enrich population of CSCs from cardiac cell mixture through alteration of cell culture substrate using different coating solution with various ratio of F127 and gelatin and using cardiac cells at different passage numbers.

METHODS: Cardiac cells were extracted from 2 days old rats (Schedule 1 culling). The cells in different passage number (P0, P1, P2, P3, P4) were separately transferred to normal 96-well plate, which were coated with gelatin and F127 solution in different ratio (100:0, 98:2, 95:5, 90:10, 0:100), and uncoated wells as control. Cell morphological images were taken to determine the separation efficiency, and immunofluorescent staining was applied on detecting the cell surface markers (c-kit and troponin-T) to reconfirm the purity of separated CSCs.

RESULTS: Cell aggregation alongside attached cells was observed on all coated substrates. Morphologically, effective separation was showed in the culture wells with 90:10 gelatin and F127 coating, while cells in 100% F127 coating group seemed over detached (Fig.1). Cell aggregations were reduced as passage number increasing. Moreover, P2 cells had higher myocyte concentration than P0 and P1, and good adaptability of coated materials, while P4 cells were even hardly affected by coating. The fluorescence staining results showed that aggregated cells expressed c-kit marker, whilst attached cells did not. c-kit$^+$ cells were barely observed in the groups which were coated with the solution containing 100% to 95 % of gelatin, while it was obviously showed in the groups coating with solution containing 10% and 100% F127 (Fig.2). In all groups, Troponin-T$^+$ cells can be observed, especially 100% gelatin coating (Fig.2).

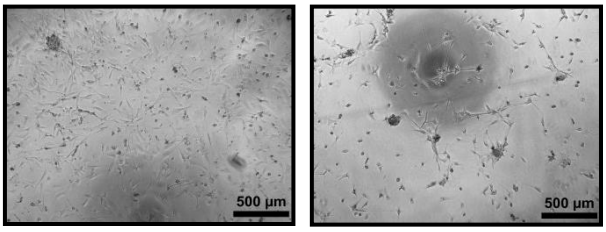

Fig 1. Cell aggregations formation in 90:10 gelatin to F127 (left) and 100% F127 (right) coating.

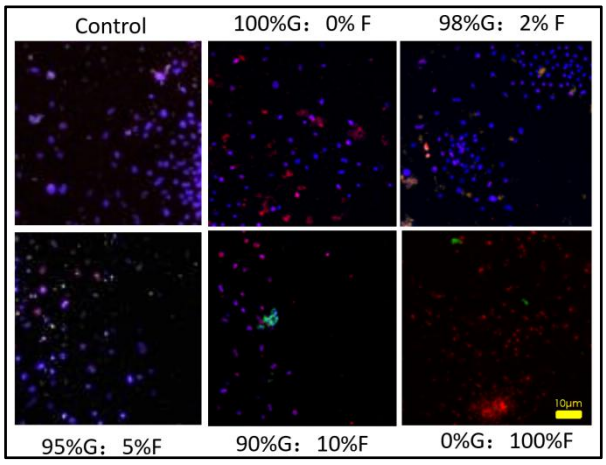

Fig 2. Cell surface marker staining of each group in P1, DAPI for nuclear staining (blue), Troponin-T (red), c-kit (green). 100% F does not show DAPI dye for better view of c-kit and Troponin-T.

DISCUSSION & CONCLUSIONS: Increasing of F127 to gelatin ratio increased the trend in formation of larger and detached cell aggregates. The coating solution containing 10% of F127 is suitable for generating CSCs aggregations as currently found. The separation efficiency was affected by the increasing number of myocytes. Better coating ratio or other materials could be investigated for further enrichment.

*Equal contribution

Assessing the feasibility of using human brain tissue slices derived from excised tissue of Chiari malformation patients as a laboratory-based neurological injury model.

J. A. Tickle[1], C. Adams[1], J. Sen[1], R. Price[2], S. Harrisson[2], N. Tzerakis[2†], D. Chari[1*]

[1]*Neural Tissue Engineering Group, Institute for Science & Technology in Medicine, Keele University, Keele, Staffordshire. ST5 5BG.* [2]*Division of Neurosurgery, Royal Stoke University Hospital, Staffordshire, ST4 6QG.* [†]*Lead Clinical Investigator; *Chief Investigator.*

INTRODUCTION: Use of live animal models to test new therapies for brain and spinal cord repair is a controversial subject, with major concerns shared by both public and scientific communities, namely i) the potential for substantial suffering in animals, and ii) the failure of animal models to predict human responses [1-2]. This study aims to address these issues by developing an *in vitro* model of brain injury using adult human brain tissue.

METHODS: A collaborative team of neuroscientists from Keele University and neurosurgeons from University Hospital of North Midlands has worked together to grow 'organotypic' slices of cerebellum removed from patients with Chiari malformation (cerebellar herniation through the foramen magnum towards the brainstem) treated by foramen magnum decompression (NHS REC No. 17/YH/0010; IRAS 195636). The time from collection of excised tissue to processing within the laboratory is = < 1 hr, with a total processing time of approximately 5 hrs. Two growth media and a range of slice thicknesses were tested.

RESULTS: We show for the first time that human brain slices derived from surgically excised tissue can be kept alive using the slice 'interface' method [3] *in vitro* for up to a month. Major neural cell types contributing to pathology can be reliably detected in slices. Importantly, for testing clinical therapies, focal injuries can be introduced into the slices to mimic a traumatic neurological injury, within which pathological responses can be detected.

DISCUSSION & CONCLUSIONS: It is suggested that "*best predictability is achieved with human organotypic models that mimic the microenvironment of human tissues*" [4]. Previous human slice models have relied on epileptiform or tumour tissue. By contrast, the tissue used in this study is herniated and is widely considered to be normal. As such, the model could serve as a useful predictor of pathological responses seen following neurological injury. Models such as these can have significant impact in reducing animal usage and ensuring rapid progression of effective and safe therapies for CNS disorders, improving reliability and patient safety.

REFERENCES: [1] M. Leist and T. Hartung (2013) *ALTEX* **30**(2):227-230. [2] R. Lowenstein and M.G. Castro (2009) *Curr. Gene Ther.* **9**(5):368-374. [3]A.P. Weightman, M.R. Pickard, Y. Yang and D.M. Chari (2014) *Biomaterials* **35**(12):3756-65. [4]T. Heinonen (2015) *Altern. Lab. Anim* **43**(1):29-38.

ACKNOWLEDGEMENTS: North Staffordshire Medical Institute provided funding for this study.

Assessment of 2D and 3D electrospun structures for use as tissue engineered ligaments: A mechanical and morphological perspective.

Elisa Roldán[1], Neil D. Reeves[2], Glen Cooper[3], Kirstie Andrews[1]

[1] School of Engineering, Faculty of Science & Engineering, Manchester Metropolitan University, Manchester, UK. [2] School of Healthcare Science, Faculty of Science & Engineering, Manchester Metropolitan University, Manchester, UK. [3] School of Mechanical, Aerospace & Civil Engineering, University of Manchester, Manchester, UK

INTRODUCTION: 2D and 3D polyvinyl alcohol (PVA) electrospun scaffolds were studied to evaluate their suitability for use as anterior cruciate ligament (ACL) grafts. ACL *in-vivo* mechanical properties were previously determined [1,2]. The aim was to establish which electrospun structure would provide the morphology and mechanical properties most comparable to the natural ligament, in dry/wet, tensile and shear cyclic loading conditions (not previously investigated). It was assumed that similar fibre networks to the extra-cellular matrix would promote tissue ingrowth; and similar morphological structure and comparable mechanical behaviour to the natural ACL would provide the mechanical properties required.

METHODS: 2D optimized electrospun scaffolds were manufactured using 12% w/v of PVA (Sigma Aldrich, UK) dissolved in distilled water, 20 kV of applied voltage, a flow rate of 1 ml/h, 18 G needle, 8 cm between the needle tip and the collector, 9.65 cm diameter rotating collector, 2000 rpm and 3 hours spin time. 2D samples were cut with a dogbone cutter (25 x 4 mm, test length x width). To fabricate the 3D structures, the 2D electrospun meshes were cut in rectangles of 2 x 15 cm and manually twisted clockwise to form scaffolds of: one twisted filament, three twisted filaments and three twisted/braided filaments. 2D and 3D structures were crosslinked with 25% glutaraldehyde for 24 hours. Cyclic tensile and shear tests with crosslinked and non-crosslinked samples were performed in dry and wet conditions (n=8 samples per condition). The tests were performed using an Instron H10KS, 10 cycles to 13% strain and then tested to failure, with a 100 N load cell and 5 mm/min test speed. Fibre diameter and thickness of the fibre bundles and fascicles were measured from SEM images using AxioVision SE64 Rel. 4.9.1. 20 fibres, 3 fibre bundles and fascicles (as relevant) were measured for each sample and test condition.

RESULTS: Three twisted/braided filaments scaffolds produced a maximum tensile stress of 38.0 ± 3.0 MPa and a Young's modulus after 10 loading cycles of 148.7 ± 13.0 MPa in dry conditions, being the most comparable structure to the ACL mechanical properties (Fig.1) [1-3]. All wet PVA scaffolds exhibited elastic behaviour with a well-defined toe region. Three twisted/braided crosslinked filament structures showed the highest maximum shear stress across all samples. The manufacturing process did not damage the nanofibres or alignment and it was demonstrated that 3D structures exhibited more consistent mechanical properties than 2D structures. The dimensions of the PVA fibres, fibre bundles and fascicles were statistically comparable with the diameters of the collagen fibrils, fibres and fascicles in the natural ligament [4].

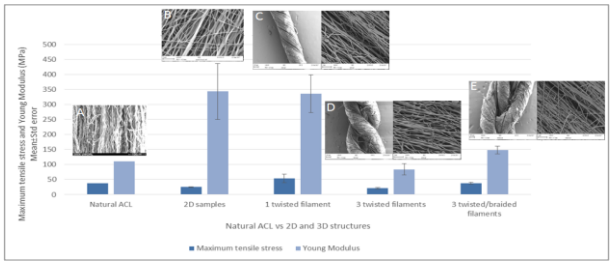

Fig. 1: Mechanical properties and SEM images of natural ACL vs 2D and 3D structures A) Natural ACL B) 2D samples C) 1 twisted filament D) 3 twisted filaments E) 3 twisted/braided filaments

DISCUSSION & CONCLUSIONS: Three twisted/braided crosslinked filament structures mimicked the ACL mechanical and morphological properties, showing significant potential for use in ACL reconstruction.

REFERENCES: [1] Roldán E. et al. *Procedia CIRP* 49, 133–138, 2016; [2] Roldán E. et al. *Gait Posture* 58, 201–207, 2017; [3] Noyes FR, Grood ES. *J.Bone & Joint Surg. Am.* 58, 1074–1082, 1976. [4] Shino K. et al. *Am. J. Sports Med.*, 23, 203–208, 1995.

ACKNOWLEDGEMENTS: This research was funded by the Faculty of Science & Engineering, Manchester Metropolitan University.

Assessment of metabolic response to biochemicals and shear stress within a 3D tissue engineered Tenon's capsule + conjunctival model

R Gater[1], S Bodbin[1], D Nguyen[1,2], L Jones[3], AJ El Haj[1], Y Yang[1]

[1] Institute for Science and Technology in Medicine, School of Medicine, Keele University, UK.
[2] Mid Cheshire Hospitals NHS Trust. [3] University Hospitals of North Midlands NHS Trust.

INTRODUCTION: Glaucoma is a major cause of vision loss, leading to blindness in approximately 4.5 million people worldwide [1]. Surgical techniques such as trabeculectomy aim to treat glaucoma by increasing aqueous fluid outflow from the anterior chamber into the sub-conjunctival space, causing a reduction in intraocular pressure. However, fibrosis and wound healing occurring after these procedures can significantly reduce their success rate [2]. Therefore, more efficient anti – inflammatory agents are required to reduce fibrosis. This study uses a 3D Tenon's capsule + conjunctival tissue (TCCT) model to investigate the metabolic activity which may influence fibrosis after glaucoma surgery.

METHODS: TCCT fibroblasts were obtained from porcine eyes via enzymatic digestion using dispase and collagenase. Porcine aqueous humour from the anterior chamber was also isolated using a 23G needle. The TCCT model was constructed by incorporating the cells from passage 2 into 3mg/ml concentrated collagen hydrogels at a density of 8 x 10^5 cells/mL. After 24 hours, growth factors TGF-β1, TNF-α and VEGF were administered to the model via addition to the culture medium. Additionally, samples were administered with isolated aqueous humour at a concentration of 50% in culture medium. The effect of shear stress on TCCT fibrosis was also tested on samples by placing culture plates on a see-saw motion rocker at a speed of 5rpm for 1 hour per day during culture. Cellular proliferation and extracellular matrix synthesis was then recorded periodically for 2 weeks via alamarBlue® assay and neocollagen labelling. Actin (phalloidin) staining was also undertaken to assess actin expression.

RESULTS: TCCT fibroblast proliferation increased significantly with doses of TGF-β1, TNF-α and VEGF (50ng/ml), in comparison to the control. Furthermore, fibroblasts exposed to 50% aqueous humour had significantly increased proliferation and actin expression, as shown in figure 1. Shear stress induced mechanotransduction was also found to promote metabolic activity across experimental conditions.

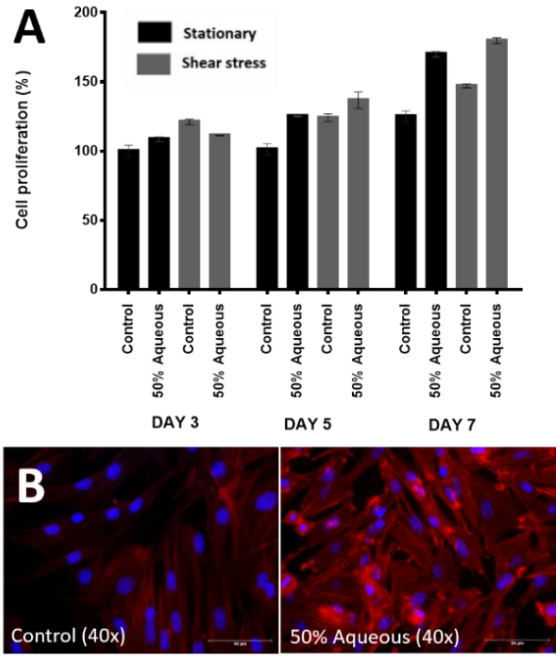

Fig. 1: (A) alamarBlue® assay results to indicate proliferation of 3D TCCT fibroblasts cultured in 50% aqueous humour, with and without exposure to shear stress. (B) Actin expression of 2D fibroblasts maintained in standard culture medium (left) and 50% aqueous humour (right).

DISCUSSION & CONCLUSIONS: A reliable and convenient 3D TCCT model has been developed to investigate the factors which may influence the metabolic activity of TCCT fibroblasts. Results indicate that a combination of growth factors and shear stress during aqueous fluid outflow are likely to influence the fibrosis and scar tissue formation in TCCT after glaucoma surgery.

REFERENCES: [1] World Health Organisation (2016) WHO | Priority eye diseases in *www.who.int/blindness/causes/priority/en/index6.html.* [2] C.H. Hong et al (2005) Glaucoma drainage devices: a systematic literature review and current controversies in *Surv Ophthalmol* **50**:48-60.

ACKNOWLEDGEMENTS: PhD studentship supported by the Keele University ACORN fund and Faculty of Health.

Atorvastatin effect on migration of endothelial cells and bone marrow stem cell homing in a wound model

Njoroge W[1], Harper A[1], Butley R[1,2], Sandhu K[2], Yang Y[1]

[1] *Institute of Science and Technology in Medicine (ISTM), Keele University.*

[2]Cardiology Department, University Hospitals of North Midlands, Stoke-on-Trent, ST4 6QG

INTRODUCTION: Statins are the standard prescription for lowering levels of circulating low density lipoprotein (LDL). Numerous studies have demonstrated positive effects of statins prior to an alteration of the lipid profile. These pleiotropic effects are believed to be associated with changes to the endothelial layer in blood vessels and associated progenitor cells. Given the ubiquity of statin use for the treatment of cardiovascular disease, the mechanisms behind the protective effects of statins need to be investigated.

METHODS: Human umbilical vein endothelial cells (HUVECs) and rat bone marrow stem cells (rMSCs) were used to evaluate a dose dependent migratory response to atorvastatin. The HUVECs were seeded at a density of $4x10^4$/well in a 48 well plate. A scratch wound was created on the confluent layer of HUVECs and exposed to atorvastatin at the following concentrations; 0, 30, 60, 80, 100, 120 and 140 µg/ml. The fluorescently labelled rMSCs were added at the same time as the addition of the drug with density of $5x10^3$/well. The extent of wound closure was evaluated after 24 hours using fluorescence microscopy. A comparative of cell numbers within the scratch wound was used for quantification. To evaluate atorvastatin effect on homing, a 3D blood vessel model (TEBV), incorporating the medial (smooth muscle cells-HCASMCs) and intimal layers (HUVECs), was lesioned with ferric chloride ($FeCl_3$). The TEBV was then incubated for 5 hours with 60µg/ml atorvastatin and perfused with human MSCs (hMSCs) and 60 µg/ml atorvastatin for 45 minutes at 15dyne/cm^2. Attachment of MSCs was observed using fluorescence microscopy.

RESULTS: There was a distinct effect of atorvastatin concentration on the size of the wound after 24 hours with peak infiltration of endothelial cells occurring at 120 µg/ml. This trend was similar in the rMSCs. The elevated cell counts observed at 120 and 140 µg/ml were not associated with complete wound closure as was observed at 60 µg/ml, but rather a clustering of cells towards the centre of the well (Figure 1, $P<0.05$). There was an increased density of attached cells (hMSCs) on the surface of the lesioned TEBV after incubation and perfusion with atorvastatin, versus without, under the same conditions (Figure 2). This suggests atorvastatin enhances homing of cells to sites of injury. Specific contributing factors to this observation are currently under investigation.

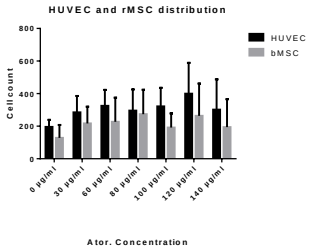

Fig. 1: HUVEC and rMSC distribution in scratch wound after 24hrs.

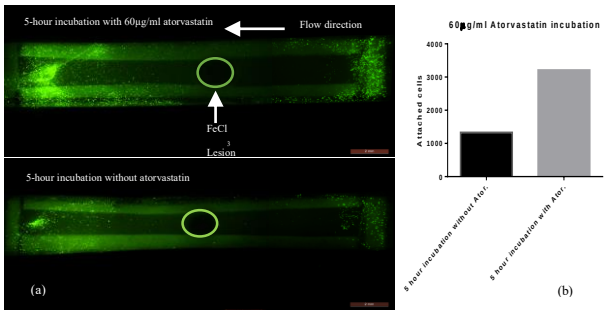

Fig. 2: Effect of 60µg/ml atorvastatin on (a) hMSC (green) attachment on lesioned TEBV. (b) quantification of attached hMSCs.

DISCUSSION & CONCLUSIONS: Incubation of HUVECs and rMSCs with atorvastatin impacted rate of migration, proliferation and density of homing of these cells and induces faster wound closure. This is possibly due to modulated chemokine production or an enhanced cytokine response within these cells.

REFERENCES: Sandhu, K., Mamas, M. and Butler, R. (2017). *Endothelial progenitor cells: Exploring the pleiotropic effects of statins*. World Journal of Cardiology, 9(1), p.1. Chamberlain, G., Smith, H., Rainger, G. and Middleton, J. (2011). *Mesenchymal Stem Cells Exhibit Firm Adhesion, Crawling, Spreading and Transmigration across Aortic Endothelial Cells: Effects of Chemokines and Shear*. PLoS ONE, 6(9), p. e25663.

Bio-printing self-assembled peptide hydrogels / cells constructs

VL Workman[1], AF Miller[3], A Saiani[1]
[1]*School of Materials,* [2]*School of Biological Sciences,* [3]*School of Chemical Engineering and Analytical Sciences, The University of Manchester, UK*

INTRODUCTION: Bio-printing/bio-fabrication has become a promising approach to design and manufacture complex cell-laden structures. One of the main challenges remains the development of bio-inks that allow the printing of 3D cell-laden constructs. Usually bio-ink requirements include high viscosity, high yield stress and rapid gelation that tend to be antagonistic to cell survival, migration and neo-tissue formation. Recently self-assembling peptide (SAP) hydrogels have come to the forefront as potential bio-inks due to their ability to sustain the growth of a large variety of cells in 3D as well as their unique shear-thinning and recovery properties [1].

METHODS: SAP hydrogels were purchased from PeptiGelDesign.Ltd (UK) as well as formulated in-house depending on required peptide design and gel characteristics. Hydrogels were 3D-printed using a variety of pressure driven extrusion based bio-printers including 3D Discovery (regenHU, Switzerland) and Fisnar Intertronics (UK) F7000N Dispensing Robot.

RESULTS & DISCUSSION: One of the main downside of SAP hydrogels is their weak mechanical properties and their tendency to break or creep under stress. In order to construct 3D large scale structures novel approaches need to be developed. In a first project we used a sacrificial hydrogel that can be washed away with water at pH 7 and designed a SAP that gels at pH 7 to bio-print a large scale structure using a gel-in-gel printing approach (Fig 1).

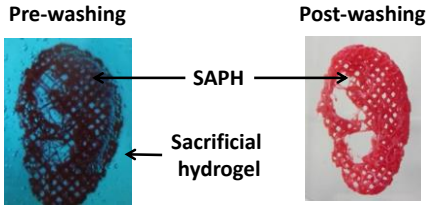

Fig. 1: Left: Structures printed with a SAP hydrogel, within a sacrificial hydrogel. Right: SAP hydrogel structure left after washing the sacrificial gel at pH 7 [In collaboration with Dr C. De Maria, University of Pisa]

Subsequently in order to show that our SAP hydrogels allow the printing of cell-laden scaffolds, mouse mammary epithelial cells (EpH4) were bio-printed [2]. After 24hrs of culture within the printed hydrogel, cells were seen to be homogenously distributed and viability was good (Fig 2). Low viability was seen on the edge of the gel "tube" where shear stress is highest due to the proximity of the syringe wall.

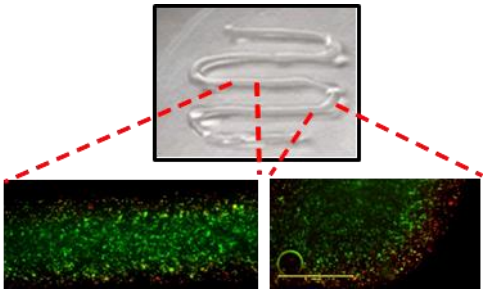

Fig. 2: Live/Dead images of EpH4 mouse mammary epithelial cell 24hrs after bio-printing in SAPH with a 3D Discovery printer. [In collaboration with Drs D. Kumar, M. Domingos and Prof C. Streuli, University of Manchester]

Finally high aspect ratio villus structures were fabricated by direct printing SAP hydrogels onto transwell membranes to replicate the structures lining the apical side of the gastrointestinal tract (Fig. 3). These structures were then seeded with Caco-2 cells.

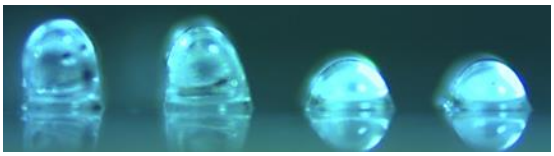

Fig. 3: Images of villus structures fabricated from SAPH using a Dispensing robot. [In collaboration with Prof C. Mills and Ms H. Mattar, University of Manchester]

CONCLUSIONS: Using different bio-fabrication procedures and equipment a variety of structures have been formed. This work shows the potential of SAP hydrogels as bio-inks for the bio-printing/bio-fabrication of complex cell-laden structures that could be used in a variety of applications from tissue engineering to drug testing.

REFERENCES: [1]S. Wan et al (2016) *Acta Biomater.* **46**:29-40 [2]B. Raphael et al (2017) *Mater. Lett.* **190**:103-106.

ACKNOWLEDGEMENTS: The authors acknowledge EPSRC Fellowship EP/K016210/1 for funding.

Blended electrospinning provides new environments for liver tissue engineering

R Grant[1], J Hallet[2], S Forbes[2], D Hay[2], A Callanan[1]

[1]*Institute for Bioengineering, School of Engineering, The University of Edinburgh, Scotland.*
[2]*Scottish Centre for Regenerative Medicine, The University of Edinburgh, Scotland.*

INTRODUCTION: A combination of increasing liver disease incidence and a shortage of organs available for patient treatment and research[1] has led to a need for liver 'organoids'. Biofunctionalization of electrospun polymer scaffolds with cell-derived extracellular matrix [ECM] has been shown to influence hepatocyte function[2,3], With this in mind we created blended protein/polymer scaffolds – directly incorporating bioactive proteins into electrospun polylactic acid [PLA] fibrous scaffolds. We demonstrated that hLECM has an influence on hepatocytes which cannot be recapitulated by individual ECM components, confirming that there is a complex and not fully understood relationship between cells and the native extracellular matrix.

METHODS: Scaffolds were fabricated containing each of the following; Collagen I [hBTC1], Fibronectin [hFN], Laminin-521 [hRL521] and decellularized whole human liver ECM [hLECM]. Decellularized tissue was obtained following 4 hours of perfusion decellularization of human liver tissue using 0.5% sodium dodecyl sulphate [SDS]. THLE-3 cells were seeded onto the scaffolds and assessed for survival and function at 5, 10 and 16 days using scanning electron microscopy [SEM], mechanical and biochemical quantification, histology, and gene expression analysis.

RESULTS: Results indicate that the incorporation of proteins into the scaffold influences cell survival and function, with alterations in albumin production and gene expression between conditions observed.

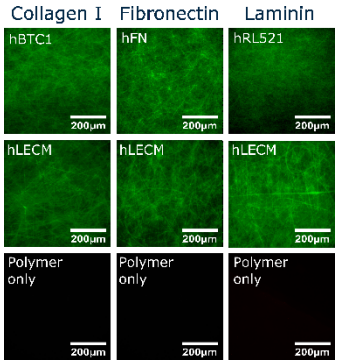

Figure 1; Staining for each ECM components clearly demonstrates the presence of each protein in the scaffolds, with none observed in the polymer only control

Figure 2; Cell titre blue [A] results demonstrate the metabolic viability of the THLE3 liver cells on each scaffold until 16 days

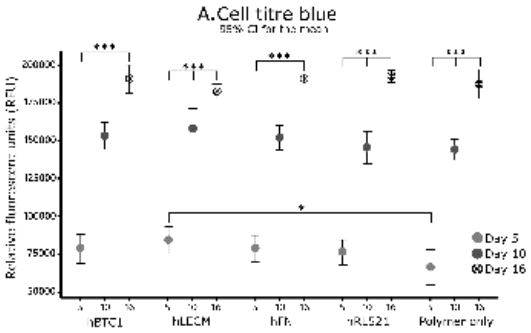

Figure 3; Albumin production also increases over time on the scaffolds, with significant differences observed.

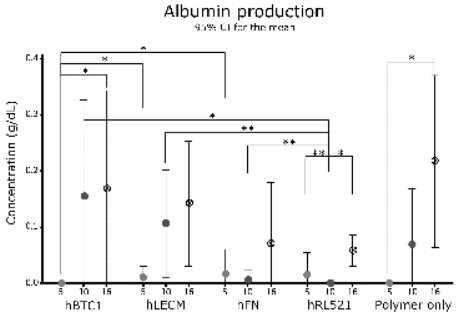

DISCUSSION & CONCLUSIONS: Our results demonstrate a method of incorporating proteins directly into a scaffold environment and of making impactful use of a valuable tissue resource which would otherwise be wasted. Protein:polymer scaffolds containing human liver ECM exert a significant positive influence on the gene expression profile, albumin production, attachment, and survival of liver cells which cannot be recapitulated by individual ECM components. These scaffolds show great potential not only for the future of liver tissue engineering and patient treatment, and are easily adaptable for other organs and tissues.

REFERENCES: 1. Williams, R. et al. Lancet 384, 1953–1997, 2014. 2. Takebe, T. et al. Cell Stem Cell 16, 556–565, 2015. 3. Grant, R., Hay, D. & Callanan, A. Tissue Eng. Part A [2017].

ACKNOWLEDGEMENTS: We are grateful to the donors and NHS staff who enable this research. This work is funded by; EPSRC doctoral training partnership, UKRMPII grant MR/L022974/1 and MRC CCBN grant MR/L012766/1.

BMP-2 localisation in nanoclay containing hyaluronic acid hydrogels enhances osteoinduction

Yang-Hee Kim[1], Dmitri Ossipov[2], Stuart Lanham[1], Jöns Hilborn[2], Richard O.C. Oreffo[1], Jonathan I. Dawson[1]

[1] Bone and Joint Research Group, Centre for Human Development, Stem Cells and Regeneration, Institute of Developmental Sciences, University of Southampton, UK. [2] Science for Life Laboratory, Department of Chemistry, Uppsala University, Sweden

INTRODUCTION: Hydrogels are extensively used as carriers for bioactive molecules, such as growth factors. Bone morphogenetic protein-2 (BMP-2) is licensed for spinal fusion and well known as a potent growth factor capable of inducing bone formation, however the high doses necessary for efficacy have complicated and limited clinical application. We have previously demonstrated the potential of hyaluronan (HA) hydrogels functionalized with bisphosphonate ligands to achieve slow release of BMP-2 [1]. Laponite nanoclay particles (LAP) display a high affinity for BP ligands and, furthermore, can also bind BMP-2 to localize its activity for enhanced bone induction [2, 3]. We hypothesized that functionalizing HABP gels with LAP (HABP-LAP) will further retard BMP-2 release and modify *in vivo* bone induction.

METHODS: We prepared HABP, LAP, and HABP-LAP gels incorporating lysozyme, a widely used model protein for BMP-2, and incubated the gels in PBS for 7 days. At each time point (1, 2, 6 hours, and 1, 3 and 7 days), we collected the supernatant and measured the concentration of lysozyme, HA and LAP released into the media. For *in vivo* release evaluation, we prepared HABP, LAP, and HABP-LAP gels incorporating fluorescent (Cy7) labelled lysozyme and subcutaneously implanted them in mice. Scans were taken via an *in vivo* imaging system at day 0, 3, 7, 14, 21, and 28. In order to evaluate bone formation ability, the HABP, LAP, and HABP-LAP gels incorporating BMP-2 (5 µg/ml) were implanted into subcutis of mice. At week 0, 2, 4, and 6, the mice were scanned using micro-computed tomography (µ-CT, Skyscan 7760) and bone mineral density and bone volume calculated.

RESULTS: *In vitro*, analysis confirmed 16% and 24% of lysozyme was released from LAP and HABP gels respectively after 24 hours incubation, compared with only 2% from HABP-LAP gel. *In vivo*, negligible fluorescence was observed in HABP gels 24 hours post implantation. However, Cy7 was apparent after 1 week in LAP and after 4 weeks in HABP-LAP gels. Following subcutaneous implantation of gels with BMP-2, bone mineral density and bone volume were observed to significantly increase over time in the presence of BMP-2 across treatments. Importantly, HABP-LAP gels incorporating BMP-2 showed a significantly higher bone volume compare to HABP and LAP gels ($P < 0.0001$).

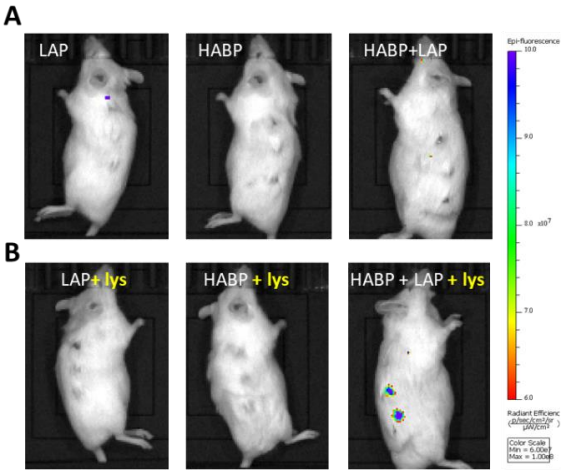

Fig. 1: In vivo imaging of un-(A)/fluorescent-labelled (B) lysozyme (lys) in mice at 4 weeks after implantation of gels.

DISCUSSION & CONCLUSIONS:

We have demonstrated that nanoclay functionalization of HABP hydrogels sustains the localized presence of encapsulated proteins for sustained periods *in vivo*. Consequently, HABPLAP gel incorporating BMP-2 enhanced bone formation. This study demonstrates the importance of sustained localized presentation of growth factors for enhanced regenerative responses.

REFERENCES: [1] Hulsart-Billstrom G, et al. (2013) *Biomacromolecules* **14**(9):3055-63. [2] Gibbs DM, et al. (2016) *Biomaterials* **99**:16-23. [3] Dawson JI, et al. (2013) *Adv Mater.* **25**(30):4069-86.

ACKNOWLEDGEMENTS: Thank Dr Janos Kanczler (Bone and Joint Research group, University of Southampton) for the animal experiment support. Funded by an EPSRC fellowship (grant number EP/L010259/1).

Can we identify altered biological pathways and novel candidate biomarkers in individuals who do not respond clinically following Autologous Chondrocyte Implantation?

Charlotte H Hulme[1,2], Emma Wilson[2,2], Heidi R Fuller[1], Sally Roberts[1,2], James Richardson[1,2], Pete Gallacher[2], Mandy Peffers[4], Sally Shirran[5], Catherine Botting[5], Karina T Wright[1,2]

[1]Institute for Science and Technology in Medicine , Keele University, UK. [2]Robert Jones and Agnes Hunt Orthopaedic Hospital, Oswestry, UK. [3]Chester Medical School, Chester University, UK. [4]Institute of Ageing and Chronic Disease, University of Liverpool, UK. [5]BSRC Mass Spectrometry and Proteomics Facility, University of St Andrews, UK

INTRODUCTION: Autologous Chondrocyte Implantation (ACI) is a National Institute of health and Care Excellence (NICE) recommended treatment for chondral/osteochondral defects of the knee. ACI involves two surgical stages. Initially (Stage I) healthy cartilage is harvested from the joint for extracting and culture expanding chondrocytes for 3-4 weeks in a GMP laboratory. In a second surgery (Stage II), these chondrocytes are implanted into the cartilage defect under a commercial collagen membrane. We have demonstrated that ACI is not clinically effective in all patients (1), therefore a better understanding of the biological mechanisms underlying treatment success/failure is needed to aid patient stratification.

METHODS: Two independent proteomic approaches were applied to holistically assess the proteome of synovial fluid (SF) collected from 14 ACI responders (Stage I, n=8; Stage II, n=12) and 13 non-responders (Stage I, n=7; Stage II, n=12), immediately prior to the two stages of surgery. Response was determined by change in Lysholm score at 12 months (the Lysholm is a scale of 0-100; 100 represents a 'perfect' functioning knee); mean improvement was 33 points (range 17-54) in responders and mean worsening was 14 points (range 4-46) in non-responders. Isobaric tag for relative and absolute quantitation (iTRAQ) LC-MS/MS and label-free quantitation (LF) LC-MS/MS of dynamically range compressed (ProteoMiner^{TM}) SFs were used to assess the proteome of high and low abundance proteins, respectively (2,3). Biological pathways associated with proteome changes were identified using network ontology analysis (Ingenuity). Candidate protein biomarkers were biochemically validated in these patients using ELISA (R&D Biosystems).

RESULTS: There was a marked proteome shift between Stages I and II of ACI with 84 and 115 differentially abundant (≥2.0 fold) proteins identified in responders and non-responders, respectively. Acute phase response signalling was the biological pathway most significantly associated with response to Stage I surgery (p=1.10x10-9; Fisher's Exact), in those who did not improve clinically. Twenty-two of the 39 proteins that were bioinformatically predicted to be increased in the fluid during the acute phase response were more abundant (≥1.2 fold) in the SF at Stage II compared to Stage I. Further, two of the ten proteins that were predicted to be downregulated demonstrated decreased abundance in the SF at Stage II compared to Stage I. Three candidate biomarker proteins that demonstrated significantly differential abundance at Stage II compared to Stage I in non-responders were further assessed. Biochemical validation confirmed that matrix metalloproteinases (MMP)-1 and -3 were increased (MMP-1, p=0.006; MMP-3, p=0.002, Mann-Whitney U) and S100 calcium binding protein was decreased (p=0.02, Mann-Whitney U) at Stage II cf. Stage I in ACI non-responders.

DISCUSSION & CONCLUSIONS: Acute phase response signalling has been identified as a functional pathway, which is associated with the marked proteome shift that exists in response to cartilage harvest in patients who do not clinically improve following ACI. The acute phase response is the first systemic reaction to surgery or trauma indicating that clinical non-responders may have a greater/abnormal innate response to cartilage biopsy or cartilage injury initial surgery. Further, we have identified 3 novel candidate biomarkers that have the potential to inform as to a patients' suitability to proceed to the Stage II procedure for completion of ACI treatment.

REFERENCES: 1. Wright et al. (2016). Am J. Sports Med. 2. Hulme & Wilson et al. (2017). Arth Res Ther. 3. Hulme et al. (2018). Arth Res Ther.

ACKNOWLEDGEMENTS: ARUK grants 19429, 20815 & 21122. The Wellcome Trust [094476/Z/10/Z] funded the TripleTOF 5600 MS at the BSRC Mass Spectrometry Facility and MJP through a Clinical Intermediate Fellowship.

Cartilage tissue engineered scaffolds: A multizone approach

N. Munir, A. Callanan

Institute for Bioengineering, *School of Engineering, University of Edinburgh, United Kingdom*

INTRODUCTION: Osteoarthritis is predicted to become the fourth leading cause of disability by 2020[1]. Tissue engineered scaffolds have shown promise in the field of cartilage tissue engineering. Recent research has been focusing on integrating scaffold fabrication techniques in order to overcome challenges including adequate mechanical properties, effective nano- and sub-micrometer structures, zonal architecture and physiological levels of ECM formation[2-3]. The present study combined cryo-printing and electrospinning to create functional multizone scaffolds which capture the zonal architecture of the native cartilage. Moreover, articular cartilage is able to adapt to the amount of mechanical loading and has an important role in transmission, bearing, distribution and absorption of applied loads[4]. Thus, the current study also investigated multi axial compressive properties to analyse the load transmission as well as the biochemical properties of multizone scaffolds.

METHODS: Multizone scaffolds consist of three different zones. The bottom helix scaffold was fabricated using cryo-printing, which involves printing of an 8% w/v Polycaprolactone (PCL)/1, 4-Dioxane solution directly onto a cold plate set at -40°C. The middle and top electrospun layers are composed of randomly orientated and aligned electrospun fibres, respectively (8% w/v PCL and HFIP). Multizone scaffolds were seeded with primary human chondrocytes and cultured for 24 hours, 1, 3 and 5 weeks. Electrospun (ESP) and directionally frozen (D/F) scaffolds were used as controls. Scaffold morphology was assessed using scanning electron microscope (SEM). Multi-axial mechanical, biochemical quantification and gene expression were analysed at all time points.

RESULTS: Multizone scaffolds successfully captured the zonal architecture of the native cartilage (Fig 1A). Moreover, these scaffolds supported cell attachment and viability (Fig 1B and C) and demonstrated improved multi-axial mechanical properties compared to the directionally frozen control. Trends in the expression of key genes and DNA quantification were also examined.

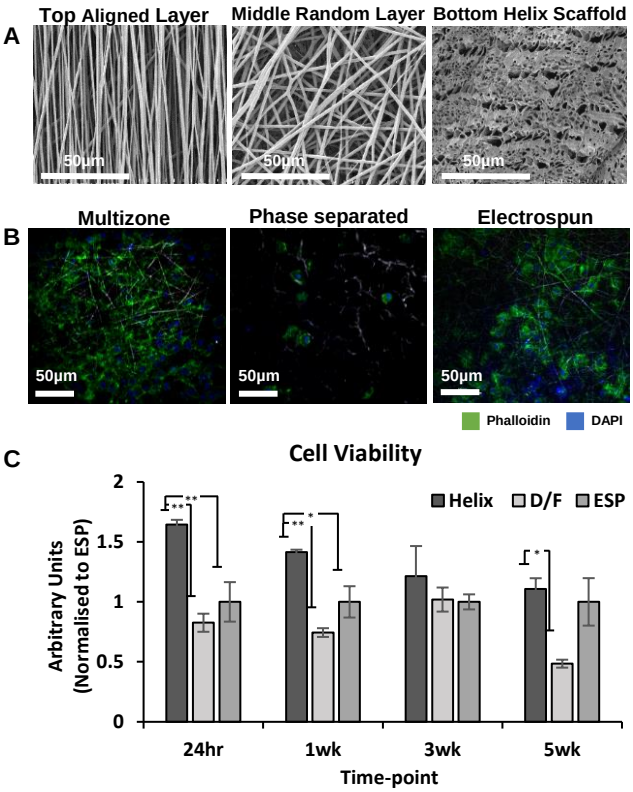

*Fig. 1: (A) SEM images of multizone scaffolds layers. (B) Fluorescence imaging of scaffolds. (C) Cell viability of seeded scaffolds, values normalised to ESP control. Error bars=SE, n=4. *p<0.05, **p<0.01; one-way ANOVA.*

DISCUSSION & CONCLUSIONS: Multizone scaffolds displayed interesting multi-axial compressive properties. Moreover, they supported long-term chondrocyte attachment with expression of key genes and the production of essential chondrogenic biomolecules, glycosaminoglycans, highlighting their potential in cartilage tissue engineering.

REFERENCES: [1] T. Lu et al (2013) International *Journal of Nanomedicine*. **8**: 337-350. [2] S. Reed et al (2016) *Biofabrication.* **8**: 1-16. [3] J. A. M. Steele et al (2013) *Acta Biomaterialia*. **3**: 1-13. [4] M. Giuseppe (2016) *Journal of Functional Morphology and Kinesiology*. **1**: 154-161.

ACKNOWLEDGEMENTS: EPSRC (EP/N509644/1) and MRC grant MR/L012766/1. Many thanks to Alison McDonald for fluorescence imaging.

Characterisation of microstructural, mechanical and biological properties of a novel fibrin-based bio-intelligent scaffold for in situ skin tissue engineering

C Inverarity[1], J Cuenca[2], D Banks[1], M Bootman[1], M Khoury[2], JF Dye[3]

[1] *Dept. of Life, Health and Chemical Sciences, The Open University, Milton Keynes, UK.* [2] *Center for Regenerative Medicine, Universidad de Los Andes, Santiago, Chile.* [3] *Tissue Engineering & Bioprocessing Group, Dept. of Engineering Science, University of Oxford, UK*

INTRODUCTION: Chronic wounds affect over 200,000 [1] people in the UK. Their management costs the NHS £3bn/year [2]. Various cell therapies offer great potential for stimulating healing but a physical environment is needed for tissue reconstruction. Biomaterial scaffolds, exhibiting particular mechanical, biological and structural properties, can provide such functionality. They must support cell ingress and withstand the demanding in vivo environment. This is especially true of chronic wounds, where scaffolds must withstand enzymatic degradation by elevated levels of enzymes secreted by neutrophils such as elastase and matrix metalloproteinases [3]. Here, novel fibrin-based scaffolds intended for in situ skin tissue engineering substrates are described and characterised

METHODS: Highly porous fibrin scaffolds were manufactured to obtain differential microstructures (method confidential). This variety was achieved by varying material composition or method of mixing. The effect of cross-linking and addition of a specific polymer ("P*x*") on scaffold functionality was examined. The effect of the secondary co-polymer on microstructure was determined by scanning EM imaging of the lyophilised scaffolds.

Tensile testing (Instron 5582 UTM) was used to examine the effect of both microstructure (pore size and size distribution) and the presence co-polymer on the tensile strength of the fibrin scaffolds, both in lyophilised and rehydrated forms.

Cytotoxicity and proliferation of MSC was measured using the CCK-8 reagent.

RESULTS: Increasing P*x* concentration (0.2-2%) has a large effect on microstructure. At low concentrations, a hierarchical fibrous structure is evident (Fig. 1) but at higher concentrations, P*x* adheres to the fibrin framework and closes up the nano-scale structure.

Cross-linking fibrin increases mechanical strength and resistance to mechanical degradation at the cost of elasticity and flexibility. However, addition of P*x* increases elasticity, even at very low concentrations.

CCK-8 indicated no cytotoxic effect, with scaffold populations comparable to the 2D plate control after 120h.

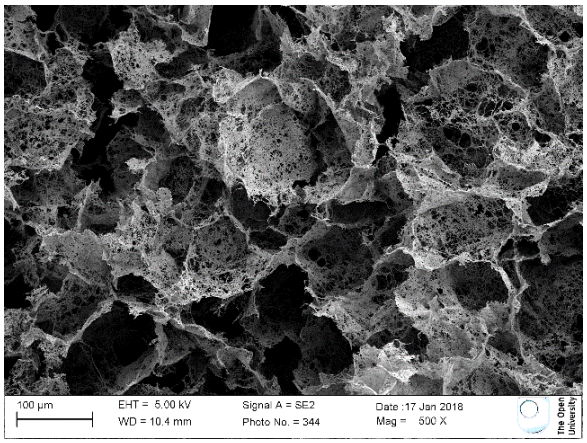

Fig. 1: SEM cross-sectional micrograph of a lyophilised fibrin-based scaffold, containing 0.2% Px, showing rounded, highly interconnected pores and a hierarchical fibrous structure.

DISCUSSION & CONCLUSIONS: Porous biocompatible scaffolds have a complex microstructure, which affects mechanical and biological properties. Understanding the interplay between manufacturing parameters allows fabrication of a scaffold with a specific set of properties for optimised performance.

Optimising P*x* content and cross-linking produces a strong, flexible biocompatible scaffold with low shrinkage, suitable biodegradation and excellent handling capabilities (when dried and rehydrated).

The method and materials used are cost-effective and scalable, making the scaffold suitable for clinical and commercial use.

REFERENCES: [1] J. Posnett and P. Franks (2008) *Nurs Times* **104**: 44. [2] J.F. Guest, K. Vowden and P. Vowden (2017) *J Wound Care* **26**: 292-303. [3] A.H. Annor, M.E. Tang, C.L. Pui et al (2012) *Surg Endosc* **26**: 2767-2778.

ACKNOWLEDGEMENTS: This project is funded by The Open University and Consorcio Regenero/Cells for Cells, and hosted by IBME at the University of Oxford.

Characterisation of Quantum® Expanded Human Mesenchymal Stromal Cells Derived From Bone Marrow & Umbilical Cord.

Claire Mennan[1,2], John Garcia[1,2], Charlotte Hulme[1,2],
Sally Roberts[1,2], James Richardson[1,2], Karina T Wright[1,2]

[1]Institute for Science and Technology in Medicine, Keele University, UK. [2]Robert Jones and Agnes Hunt Orthopaedic Hospital, Oswestry, UK.

INTRODUCTION: The Quantum® bioreactor (Terumo BCT) is an automated hollow fibre system, which has an internal surface area of 2.1m^2, allowing for large scale expansion of monolayer cells. The purpose of this study was to comprehensively characterise mesenchymal stromal cells (MSCs) from human bone marrow (BM) and umbilical cord (UC) after expansion in the system and compare them to cells grown on tissue culture plastic (TCP).

METHODS: Quantum® fibres were coated with human cryoprecipitate prior to cell seeding to enable cell adherence. The Quantum® was loaded with 20ml of bone marrow and BM-MSCs were harvested and characterised at the end of the first passage and also after a second expansion in the system after re-seeding 5-10M BM-MSCs. A 'hybrid' process was used for UC-MSCs, whereby cells were expanded first on TCP as described previously (1) and within 14 days 5M UC-MSCs were loaded into the Quantum® system.

Flow cytometry was used to assess the MSC immunoprofile (2) of each Quantum and TCP cell product, as well as a panel of chondrogenic markers, CD44, CD166, CD49c, CD39, CD151, CD271, FGFR3 and ROR2. Immunomodulatory markers, CD40, CD80, CD80, HLA-DR, CD317 and CD106, were also assessed before and after inflammatory stimulation (+25ng/ml IFN-g). Quantum and TCP cultured BM-MSCs were also investigated using a panel of integrin markers and macrophage markers (Quantum only) at P1. Further, each Quantum product was assessed for immunomodulatory gene expression profiles and trilineage capacity (3). Telomere lengths of donor matched cells grown in the Quantum and on TCP were compared as described previously (4) and cells are also being used in a murine joint surface injury model (collaborators Professor Cosimo De Bari and Dr Anke Roelofs) to assess their ability to repair cartilage *in vivo* (data not shown).

RESULTS: The mean BM-MSC harvest after passage 1 was 23±16M cells in 14±1.5 days. After seeding 10M cells, at passage 2, the mean cell harvest was 131±84M cells in 13±1 days.

The mean UC-MSC harvest after passage 1 in the Quantum was 168±52M cells in 7.7±2 days. Cell imaging and flow cytometry analyses indicated a 15-30% macrophage contamination in the Quantum BM-MSC cultures at passage 1. Following a second expansion in the Quantum macrophages were no longer detected. All Quantum expanded populations demonstrated trilineage potential. BM-MSCs and UC-MSCs cultured in the Quantum and on TCP displayed similar immunopositivity for cell surface markers indicative of MSCs, immunomodulatory potential and chondrogenic potency.

Analysis of telomere length showed that the shorter cell doubling times seen in the Quantum cultures did not cause shortened telomeres for UC-MSCs when compared to those grown on TCP.Results for BM-MSCs were inconclusive. Immunomodulatory gene expression profiles were variable between different patients but showed that Quantum expanded MSCs retained the ability to up-regulate genes for potentially therapeutic proteins such as indoleamine 2,3-dioxygenase (IDO). Flow cytometry and live cell imaging indicated that Quantum® expanded BM-MSCs and UC-MSCs at second passage adhered to the ISCT criteria for MSCs and had comparable chondrogenic potency and immunomodulatory immunoprofiles before and after pro-inflammatory stimulation.

DISCUSSION & CONCLUSIONS: These preliminary results suggest that the Quantum system can be used to expand large numbers of MSCs from BM and UC tissues. Further *in vitro* and *in vivo* work will establish the potential of these cells for use in orthopaedic allogeneic cell-based therapies for cartilage repair.

REFERENCES: 1. Mennan et al. (2013). Bio Med Res Int. 2. Dominici et al. (2006). Cytotherapy. 3. Johnstone et al. (1998). Exp Cell Res. 4. Mennan et al. (2016) FEBS Open Bio.

ACKNOWLEDGEMENTS: Arthritis Research UK grants 19429, 20815 & 21122. With thanks to Brent Rice of Terumo BCT for technical support.

Comparing methods to reliably and reproducibly characterise fibre orientation

S N Beal,*[1,2] P V Hatton[1], M Placzek[2] & I Ortega[1]

[1]School of Clinical Dentistry, University of Sheffield, UK, [2]Department of Biomedical Science, University of Sheffield, UK

INTRODUCTION: Electrospinning is utilised to manufacture fibrous scaffolds, which can be powerful tools for the creation of intricate 3D *in vitro* models as well as for the development of medical devices for regenerative medicine. Electrospinning is a versatile method that allows for the control of fibre diameter and orientation. Recent research has suggested that fibre orientation can influence cell behaviour[1], however, there is a still a need for the development of reliable and reproducible methods to quantify this property. This study therefore compares two methods to determine the level of fibre alignment present within a scaffold in order to determine the most appropriate approach prior to investigating cell response.

METHODS: Electrospinning was used to manufacture PCL scaffolds (Sigma, UK, for preliminary study and Corbion, The Netherlands). Collection of fibres onto a flat plate produced randomly orientated fibre mats while collection onto a drum introduced fibre alignment. Attachment of metallic templates (Fig 1D) onto the flat plate allowed the incorporation of complex features into the mat. Scaffolds were imaged at high power to visualise fibres using scanning electron microscopy (SEM). Fibres were then characterised either by automatic software (Lambda Photometics, UK) or a manual method which uses ImageJ (Fiji[2]). Statistical analysis was performed using ANOVA.

RESULTS: Electrospun meshes were reproducibly manufactured with random and aligned fibres orientations (Fig 1). Utilising metallic templates complex microfeatures were introduced to produce complex meshes in which both random and aligned fibres were located within the same scaffold. The determination of fibre alignment was achieved by both the automatic and manual methods. Both methods showed a statistically significant difference between random and aligned fibres ($p<0.0001$). The automatic method was capable of collecting a large data set (200 fibres) in a short time frame (seconds), while the manual method produced a smaller data set (10 fibres) in a longer time frame (15 minutes). However, the automatic method also had limitations, such as it could not always distinguish between several close fibres and collected data as one large fibre. Fibre diameter was also characterised for the random and aligned scaffolds via both automatic and manual methods. Work is in progress to investigate how changes in fibre orientation can influence neural stem cell behaviour (alpha-tanycytes of the vertebrate hypothalamus).

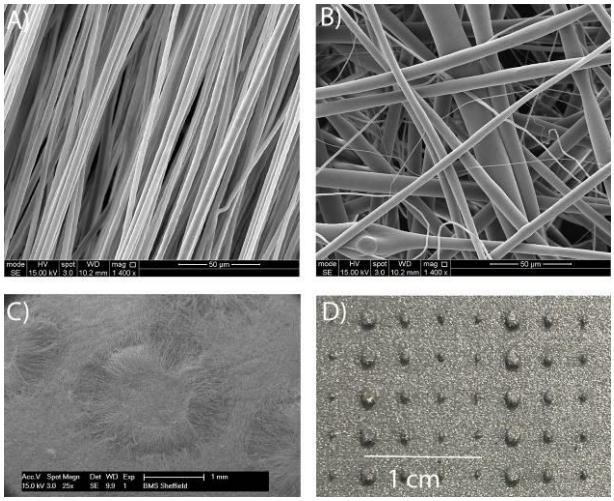

Fig. 1: Electrospun scaffolds. A) Random scaffold and B) Aligned scaffold made with Corbion PCL. C) A microfeature introduced by metallic templates D).

DISCUSSION & CONCLUSIONS: Both the automatic and manual methods have benefits and limitations. Both have shown their reproducibility and ability to measure fibre orientation. The automatic method is recommended due to its benefits in terms of scale and time however, the manual method is an equally effective alternative. Should the software not be available, the manual method provided a reliable and cost-effective alternative to characterise the fibre properties of a mesh. This characterisation of the fibre properties of a scaffold is essential prior to the investigation of differences in cell behaviour in response to these morphological features.

REFERENCES: [1] TJ Sill and H A Von Recum (2008) *Biomaterials.* **29**:1989-2006. [2] J Schindelin, I Arganda-Carreras, E Frise, et al. (2012) *Nature Methods.* **9**:676–82.

ACKNOWLEDGEMENTS: The University of Sheffield for financial support. MeDe Innovation (Grant no: EP/K029592/1) for financial contribution and The Electrospinning Company for collaboration.

Composite auxetic scaffolds show potential for use in tissue engineering

P Mardling[1], N Jordan-Mahy[1], A Alderson[1], P Godbole[2], CL Le Maitre[1]

[1]Sheffield Hallam University, UK, [2]Sheffield Children's Hospital and Pioneer Healthcare, UK.

INTRODUCTION: Tissue engineering scaffolds for regenerative medicine have to withstand a variety of loading conditions, as well as support and stimulate cell growth. Natural biological tissues display auxetic properties where upon stretching they become thicker which corresponds with a negative Poisson's ratio. A porous auxetic scaffold has the potential to mimic the properties of natural tissue which would enable a more natural environment to support cells for eventual use in tissue engineering.

This study aimed to investigate the possibility of composite auxetic scaffolds to create a laminar structure and support human smooth muscle cells (SMC) and human mesenchymal stem cell (HMSC) adhesion and growth.

METHODS: Auxetic scaffolds were manufactured from polyurethane foam (Custom Foams) using a previously developed thermo-mechanical technique under tri-axial compression [1]. The auxetic properties of the foams were assessed using an Instron 3367 and the Poisson's ratio was calculated. The foams were cut into 12mm outside diameter x 2mm cylinders and sterilised. Cylinders were coated with fibronectin (50µg/cm^3). SMC cells were suspended in pNIPAM-Laponite hydrogel (1C10) at 4 x 10^6 cells/ml at 37°C. The hydrogel was absorbed into the foam and set at by lowering the temperature below 32°C. HMSCs were then layered onto the upper surface of the scaffold. Scaffolds were cultured in low adhesion plates under standard conditions for up to 6 weeks. Samples were sectioned at 10µm for H & E analysis. Replicate foams were snap-frozen and freeze dried overnight, before Scanning Electron Microscopy (SEM) was used for analysis of pore structure/size and cellular localisation within the auxetic foams.

RESULTS: Polyurethane foams were successfully converted to gain auxetic properties demonstrated by the gaining of a negative Poisson's ratio when compared to the unconverted control. SEM images show the change in the pore structure of foams before and after conversion (Fig.1a-b). Haematoxylin and eosin stained sections demonstrated hydrogel was incorporated into the foam (Fig. 1c) and the composite scaffold supported the adherence and growth of SMCs which were suspended within the hydrogel, demonstrated by growth of cellular layers/clusters (Fig. 1d). Fluorescent images of Hoechst stained sections showed cell nuclei with low levels of auto-fluorescence within the hydrogel (Fig. 1e-f).

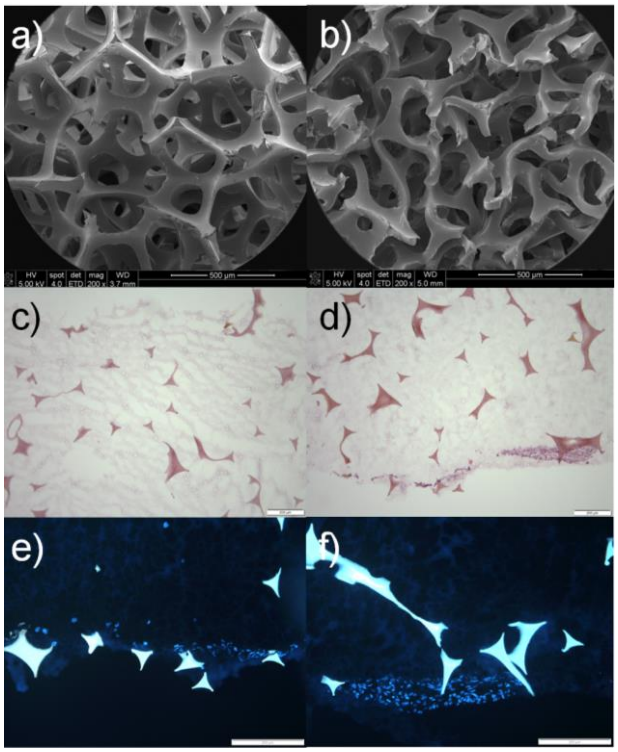

Fig.1: SEM images demonstrating alteration of pore structure of a) unconverted and b) converted foams. Brightfield images of haematoxylin and Eosin stained 10µm sections of c) acellular controls and d) cell seeded constructs. e) & f) Fluorescent images of hoechst stained sections of cell seeded constructs. (Scale bar a-b 500µm, c-f 200µm)

DISCUSSION & CONCLUSIONS: This study has shown, that a composite auxetic scaffold can be utilised to support the growth of cells in a laminar configuration, and allows multilayers of cells to be cultured. Such a system has potential for use in tissue engineering applications of tissues where multiple layers are seen such as epithelial layers.

REFERENCES: [1] A. Sanami *et al*, (2014), Smart materials and Structures, (23), 1-13.

ACKNOWLEDGEMENTS: This work was supported by a grant from Sheffield Children's NHS Foundation Trust, Sheffield Hallam University and Pioneer Healthcare.

Developing 3D neurovascular unit co-culture models to investigate Alzheimer's disease related neurovascular dysfunction

G Potjewyd[1-3], S Moxon[1], T Wang[2], M Domingos[3], N Hooper[1]

[1] Division of Neuroscience and Experimental Psychology, [2] Division of Evolution and Genomic Sciences, [3] Manchester Institute of Biotechnology (MIB), The University of Manchester, Manchester, UK.

INTRODUCTION: The neurovascular unit (NVU) consists of the neural and vascular components of the brain, which interface at the blood-brain barrier [1]. NVU dysfunction has been implicated in Alzheimer's disease pathology; with altered transport of Aβ protein and reduced expression of endothelial junction proteins and glucose transporters [2]. To investigate underlying mechanisms of NVU dysfunction there is a need to replicate the *in vivo* physiology of the brain *in vitro*, with 3D architecture and cell-cell cross talk. In this study, NVU cells are co-cultured in a model which allows for inter-cellular interactions at a biochemical and biophysical level, whilst enabling analysis of NVU functionality. Eventually this model could be used to elucidate the mechanisms underlying NVU dysfunction in Alzheimer's disease by using Aβ producing neuron-like cells to attempt recreating the diseased brain parenchyma and its effects on the brain endothelium.

METHODS: Human neuron-like cells (SH-SY5Y) were pre-encapsulated within Purecol EZ Gel type I collagen hydrogels for two days before mouse brain endothelial cells (BEND.3) were seeded on top of the gel in the absence or presence of Matrigel. The cells were then co-cultured in supplemented DMEM (10% FBS, 1% L-glutamine) for 7 days to allow for growth within and on top of the hydrogel. Cultures were fixed in 4% paraformaldehyde, immunostained and analysed for endothelial and immature neuron markers using an Olympus Orca ER camera. Immunostained co-cultures were also embedded in 6% agarose gel and sectioned for imaging of vertical cross-sections [3].

RESULTS: In the absence of the Matrigel on top of the collagen hydrogel, the brain endothelial cells did not grow to a full monolayer after 7 days, whereas when the hydrogel was coated in Matrigel a full monolayer was formed. Identification of brain endothelial cells, neuron-like cells and nuclei was achieved effectively using immunofluorescence microscopy. Upon vertical sectioning of the co-culture, the distribution of neuron-like cells and the formation of a full endothelial monolayer was visible.

DISCUSSION & CONCLUSIONS: Collagen hydrogels provide an appropriate stiffness substrate for brain tissue (~300 Pa), but required further functionalisation through Matrigel coating to allow a complete endothelial cell monolayer to form. The encapsulation of SH-SY5Y cells within the collagen matrix and seeding of BEND.3 cells on top of the matrix enabled the formation of a neurovascular interface which can enable the biochemical and biophysical interactions to be investigated. This model sets a platform for future research into how Alzheimer's disease mutations in neuronal cells can cause NVU dysfunction.

REFERENCES: [1] Potjewyd, G. et al. (2018) Tissue Engineering 3D Neurovascular Units: A Biomaterials and Bioprinting Perspective. Trends Biotechnol. 36, 457–472. [2] Sweeney, M.D. et al. (2018) Blood–brain barrier breakdown in Alzheimer disease and other neurodegenerative disorders. Nat. Rev. Neurol. DOI: 10.1038/nrneurol.2017.188. [3] Short, A.R. et al. (2017) Imaging Cell–Matrix Interactions in 3D Collagen Hydrogel Culture Systems. Macromol. Biosci. 17, 1–8

ACKNOWLEDGEMENTS: The authors would like to thank the MRC and EPSRC for funding the CDT in Regenerative Medicine program, as well as the Bioimaging Facility at The University of Manchester for providing the microscopes and their assistance in training.. Grant reference number: EP/L014904/1.

This template was modified with kind permission from eCM Journal

Developing a novel system to aid tissue expansion via tensile strain for skin regeneration

N Jarangdej[1], E Antanaviciute[1], E Kritikaki[1], C Lopez Orts[1], R Unadkat[1], A Hamilton[2] and MO Riehle[1]

[1]Institute of Molecular Cell and Systems Biology, College of Medical, Veterinary and Life Sciences. [2]School of Medicine, Dentistry and Nursing, University of Glasgow, Glasgow

INTRODUCTION: Skin develops when dermal fibroblasts primarily establish scaffold, provides the tensile strength and extensibility in support of the structural integrity of the skin. Injuries to the skin lead to loss of this framework and function[1]. Even though there has been progress in skin regeneration after injuries using autologous transplant, the ongoing challenges include availability of donor skin and limited proliferative ability of primary cells. This study aims to integrate a biomechanical stimulus with cell culture to investigate more therapeutic support to tissue expansion. Skin fibroblasts respond to mechanical challenges in their environment as they can sense deformation of their shape and that of their environment. The molecular mechanisms by which these cells sense forces are through transmembrane proteins e.g. integrins that link the extracellular matrix (ECM) to the cytoskeleton within. One of the major regulators of actin cytoskeleton dynamics is RhoA, which plays a vital role in cell shape, motility, intracellular tension and can also indirectly couples intracellular tension to cytoskeletal gene expression through MRTF-A[2]. In this study, continuous unidirectional stretch was applied to human dermal fibroblasts and effects of stretch on phenotype were assessed using high throughput fluorescence microscopy.

METHODS: Polycaprolactone (PCL) membrane. The PCL membranes were prepared by spin coating on silicon wafer with 12% PCL solution. To create amorphous PCL, the coated wafer was heated and treated with low temperature using a liquid nitrogen cooled cylindrical copper block. Then, air plasma treatment was used to increase hydrophilicity of the surfaces for 1 min 10 secs.

Cell stretching, immunofluorescence and data analysis. The cells were seeded at 2 x 10^5 cells for 48 hrs and applied stretch at 1 mm/day. Then, cells were fixed and stained with anti-MRTF-A and conjugated with phalloidin-rhodamine to visualise f-actin. Mounting medium with DAPI was used to visualise cell nuclei. Finally, images were analysed using CellProfiler software for MRTF-A position, cell shape, orientation and f-actin cytoskeleton.

RESULTS: To determine the degree of MRTF-A translocation in response to unidirectional stretch, the position (nuclear/cytoplasmic) of MRTF-A in the stretched cells were compared to non-stretched groups as a control. The results of n/c MRTF-A ratios revealed that MRTF-A ratio in stretched groups were increased by 13% as compared to control. Furthermore, the orientation of cells along with directional axis of stretch was examined. Our results determined that cells reoriented under stretch activated growth (Figure1).

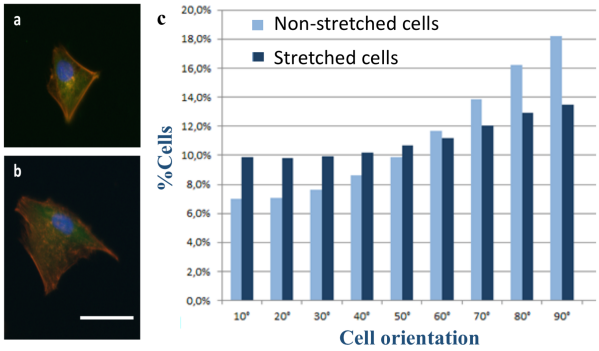

Figure 1: Cell alignment after stretching in a) non-stretched b) stretched cells. Fiber in stretched cells aligned to the direction of stretching while, non-stretched group showed a random distribution. For fluorescent images; actin (red), MRTF-A (green), nucleus (blue). Scale bar = 20 μm c) the angle of major axis of the cells between non-stretched and stretched cells.

DISCUSSION: The result indicated that the intensity of MRTF-A was a gradual increase in stretched cells. In a study by van Leeuwen et al (2002), highlighted that lysophosphatidic acid is able to enhance intracellular tension through RhoA activation. According to Neidlinger-Wilke et al (2002), showed that fibroblast orientation initially occurred by 2-3 hours and nearly complete by 24 hours of stretch[3] which similar to the cells reorientation in this study.

REFERENCES: [1]Kishi, K., Okabe, K., Shimizu, R. and Kubota, Y. (2012) 'Fetal skin possesses the ability to regenerate completely: complete regeneration of skin', *Keio J Med,* 61(4), pp. 101-8. [2]Vining, K. H. and Mooney, D. J. (2017) 'Mechanical forces direct stem cell behaviour in development and regeneration', Nat Rev Mol Cell Biol, 18(12), pp. 728-742. [3]Neidlinger-Wilke, C., Grood, E., Claes, L. and Brand, R. (2002) 'Fibroblast orientation to stretch begins within three hours', *J Orthop Res,* 20(5), pp. 953-6.

Development and characterization of a novel drug – loaded PLGA microparticle bandage for topical wound healing applications

R.A. Mensah, E.A. Hoffman, M.T. Cook, S.B. Kirton, V. Hutter, D.Y.S. Chau

Department of Pharmacy, Pharmacology and Postgraduate Medicine, School of Life and Medical Sciences, University of Hertfordshire, Hatfield, UK

INTRODUCTION: Material science has contributed to the development of numerous medical therapeutics that include wound dressing for the management of eye diseases, treatment of burns and chronic ulcers. Biomaterials are intended to provide structural, cellular and biochemical support for wound healing [1, 2]. Eggshell membrane (ESM) is an exceptional biomaterial in nature. ESM not only possesses appropriate physical and mechanical properties but also expresses a wide content of bioactive components and unique biocompatibility/ biodegradability characteristics which suggests that it may be exploited as a potential wound dressing for skin and eye applications [3]. Moreover, the treatment for wound healing generally requires repeated administration of drugs at regular time intervals or for extended durations. Polymer based microparticulate systems are often used in wound healing applications as controlled and sustained release carriers for drugs and growth factors. Poly (lactic-co-glycolic) acid (PLGA), a biocompatible, biodegradable and non-toxic polymer was utilized in this study for the creation of drug-loaded microparticles (MPs) [4]. The aim of this study was to generate and characterize a potential novel bandage consisting of ESM and drug-loaded PLGA microparticles for topical wound healing applications. Within this, a sub-study using Taguich design to optimize manufacturing process parameters and generate a protocol for the fabrication of 10-100 µm drug-incorporated PLGA MPs for topical drug delivery was also validated.

METHODS: ESMs were extracted using an optimised acetic acid and sterilization protocol. The physico-mechanical and biological properties of the ESM were evaluated using a number of standard test including texture analyses, permeation/penetration studies and scanning electronic microscope (SEM). The drug-loaded PLGA were created using an established single emulsion technique. Taguich design was implemented to optimize the parameters involve in the manufacturing process and generate a desirable protocol for the fabrication of 10 -100 µm MPs. The drug loaded-MPs were then characterized accordingly: morphology (imaging), size (SympaTec, laser diffraction) and FT-IR (chemical composition). A simple surface adsorption technique was used to deposit the MPs onto the ESM. A combination of *in vitro* tests i.e. cell culture, Franz cells and chorioallantoic membrane (CAM) assay were used in assessing the release profiles, toxicity and pro-angiogenic responses of the bandage generated.

RESULTS: The ESMs generated using the acetic acid and sterilization methods had suitable physical and mechanical behaviors crucial to their performance. The Taguchi design suggested the best combinations of the manufacturing parameters in generating MPs with the desired sizes. Their characterization protocols and *in vitro* tests exhibited suitable entrapment efficiency, tailorable release profiles and pro-biological effects required for the therapeutic applications.

DISCUSSION & CONCLUSIONS: Intact and complete eggshell membranes were successfully obtained using acetic acid method. The sterilized membranes demonstrated high biocompabiltiy, durability and flexibility. Drug-loaded PLGA-MPs, 10-100µm, were successfully fabricated using the predicted Taguchi design protocol. These were characterized and assessed using a range of *in vitro* tests and techniques which demonstrated that the desired profile(s) were obtained to suit the final application. The final bandage produced has potential for wound healing applications.

REFERENCES: [1]R. Langer, J.P. Vacanti (2013) *Tissue engineering Science*, 260 (5110), pp. 920-926. [2]D.F. Williams (2009) On the nature of biomaterials *Biomaterials*, 30 (30), pp. 5897-5909 [3]W.T. Tsai, J.M. Yang, C.W. Lai, Y.H. Cheng, C.C. Lin, C.W. Yeh. (2006) Characterization and adsorption properties of eggshells and eggshell membrane, *Bioresource. Technol*. 97 488–493. [4]D.Y. Chau, N.L. Tint, R.J. Collighan, M. Griffin, H.S. Dua, K.M. Shakesheff, F. Rose. (2010) The visualisation of vitreous using surface modified poly (lactic-co-glycolic acid) microparticles. British *Journal of Ophthalmology*, 94(5), pp.648-653.

Development of a biomechanical simulation model of traumatic spinal cord injury in vitro.

TK Nguyen[1] , JCF Kwok[2, 3] , JB Phillips[4] , RM Hall[1] , JL Tipper[5]

[1] Institute of Medical and Biological Engineering, University of Leeds, England. [2] School of Biomedical Sciences, University of Leeds, England. [3]Institute for Clinical and Experimental Medicine, Prague, Czech Republic. [4] Department of Pharmacology, UCL School of Pharmacy, University College London, England. [5] Faculty of Engineering and IT, University of Technology Sydney, Australia.

INTRODUCTION: Traumatic injuries to the spinal cord lead to a physicochemical microenvironment in which regeneration is poor. Replicating the biomechanics of injury has increasingly been shown to be important in understanding the heterogeneity of pathophysiological events and predicting neurological outcomes [1]. The aim of this work was to determine the feasibility of using an adapted materials testing machine, to investigate the interactions between injury biomechanics and neural cellular responses in a simple 3D hydrogel model.

METHODS: Characterisation of the BOSE Electroforce BioDynamic 5110 was performed, in air, to determine whether the apparatus was suitable for simulating contusion injuries *in vitro*. The waveform setup was as follows: 10 ms dwell, 1000 $mm.s^{-1}$ acceleration to 25, 50, or 75% gel height, 100 ms dwell, 1000 $mm.s^{-1}$ deceleration to 0%.

RESULTS: Manual (PID) tuning improved concordance between the theoretical and experimental displacement profiles; whereas increasing the working distance from the surface of the gel (0 mm) to 8 mm allowed for acceleration up to 1000 $mm.s^{-1}$. A 220 N load cell was able to resolve differences in load applied in 25, 50, and 75% displacement of a gel, with increasing loads measured with increasing displacement (Fig. 1). The peak load was achieved towards the end of the dwell period.

The natural source and viscosity of collagen resulted in variation of gel heights: 1.536 ± 0.046 mm (gel heights combined from four independent experiments; mean ± 95% CI). However, average gel heights across the experiments were not significantly different. Displacement controlled contusion requires accurate determination of the height of the gel. Thus, subsequent measurement of each gel was performed for accurate calculation of the desired injury displacement.

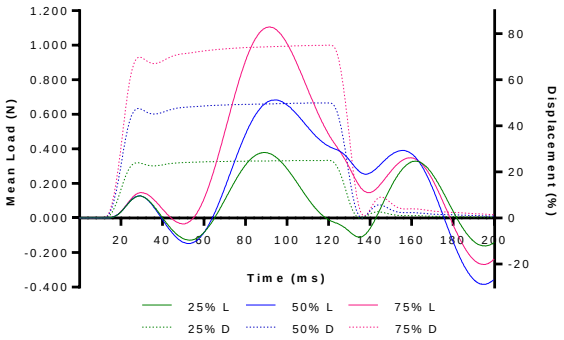

Fig. 1: Load and displacement profiles of gels displaced to different depths at 1000.mm.s^{-1} – n=9 per condition. L: load, N; D: displacement, %.

DISCUSSION & CONCLUSIONS: Characterisation of the BOSE Electroforce Biodynamic 5110 determined that it was an apparatus capable of simulating defined biomechanical inputs in a controlled manner, with outputs comparable to literature [2]. Increased load with impact depth is likely due to the viscous response of the gel. There is potential for the development of additional common injury mechanisms, such as distraction and dislocation [3]. Simulation of a range of contusion injuries in primary rat astrocyte seeded collagen gels has been performed. Comparison of astrocyte reactivity over a 14 day period will be performed using 3D analysis methods.

REFERENCES: [1] S. Mattuci, J. Speidel, J. Liu, et al (2018) Clin Biomech **18**: [Epub ahead of print]. [2] C.J. Lam, P. Assinck, J. Liu, et al (2014) J Neurotrauma **14**:1985-97. [3] A.M. Choo, J. Liu, C.K. Lam, et al (2007) J Neurosurg Spine **3**:255-66.

ACKNOWLEDGEMENTS: This research was funded by the EPSRC Centre for Doctoral Training in Tissue Engineering and Regenerative Medicine – Innovation in Medical and Biological Engineering, multidisciplinary collaboration of Faculties at the University of Leeds. Grant number EP/L014823/1.

Development of a hierarchical scaffold to stimulate angiogenesis and wound healing for skin tissue engineering

David H. Ramos[1], Sheila MacNeil[2], Frederik Claeyssens[2], Iida Ortega[1]

[1] *The School of Clinical Dentistry, University of Sheffield, Sheffield, United Kingdom,*
[2] *Kroto Research Institute, North campus, University of Sheffield, Sheffield, United Kingdom*

INTRODUCTION: The treatment of superficial burns and scalds remains a big challenge worldwide [1]. These injuries are not of uniform depth which makes it difficult to determine the right treatment to follow and to decide if grafting is needed within the first two weeks (which is crucial to achieve successful healing [2]). The regeneration process of scalds and superficial burns is accelerated when the presence of blood vessels is encouraged in the damaged area but, unfortunately, angiogenesis remains a challenge in wound healing and there is a need of innovative approaches to stimulate blood vessel formation [3]. Recent work from the MacNeil laboratory has shown that 2 deoxy D ribose [3] and oestradiol [4] are both potent proangiogenic agents. The fabrication of multifunctional and biodegradable nanofibrous dressings is a potential approach in which angiogenic agents can be included and complemented with anti-inflammatories and/or anti-microbials. The aim of this project is to manufacture angiogenic poly(lactide-co-glycolic acid) (PLGA) electrospun scaffolds and include small pro-angiogenic molecules (2-deoxy-D-ribose [3] and oestradiol) [4] to ultimately develop a multifunctional wound dressing to be used in skin tissue engineering.

METHODS: Electrospun scaffolds were fabricated using PLGA 50:50. Dichloromethane (DCM) and dimethylformamide (DMF) were used as solvents to prepare 20% PLGA solutions. The composition of the solvent system was controlled by dissolving 2-deoxy-D-ribose and 17β-oestradiol in DMF, and then added to the DCM-PLGA solution in concentrations of 1%, 5%, and 10% wt. The parameters used to electrospun PLGA fibers loaded with sugar were a voltage of 17 kV, a collector distance of 15cm, and a flow rate of 0.5 mL/h. Mechanical testing was performed with a uniaxial tensiometer (BOSE) to establish a relationship between the macro-mechanical properties of the materials and the concentration of sugars. SEM micrographs were used to analyse the morphology of the electrospun fibres.

RESULTS: We have shown that is possible to produce PLGA fibres loaded with different concentrations of 2-deoxy-D-ribose and oestradiol by using an in-house electrospinning set up. Preliminary characterisation of the sugar-loaded membranes suggests that he inclusion of 2-deoxy-D-ribose and oestradiol might have an effect on the physicomechanical properties of the materials. We envisage that changes in mechanical properties and in fibre morphology will have an effect on the *in vitro* response and bioactivity of the manufactured membranes, ultimately encouraging angiogenesis (it has been previously reported that these sugars can encourage angiogenesis by different biochemical pathways [3-4]).

DISCUSSION & CONCLUSIONS: The inclusion of angiogenic agents into biodegradable dressings made of FDA approved polymers such as PLGA can be a powerful strategy to accelerate wound healing. We have shown that electrospinning is a promising technique to include 2-deoxy-D-ribose and oestradiol into biological systems. Further studies will aim (i) to characterise the *in vitro* and *ex vivo* effects of the sugar-loaded scaffolds using skin models; (ii) to explore the introduction of anti-microbial and anti-inflammatory agents within the optimised angiogenic systems to create a multifunctional and bioactive membrane for skin regeneration.

REFERENCES: [1] A. Oryan, E. Alemzadeh and A. Moshiri (2017) *Burn wound healing: present concepts, treatment strategies and future directions*, J. Wound Care, vol. 26, no. 1, pp. 5–19. [2] N. S. Brown and R. Bicknell (1998) *Thymidine phosphorylase, 2-deoxy-D-ribose and angiogenesis* Biochem. J., vol. 334 Pt 1, pp. 1–8. [3] M. Yar, L. Shahzadi, A. Mehmood, M.I Raheem, S. Román, A.A. Chaudhry, I. ur Rehman, C.I. Douglas, and S. MacNeil, (2017) *Deoxy-sugar releasing biodegradable hydrogels promote angiogenesis and stimulate wound healing*, Materials Today Communications, 13, pp.295-305. [4] N. Mangır, C.J. Hillary, C.R. Chapple, and S. MacNeil (2017) *Oestradiol-releasing Biodegradable Mesh Stimulates Collagen Production and Angiogenesis: An Approach to Improving Biomaterial Integration in Pelvic Floor Repair*. European urology focus.

ACKNOWLEDGEMENTS: The authors would like to thank CONACYT for funding this research.

Development of injectable thermoresponsive clay-polymer nanocomposite formulations for tissue engineering strategies

SW Partrdge[1,2], AA Thorpe[1,2], CL Le Maitre[2], C Sammon[1]
[1]*Materials Engineering Research Institute*, [2]*Biomolecular Sciences Research Centre*, *Sheffield Hallam University, S1 1WB, UK*

INTRODUCTION: Injectable hydrogels via minimally invasive surgery offer benefits to the healthcare system, reduced risk of infection, scar formation and the cost of treatment. Degradation of the intervertebral disc (IVD) currently has no preventative treatment; an injectable hydrogel material could reinforce disc mechanical properties and promote tissue regeneration. We present a hydrogel material based on Laponite® associated poly(N-isopropylacrylamide)-co-poly(dimethylacrylamide). Previous research from our group has already demonstrated *in vivo* and *in vitro* efficacy for cell differentiation, migration and tissue integration for both nucleus pulposus and bone tissues [1-3]. Understanding how the components of this hydrogel system influence properties such as pre-injection viscosity (38°C - 40°C), gelation, final mechanical properties and 'pore' size is crucial for tailoring treatment strategies for the IVD and other tissues.

METHODS: The hydrogels were synthesised using a one-pot process described previously in [1-3], and illustrated in Fig 1A. The effect of hydrogel wt./wt., clay and co-monomer percentages were assessed using a box-Behnken experiment design. An Anton Paar Rheometer was used to measure dynamic changes in material properties. SEM, FTIR and swelling was used to characterise freeze dried material properties. The lower critical solution temperature (LCST) was evaluated spectroscopically using a Biotek® Cytation™ 5.

RESULTS: Rheometry revealed gelation temperature of hydrogel materials could be modified with increased dimethyl-acrylamide co-monomer; however, final maximum mechanical properties remained unaffected. Spectroscopy also showed a linear correlation between co-monomer concentration and change in LCST. Increasing the weight % and clay % increased resultant mechanical properties from ~500-2500 G' (Pa), increased viscosity, but retained the ability to flow through a 26g needle at 39°C. SEM demonstrated a decrease in porosity correlating with increased clay percentage.

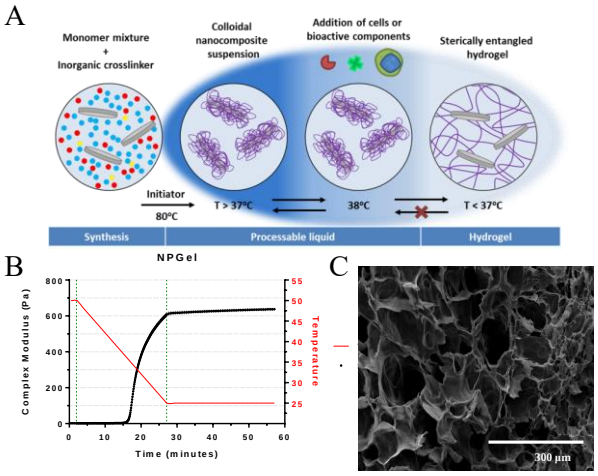

Fig. 1: A) Illustration of hydrogel synthesis. B) Example: Temperature gelation profile of hydrogel. C) SEM of freeze dried hydrogel.

DISCUSSION & CONCLUSIONS: By increasing the total weight percentage of the material system we can attain greater mechanical properties, which have potential benefits for other orthopaedic or dental applications. By modifying the co-monomer percentage we can control gelation temperature, which open opportunities for thermoresponsive drug release from topical or implanted materials. The clay content has demonstrated changes in SEM 'pore' size which indicates control over material cross-link density which could be used to regulate cell migration in 3D printed devices.

REFERENCES: [1] Thorpe AA, Creasey S, Sammon C, Le Maitre CL (2016b) Eur. Cells Mater. 32: 1–23.

[2] Thorpe AA, Dougill G, Vickers L, Reeves ND, Sammon C, Cooper G, Le Maitre CL (2017) Acta Biomater. 54: 212–226.

[3] Thorpe AA, Freeman C, Farthing P, Callaghan J, Paul V, Brook IM, Sammon C, Lyn C, Maitre L (2018) Oncotarget 9: 18277–18295.

ACKNOWLEDGEMENTS: We would like to thank Arthritis Research UK grant number 21497 for supporting this research.

Development of reproducible and scalable 3D printed scaffolds enable the high content screening of functional human and perfused murine tissue engineered skeletal muscle

RP Rimington[1], AJ Capel[1], JW Fleming[1], DJ Player[3], LA Baker[1], MC Turner[1], J Jones[3], NRW Martin[1], SD Christie[2], VC Mudera[3], MP Lewis[1]

[1]School of Sport, Exercise and Health Sciences, [2]School of Science, Loughborough University, Loughborough, United Kingdom. [3]Institute of Orthopaedics and Musculoskeletal Sciences, RNOH, University College London, Stanmore, United Kingdom

INTRODUCTION: Tissue engineered skeletal muscle provides a platform to investigate the cellular and molecular mechanisms that regulate skeletal muscle physiology in health and disease. To enable effective use in this manner, the fabricated model must resemble characteristics of native *in vivo* tissue. Scaffolds to support the development of such tissues have been manufactured using a diverse range of materials and methods. However, constructs that are scaled in size to facilitate the generation of primary human constructs from muscle needle biopsies are scarce. Furthermore, little work has been undertaken regarding replicating the perfused nature of the skeletal muscle cellular macroenvironment. Critical for nutrient replenishment and removal. Advances in three-dimensional (3D) printing technology allows for the rapid manufacture of such scaffolds and systems from biocompatible materials.

METHODS: To this end, a scalable model 3D printed via fused deposition modelling (FDM) and selective laser sintering (LS) techniques has been developed (50, 100, 250 and 500 µL construct volumes, 4 x 10^6 cells per mL) that can be utilised for a diverse range of tissue engineering, analytical and mechanistic investigations. Chamber and post dimensions of scaffolds were scaled to match the volume of matrix required for each specific construct and designed to fit into a standard 6 or 12 well culture plate. 50 µL constructs were assembled in 2-parts with a removable barrier. Tissue engineered murine (All sizes) and primary human (50 µL) skeletal muscle constructs were cultured for 14 days as previously published by our group.[1] Further design and development has facilitated the generation of 3D printed perfusion systems via LS that incorporate 50 µL scaled construct volumes. After 24 h in culture, tissue engineered hydrogels were cultured under perfused conditions for a further 13 days at 250 µL per minute continuous flow. After twitch and tetanic force measures, constructs were then harvested for immunocytochemistry and mRNA analysis.

RESULTS: Using a fixed mechanically loaded type-1 collagen or collagen/Matrigel® hydrogel, embedded C_2C_{12} murine skeletal myoblasts align and fuse to form highly mature striated multinucleated myotubes at all construct volumes. Effective scaling toward mature primary human derived constructs explanted from donor biopsies is also evident at 50 µL construct volumes. The functional capacity of murine and primary human tissue laden (50 µL) hydrogels were confirmed via electrical field stimulation to promote maximal twitch and tetanic contractions. Incorporation of 50uL scaffolds within developed 3D printed perfusion systems facilitated the *in situ* differentiation of skeletal muscle 3D tissue engineered constructs. In addition to comparable morphological maturation, MuRF1, myostatin, TNF-α and IL-1β mRNA expression was significantly reduced in response to 13 days continuous flow ($P \leq 0.05$). Furthermore, mRNA analyses of myosin heavy chain (MyHC) isoform transcription (MYH1, 2, 3, 7 and 8) outlined decreased expression in perfusion conditions. This appears to indicate a reduced basal equilibrium of MyHC protein turnover, due to decreased transcription of MuRF1 and its ubiquitin of MyHC proteins resulting in reduced isoform expression.

DISCUSSION & CONCLUSIONS: These models hold the flexibility to adapt to desired experimental designs, cell source and application. Crucially, this research provides effective strategies to overcome donor biopsy cell number limitations, and facilitate cost-effective, high content screening of functionally mature human tissue engineered skeletal muscle. Incorporation of perfusion further enhances the physiological biomimicry and technological translation of these models to pharmaceutical environments.

REFERENCES: [1]Smith, A. S. T., Passey, S., Greensmith, L., Mudera, V. & Lewis, M. P. Characterization and optimization of a simple, repeatable system for the long term in vitro culture of aligned myotubes in 3D. J. Cell. Biochem. 113, 1044–53 (2012).

ACKNOWLEDGEMENTS: This work was supported in part by EPSRC Grant REF: EP/ L02067X/2.

Development of small-diameter vascular grafts using a combination of electrospun micro and nanofibre scaffolds

RK Kampa[1], S MacNeil[1]

[1] *Department of Materials Science and Engineering, Kroto Research Institute, University of Sheffield, S37HQ, United Kingdom.*

INTRODUCTION: Recent advances in vascular tissue engineering have led to the development and early-stage clinical translation of tissue engineered blood vessel grafts. However, while results are promising with larger diameter grafts[1] they also show that small-diameter grafts (<6mm) suffer from thrombogenicity issues post implantation *in vivo* and have high failure rates in comparison to autologous grafts[2]. The ideal small-diameter tissue engineered blood vessel must be able to resist thrombi formation, withstand the *in vivo* mechanical environment, be bioresorbable and be able to be remodelled. Our study aims to produce a viable small-diameter blood vessel that can be lined with endothelial cells and which can be perfused and will resist blood clotting.

METHODS: We have developed multi-layered tubular 3D scaffolds by co-electrospinning blends of Poly(3-hydroxybutyrate-co-3-hydroxyvalerate) (PHBV) and Poly(lactic-acid) (PLA) such that they do not delaminate and can support multi-cell type cultures as previously described from our laboratory[3]. Nanofibres of PHBV followed by microfibers of PLA were co-electrospun onto a metal rod of diameter 4.7mm to produce scaffolds of length 3.5cm and internal diameter of 4.7mm and external 4.9mm. Scaffolds were then examined using scanning electron microscopy. We assembled the scaffolds into a transparent single-use bioreactor made out of a biocompatible plastic and perfused with cell-media at incremental flow-rates.

In initial experiments scaffolds were seeded with human dermal fibroblast (HDFs) and cultured under static conditions for 7 weeks. We then used confocal laser endomicroscopy to monitor cellular growth.

RESULTS: Scanning electron micrographs revealed interconnected PHBV nanofibres and PLA microfibres. Electrospun scaffolds cultured with HDFS displayed neo-tissue at 7 weeks with excellent cell viability and the continuous spread of cells throughout the length of the scaffolds.

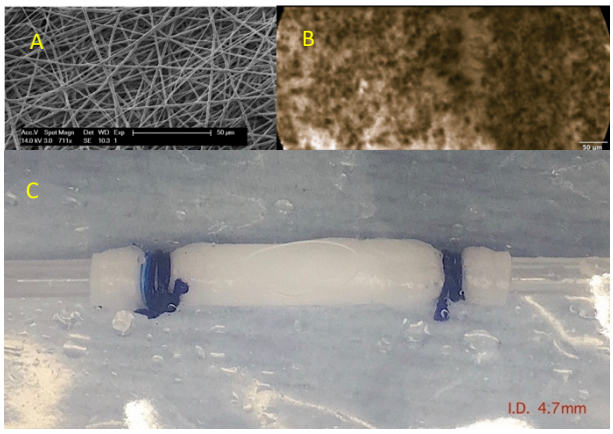

Fig. 1: Images of the TEBV – (A) scanning electron micrograph of the scaffold PHBV nanofibre surface; (B) Confocal laser endomicroscopic image showing the neo-tissue represented in dark sepia colour at 7 weeks of static culture; (C) Top-view of the whole scaffold assembled inside a perfusion bioreactor.

DISCUSSION & CONCLUSIONS: We report a convenient methodology for making a tubular small-diameter scaffold for vascular tissue engineering by combining an inner layer of nano fibres to support endothelial cells surrounded by an outer layer of microfibres to encourage ingrowth of stromal cells. Future work will focus on endothelial and stromal vascular cell co-culture study within a single-use perfusion bioreactor.

REFERENCES: [1]Drews, J. D., Miyachi, H. & Shinoka, T. Tissue-engineered vascular grafts for congenital cardiac disease: Clinical experience and current status. *Trends Cardiovasc. Med.* **27,** 521–531 (2017). [2]Dahl, S. L. M. *et al.* Readily available tissue-engineered vascular grafts. *Sci. Transl. Med.* **3,** 68ra9 (2011). [3]Bye, F. J. *et al.* Development of bilayer and trilayer nanofibrous/microfibrous scaffolds for regenerative medicine. *Biomater. Sci.* **1,** 942 (2013).

DEVELOPMENT OF SYNTHETIC CORNEAL MICROFABRICATED MEMBRANES WITH CONTROLLED STIFFNESS

Danilo Villanueva[1], Tom Paterson, Sheila MacNeil[2], Frederik Claeyssens [2], Ilida Ortega[1].

[1]The School of Clinical Dentistry, University of Sheffield, S10 2TA, Sheffield, United Kingdom
[2] Kroto Research Institute, North campus, University of Sheffield, S3 7HQ, Sheffield, United Kingdom.
dvillanueva1@sheffield.ac.uk

INTRODUCTION: It is estimated that approximately 10 million people in the world suffer from bilateral corneal blindness being this condition highly prevalent in developing countries. Although corneal transplantation is well established and the use of membranes for corneal cell delivery is starting to take off, these treatments are generally expensive and, unfortunately, not available to all surgeons worldwide. Therefore, there is a pressing need for the development of new cost-effective and off-the-shelf approaches to aid in corneal regeneration. Previous work from our group at Sheffield, showed that electrospun scaffolds made of poly(lactic-co-glycolic acid)PLGA can successfully support the growth of corneal limbal epithelial cells and explants. Additionally, recent research in corneal biology has demonstrated the importance of controlling mechanical properties when developing substrates for corneal regeneration [1]. The aim of this project is to optimise the fabrication of mechanically-controlled PLGA-based electrospun membranes for then study corneal cell response to stiffness using *ex vivo* corneal models.

METHODS: Poly lactide-co-glycolide (PLGA) and Polycaprolactone (PCL) solutions were prepared in 100:0, 99:1, 95:5, and 90:10 respectively using Dichloromethane and Dimethylformamide as solvents, then the solutions were electrospun using an in-house set up at a voltage of 17.5 kV and with 14 cm needle-collector distance.

Mechanical properties of the electrospun materials and biological controls (cornea and amniotic membrane) were tested using a uniaxial tensiometer (BOSE). Scanning electron microscope (SEM) was used to determine morphological characteristics and measure fibre diameter. Porcine corneas were used for corneal epithelial cell culture; tissue explants were isolated from the corneal limbus and placed on the scaffolds for periods of 2-3 weeks after which cell outgrowth was analysed.

RESULTS: Electrospun PLGA scaffolds and PLGA-PCL electrospun blends have similar morphological characteristics, but, in terms of mechanical properties, the addition of PCL seems to reduce the stiffness of the scaffolds. Adding PCL does not involve significant changes in the morphology of the fibres under our electrospinning conditions, in which all of our materials present average fibre diameters under 1 µm.

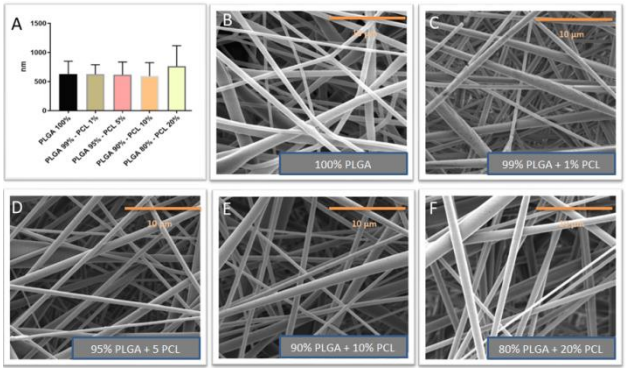

Fig.1: A- Fibre diameter comparison between electrospun PLGA scaffolds with different amounts of PCL. N=1, n=30. No statistic difference can be appreciated between the average fibre diameter (P<0.05). B to F- SEM images of the electrospun PLGA scaffolds with different amounts of PCL.

DISCUSSION & CONCLUSIONS: We have shown a simple and reproducible one-step strategy for the fabrication of mechanically-tailored electrospun scaffolds using FDA approved polymers (PLGA and PCL). These scaffolds will aid in the development of the next generation of synthetic electrospun substrates for corneal regeneration. Initial work for the study of cell behaviour on the membranes with different stiffness has now started and we aim to use these newly developed substrates in our porcine and rabbit cornea models as well as in human corneal models (in collaboration with LVPEI, India

REFERENCES:

[1] Gouveia, R.M. et al., 2017. Controlling the 3D architecture of Self-Lifting Auto-generated Tissue Equivalents (SLATEs) for optimized corneal graft composition and stability. Biomaterials, 121, pp.205–219.

ACKNOWLEDGEMENTS: The authors would like to thank CONICYT for founding this research.

Direct electrical stimulation may promote human MSC proliferation in donor- and tissue-dependent manner

K Srirussamee[1], S Mobini[2], NJ Cassidy[3], SH Cartmell[1]

[1] *School of Materials, The University of Manchester, UK.* [2] *J Crayton Pruitt Family Department of Biomedical Engineering, The University of Florida, USA.* [3] *Department of Civil Engineering, University of Birmingham, UK*

INTRODUCTION: It was presented earlier by our group that direct electrical stimulation (ES) could promote human bone marrow-derived mesenchymal stem cells (BM-MSCs), or later regarded as stromal cells, through the generation of H_2O_2 as a faradic by-product [1]. This study aims to address the question of whether or not this cellular response is dependent on donor and tissue source. We have obtained BM-MSCs from the second donor and also those derived from adipose tissue (AT-MSCs). Their proliferative responses after ES will be characterised and discussed.

METHODS: BM- and AT-MSCs were seeded into 6-well plates at 90,000 cells per well and treated with DMEM-based growth medium (GM) and osteogenic medium (OM). ES was applied for 1 hour daily through Pt electrodes using the device that is modified from Mobini, et al [2]. The voltage was set constant at 2.2 VDC. Cell metabolic activity was measured using resazurin assay after 10 days of ES.

RESULTS: A significant increase in cell proliferation is observed after 10 days of ES in both types of MSC. However, it is noticed that ES was effective for promoting BM-MSC proliferation only in GM (Fig. 1), whilst AT-MSC proliferation is enhanced only when treated with OM (Fig. 2).

DISCUSSION & CONCLUSIONS: The variation in cell proliferative response between BM- and AT-MSCs signifies the influence of the tissue source. Moreover, the difference is also observed when comparing BM-MSCs from this study with those derived from another donor [1]. The results suggest that cells derived from distinct donors or tissues may require different level of H_2O_2 for promoting their proliferation due to dissimilar anti-oxidative capability. As there is ascorbic acid in OM, it is our thought that it would reduce the level of H_2O_2 in the media during ES, which results in lower intracellular H_2O_2 concentration than the cells in GM. Hence, the cells react differently between the two media, and the mechanism behind this is being studied alongside their osteogenic differentiation. This study highlights the donor- and tissue-dependent behaviours of MSCs when stimulated by similar regime, which is also addressed in the literature [3]. This issue needs to be considered when designing an experiment for future ES studies that involve reactive oxygen species.

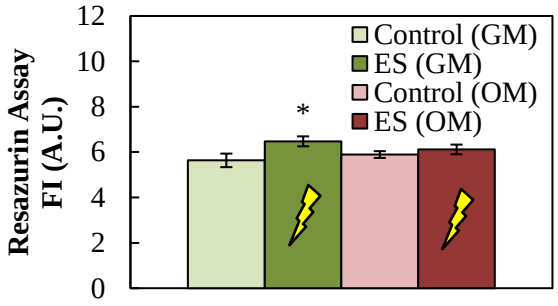

*Fig. 1: Cell metabolic activity of BM-MSCs after 10 days of ES. Error bars represent SD (n=2 for ES (GM) and n=3 for the rest). * represents p<0.05 when compared with Control (GM) group.*

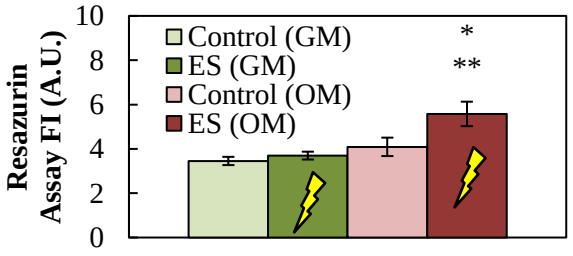

*Fig. 2: Cell metabolic activity of AT-MSCs after 10 days of ES. Error bars represent SD (n=3). * and ** represent p<0.05 when compared with Control (GM) and (OM) groups, respectively.*

REFERENCES: [1] K. Srirussamee, S. Mobini, and S.H. Cartmell (2017) *eCM Meeting Abstracts* **2**:194. [2] S. Mobini, L. Leppik, and J.H. Barker (2016) *Biotechniques* **60**(2):95-98. [3] S. Mobini, L. Leppik, V.T. Parameswaran, et al (2017) *PeerJ* **5**: e2821.

ACKNOWLEDGEMENTS: This work is financially supported by BBSRC BB/M013545/1 grant and The Royal Thai Government Scholarship.

Discrimination of meniscal cell and chondrocyte phenotypes in degenerate meniscus and cartilage.

J Wang[1,2,3], S Roberts[1,2], J Richardson[1,2], K Wright[1,2]

[1] Keele University, Stoke-on-Trent, Staffordshire, United Kingdom [2] Robert Jones & Agnes Hunt Orthopaedic Hosp., Oswestry, United Kingdom [3] Dalian Medical University, LiaoNing, China.

INTRODUCTION: There are many challenges in the field of meniscus tissue engineering[1] and no consensus has been reached regarding which cell type should be used in cell-based therapies for the meniscus. Currently, few studies have characterised cells in the meniscus (avascular and vascular zones) and articular chondrocytes from the same joint. However, previous studies have shown that meniscal cells display distinct immunoprofiles cf. (non-donor-matched) articular chondrocytes derived from non-degenerate tissues[2]. The purpose of this study is to identify and compare cell behaviours and phenotypical markers of meniscal cells derived from the inner and outer meniscus (avascular and vascular zones) as well as donor-matched articular chondrocytes from degenerate meniscus and cartilage.

METHODS: Donor-matched avascular and vascular meniscal cells (MC) and chondrocytes (C) were isolated from the menisci and condylar cartilage of total knee replacement (TKR) patients (n=3). H&E staining and trypan blue were used to assess meniscus tissue histologically (figure 1). The Cell-IQ® live cell imaging platform was used for image capture and analysis. Cell growth kinetics were calculated using population doubling times (PDTs). Immunopositivity for 16 molecules which are indicative of chondrogenesis, immunomodulation or MSC-phenotype were examined by flow cytometry after monolayer culture expansion to passage 2.

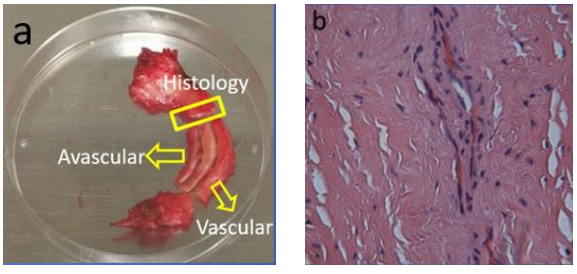

Fig. 1: (a) Menisci were divided into inner (avascular), middle and outer (vascular) zones. (b) H&E staining of the vascular zone (x 40)

RESULTS: Histological assessments confirmed that avascular dissections contained no blood vessels. No significant differences in PDTs were observed in meniscal cells cf. articular chondrocytes. Live cell imaging showed that donor-matched avascular zone derived MCs were morphologically distinct compared to their vascular zone counterparts (figure 2).

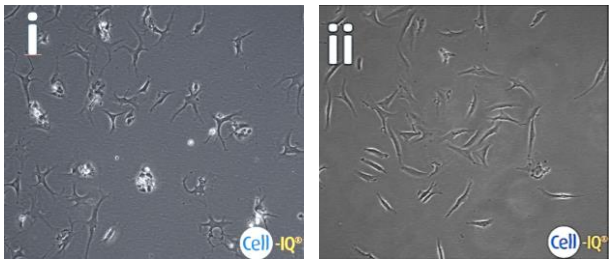

Figure 2: Avascular (i) and vascular (ii) meniscal cells display distinct morphologies in monolayer.

For the majority of the markers examined, meniscal cells and articular chondrocytes exhibited similar immunoprofiles. However, a greater percentage of meniscal cells were positive for CD34 (hematopoietic progenitor/endothelial cell marker) and CD49b (α2 integrin sub-unit) compared to articular chondrocytes (figure 3).

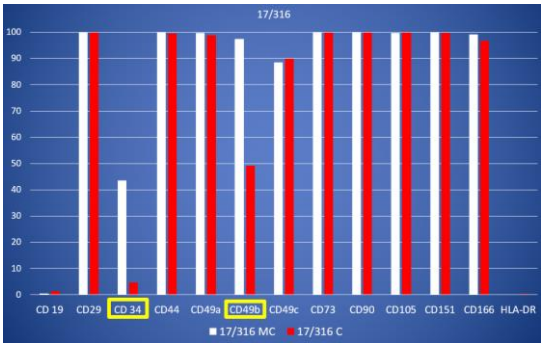

Figure 3: Representative immunoprofile. White bars: meniscal cells; Red bars: chondrocytes.

DISCUSSION & CONCLUSIONS: We have started the process of characterising distinct cell populations from donor-matched degenerate cartilaginous tissues. Future work will assess their chondrogenic potency and biocompatibility with commercially available meniscus scaffolds in the development of a tissue engineered meniscus graft.

REFERENCES: 1. Son et al. (2012) Eur Cell Mater. 2. Grogan et al. (2017). Conn Tiss Res.

Dual anti-bone cancer and osteoinductive effects of fucoidan from *Fucus vesiculosus*

D Gupta[1,2], VL Hearnden[1], MA Puertas-Mejia[3], GC Reilly[2]

[1]*Department of Materials Science and Engineering, University of Sheffield, UK.* [2]*Insigneo Institute for in Silico Medicine, University of Sheffield, Sheffield, UK.* [3]*Institute of Chemistry, University of Antioquia, Medellín, Colombia.*

INTRODUCTION: Recently, fucoidan from brown seaweed has been shown to have several biomedical activities such as anti-cancer, anti-inflammatory and anti-coagulant activities. More recently, it has been shown to induce bone formation in osteogenic cells[1]. The bioactivity of fucoidan is a function of its molecular structure which in turn depends on species type, season of harvest, extraction method, molecular weight and sulphur content in fucoidan[2]. Here we investigate anti-bone cancer and pro-osteogenic properties of fucoidan derived from *Fucus vesiculosus* for simultaneous anti-cancer and bone regeneration treatment in bone cancer patients.

METHODS: Human embryonic stem cell derived mesenchymal progenitor cells (hES-MPs) and osteosarcoma cells (MG63s) were used in this study. For assessment of cell attachment, cells were seeded in medium supplemented with or without varying doses of fucoidan and cell metabolic activity assay and actin staining were performed after 24 h of cell seeding. For assessment of cell growth, cells were seeded and the next day, culture medium was supplemented with varying fucoidan doses. After 3 days, DNA assay was performed. To assess osteogenic differentiation, hES-MPs were cultured with or without varying doses of fucoidan and alkaline phosphatase (ALP) activity, Sirius Red (collagen) and Alizarin Red (mineral) assays were performed over 3 weeks of culture. *, ** and *** indicate $p<0.05$, $p<0.01$ and $p<0.001$, compared to medium with 0 µg/ml fucoidan dose.

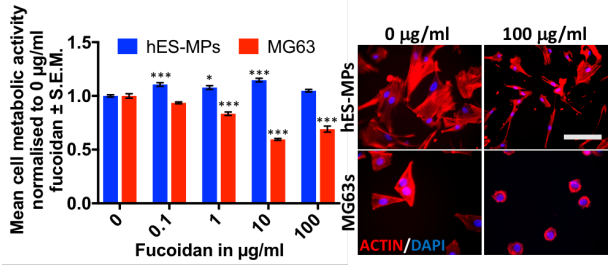

Fig. 1: Effect of fucoidan on cell attachment. Left- Presto Blue assay, Right- Actin staining, after 24 h cell seeding. Scale bar- 125 µm.

RESULTS: The hES-MPs attached normally even at higher concentrations of fucoidan (Fig. 1). However, for MG63s attachment efficiency was lower at higher fucoidan concentrations and cells were visibly rounded. Fucoidan inhibited both hES-MPs and MG63 growth by Day 3 (Fig. 2). However, it affects MG63 in dose-dependent manner but not hES-MPs. hES-MPs have higher ALP activity on day 7 at all fucoidan doses and this is also complemented by higher collagen production and mineral deposition on day 21 of culture, especially at 0.5 µg/ml fucoidan (Fig. 3).

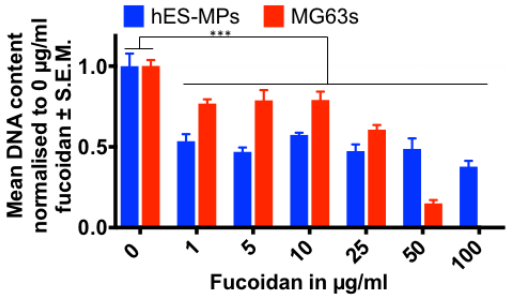

Fig. 2: Effect of fucoidan on hES-MP and MG63 growth after 3 days of culture.

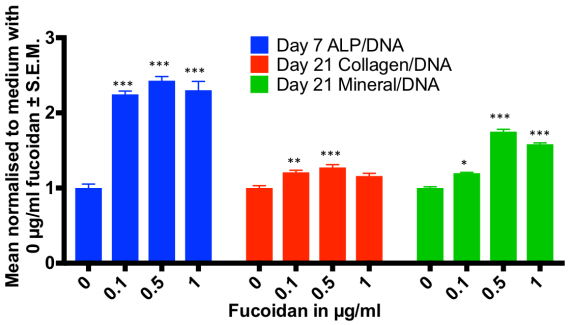

Fig. 3: Effect of fucoidan on hES-MP ALP activity, collagen production and mineral deposition.

DISCUSSION & CONCLUSIONS: The results suggest that fucoidan inhibits MG63 cytoskeletal remodelling and induces cell death. However, in case of hES-MPs, it does not interfere with cell attachment and induces osteogenic differentiation. Future work will involve investigation of molecular pathways targeted by fucoidan in normal and cancer cells in bone.

REFERENCES: [1]J.H. Fitton, et al (2015) *Mar. Drugs* **13**:5920-46. [2]L. Wu, et al (2016) *Carbohydr Polym.* **154**:96-111.

ACKNOWLEDGEMENTS: This work is funded by Newton Fund - British Council 2017-2019.

Effect of DL-Methionine on mesenchymal stem cells for the enhancement of the wound healing processes

Abed F. Ali[1], Yvonne Reinwald[1*]

[1] *Department of Engineering, School of Science and Technology, Nottingham Trent University*
*yvonne.reinwald@ntu.ac.uk

INTRODUCTION: Skin injury stimulates a cascade of cellular and biochemical events, which intend to repair tissues. Several different cell types are involved in the wound-healing process including mesenchymal stem cells. Mesenchymal stem cells (MSCs) are key to regenerative wound healing through cellular differentiation, immune-modulation, secretion of growth factors and mobilization of resident stem cells. Proteins are one of the most important nutritional factors affecting wound healing. Protein deficiency can impair fibroblast proliferation, proteoglycan synthesis, collagen synthesis, and wound remodeling. DL-Methionine is a sulfur-containing essential amino acid and a precursor for succinyl-CoA, homocysteine, cysteine, creatine, and carnitine[1]. Engineered skin substitutes are an alternative treatment for acute and chronic skin wounds. The aim of this project is to investigate the effects of DL-Methionine on cell behaviour and to further understand the role of this specific amino acid in skin tissue repair and regeneration for the production of bioactive wound healing products.

METHODS: Therefore, bone marrow-derived mesenchymal stem cells (BM-MSC) at passage 3 were seeded 24 wells plates and cultured in basic medium. (When cells reached ~ 70% confluence, different concentrations of DL-Methionine ranging from 0 - 4.5 mg/ml were added to the basic media (n=4). The cells were monitored for two days. Scratch assay was performed and monitored over 24 hours. Alamar blue and Pico Green assays where was performed at specific time points during the DL-Methionine treatment. Cells were fixed with 10% buffered formalin and histologically stained to assess their morphology. Data were statistical analysis by one-way ANOVA in SPS.

RESULTS: The results illustrate that DL-Methionine enhanced cell proliferation and viability. The scratch assay revealed that treated cells started to migrate and proliferate to fill the gap after two hours and filled the gap completely after 8 hours compared to untreated cells. DL-Methionine treatment seemed to enhance cell metabolic activities. Statistical significant differences were found between 2h, 24h and 48h for all concentrations at $p \leq 0.001$ and between 0 mg/ml and 0.05 mg/ml. All other concentrations were significant different from each other for $p \leq 0.001$ at 24h and 48 h (Figure 2).

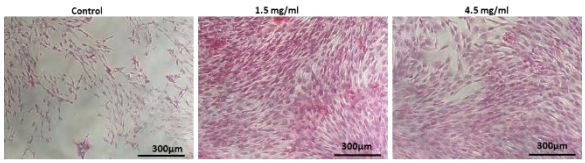

Figure 1: Images of mesenchymal stem cells showed the cell morphology in the different concentration of DL-Methionine. Images were taken at 10x magnification, scale bar = 300 µm.

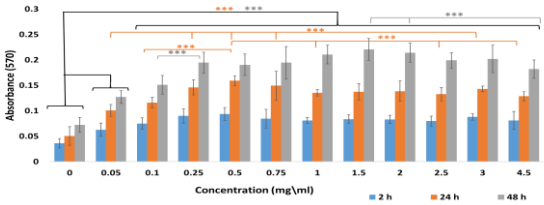

Figure 2: Cell metabolic activity was assessed by alamar blue assay. Absorbance was read at 570 nm.

DISCUSSION & CONCLUSIONS: MSCs can differentiate into multiple mesenchymal lineages depending on the cellular environment. The presence of MSCs in normal skin and their critical role in the inflammatory, proliferative, and remodeling phases of wound healing[2]. The uses of DL-Methionine as medium supplement seem to enhance cell proliferation. Future work will investigate stem cell fate in response to DL-Methionine.

REFERENCES: [1]Martínez, Y. et al. 2017. Amino Acids 49, 2091–2098. Hocking, A.M., Gibran, N.S., 2010. Exp Cell Res. 316, [2]Maxson, S., et al.2012. Stem Cells Transl. Med. 1, 142-149.

ACKNOWLEDGEMENTS: The authors would like to acknowledge Michael Shaw, Gareth Williams and Jacqueline Greef for their technical support.

Encapsulation of adenosine into biodegradable microspheres for bone regeneration

Hadi Hajiali,[1], Manuel Salmerón-Sánchez [2] , Matthew J. Dalby [3], Felicity R. A.J. Rose [1],

[1] *Division of Regenerative Medicine and Cellular Therapies, Centre for Biomolecular Sciences, School of Pharmacy, University of Nottingham, Nottingham, NG7 2RD, UK.* [2]*Division of Biomedical Engineering, School of Engineering, University of Glasgow, Glasgow G12 8LT, UK.* [3] *Center for Cell Engineering, Institute of Molecular Cell and Systems Biology, University of Glasgow, Glasgow G12 8QQ, UK.*

INTRODUCTION: In bone regeneration, a complex cascade of biological events is controlled by several factors at the site of injury to induce the healing process. Much research has been conducted into the delivery of factors, such as small molecules, to support and augment new bone formation. There is a need to control the spatio-temporal release kinetics of such factors in order to improve their efficiency and reduce side effects of their high dose. Spatio-temporal control of factor delivery can be obtained by encapsulation within biodegradable microspheres as a controlled release strategy.[1] Recently, it has been demonstrated that human pluripotent stem cells can be differentiated into functional osteoblasts through the supplementation of adenosine.[2] Therefore, we aimed to investigate the encapsulation of adenosine into biodegradable polymer microspheres for bone regeneration. To incorporate adenosine into these microspheres, double emulsion encapsulation (water/oil/water)[1] was not an appropriate approach. In this study, we therefore utilized and compared different methods and conditions for adenosine incorporation into biodegradable microspheres.

METHODS: In the first approach, poly(lactic acid) (PLA) microspheres were formed using a water-in-oil-in-water (w/o/w) emulsion method as previously described [1]. Briefly, an aqueous solution of adenosine was added to a solution of PLA in dichloromethane (DCM). These phases were homogenised to form the w/o emulsion. The primary emulsion was transferred to a poly(vinyl alcohol)) solution and was homogenised for a second time. The obtained double emulsion was stirred, and then filtered, washed and lyophilized until dry. In the second approach, the microspheres were formed using a solid-in-oil-in water(s/o/w) emulsion. In the s/o/w system, the adenosine was added into PLA solution directly in the solid phase and then the previous procedures of the second emulsion of w/o/w system were followed. After the microspheres were prepared, their morphology, encapsulation efficiency and their release profile were investigated.

RESULTS: The morphology of the microspheres were evaluated by scanning electron microscope (SEM) (Fig. 1).

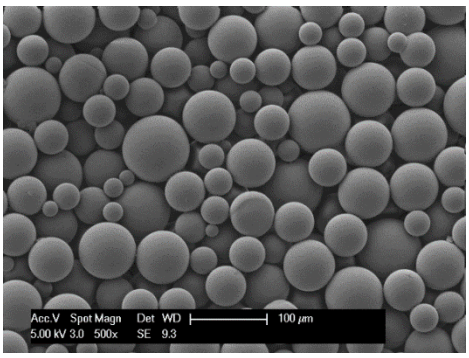

Fig. 1: SEM Image of PLA microspheres.

To measure the encapsulation efficiency (the ratio of actual and theoretical adenosine loading), the microspheres first were dissolved in dimethyl sulfoxide and analysed for adenosine content by UV spectroscopy. The data showed a significant enhancement of loading efficiency in the s/o/w system compared to w/o/w method.

DISCUSSION & CONCLUSIONS: The small size of the adenosine molecule and low solubility of adenosine in water limited the usage of common encapsulation methodologies such as w/o/w emulsion. The low encapsulation efficiency of the w/o/w method was likely to be due to the small size of the molecule and the washing process which allows escape of adenosine from microspheres. In this study, it has been demonstrated that the s/o/w emulsion is a more efficient system for adenosine loading. Finally, a delivery system for adenosine, capable of providing both structural support and controlled release kinetics, can be developed for bone regeneration.

REFERENCES: [1] L. J. White, et al (2013) *Materials science & engineering. C, Materials for biological applications* **33**: 2578-2583. [2] H. Kang, et al (2016) *Science advances* **2**: e1600691.

Engineering a spinal cord injury: developing an *in-vitro* model of non-traumatic spinal cord injury

K. V. Timms[1,2], J. L. Tipper[3], R. M. Ichiyama[1], J.B. Phillips[4], J.C.F. Kwok[1, 5], L. Urdzikova[5], R.M. Hall[2]

[1]School of Biomedical Sciences, University of Leeds, UK. [2]Faculty of Engineering, University of Leeds, UK. [3]Faculty of Engineering, University of Technology Sydney, Australia. [4]UCL School of Pharmacy, University College London, UK. [5]Institute for Clinical and Experimental Medicine, Prague, Czech Republic

INTRODUCTION: Non-traumatic spinal cord injury (NT-SCI) involves spinal cord stenosis which increases over months to years; as opposed to the millisecond duration of traumatic spinal cord injuries. NT-SCI affects up to 150000 people in total in the UK[1]. The pathological process of NT-SCI is poorly understood and requires further investigation. The progressive and prolonged nature of NT-SCI allows neural cells to respond to changes in the mechanical environment and induces plasticity in the spinal cord. This is exemplified by the fact that clinically the radiological degree of stenosis does not correlate with symptoms[2]. For instance, a patient with 60% stenosis may have no symptoms; or be symptomatic, indicating plasticity in the spinal cord. This research aims to develop experimental models of NT-SCI in order to better understand the neural cell responses to low-velocity mechanical insults. Ultimately, an *in-vitro* and *in-vivo* model will be established. Initial aims for the *in-vitro* model included developing a 3D environment where primary astrocytes expressed a relevant phenotype. Further, cellular responses to TGF-beta treatment, a known chemical stimulant inducing spinal cord injury-like phenotypes, were established as a positive control.

METHODS: Primary rat astrocytes were isolated from pre-weaner rats. The population was validated using immunocytochemistry for glial fibrillary acidic protein (GFAP) expression. Subsequently, primary rat astrocytes were seeded into rat collagen I (1.6 mg.mL^{-1}) hydrogels at a cell density of 1x10^6 cells per mL of gel. Half of the samples were treated with 10 ng.mL^{-1} TGF-beta in the media, and the others remained untreated. Over 14 days, cell viability was determined using ethidium homodimer and Hoechst staining; and reactivity was determined via GFAP expression. Image analysis was undertaken using FIJI.

RESULTS: A total of 89.7 ± 3.5% (mean ± S.E.M.) of primary glial cells were positive for GFAP. Thus, based on previous studies, the population could be described as astrocytes[3,4]. These cells remained viable in collagen hydrogels, with viability increasing by 18% over 14 days in treated and untreated conditions (Figure 1, $p<0.05$ day 1 vs 14). GFAP expression did not change over time in untreated samples. In TGF-beta treated samples, GFAP-stained area increased by 2.27 fold (Figure 1, $p<0.05$ day 1 vs 14); indicating a more reactive phenotype as seen in previous studies[3].

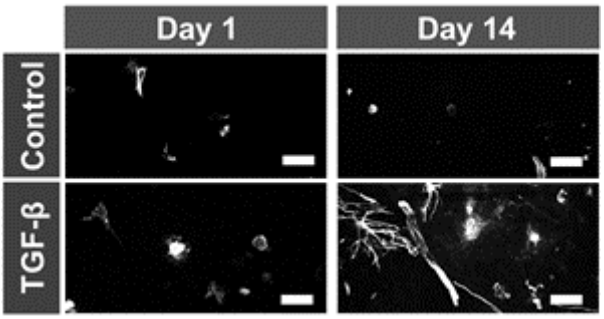

Fig 1: GFAP staining of primary astrocytes in collagen hydrogels, untreated (control) and TGF-beta treated (10 ng.mL^{-1}). Scale bar 50 µm

DISCUSSION & CONCLUSIONS: Primary astrocytes were compatible with a collagen hydrogel system. The cells expressed relevant physiological and chemical-induced reactivity phenotypes which have been previously characterised in the literature[3,4]. Further steps will be to use the BOSE Electroforce 5110 Biodynamic to apply controlled mechanical insults to the seeded hydrogels simulating NT-SCI. Further, an *in-vivo* model is yet to be established, but should replicate the temporal profile of non-traumatic injuries; and incorporate a ventral lesion.

REFERENCES: [1]New, P. W., Marshall, R. (2014). *Spinal Cord.* **52**: 123-32. [2]Nakashima, H. et al.(2016) *Eur Spine J* **25**: 2149-54. [3]East, E., Golding, J.P., Phillips, J.B. (2009) *J Tissue Eng Regen Med*. **3**:634-46. [4]Kerstetter, A.E., Miller, R.H. (2012) *Methods Mol. Biol*. **814**:93-104

ACKNOWLEDGEMENTS: Funded by EPSRC Centre for Doctoral Training: Tissue engineering & regenerative medicine; grant number EP/L014823/1

Epigenetic regulators enhance osteogenesis of human dental pulp stromal cells in 2D & 3D silk scaffolds

K Man[1,*], L.-H Jiang[2], R Foster[3], X.D. Manz[4,5], J Rnjak-Kovacina[4] and X.B Yang[1]

[1]BMTE Group, [4]School of Dentistry, [2]School of Biomedical Sciences, [3]School of Chemistry, University of Leeds, UK. [4]Graduate School of Biomedical Engineering, UNSW, Australia. [5]Department of Pulmonary Diseases, VU University Medical Center, The Netherlands. *Email: mnkklm@leeds.ac.uk.,

INTRODUCTION: The key challenge for functional tissue engineering is to effectively control lineage specific differentiation of stem cells. Limitations in current strategies in particular gene therapy have led to the search for alternative methods. Epigenetic approaches are capable of controlling stem cell fate without altering the genome. Inhibition of histone deacetylase (HDAC) isoform 3 has been linked to osteogenesis. This study aimed to evaluate the potential of using a HDAC2/3 inhibitor - MI192 to enhance *in vitro* osteogenesis of human dental pulp stromal cells (hDPSCs) cultured in 2D monolayer culture and 3D silk scaffolds.

METHODS: Following MI192 treatment, hDPSCs were cultured in osteoinductive medium (OIM) either in monolayer and within 3D porous lyophilized Bombyx mori silk scaffolds. Cell viability was assessed via AlamarBlue quantification. Osteogenesis was confirmed by qPCR, ALP specific activity (ALPSA), in-cell western (ICW) and histological analysis.

RESULTS: 1) A time-dose dependent decrease in cell viability was observed following treatment with different MI192 doses, with ≥ 20 µM at 24 h; ≥ 5 µM at 48 h and ≥ 1 µM at 72 h significantly reducing viability compared to untreated cells at the same time points ($p \leq 0.01$). 2) ALPSA was significantly enhanced in cells pre-treated with 2 and 5 µM MI192 for 48 h compared to the untreated control groups ($p \leq 0.001$) and 1 µM MI192 group ($p \leq 0.01$). 2 µM MI192 for 48 h pre-treatment was utilised for the rest of this study (Fig 1A). 3) Gene expression of Runx2, ALP, OCN, BMP2 and Col1a was significantly increased in the MI192 pre-treated group compared to the untreated group. 4) ICW showed a significant increase in Runx2 ($p \leq 0.05$), ALP ($p \leq 0.001$), OCN ($p \leq 0.001$), BMP2 ($p \leq 0.01$) and Col1a ($p \leq 0.01$) protein production in pre-treated cells compared to untreated cells (Fig 1B). 5) Calcium accumulation and mineralisation were extensively enhanced in pre-treated cells confirmed by Alizarin Red & Von Kossa staining (Fig 1C). 6) In 3D culture, MI192 pre-treatment significantly enhanced the ALPSA in both 2% and 5% (wt/v%) silk scaffolds ($p \leq 0.001$) (Fig 2A), with the 5% silk scaffold possessed significantly enhanced ALPSA compared to 2% silk scaffolds within both the untreated/MI192 pre-treated cells ($P \leq 0.001$).

7) Immunohistochemistry showed increased protein production (ALP, OCN and Col1a), whilst mineralisation was enhanced in cells pre-treated with MI192 compared to untreated cells in both 2 and 5% scaffolds (Fig 2B).

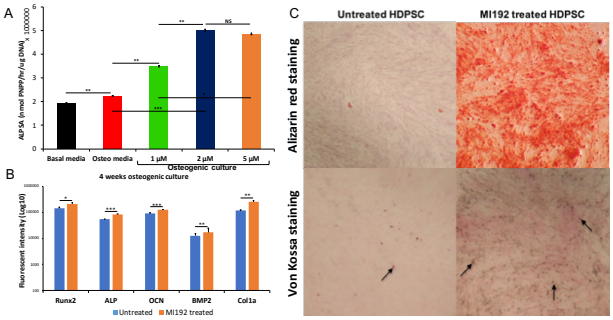

Figure 1. Effects of MI192 on hDPSC osteogenesis in 2D. *a) ALPSA of hDPSCs pre-treated with 1, 2 & 5 µM MI192 for 48 h prior to culture in OIM for 14 days. b) ICW showed the effects of MI192 on osteogenic protein expression after 4 weeks OIM culture. c) Alizarin Red/Von Kossa staining of hDPSC pre-treated with/without MI192 prior to 4 weeks in OIM. Mean ± SD (n=3). * p≤0.05, **p≤0.01, ***p≤0.001. Mag: ×100*

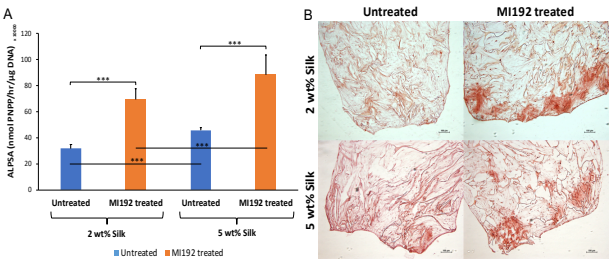

Figure 2. Effects of MI192 on hDPSC osteogenesis within 3D B. mori silk scaffolds. *a) ALPSA of untreated/MI192 pre-treated hDPSC on silk scaffolds after 2 weeks in OIM. b) Alizarin Red staining of hDPSC pre-treated with/without MI192 prior to 4 weeks osteogenic culture silk scaffolds.*

DISCUSSION & CONCLUSIONS: These results demonstrate that the selective HDACi - MI192 is capable of promoting hDPSC osteogenesis and mineralisation *in vitro* both in monolayer and in 3D *B.mori* silk scaffolds, indicating the potential of this novel epigenetic approach for controlling hDPSC osteogenesis for bone augmentation.

ACKNOWLEDGEMENTS: *EPSRC CDT; EU FP7/2007–2013-IRSES, No [318553] – 'Skelgen'.*

Evaluating donor variability of ovine adult stem cells oMSCs - implications for orthopaedic animal models

E A Al-Mutheffer[1,2], Y Reinwald[1,3], A J El Haj[1]

[1]Institute for Science and Technology in Medicine, Keele University, Stoke-on-Trent, UK. [2]Department of surgery and obstetrics, College of Veterinary Medicine - Baghdad University Baghdad, Iraq. [3]School of Science and Technology, Department of Engineering, Nottingham Trent University, Nottingham, UK

INTRODUCTION: Cell-based therapy using ovine mesenchymal stem cells (oMSCs) are promising for cartilage repair. However, little is understood of how donor variability impacts the clinical outcome of cellular therapies. Due to the similarities to human in size, weight, architecture and healing mechanism, sheep animal models can facilitate clinical translation of cell-based orthopaedic treatments. As yet, oMSCs have not been fully characterized and their differentiation potential is not well understood. The present study aims to investigate donor variability in the tri-potential capacity of oMSCs to differentiate *in vitro*. In addition, we explore the individual variation in oMSCs response to mechanical stimuli[1]. Statistical analysis of this data allows us to characterise the oMSCs for use in cell-based therapies for osteoarthritis and cartilage defects

METHODS: Bone marrow-derived oMSCs were isolated and STRO-4 selected from 13 adult sheep (English mule ewes, age group 2-4 years). Cells were cultured for 20 days to assess the differentiation potential of oMSCs for both adipogenesis and osteogenesis in 2D and for chondrogenesis in 3D cell organoids, using Oil-o-Red, Alizarin red and Alcian blue staining respectively. Donor variation was also assessed semi-quantitatively for both adipogenesis and osteogenesis, while chondrogenesis potential, was assessed by DMMB assay for GAG production. For native sheep cartilage study, native sheep cartilage samples (6 donors, 8mm diameter samples, n=3) were harvested from femoral distal condyle, tissue matrix composition were assessed histologically, immunohistological and biochemically. Young modulus was determined by compressive testing.

RESULTS: Results revealed donor variation in the tri-lineage differentiation and CD marker expression across the thirteen donors. No clear correlation between donors was observed among the three lineages. For example, a donor that was highly responsive during osteogenic differentiation was not necessarily as responsive to chondrogenic or adipogenic differentiation. Similarly, regarding to the native sheep cartilage, there are apparently individual differences (Figure 1 and 2).

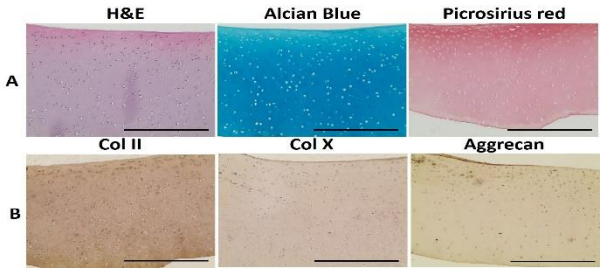

Figure 1: Bright field micrograph of the histology, (A) and immunohistology, (B) stained 7µm paraffin sections of the native sheep cartilage x20 magnification, scale bar = 300 µm

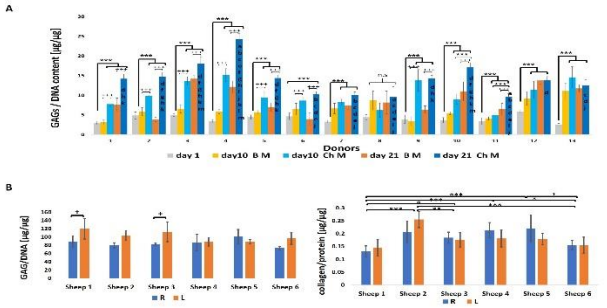

*Figure 2: (A) GAG/DNA content chondrogenesis variation study, (B) GAG/DNA content with collagen/total protein, native sheep cartilage study. Data are expressed as mean ± standard deviation, n=3, *p≤0.05, **p≤0.01, ***p≤0.001.*

DISCUSSION & CONCLUSIONS: oMSCs appear to share some similarity in characteristics across individual donors, but at the same time, express differences regarding biological properties that may influence the number, phenotype and *in vitro* biological characteristics. This study investigated the use of 2D and 3D assays to predict outcomes in differentiation capacity between different donors before being successfully transmitted to preclinical animal studies.

REFERENCES: [1] H Markides et al. (2018) Translation of remote control regenerative technologies for bone repair. npj Regenerative Medicine 3:9

ACKNOWLEDGEMENTS: Al-Mutheffer was supported by Iraqi Ministry of Higher Education. Special thanks Dr J McLaren from the University of Nottingham for her assistance in collecting sheep bone marrow and cartilage and to Prof El Haj's group.

Expression of xenobiotic metabolising enzyme expression in tissue engineered oral mucosa

K Slowik[1], H.E Colley[1], C. Murdoch[1]

[1]*School of Clinical Dentistry, University of Sheffield, Sheffield, S10 2TA,UK*

INTRODUCTION: Xenobiotic compounds are external foreign molecules, such as drugs, that interact with our tissues and cells. To maintain homeostasis these foreign molecules are converted to usually less toxic and more soluble metabolites by cellular xenobiotic metabolising enzymes enabling excretion. The liver is an abundant source of metabolising enzymes [1] and recent evidence suggests that these enzymes are also present in the skin [2,3]. Drugs can be delivered via the oral mucosa, however, the expression of xenobiotic metabolizing enzymes in the oral mucosa is unknown. Here we characterised, for the first time, the expression of a sub-set of metabolising enzymes in native oral mucosa, and compared these to tissue-engineered oral mucosal (TEOM) equivalents and cells cultured as monolayers.

METHODS: Immunohistochemistry using antibodies directed against selected phase I and phase II enzymes was performed on wax-embedded sections of normal oral mucosa (NOM) and TEOM equivalents to determine protein expression and localisation within tissue. Total RNA extracted from the epithelium of TEOM equivalents or keratinocytes grown as monolayers were reverse transcribed and subjected to qPCR using TaqMan primers; β-actin was used as a reference control.

RESULTS: qPCR analysis showed that gene expression of xenobiotic metabolising enzymes CYP2A6 (Fig.1A), CYP3A4 and CYP3A5 were all significantly increased ($p<0.001$) in the RNA isolated from the stratified epithelium of 3D cultured TEOM equivalents when compared to expression in RNA isolated from keratinocytes grown in 2D monolayer culture.

Immunohistochemical results revealed that the location of xenobiotic enzyme expression varies between NOM and TEOM. Expression of GST-Pi, FMO4, FMO5 (Fig. 1B&C), NAT-1, ALDH2, CYP3A4 was similar in all tissues with immune-reactivity throughout the epithelium. CYP2E1 expression was mainly restricted to the basal epithelium as was expression for CYP3A5. UGT1A6 was expressed in the basal cells of NOM but expression was absent in TEOM equivalents. Immunoreactivity toward FMO3 was strong and throughout the entire epithelium of NOM, but was weak in TEOM equivalents.

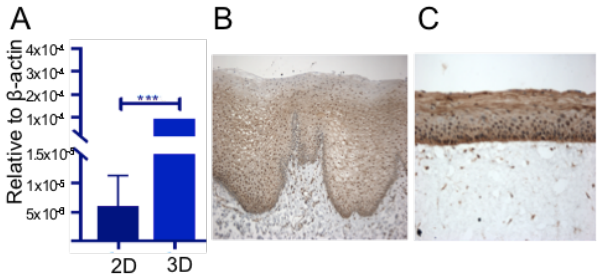

Fig. 1. (A) Gene expression of CYP2A6 in monolayer keratinocytes compared to the epithelium from 3D TEOM. Protein expression of FMO5 in (B) NOM and (C) TEOM equivalents; expression is uniform throughout both tissues

DISCUSSION & CONCLUSIONS:

Metabolising enzyme expression has been described in skin but this study is the first to show expression of xenobiotic metabolising enzymes in the epithelium of the oral mucosa. Location of enzyme expression within the oral epithelium varies from enzyme to enzyme. Expression in 3D TEOM equivalents was similar to that of the NOM for all enzymes tested, suggesting that TEOM equivalents are good representative models for analysing enzyme function in the oral mucosa. 3D TEOM equivalents expressed elevated levels of enzymes than cells cultured in 2D, reinforcing the necessity to use tissue-engineered models. Our data will be a useful when investigating xenobiotic metabolism of topically delivered compounds in the oral mucosa.

REFERENCES: [1]Guengerich F.P *et al* (2008) *Chem. Res. Toxicol.* **21**:70. [2]Wiegand C. *et al* (2014) *Skin Pharmacol. Physiol.* **27**:263. [3]Smith S *et al* (2017) *Exp. Dermatol.* (in press doi:10.1111/exd.13483)

ACKNOWLEDGEMENTS: The authors would like to thank volunteers for donation of oral mucosal biopsy tissue.

Fabrication of an aligned 3D neural model for tissue engineering

D Merryweather[1], S Bodbin[1], M Lewis[2] , P Roach[1]

[1] Department of Chemistry, School of Science, Loughborough University, Leicestershire. [2] School of Sports Science, Loughborough University, Leicestershire

INTRODUCTION: A wide variety of hydrogels have been employed to generate 3D cell cultures. Hydrogels can have a wide variety of chemistries which may be permissive or non-permissive to cell adhesion. Whilst significant difference have been found in 3D vs 2D *in vitro* cultures, evidence suggests that the geometry of the hydrogel matrix may create a number of distinct microenvironments as found in the complex hierarchical structures of biological matrices *in vivo*. Development of a simple system that allows for the fabrication of complex micro-topographies within a 3D culture environment that can be manufactured in large quantities critical to the investigation of 3D culture environments *in vitro* and would be of great use in the production of therapeutics involving the introduction of cell-laden scaffolds to the body.

METHODS: Dilutions of a commercial rat-tail collagen type I were seeded with $0.5x10^5$ SH-SY5Y human neuroblastoma cells in 500µl of each gel. Cultures were maintained for 3 days and then differentiated using 2µM retinoic acid with 50ng/ml BDNF. After seven days of differentiation cultures were fixed and stained for β-III-tubulin to determine the expression of neuronal markers. Microfluidic devices with microchannels 50µm in diameter were prepared using reverse replica moulding of Qsil PDMS. Devices were bonded to clean glass slides using a high-pressure air plasma to induce a radical-mediated bond between these two chemistries. Loading of collagen through the microchannels was confirmed using transmission FTIR. Collagen-loaded devices were also fixed and coated with an Au/Pd vapour after removal of the devices, allowing for SEM imaing of the collagen both in its native form and after loading into microchannels. Collagen-loaded devices were also seeded with SH-SY5Y and cultured for a period of 10 days.

RESULTS: SH-SY5Y neuroblastoma cells are capable of growth and differentiation within collagen I hydrogels as determined by β-tubulin expression after 7 days of exposure to differentiation media. Lower dilutions of collagen allowed for a significantly greater level of remodelling within the cell-laden gels. Neurite extension was observed in all gels, though it proved impractical to determine the origin of specific neurites for length measurement. Collagen was successfully loaded through all microchannels. Scanning electron microscopy putatiatively confirmed collagen fibril alignment through the microchannels and allowed for a determination of collagen fibril diameter to be 88nm±5nm with the distinctive D-Banding pattern of collagen in vivo (fig. 1).

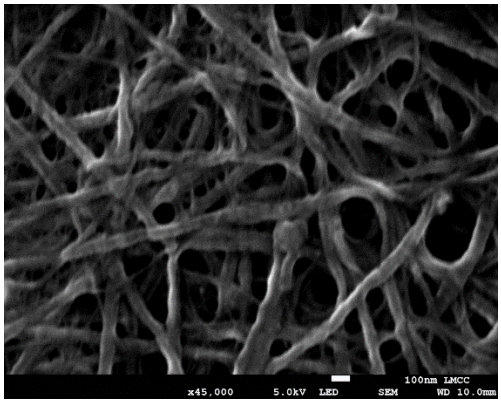

Fig. 1: SEM of collagen I fibrils within a dehydrated collagen gel.

DISCUSSION & CONCLUSIONS: Collagen has been widely used as a base material for nerve guides and other medical devices. Its use in guiding neurite outgrowth *in vivo* is thus widely established. Current fabrication methods however do little to control the micro- and nanoscale topography of the substrate which limits their application in the development of complex biological models *in vitro* and in the repair of nervous damage *in vivo*. Here we have demonstrated that microfluidic flow can be used to trivially create complex microscale topographies that can readily guide neurite outgrowth in specified directions.

ACKNOWLEDGEMENTS: EPSRC for funding, Jordan Roe for assistance with SEM

This template was modified with kind permission from eCM Journal.

Heparin-biofunctionalised and topographically-modified electrospun scaffolds as new *in vitro* platforms to study bone regeneration

BJC Monteiro[1,2], T Paterson[1], P Hatton[1], S Cool[2], I Ortega[1]

*[1]Bioengineering and Health Technologies Group, School of Clinical Dentistry, University of Sheffield, United Kingdom [2]Institute of Medical Biology, Agency for Science, Technology and Research (A*STAR), Singapore*

INTRODUCTION: Musculoskeletal disorders affect millions of people worldwide, having the potential to severely reduce quality of life; specifically. There is an increasing need for the development of new *in vitro* models to explore the mechanisms underlying the bone regeneration process. The use of key molecules for the fabrication of biofunctional fibrous membranes is a promising approach. For example, heparin, has been reported to potentiate bone formation by increasing growth factors availability and enhancing osteogenic activity [1]. The aim of this research is to fabricate electrospun 3D biofunctional microfabricated membranes incorporating specific biomolecules (heparin) to create new 3D *in vitro* models to study stem cells behaviour towards osteogenic differentiation pathways.

METHODS: Medical grade polycaprolactone (PCL) was electrospun onto plain or patterned collectors to produce 3D-fibrous scaffolds. The obtained fibre diameter and alignment were characterised using scanning electron microscopy (SEM) and ImajeJ. PCL scaffolds were biofunctionalised using three different heparin incorporation methods (simple adsorption, emulsion, covalent binding). Heparin content was assessed by X-ray photoelectron spectroscopy (XPS) and quantified overtime by Toluidine Blue assay. After scaffold characterisation, Rat MSCs were cultured on the PCL-heparin membranes in order to assess cell morphology and cell viability over time (Presto Blue®) (n=3).

RESULTS: Fibers disposition within micropatterns cues have showed different alignments (Fig.1) while fibre diameters have showed similar sizes. Toluidine Blue assays corroborated the presence of heparin for the 3 biofunctionalisation methods, showing differences in the heparin distribution for the 3 different types of PCL-heparin scaffold. Cell metabolic assays showed that the functionalised membranes can support cells survival and viability over time.

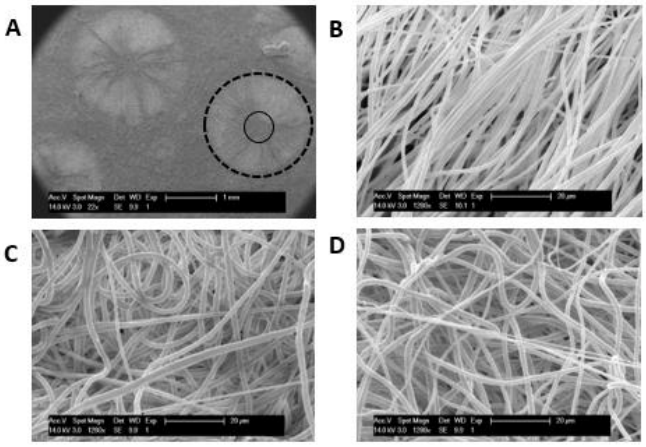

Fig. 1: SEM images of micropatterned PCL scaffolds and zoom in images of the different existing fibre distributions within a micropattern. A) Micropatterned topographical cue. B) Fibre morphology at the central area C) in the walls and D) outside of the topographical cue.

DISCUSSION & CONCLUSIONS: The combination of intricate topographical cues with biomolecules into 3D fibrous scaffolds is a novel approach towards the development of cell responsive environments. Our current work is focusing now on the quantification and chemical characterisation of heparin on the scaffolds using XPS and nuclear magnetic resonance (NMR) respectively. This new strategy will ultimately provide us with a new generation of membranes with the ability to control cell behaviour and therefore with key data for achieving a better understanding of bone regeneration mechanisms and ultimately facilitate the design of biomedical devices for musculoskeletal regeneration.

REFERENCES: [1] Ling, L., Dombrowski, C., Foong, K.M., Haupt, L.M., Stein, G.S., Nurcombe, V., van Wijnen, A.J., and Cool, S.M. (2010). Synergism between Wnt3a and heparin enhances osteogenesis via a phosphoinositide 3-kinase/Akt/RUNX2 pathway. J. Biol. Chem. *285*, 26233–26244.

ACKNOWLEDGEMENTS: The University of Sheffield and A*STAR for financial support. MeDe Innovation (Grant no: EP/K029592/1) for financial contribution.

Regenerating articular cartilage through the use of decellularised osteochondral matrices to support autologous cell therapies

P Lawson-Statham[1], E Jones[2], RJ Wilcox[1], L Jennings[1], M Izon[3] and HL Fermor[1]
[1]Institute of Medical and Biological Engineering, University, Leeds.[2]Faculty of Medicine and Health, St James University Hospital, Leeds.[3] Tissue Regenix PLC, Leeds

INTRODUCTION: It is estimated that 10,000 people in the UK alone suffer cartilage lesions which require treatment every year [1]. These lesions may progress to osteoarthritis (OA) under normal joint loading and articulation, resulting in joint immobility and pain for patients. For younger and more active patients, total knee replacement is unfavourable due to their limited lifetime. Other treatments such as mosaicplasty, debridement and microfracture, also bear respective limitations in donor site morbidity and fibrocartilage repair [2].

In 2017, new guidance by NICE recommended the use of autologous chondrocyte implantation (ACI), by which the patient's own chondrocytes are delivered to the defect to encourage regeneration as a cost effective treatment for cartilage defects. Iterations of this process utilise a collagen matrix (ACI-C) to aid cell delivery and to provide a scaffold for tissue regeneration. Neither of these approaches offers immediate restoration of cartilage biomechanics and therefore have limited function prior to regeneration [3].

We propose that native decellularised osteochondral xenogeneic scaffolds will provide an optimum 'off the shelf' immunocompatible matrix to support autologous cell therapies. These biological scaffolds retain near native tissue biochemical composition, extracellular matrix structure and biomechanical function, offering an ideal tissue replacement and microenvironment for cartilage regeneration.

AIMS: Our aims are principally to investigate the applicability of these scaffolds as a matrix to support cell therapies. Alongside investigating the use of a self-assembling peptide (SAP) technology developed at Leeds combined with chondroitin sulphate (SAP-CS) as a novel biocompatible cell carrier permitting cell encapsulation and control of cartilage stiffness.

METHODS: Bioprocesses to decellularise osteochondral rods (9 mm diameter) have been developed, and these will be adapted to produce a stratified range of scaffolds appropriate for lesions of various dimensions. Following this, the optimum cell delivery method to the scaffold will be investigated, with a focus on the SAP-CS system. Stratification opportunities exist to target the number and density of cells which will be delivered as well as need for cell pre-conditioning. Finally, we aim to study exactly how the cell populations respond to the matrix in terms of viability, proliferation and differentiation and establish whether biomechanical stimuli are required to produce optimal recellularisation.

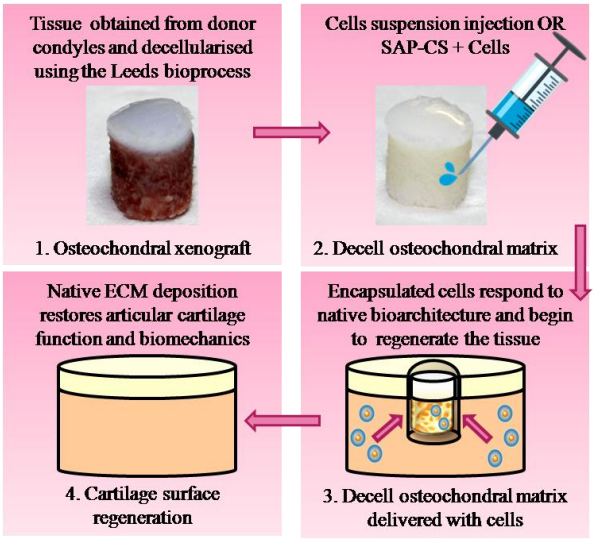

Fig. 1: Treatment rationale

CONCLUSIONS: The project scope here demonstrates potential for the development and translation of a stratified range of functional matrix associated autologous cell therapies for cartilage repair. The long-term translational goal is to develop a technology which will facilitate rapid recovery time for patients and prolong the lifetime of their natural knee, delaying the requirement for prosthetic intervention.

REFERENCES: [1]NICE (2017) Autologous chondrocyte implantation for treating symptomatic articular defects of the knee. www.nice.org.uk. [2] TF Tyler and JY Lung (2012) Rehabilitation following osteochondral injury to the knee in *Curr Rev Musculoskelet Med*, 5(1), pp72-81. [3]L Zhang *et al*. (2011) The Role of Tissue Engineering in Articular Cartilage Repair and Regeneration in *Crit Rev Biomed Eng*, 37(1-2), pp1-57

ACKNOWLEDGEMENTS: iMBE (University of Leeds) and Tissue Regenix PLC.

Human model of the neuromuscular junction using iPSCs and 3D tissue engineering constructs

L Marani[1], M Pardo-Figuerez[1,2], A Capel[1], Z Nilson[3], A Stolzing[4], M Lewis[1]

[1] *School of Sports, Exercise and Health Sciences, Loughborough University, England. Institute of Agrochemistry and Food Technology (IATA), Spanish Council for Scientific Research (CSIC), Spain. [3]Axol Bioscience, Cambridge, England [4]Wolfson School of Mechanical and Manufacturing Engineering, Centre for Biological Engineering - Garendon Wing, Loughborough University, UK*

INTRODUCTION: The use of induced Pluripotent Stem Cells (iPSCs) is growing globally[1]. A human *in vitro* model of the neuromuscular junction (NMJ) is essential to study physiology and pathophysiology of the tissues, as well as developing a platform for drug screening[2]. This work focuses on the optimisation of a human skeletal muscle (hSkM)/human iPSC-derived motor neurons (MNs) co-culture model, both in monolayer and in 3D tissue engineering constructs.

METHODS: Primary hSkM was obtained from vastus lateralis biopsies at Loughborough University and expanded on gelatin coated tissue culture plastic in Dulbecco's Modified Eagles Medium (DMEM), supplemented with 20% fetal bovine serum (FBS). iPSC-derived MNs were kindly provided by Axol Bioscience and cultured according to the manufacturer's protocol. The co-culture was performed expanding hSkM up to confluence, and then seeding the MNs on the myoblast layer. The differentiation of both cell types was carried out for 5 days using MN Maintenance Medium (MM). The morphological immunostaining was performed using Rhodamine-Phalloidin for actin filaments, β-III Tubulin for microtubules and 4',6-diamidino-2-phenylindole (DAPI) for nuclei.

RESULTS: The optimisation of the primary co-culture showed that hSkM fuses into myotubes more on Gelatin (vs SureBond+ReadySet, substrate used to culture MNs). The 2 cell types co-exist in all co-culture conditions (*Figure 1*) and the MNs stained positively for the cholinergic marker Choline Acetyltransferase (ChAT) up to 35 days in culture (data not shown). Interaction staining (α-Bungarotoxin for Achetylcholine receptors and Synaptic Vesicle 2) showed co-localisation of the 2 markers, indicating a potential interaction of hSkM and MNs in monolayer. Promising morphological analysis was also performed on the 3D co-cultures and showed neurite extension through the matrix.

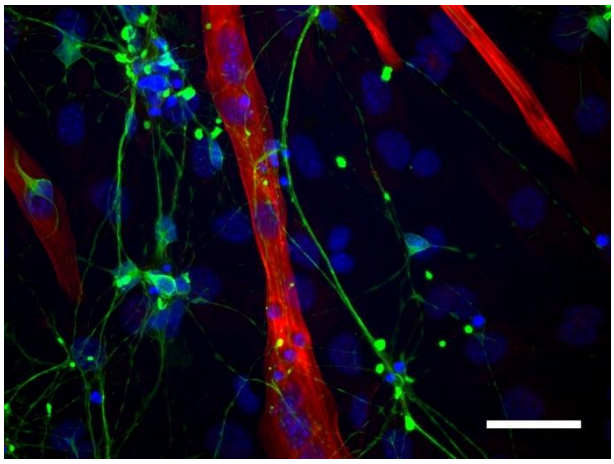

Figure 1: Human skeletal muscle and human iPSC-derived MNs co-exist in culture. Rhodamine Phalloidin (red), β-III Tubulin (green), DAPI (blue). Scale bar 100 µm.

DISCUSSION & CONCLUSIONS: Despite the numerous challenges to be faced while generating iPSC-derived MNs, promising models were developed[2].This work shows that iPSC-derived MNs are cholinergic and can be co-cultured with primary hSkM cells in different conditions, to maximise the interaction and formation of the NMJ. Once fully optimised, this model will be a promising platform for industries to test therapeutic compounds and predict the outcome of drug treatments for patients affected by musculoskeletal and neurological diseases.

REFERENCES: [1]S Yamanaka (2012), *Cell Stem Cell*, **10**:678-684. [2] S Thomson, T Wishart, R Patani, S Chandran, T Gillingwater (2012), *Journal of Anatomy*, **220**:122-130.

ACKNOWLEDGEMENTS: This work is supported by the Centre for Doctoral Training in Regenerative Medicine. The author would like to thank Prof. Mark Lewis and his group, and Dr. Zoe Nilsson for the support received.

This template was modified with kind permission from eCM Journal.

Human platelet lysate – a viable alternative to FBS for periosteum derived stem cell expansion and intramembranous bone formation

P Gupta[1,2], G.N Hall[1,2], F. Luyten[1,2*] , I. Papantoniou[1,2*]

[1]Prometheus, KU Leuven, BE, [2] Skeletal Biology and Engineering Research Center, KU Leuven, BE

INTRODUCTION: Due to their low regulatory restrictions and multipotent nature, mesenchymal stem cells (MSCs) are considered to be an important cell source for Tissue Engineering and Regenerative Medicine (TERM). The use of human platelet lysate (HPL) as an alternative to FBS for MSC culture has gained momentum in recent time[1, 2]. Here, we report, the use of HPL for spinner flask based expansion of human periosteum derived stem cells (hPDCs). Apart from highlighting the suitability of HPL for the expansion of hPDCs, we also report for the first time the role of HPL in bone forming capacity of hPDCs in an ectopic mouse model.

METHODS: Preliminary 2D comparison between 2%, 5% and 10% HPL was carried out to select the best suited concentration for hPDCs. Selected HPL concentration was used for spinner flask based culture using Cultispher-S microcarriers following previously published method[3]. FBS supplemented media was used as control. Cell and media sample were collected at regular interval for various analysis (cell count, q-PCR, FACS). At the end of 10 days, expanded cells were ectopically implanted in nude mice models using calcium phosphate (CaP) scaffolds. 8weeks explants were analysed to quantify bone formation.

RESULTS: Preliminary 2D comparison showed that 10% HPL consistently maintained higher cell proliferation in comparison to other conditions for hPDCs. Hence, 10% HPL was selected for further bioreactor based culture. Throughout the culture period HPL supplemetation resulted in a faster cell expansion in comparison to FBS. At the end of 10 days, HPL resulted in a 5.2±0.61 fold increase in cell number in comparison to a 2.7±0.22 fold increase with FBS. The cells were able to maintain MSC characteristic marker (CD 73, CD90 and CD105) expression along with their trilienage differentiation property, although adipogenic differentiation capability was reduced in HPL expanded hPDCs. 8 week explants of FBS and HPL expanded hPDCs showed clear difference in terms of mineralised tissue formation. The use of HPL in spinner flask culture resulted in a higher volume of well-formed mineralisation within the scaffolds while FBS resulted in less volume and a more fibrous structures. Representative images are shown in figure 1.

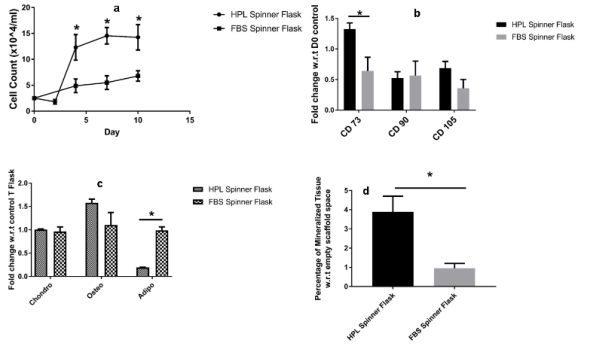

Fig.1:(a)Viable cell count for spinner flask culture, (b qPCR analysis of CD markers, (c)trilineage differentiation potential analysis, (d)mineralised tissue within quantification of 8week old explants.

DISCUSSION & CONCLUSIONS: We report for the 1st time, spinner flask based expansion of hPDCs using HPL supplemented media and their ectopic bone forming capacity. HPL resulted in faster cell proliferation in comparison to FBS while maintaining their characteristics CD markers and trilineage differentiation capabilities. It is well established at Prometheus that 2D FBS expanded hPDCs are capable of forming mineralised bone tissue in CaP scaffolds, the use of spinner flasks changed this. Spinner flask culture with FBS resulted in less mineralised and more fibrous tissues while HPL resulted in well-formed higher volume of mineralised bone tissue. These data highlight the need for individual process optimisation for bioreactor based culture. HPL is also shown to be a valid alternative for replacement of FBS.

REFERENCES:1.Heathman,T.R. et al. Scalability and process transfer of mesenchymal stromal cell production from monolayer to microcarrier culture using human platelet lysate. *Cytotherapy* **18**, 523-535 (2016).2.Petry,F.et al. Manufacturing of human umbilical cord mesenchymal stromal cells on microcarriers in a dynamic system for clinical use. *Stem cells international* **2016** (2016).3.Gupta, P. et al. An Integrated Bioprocess for the Expansion and Chondrogenic Priming of Human Periosteum-Derived Progenitor Cells in Suspension Bioreactors. *Biotechnology journal* **13** (2018).

ACKNOWLEDGEMENTS:P.G. was funded by ERC Grant Agreement No. 294191 I.P. was funded by FWO fellowship, project 12O7916N.

Identification and *in vitro* screening of osteogenic metabolites through supplement-free nanovibration-driven mesenchymal stem cell differentiation

T Hodgkinson[1], K Burgess[2], D France[3], P Campsie[4], S Robertson[4], D Phillips[4], P Childs[1], ROC Oreffo[5], S Reid[3], M Sanchez-Salmeron[1], MJ Dalby[1]

[1]Centre for the Cellular Microenvironment, College of Medical, Veterinary and Life Sciences, University of Glasgow, Scotland. [2]Glasgow Polyomics, University of Glasgow, Scotland. [3]School of Chemistry, University of Glasgow, Scotland [4]SUPA, University of Glasgow, Scotland. [5]Centre for Human Development, Stem Cells and Regeneration, University of Southampton

INTRODUCTION: There is a need for the development of effective tissue engineered approaches to produce bone. In the laboratory, these approaches typically involve osteogenic differentiation of mesenchymal stem cells (MSCs) through media supplementation. We recently developed a supplement-free osteogenic differentiation protocol through nanovibrational-stimulation of MSCs[1]. Here, we hypothesised that nanovibrational differentiation of MSCs would allow metabolomic analysis of differentiation without confounding exogenous media supplements. We aimed to investigate MSC nanovibration-driven osteogenesis in 2D and 3D cultures, identify key osteogenic metabolites and metabolomic processes and investigate their osteogenic potential by supplementing these pathways *in vitro*.

METHODS: Human MSCs were cultured in standard tissue culture well plates (2D) or in type I collagen gels (3D) and cultured over 28 days in three groups- nanovibrational stimulation, osteogenic media (dexamethasone) and MSC expansion media. Differentiation was tracked through changes in gene expression (qPCR), protein expression (immunofluorescent staining (IFS)). At key points, cell metabolomic analysis was performed (LC-MS; ZIC-pHILIC). We selected the most promising metabolite during osteogenic differentiation. This was synthesised along with several chemical analogs. The osteogenic potential of these metabolites was then investigated through gene and protein expression following supplementation to 2D and 3D MSC cultures.

RESULTS: Nanovibration upregulated key osteogenic genes in both 2D and 3D cultures comparably to osteogenic media, including early upregulation of RUNX2 (2D x14.5, $p<0.05$; 3D x11.5, $p<0.05$) followed by maturation marker osteopontin (2D x19, $p<0.05$; 3D x7.2, $p<0.05$). Corresponding increases in osteogenic proteins were also observed. Metabolomic analysis identified several key networks, with cholesterol sulphate (CS) identified as a promising metabolite target. When CS and several analogs were supplemented at 1 μM to 2D and 3D cultures they induced osteogenic gene and protein expression, comparably to osteogenic media, while having less off target effects. In particular, fludrocortisone and fludrocortisone acetate significantly increased osteogenic marker expression, even versus osteogenic media.

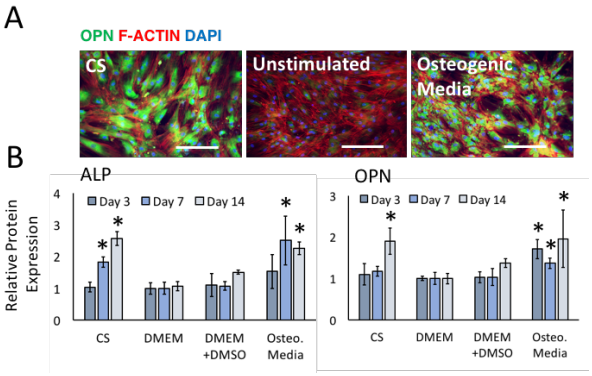

*Fig. 1: (A) Osteopontin IFS after 14-days culture with Cholesterol sulphate (CS) or osteogenic media (B) ALP and OPN protein expression with cholesterol sulphate supplementation, expansion media or osteogenic media. (n=3;*p<0.05).*

DISCUSSION & CONCLUSIONS:
Nanovibration is an exciting tool for the supplement-free study of MSC osteogenic differentiation, while this work also validates a targeted metabolite supplementation approach for controlling cell fate decisions, which may prove cheaper and more specific than conventional approaches.

REFERENCES: [1]Tsimbouri, P.M., *et al.* (2017) Nature Biomedical Engineering, 1:758.

ACKNOWLEDGEMENTS: We would like to thank the EPSRC (EP/N013905/1) for funding this project and CeMI lab members for assistance.

This template was modified with kind permission from eCM Journal.

Impact of human platelet lysate on the expansion and chondrogenic capacity of cultured human chondrocytes for cartilage cell therapy.

JG. Sykes[1], JH. Kuiper[1], JB. Richardson[1], S. Roberts[1], KT. Wright[1] and NJ. Kuiper[1]
[1]*Institute of Science & Technology in Medicine (ISTM), University of Keele, Arthritis Research Centre, The Robert Jones & Agnes Hunt Orthopaedic Hospital, Oswestry, Shropshire, UK.*

INTRODUCTION: High hopes have been pinned on regenerative medicine strategies to meet the challenge of preventing the progression to osteoarthritis, particularly autologous chondrocyte implantation (ACI). The loss of chondrocyte phenotype during *in vitro* monolayer expansion, a necessary step to obtain sufficient cell numbers, may be a key limitation in ACI[(1)]. In this study, we determined whether a shorter monolayer expansion approach could improve chondrogenic differentiation. Stemulate™ (a commercially available source of human platelet lysate from Cook Regentec) has been shown to increase proliferation in several different cell types, including mesenchymal stem cells and fibroblasts[(2,3)]. However, no published studies investigated the effect of Stemulate™ on human chondrocytes, and the subsequent effect on the quality of the extracellular matrix produced. We compared the effects of two supplement types: foetal bovine serum (FBS) and Stemulate™, on the expansion and re-differentiation potential of human chondrocytes.

METHODS: Human articular chondrocytes were harvested from five patients undergoing total knee replacement surgery at our centre, and monolayer expanded with 10 % FBS or 10 % Stemulate™. Growth kinetics were determined whilst in monolayer culture. Chondrocytes were seeded into chondrogenic pellets and were cultured for 28 days in chondrogenic differentiation medium. Assessments for the synthesis of two key cartilage matrix molecules: sulphated glycosaminoglycans (sGAGs) and total collagen were performed with biochemical assays. Assessments for markers and genes associated with chondrogenicity were performed using RT-qPCR. Histological analysis was performed using toluidine blue to assess proteoglycan content and haematoxylin and eosin (H&E) to assess general morphology.

RESULTS: Stemulate™ significantly enhanced proliferation rates of the chondrocytes during monolayer expansion (average population doubling times; FBS 25.07 days ±6.98 standard error of mean (SEM) vs Stemulate™ 13.10 days ±2.57 SEM; p=0.05). sGAG, total collagen and qRT-PCR analyses of cartilage genes showed that that FBS-expanded chondrocytes demonstrated significantly better chondrogenic capacity than Stemulate™-expanded chondrocytes. Histologically, FBS-expanded chondrocyte pellets appeared to be more stable, with a more intense staining for toluidine blue, indicating a greater chondrogenic capacity, histologically.

DISCUSSION & CONCLUSIONS: Overall we have shown that although Stemulate™ positively influences chondrocyte proliferation, it has a negative effect on chondrogenic differentiation potential. FBS appears to recover the chondrogenic potential quicker than Stemulate™. This suggests that Stemulate™ may not be the ideal supplement for the expansion of chondrocytes, maintaining chondrocyte phenotype and hence for cell therapies, including ACI, in the treatment of cartilage defects.

REFERENCES:

[1.] Schulze-Tanzil G. (2009). Activation and dedifferentiation of chondrocytes: Implications in cartilage injury and repair. *Ann Anat - Anat Anzeiger.* **191**(4):325–38. [2.] Hildner F, Eder MJ, Hofer K, *et al*. (2015). Human platelet lysate successfully promotes proliferation and subsequent chondrogenic differentiation of adipose-derived stem cells: a comparison with articular chondrocytes. *J Tissue Eng Regen Med.* **9**(7):808–18. [3.] Hemeda H, Giebel B, Wagner W. (2014). Evaluation of human platelet lysate versus fetal bovine serum for culture of mesenchymal stromal cells. *Cytotherapy.* **16**(2):170–8.

ACKNOWLEDGEMENTS: We are grateful for the financial support kindly provided by the Orthopaedic Institute Ltd., The Robert Jones & Agnes Hunt Orthopaedic Hospital, Oswestry, UK. We would like to thank Cook Regentec for supplying the Stemulate™, Dr Sharon Owen and Mrs Annie Kerr for obtaining patient consent.
The authors would like to acknowledge the sad passing of their friend and colleague Professor James Richardson.

In situ melanoma biomarker detection on a novel skin cancer 3D model via immunodiagnostic microneedles

S Totti [1], KW Ng[2], G Lian[1,3], T Chen[1], EG Velliou[1]

[1] *Bioprocess and Biochemical Engineering group (BioProChem), Department of Chemical and Process Engineering, University of Surrey, Guildford.* [2] *School of Pharmacy, Newcastle University, Newcastle upon Tyne.* [3] *Unilever R&D Colworth, Bedfordshire*

INTRODUCTION: Metastatic melanoma is the most lethal skin cancer. The prognosis for patients with distant metastasis is particularly poor and the 5-year survival rate is a dismal 20% [1]. To improve these disappointing statistical figures, it is essential to better understand the tumour's behaviour, progression and response and/or resistance to treatment options. Recent advances in tissue engineering enable the development of more physiologically relevant models that can recapitulate important features of the tumour tissue, i.e., the so-called tumour microenvironment (TME). More specifically, biomaterial based scaffolds can simulate important topological tissue features that affect the disease's progression and response to treatment, such as porosity, structure, extracellular matrix presence, cell-cell and cell-matrix interactions, environmental gradients and vascularization [2-4]. To date, the most effective treatment for melanoma is early diagnosis followed by surgical resection. Towards rapid diagnosis, minimally invasive microneedles are solid or hollow microstructures that enable rapid and pain-free biomarker detection *in situ* [5]. *The aim of this work was to develop and further validate the S100, a marker that is upregulated in melanoma, on a microporous polymer based 3D melanoma model. S100 expression in the model was confirmed using an immunodiagnostic microneedle device.*

METHODS: The overall procedure followed is depicted in Figure 1. 3D polymer (PU) based microporous scaffolds were developed and the metastatic melanoma cell line A-375 was injected and cultivated in those scaffolds for 5 weeks. Quantitative assessment of cell viability took place with the MTS metabolic assay and evaluation of cell distribution within the PU matrix was conducted with Scanning Electron Microscopy (SEM). Viable (live) cells were visualised *in situ* with confocal laser scanning microscopy (CLSM) of several sections of each scaffold. Furthermore, the detection of the S100 melanoma specific marker was carried out with microneedles via immunoassay analysis on their surface.

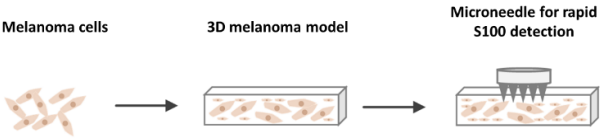

Fig 1. Developed platform for S100 detection in the 3D melanoma model.

RESULTS: The 3D microporous scaffolds were able to support the long term cultivation of the A-375 cells, with the majority of them being viable until the culture endpoint. Dense melanoma cell masses adhered to the scaffold pores and were distributed throughout the 3D matrix. Additionally S100 detection was achieved via immunodiagnostic microneedle administration on the surface of the 3D scaffolds.

DISCUSSION & CONCLUSIONS: Our findings indicate that this 3D polymer based microporous system is a promising tool for *ex vivo* modelling of metastatic melanoma. Furthermore, to our knowledge, this is the first time that a 3D *in vitro* melanoma model is used for validation of biomarker detection with microneedles. Our findings suggest that this 3D microporous melanoma scaffold can be used as a low cost tool for validation/screening of novel cancer detection methods and/or kits, replacing and/or reducing animal testing for the validation of such kits.

REFERENCES: [1] R.L. Siegel, K.D. Miller, and A. Jemal. (2018) *CA Cancer J Clin* **68**:7-30. [2] S. Totti, S.I. Vernardis, L. Meira, et al (2017) *Drug Discov Today* **22**, 690-701. [3] S. Totti, M. Allenby, S B. Dos Santos, et al (2017) *Eur Cells Mater* **33** (Suppl. 2), 0249, [4] S. Totti, S B. Dos Santos, M. Allenby, et al (2016) *Eur Cells Mater* **31**(Suppl. 1), P441**,** [5] K.W. Ng, W.M. Lau, and A.C. Williams (2015) Drug Deliv and Transl Res **5**, 387-96.

ACKNOWLEDGEMENTS: This work was supported by University of Surrey as well as an Impact Acceleration Grant (IAA-KN9149C) of the University of Surrey, an IAA –EPSRC Grant (RN0281J) and the Royal Society.

In vivo evaluation of a biofabricated nanocomposite cell-laden bioink for skeletal tissue regeneration

G.Cidonio[1,2], T. Ahlfeld[3], M. Glinka[1], Y. Kim[1], J. Kanczler[1], S. Lanham[1], S. Yang[2], A. Lode[3], J.I. Dawson[1], M. Gelinsky[3], R.O.C. Oreffo[1]

[1]Bone and Joint Research Group, Centre for Human Development, Stem Cells and Regeneration, Institute of Developmental Sciences, University of Southampton, Southampton, UK. [2]Engineering Materials Research Group, Faculty of Engineering and the Environment, University of Southampton, Southampton, UK. [3]Centre for Translational Bone, Joint and Soft Tissue Research, University Hospital Carl Gustav Carus and Faculty of Medicine, Technische Universität Dresden, Dresden, DE

INTRODUCTION: Biofabrication aims to produce complex three-dimensional scaffolds simultaneously extruding biomaterials and living cells. However, this paradigm involves the use of high polymeric content paste to ensure shape fidelity which often impacts cell viability [1]. In this study, we present a clay-based bioink for skeletal tissue regeneration and the development of viable 3D scaffolds *in vitro*, that show vessel infiltration *ex vivo* and bone tissue formation *in vivo*.

METHODS: 3% w/v nanoclay (Laponite), alginate and methylcellulose (3-3-3) paste was prepared by direct mixing of core components as previously described [2]. Human bone marrow stromal cells (HBMSCs) were expanded for an encapsulation density of 5×10^6 cells g^{-1}. Pre-labelling of cells was performed with Vybrant DiD (Thermo Fisher Scientific). Metabolically active cells were identified post-printing with Calcein AM staining (Molecular Probes) at 1, 7, 14 and 21 days. VEGF-loaded 3-3-3 scaffolds were implanted in 10 day old chick embryos. Integration and angiogenesis within the chorioallantoic membrane (CAM) determined by histology and Chalkley score after 7 days. BMP-2 loaded 3-3-3 scaffolds were implanted in a murine subcutaneous implant model. Quantitative analysis for new bone was performed using a SkyScan 1176 system (Bruker micro-CT, Kontich) and samples analysed using CTAn software v.1.17.7.2 (Bruker) to assess bone volume (BV).

RESULTS: HBMSCs-laden 3-3-3 scaffolds were viable at 1 (81.1 % ± 13.3), 7 (88.0 % ± 6.7), 14 (88.3 % ± 9.2) and 21 (88.8 % ± 8.0) days. 3-3-3 scaffolds demonstrated vascular infiltration in an *ex vivo* CAM model after 7 days. Biofabricated constructs showed significant *in vivo* bone formation in the mouse implant model. Clay-based 3D printed scaffolds both with and without BMP-2 showed a significant difference in mineralized tissue (BV 15.17 ± 1.98 mm3 ($p < 0.0001$) and 13.75 ± 3.98 mm3 ($p < 0.0001$) respectively) compared to bulk alginate control. 3-3-3 constructs loaded with BMP-2 resulted in highly significant ($p < 0.0001$) increase in mineral tissue formation compared to alginate-BMP-2 bulk hydrogel.

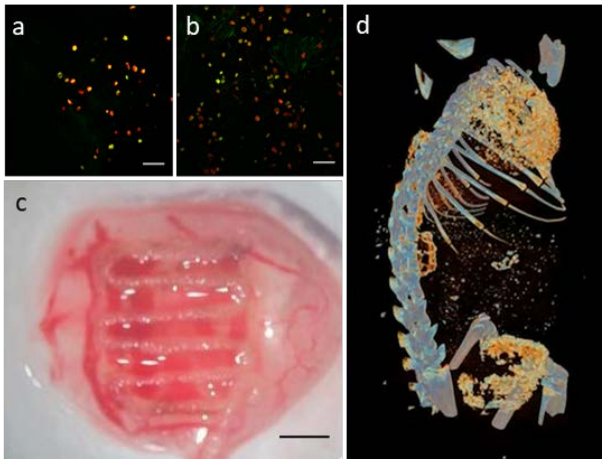

Fig. 1: a-b) Confocal images of HBMSCs-laden 3-3-3 scaffolds at day 1 and 21 respectively (Scale bar: 100 µm). c) Integrated 3-3-3 scaffolds in CAM model (Scale bar: 5 mm). d) Micro CT scan of day 28 BMP-2 loaded 3D printed 3-3-3 scaffolds.

DISCUSSION & CONCLUSIONS: The current studies demonstrate the *in vitro* viability, *ex vivo* and *in vivo* functionality of a cell laden nanocomposite bioink. CAM vascular infiltration and *in vivo* bone formation indicate the orthopaedic translational potential of this clay-based bioink.

REFERENCES: [1] J Malda, et al (2013) *Advanced Materials* **25**:5011-28. [2] T. Ahlfeld, G. Cidonio, et al (2017) *Biofabrication* **9**:034103.

ACKNOWLEDGEMENTS: Supported by Biotechnology and Biological Sciences Research Council UK (BB/ L00609X and BB/LO21072/1) and University of Southampton IfLS, FortisNet and Postgraduate awards to ROCO. This template was modified with kind permission from eCM Journal.

Influence of composition of Poly (N-Isopropylacrylamide) - Based Laponite® Hydrogels on their properties and cell behaviour.

Essa A[1], Le Maitre CL[1], Sammon C[1].

[1] *Sheffield Hallam University, Sheffield, UK.*

INTRODUCTION: We have previously reported the development of a synthetic Laponite® crosslinked pNIPAM-co-DMAc hydrogel (L-pNIPAM-co-DMAc), which can be modified to tailor stem cell differentiation to intervertebral disc[1], bone[2], or maintain gastrointestinal cells[3]. Here, a range of compositions of injectable pNIPAM-Laponite® hydrogels were studied, to determine the influence of crosslink density, comonomer type and concentration on the properties and their suitability to be used in regenerative therapies.

METHODS: Hydrogels were prepared via precipitation polymerisation of various ratios of N-Isopropylacrylamide, hydroxypropylmethacrylate and hydroxyethylmethacrylate with a thermal initiator (AIBN) with three different concentrations of Laponite®/water dispersion. The state of water was investigated using Fourier transform infrared spectroscopy (Thermo Nicolet Corp., USA). human mesenchymal stem cells (hMSCs) were embedded into different hydrogel compositions and cell viability was assessed using Alamar Blue assay (Life Technologies, Paisley UK) and phenotype assessed using histology and immunohistochemistry. Morphology of acellular hydrogels and hydrogels containing hMSC were examined using a scanning electron microscope (FEI NOVA nano-SEM 200 scanning electron microscope), and dynamic mechanical analysis (PerkinElmer DMA 8000) used to determine viscoelastic behavior of each composition.

RESULTS: Increased crosslink density increased storage moduli and decreased pore size (Fig 1), whilst incorporation of comonomer HPA decreased moduli and increased pore size. hMSCs maintained viability in pNIPAM hydrogels and increased metabolic activity with HPA but decreased activity was seen with HEMA. Interestingly cells responded differently in the different hydrogel compositions. Most notably, incorporation of HPA promoted matrix deposition of collagens and calcium deposition following 4 weeks (Fig 2).

DISCUSSION & CONCLUSIONS: Hydrogel composition was shown to affect material and cell behavior, demonstrating the hydrogel can be tuned to provide different properties.

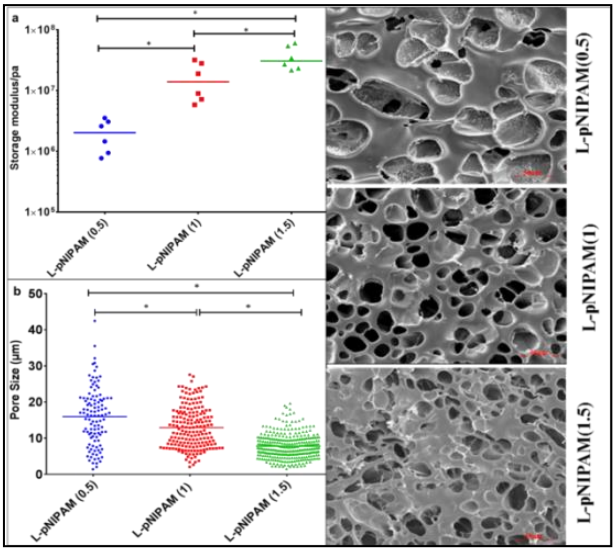

Fig. 1: a) Storage modulus for pNIPAM hydrogels with different crosslink density. b) SEM images of pNIPAM hydrogels with different crosslink density and their pore size statistical analysis.

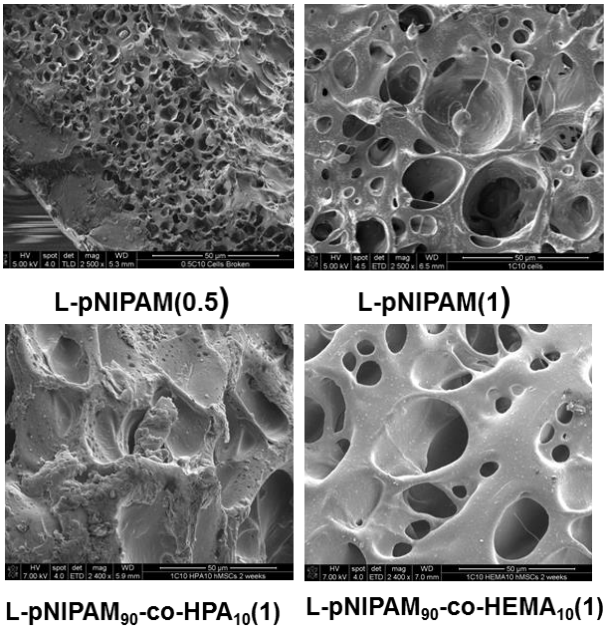

Fig. 2: SEM images of hydrogelsfollowing 4 week culture containing hMSCs

REFERENCES: [1] A.A Thorpe *et al.,* (2016). Acta Biomater. 36:99-111. [2] A.A. Thorpe *et al.,* (2016). Eur Cell Mater. 32:1-23. [3] R. Dosh *et al.,* (2017). Acta Biomater. 62:128-143.

ACKNOWLEDGEMENTS: We thank the Libyan government for funding.

Innovative manufacturing of decellularised bone scaffolds

K Cowell[1], A Herbert[1], P Rooney[2], RK Wilcox[1], HL Fermor[1]

[1] Institute of Medical and Biological Engineering, University of Leeds, Leeds, UK. [2] NHS Blood and Transplant, Tissue and Eye Services, Liverpool, UK

INTRODUCTION: Bone grafting is the second most common tissue transplantation after blood transfusion and can be used for clinical procedures from fusing bones together to assisting in securing surgical implants[1]. The gold standard method of bone grafting is the autograft, sourcing the bone graft from another part of the patient's body, usually the iliac crest. This can cause pain, blood loss and infection at the donor site and also doubles the number of surgical procedures required. An alternative to this is cadaveric allograft, however, this has been found to re-vascularise poorly and have inferior bone remodelling to autografts, leading to a higher incidence of fracture and non-union. Additionally, there are concerns about potential immune responses to allografts and increased infection rates via transfer of pathogens from donor to patient[2].

AIMS: Decellularisation of allografts has been proposed as a potential solution to these problems. Currently, methods used to produce decellularised scaffolds are labour intensive; taking up to six weeks. Therefore, the primary aim of this research is to translate the current method of decellularisation into a scalable, automated, closed system that produces clinically suitable decellularised bone grafts. The second aim of the project is to use this manufacturing process to investigate how varying the source tissue, size, shape and sterilisation method can change the mechanical and biochemical properties of bone grafts. With the intention of producing a range of stratified bone graft products for specific patient and surgeon requirements.

METHODS: To assess the quality of the novel automated decellularisation system histology will determine whether the process has removed all cells and cell fragments, the DNA will be quantified to ensure it is below the widely used decellularisation target value of 50ng per mg dry tissue weight[3]. The material and biological properties of the stratified bone products will be assessed using a variety of techniques: Young's modulus and 0.2% proof stress will be measured using compression testing; MicroCT will be used to determine bone volume; and cytotoxicity will be evaluated using cell culture. A summary of these methods can be found in Figure 1.

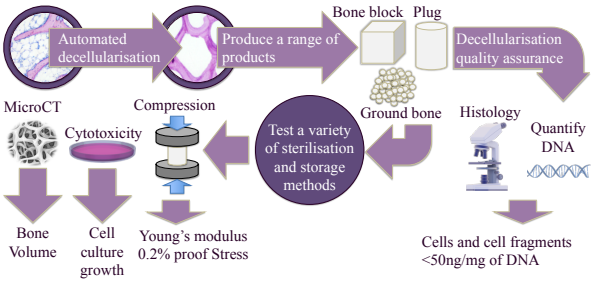

Fig. 1: Summary of prospective methods and techniques

IMPACT: Both patients and clinicians will benefit from this research as bone grafts that are easily manufactured to a precise, reproduceable quality and are customisable for a variety of functions will be an improvement over the current bone grafting methods. The economic beneficiaries from this work are the sponsors, NHS Blood and Transplant, Tissue and Eye Services, who will be able to integrate the automated decellularisation system into their current bone graft production methods. Additionally, academic groups studying decellularisation will benefit from a faster and easier decellularisation process.

REFERENCES: [1] P.V. Giannoudis, H. Dinopoulos and E. Tsiridis (2005) Bone substitutes: An update, *Injury*, **36**(3):S20-S27. [2] A.S. Brydone, D. Meek and S. Maclaine (2010) Bone grafting, orthopaedic biomaterials, and the clinical need for bone engineering *Proc Inst Mech Eng H.,* **224**(12) 1329-43 [3] P.M. Crapo, T.W. Gilbert and S.F. Badylak (2011) An overview of tissue and whole organ decellularization processes, *Biomaterials*, **32**:3233-3243.

ACKNOWLEDGEMENTS: Thank you to both EPSRC and NHS Blood and Transplant, Tissue and Eye Services for funding this research.

This template was modified with kind permission from eCM Journal.

Integrin-growth factor synergistic microenvironments to investigate metabolic mechanisms for a bone marrow niche-like phenotype

Hannah Donnelly[1], Ewan Ross[1], Christopher West[2], Bruno Peault[2], Jo Mountford[3], Manuel Salmeron-Sanchez[1] & Matthew J Dalby[1]

[1]Centre for the Cellular Microenvironment, University of Glasgow, Scotland, UK. [2]MRC Centre for Regenerative Medicine, University of Edinburgh, UK. [3]Scottish National Blood Transfusion Service, Edinburgh, Scotland, UK

INTRODUCTION: Pericytes are key bone marrow niche cells. The niche is a regulatory microenvironment that is hypoxic. They have immune modulatory and inflammatory functions, and act to support haematopoietic stem cells (HSCs). In culture, however, both pericytes and HSCs lose their niche phenotype. Noting that soft gels can support nestin[1] expression, a key niche marker, we aim to create a system supporting a niche-like pericyte phenotype. Here, poly(ethyl acrylate) (PEA) was used to assemble fibronectin (FN) into physiological-like networks, thus allowing growth factor tethering and presentation in synergy with integrin binding sites[2]. Then, a soft gel or hypoxia was used, to investigate metabolic mechanisms required to support niche phenotypes in this bone marrow-like microenvironment. We used poly(methyl acrylate) (PMA) as a control where FN is not assembled into networks[2].

METHODS: *Preparation of materials and system set up:* PEA was polymerised and then spin coated on 12 mm glass coverslips2. FN from human plasma was adsorbed (20 µg/mL) followed by BMP-2 (50 ng/mL). Pericytes, isolated from human adipose tissue were seeded at 103 cells/substrate. Then either a collagen gel (2 mg/mL to match bone marrow stiffness) or 1% hypoxia was added at 72h. *Metabolomic and transcriptomic analysis:* Metabolites were extracted 7 & 14 days after seeding. Relative abundance measured using liquid chromatography-mass spectrometry (LC-MS). RNA-Seq whole transcriptome profiling after 7 days. (N= 3; 4). *Immunocytochemistry:* Immunofluorescence was used to asses LDH levels (n=3, $p < 0.05$), levels of phenotypic markers (nestin, CD146, NCAM) and transcription factor hypoxia-inducible factor 1 (HIF1α) levels and activity (Hypoxyprobe™).

RESULTS: Immunocytochemistry revealed an increase of sustained activated HIF1α with soft gels after 3 days (+Gel), whereas similar levels of HIF1α activation were observed in the absence of gel (–Gel) and in 1% hypoxia, where activation levelled out after ~12h. Controls supporting globular FN conformation (PMA and glass) both had significantly reduced levels compared to PEA FN BMP2 (Fig 1). Correspondingly, levels of glycolytic enzyme lactate dehydrogenase (LDH) showed a trend towards increased levels with gel addition, suggesting a switch to an anaerobic metabolic profile. Metabolomic analysis revealed strong agreement in down-regulation of metabolites involved in oxidative phosphorylation with the soft gel and hypoxic system. Genome-wide transcriptomic analysis identified key genes similarly expressed, such as glycolytic enzymes, and identified genes differentially expressed, such as increased expression of nestin and HIF1α after 7 days with soft gels but not hypoxia. However, downstream analysis of HIF1α-driven VEGF production did not increase with gel addition, suggesting differing mechanisms of action.

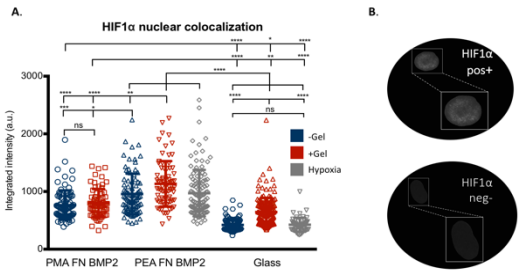

*Fig. 1: Active HIF1α levels (A.) elevated on PEA FN BMP2 surfaces, & sustained increase observed after 3 days with Gel addition vs hypoxia. (B.) HIF1α positive and negative nuclei. N=3, **p<0.01, ****p<0.0001 by one-way ANOVA.*

DISCUSSION & CONCLUSIONS: Using this material-based system, we have found that soft gel addition drives a 'hypoxic-like' mechanistic response, that could be a key facet in maintaining and supporting niche-like phenotypes in vitro. This can have large implication for production of pericytes in vitro that can be used to support, for example, tissue engineered construct implantation via enhanced anti-inflammatory & immune modulatory properties.

REFERENCES: [1]Engler AJ, et al. Cell 2006; 126: 677-89. [2]Llopis-Hernandez et al. Sci Adv 2016; 1-11.

ACKNOWLEDGEMENTS: This work was supported by grant BB/N018419/1 (BBSRC) & an EPSRC studentship. We thank Carol-Anne Smith for technical support.

Investigating fibroblast involvement in vascular inflammation using co-culture models

K Wright[1,2], S Francis[2] and J W Haycock[1]

Departments of Materials Science and Engineering[1], and Infection, Immunity and Cardiovascular Science[2], University of Sheffield. U.K.

INTRODUCTION: Coronary heart disease often goes undetected until a patient becomes symptomatic (e.g. myocardial infarction). Consequently, available treatments are primarily aimed at symptomatic relief. However, to develop preventative strategies it is firstly necessary to improve the design of current *in vitro* vascular models; these largely consider only the signalling pathways between the EC and SMC. The involvement of the adventitial fibroblast is becoming increasingly popular; thus, the aim is to determine whether its addition to *in vitro* models would enable the inflammatory processes that underpin atherogenesis to be studied in more detail. ICAM-1 is up-regulated during inflammation to aid leukocyte extravasation and is expressed by numerous cell types. Therefore, ICAM-1 was used as a marker to study the augmentation of the inflammatory response in HUVEC / HUASMC / NHDF co-cultures.

METHODS: 25 U/mL human recombinant TNF-α was used to stimulate HUVEC, HUASMC and NHDF in 2D monoculture and co-culture arrangements, as well as in conditioned medium experiments, fixing samples every 3 hours for up to 12 hours. All samples were immunolabelled against ICAM-1. ANOVA determined any significant differences in ICAM-1 expression.

RESULTS: ICAM-1 expression was significantly up-regulated ($p<0.001$) upon the introduction of TNF-α under all conditions in HUVEC (Fig. 1a). Baseline ICAM-1 expression and intensity at 12 hours was increased when co-cultured with both NHDF and HUASMC ($p<0.001$). TNF-α caused an increase in ICAM-1 expression in NHDF in monoculture ($p<0.001$) and HUVEC co-culture ($p=0.038$) (Fig. 1b). Whilst the baseline expression increased in co-culture with HUASMC ($p<0.001$), there was no significant up-regulation after TNF-α addition ($p=0.991$). Constitutive production of ICAM-1 was observed in HUASMC, whereby the introduction of TNF-α or additional cell types resulted in no significant differences after 12 hours in monoculture ($p=1.000$) or co-culture with either HUVEC ($p=0.546$) or NHDF ($p=1.000$). Conditioned medium experiments highlighted that autocrine (HUVEC/NHDF), juxtacrine (HUASMC

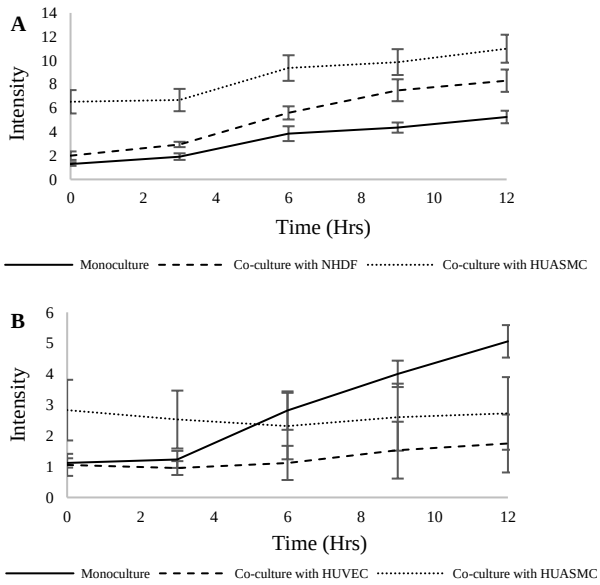

Fig. 1: ICAM-1 intensity in (A) HUVEC and (B) NHDF after the addition of 25 U/mL TNF-α in monoculture and co-culture conditions.

→HUVEC, HUVEC→NHDF) and paracrine signalling pathways exist between the different cell types (HUVEC↔NHDF, HUASMC→NHDF) (data not shown).

DISCUSSION & CONCLUSIONS: It appears that a complex communication network exists between EC, SMC and fibroblast cells. When no stimulus is present, signalling pathways appear to only present from HUVEC/HUASMC to NHDF, possibly with the aim to 'prime' the fibroblast for an inflammatory response. These pathways become more complex upon stimulation with TNF-α, enhancing ICAM-1 expression by HUVEC, thus promoting further leukocyte infiltration. Consequently, it is evident that the fibroblast contributes significantly to the vascular inflammatory response. We suggest that consideration of the fibroblast in 3D *in vitro* model design is important on the role of fibroblast activation during atherogenesis, and whether it is initiated via the endothelium and/or vasa vasorum.

ACKNOWLEDGEMENTS: This work was funded by the EPSRC.

Investigating the alignment of cellulose nanowhiskers and its potential to engineer skeletal muscle

A Eade[1], JD Aplin[2], JE Gough[1]

[1] *Biomaterials, School of Materials, University of Manchester, Manchester, UK.* [2] *Maternal and Fetal Health Research Centre, Institute of Human Development, University of Manchester, Manchester, UK.*

INTRODUCTION: Skeletal muscle has a high capacity for self-regeneration. Throughout our lives, skeletal muscle is constantly repairing itself yet it has limitations. Muscle loss due to accidents or disease results in the formation of scar tissue which restricts the original function of the tissue.[1] The application of a substrate designed to promote cell alignment and encourage myogenic differentiation could aid the repair of the muscle's functionality.

It is proposed that oriented cellulose nanowhiskers (CNWs) could be used to direct alignment of myoblasts.[2] The application of spin-coating and polyelectrolyte layers could produce substrates of physiologically relevant stiffness and serve as a guide to achieve broad areas of aligned multi-nucleated myotubes.

METHODS: Through the partial acid hydrolysis of tunicin cellulose with sulphuric acid, CNWs with dimensions of around 5 nm in diameter and lengths ranging from nanometres to microns can be produced. The sulphuric acid gives a slight negative charge which enables the building of polyelectrolyte layers through dip coating with positively charged chitosan, resulting in a layered substrate. CNWs can be spin coated resulting in a radially aligned top layer suitable for cell culture.

Myoblasts, C2C12s, were cultured on a range of CNW substrates with different numbers of polyelectrolyte layers. Alignment and myogenic expression was investigated using bright field imaging and immunofluorescence staining respectively. Further cell studies were carried out with human skeletal muscle cells (hSkMCs) to see if the cell alignment could be replicated. The number of nuclei per myotube was collected using CellProfiler.

RESULTS: Orientation of the CNWs was confirmed using atomic force microscopy. Cells were initially observed for end-to-end alignment to the topography of the spin coated top layer and further stained for the presence of myogenin, a muscle specific transcription factor that indicates that there is potential for myogenic differentiation to occur. Alignment of multi-nucleated myotubes can be observed (Figure 1).

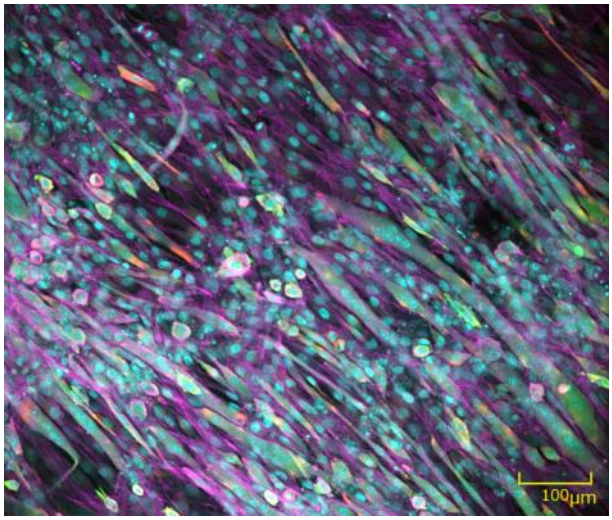

Fig. 1: Fluorescence micrograph at x40 mag. Multi-nucleated myotubes show alignment on an oriented CNW surface. C2C12s have been stained for nuclei (cyan), actin (magenta) and myogenin (green).

DISCUSSION & CONCLUSIONS: Spin-coated CNWs can be used to direct alignment and promote myogenic differentiation of C2C12s and hSkMCs in to multi-nucleated myotubes. This could provide further understanding of myotube formation. The use of CNW polyelectrolyte layers in directing myoblasts towards myogenic differentiation shows promise as a first step in aiding muscle repair, although the effect of the number of polyelectrolyte layers still needs to be determined. The application of hSkMCs gives a basis for further investigation in to the potential of myogenic differentiation in stem cells and possibly co-culture.

REFERENCES: [1] M. Juhas (2015) *Methods*, **99**: 81-90. [2] J. Dugan (2013) *Acta Biomaterialia* **9**:4707-15.

ACKNOWLEDGEMENTS: The authors would like to thank EPSRC for providing financial support for this project.

Kidney tissue engineering: Incorporation of decellularised renal extracellular matrix into an electrospun scaffold

W Shanahan, A Callanan

Institute of Bioengineering, School of Engineering, University of Edinburgh, UK

INTRODUCTION: The incidence of end stage renal disease is ever increasing[1]. Allogeneic transplant currently offers the most definitive management of this disease but a paucity of available organs meant that the average waiting time for a donor kidney, once approved for receipt, was 864 days in the UK last year[2]. Even once implanted there is a constant threat of graft failure, and a significant side effect profile associated with life-long immunosuppression. Novel strategies are needed to address these issues.

Electrospinning is a simple, scalable technique for the production of non-woven fibrous scaffolds which resemble the fibrils of the endogenous extracellular matrix (ECM)[3]. We have produced a hybrid electrospun scaffold formed of polycaprolactone (PCL) and rat renal ECM. Scaffold architecture was determined by work previously performed within the group[3], and extracellular matrix proteins were isolated using an optimised perfusion decellularisation protocol[4].

METHODS: Kidney ECM was obtained from 8 week old Sprague-Dawley rats. The abdomen was opened immediately post euthanasia and the renal artery cannulated. Kidneys were perfused with ~30 ml sodium nitroprusside to achieve blanching and subsequently washed with PBS. Kidneys were then perfused via the arterial cannula with 0.25% sodium dodecyl sulphate (SDS) while suspended within a 400ml recirculating bath for 4 hours. Resulting extracellular matrix was rinsed with PBS, assessed for remnant DNA & SDS, then milled to a fine pulp. Mats of small, randomly arranged fibres were formed by electrospinning 7wt/v% PCL in hexafluoroisopropanol with either 1wt/v% ECM, 0.25wt/v% ECM or none. Fibres were projected 11cm across a 20kV differential at 0.8ml/hour onto a mandrel rotating at 250rpm. 10mm scaffolds were punched out of the resultant mats, sterilised with ethanol, and seeded with RC124s, a non-neoplastic human renal epithelial cell line. Cell viability, DNA quantification, fluorescence imaging, and PCR were performed on cells at 5 and 10 day time-points.

RESULTS: Decellularisation was confirmed through the comparison of DNA content of decellularised kidneys with whole untreated kidneys. SEM images verified the production of small randomly arranged fibres. Biochemical assays confirmed cell attachment and proliferation over the study period. Trends were seen in the gene expression profiles.

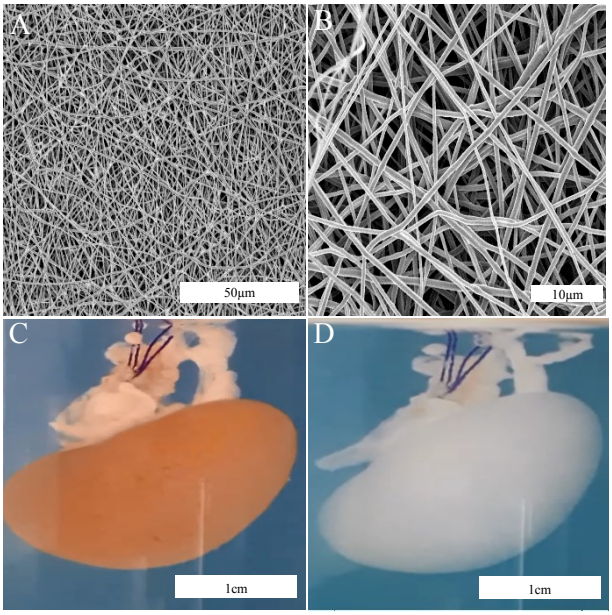

Fig. 1: SEM images of hybrid electrospun fibres (A) and (B), alongside rat kidneys before (C) and after (D) perfusion decellularisation.

DISCUSSION & CONCLUSIONS: Electrospinning of a hybrid scaffold incorporating perfusion decellularised ECM is shown here to support human renal epithelial cells and influence their proliferation. These results demand further study on the biochemical enhancement of polymer scaffolds through addition of endogenous proteins as platforms for renal tissue engineering.

REFERENCES: [1] 2017 USRDS Annual Data Report.[2] NHS Blood and Transplant. Organ donation and transplantation activity report 2016/7. [3] TP Burton, A Corcoran, A Callanan (2017) *Biomed Mater.* **13**:15006. [4] M He, A Callanan, K Lagaras et al (2016) *J Biomed Mater Res - Part B Appl Biomater*. **105**:1352-1360.

ACKNOWLEDGEMENTS: MRC grant MR/L012766/1.

Magnetic nanoparticle mediated activation for chondrogenic differentiation of MSCs

I Echevarria[1], A El Haj[1], H Markides[1]

[1] *ISTM, Guy Hilton research centre. Keele University, Stoke-on-Trent*

INTRODUCTION: The absence of a long term treatment for osteoarthritis (OA) has led to the development of new approaches which can be used for early intervention[1]. Mechanical regulators are known to play a key role in OA and present some key targets for modulation. The mechano-transductive potential of stem cells introduces the possibility of using external mechanical stimuli to promote cell differentiation and provides cues for tissue maturation[2]. For this purpose, our group has developed a new technology based on remote magnetic activation of MSCs. The magnetic nanoparticles (MNPs) are targeted and bound to specific mechano-transductive ion channels or receptors on the MSCs membrane which then allows remote forces to be delivered directly to the channels or mechano-receptive parts of the cells membrane. This effect is translated downstream into the activation of specific chondrogenic signaling pathways.

METHODS: Equine MSCs were cultured as pellets ($4x10^5$ cells) and micromass cultures ($5x\ 10^4$ cells). Cells were previously transfected with GFP dye linked to collagen type 2 expression. For this experiment, the cells were labelled with a MNP, Nanomag (250 nm) with carboxylic coating and linked to the specific antibody for each group: TRPV4, TREK1 and RGD. The cells were cultured for 21 days under the relevant media, chondrogenic media (DMEM, 10% FBS, 1% L-Glutamine, 1% Antibiotics, 1% Non-essential aminoacids, 50 mg/ml ITS, 10 ng/ml TGF-β3, 50 μg/ml Ascorbic acid, 0.1 mM Dexamethasone), chondrogenic media without TGF-β3 (key for differentiation) and basal media. The 3 different media were tested for all groups. The cells were submitted to 1h daily stimulation using the changing magnetic field generated using the MICA bioreactor (MICA Biosystems Ltd). Samples belonging to all the groups were also grown and cultured under the same conditions lacking the magnetic stimulation.

RESULTS: Collagen 2 expression was increased in all the chondrogenic groups cultured in chondrogenic media when compared to the cells cultured in basal media for all groups. In response to the mechano-activation with MNP, we observed an increase in collagen 2 production in the TRPV4 group, especially for the micromass cultured in chondrogenic media. Additional histological analysis demonstrated a similar pattern for collagen and aggrecan up-regulation. A higher production of both markers was observed for all MNPs tagged cells in both chondrogenic and incomplete chondrogenic media. The cells labelled with MNPs showed enhanced production of collagen without the addition of TGF-β3.

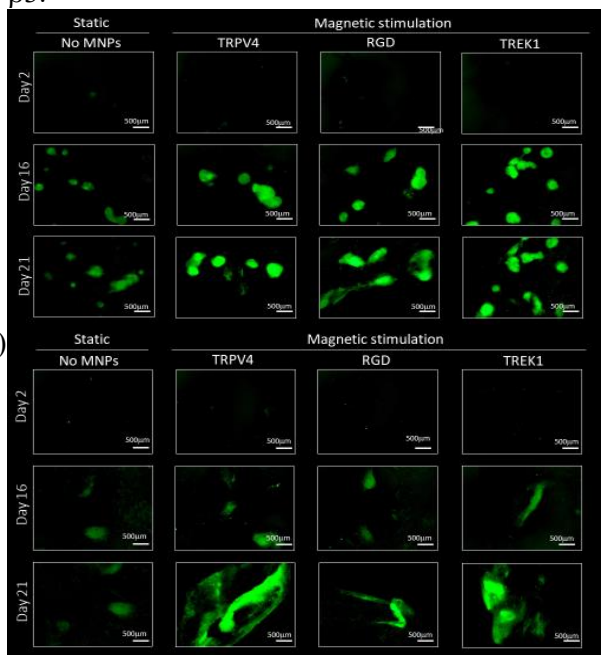

Fig. 1: Fluorescence images of micromass cultures labelled with TRPV4, TREK1, RGD and cells lacking MNPs on days 2, 16 and 21 of culture with a) chondrogenic media without TGF-β3, and b) chondrogenic media.

DISCUSSION & CONCLUSIONS: The development of injectable solutions for early OA therapy could provide solutions which would improve motility with ageing. MICA approaches using MNP tagged to mechano-responsive receptor targets has the potential to generate these new therapeutic approaches. The use of ion channels such as TRPV4 as targets for enhancing chondrogenesis is being explored further.

REFERENCES: [1] J. Burke (2016) *Clin Trans Med*, **5**:27. [2] E.A Lee etl al (2014) *Arch Pharm Res*, **37**:120-128. [3] H**.** Markides, J.S McLaren, A. El Haj (2015) *Biochem cell biol,* **69**: 162-172.

ACKNOWLEDGEMENTS: I would like to thank to the EPRSC for funding. This template was modified with kind permission from eCM Journal.

Mathematical modelling of magnetically targeted stem cell delivery

E. F Yeo[1], H Markides[2], A.J El Haj[2], J.M Oliver[1], S.L Waters[1].

[1] *Mathematical Institute, University of Oxford, UK.* [2] *Institute for Science and Technology in Medicine, University of Keele, UK*

INTRODUCTION: In stem cell therapies used in regenerative medicine a key challenge is to deliver the cells to the site of injury. One approach is to label cells with magnetic particles and use externally applied magnetic fields to guide the cells to the target site. To optimise delivery protocols it is essential to understand the interplay between the fluid mechanics, magnetic fields and stem cell properties. We develop mathematical models alongside in vitro and in vivo experimental models to provide mechanistic understanding.

METHODS: Magnetic nanoparticles (MNPs) are utilised to tag mesenchymal stem cells (MSCs) which can then be targeted using an external magnetic field. This was carried out in vivo and in vitro. In vitro we used a custom model and MSCs in concentrations of blood from 0% to 40% for various flow rate and degrees of magnetic tagging. This has shown that magnetic tagging increases trapping, with a trapping of up to 31% (versus 17.5% for untagged cells) in a blood concentration of 40%.

In our mathematical model we have assumed steady fully developed Poiseuille flow in the pipe. The magnetically tagged MSC experiences Stokes drag from the fluid and a Lorentz magnetic force. We have computed trajectories of particles in the pipe as a function of the initial position, flow rate, magnetisation of the particles and properties of the fluid.

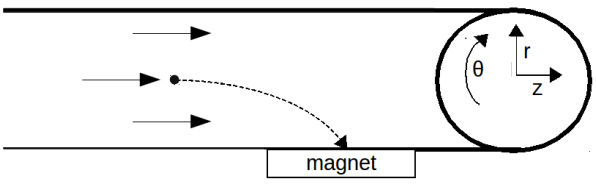

Fig. 1: Mathematical description of our system, showing the coordinates and a single particle's trajectory to the magnet.

RESULTS: Mapping the flow theoretically we have shown how a distribution of particles in the entering cross section are deposited onto the wall of the vessel. This will enable us to predict deposition of particles given their distribution in the flow.

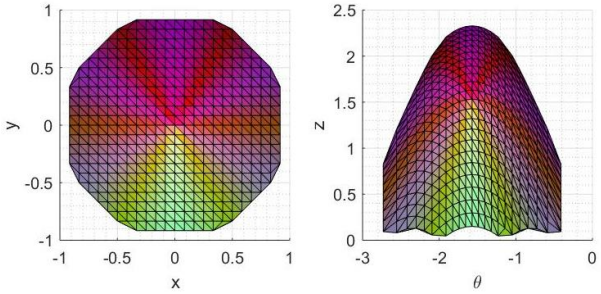

Fig. 2: Colour map indicating how particles in regions of inlet cross-section are deposited on the wall of the vessel. Left illustrates the cross section, right shows the net of the cylindrical pipe in Θ,z space.

DISCUSSION & CONCLUSIONS:
Mathematical models can allow us to gain cheap and quick insights into potential treatments. This can allow the rapid exploration of parameter space, calculating optimal regimes for trapping as well as the boundaries the space where capture is feasible.

Through this model we will be able to predict the optimal flow rate and minimum magnetic field strength required for a desired percentage of trapping. This model can be readily adapted to include variability in tagging with MNPs, whereas current studies have assumed heterogeneity of tagging. It also offers the flexibility to include time dependent effects such as pulsatile fluid flow, build of up deposited cells on the vessel wall or the extravasation of cells.

REFERENCES: [1] El Haj, A. J., Glossop, J. R., Sura, H. S., Lees, M. R., Hu, B., Wolbank, S., ... & Dobson, J. (2015). An in vitro model of mesenchymal stem cell targeting using magnetic particle labelling. *Journal of tissue engineering and regenerative medicine*, [2] Grief, A. D., & Richardson, G. (2005). Mathematical modelling of magnetically targeted drug delivery. *Journal of Magnetism and Magnetic Materials*.

ACKNOWLEDGEMENTS: AJE and SLW gratefully acknowledge funding from EPSRC in the form of a Healthcare Technologies Discipline Hopping Award, and SLW the award of a Royal Society Leverhulme Trust Senior Research Fellowship.

This template was modified with kind permission from eCM Journal.

Mechanical testing of nerve guidance conduit materials for peripheral nerve repair

KS Bhangra[1,2,3], JC Knowles[1], RJ Shipley[3,4], D Choi[5] and JB Phillips[1,2,3]

[1]Biomaterials & Tissue Engineering, UCL Eastman Dental Institute, [2]Pharmacology, UCL School of Pharmacy, [3]UCL Centre for Nerve Engineering, [4]Mechanical Engineering, UCL Engineering, [5]Brain repair and Rehabilitation, UCL Institute of Neurology

INTRODUCTION: A long-standing challenge in the development of nerve guidance conduits (NGCs) is to achieve a balance between required mechanical strength to withstand physiological stresses whilst mimicking natural nerve biomechanics to support endogenous peripheral nerve repair. Currently, there are several FDA-approved NGCs [1], however the stiffness of these hollow tubes tends to be greater than that of a nerve since they must maintain a patent lumen [2]. Conversely, conduits with an internal framework of engineered tissue can have a reduced stiffness [3]. In this study, we carried out tensile tests to investigate the breaking force of a rat sciatic nerve and that of potential NGC replacement materials, in particular natural and synthetic membranes.

METHODS: Sciatic nerves were harvested from Sprague-Dawley rats (200 – 260 g). Nerves had a diameter of 1.33 ± 0.32 mm and a length of 20 mm. Two collagen-based membranes and a Poly Lactic Acid (PLA)-based material were also evaluated, namely CM-A, CM-B and PLA. Material thickness was determined using a contact angle measurement machine (CAM 200, KSV Instruments). Samples were then prepared by cutting the membranes into an hourglass shape with a width of 10 ± 1 mm, a height of 20 ± 1 mm and a central width of 5 ± 1 mm. Each membrane was hydrated in phosphate buffered saline for 5 minutes prior to mechanical testing. Tensile testing was performed with a 10 mm gauge length in uniaxial tension using a Bose Electroforce 3200 machine with an extension rate of 10 mm/min. Ultimate tensile stress (UTS) refers to the amount of force per unit of initial cross-sectional area at tensile failure.

RESULTS: Results reveal that CM-A is thinnest of the tested membranes, closely followed by CM-B, whereas the PLA-based membrane was the thickest (*Table 1*).

Figure 1 shows that the sciatic nerve has a UTS of 3.4 ± 0.4 N/mm^2, whereas a sheet of CM-A is considerably less at 0.9 ± 0.2 N/mm^2. The CM-B material has a UTS that is greater than that of CM-A, 1.7 ± 0.2 N/mm^2. The PLA-based membrane has the greatest UTS compared to the other membranes, at 2.4 ± 0.3 N/mm^2.

Table 1. Thickness of prospective NGC materials.

Material	*Thickness, mm*
Collagen-based membrane A (CM-A)	0.29 ± 0.03
Collagen-based membrane B (CM-B)	0.33 ± 0.02
PLA-based membrane (PLA)	0.37 ± 0.03

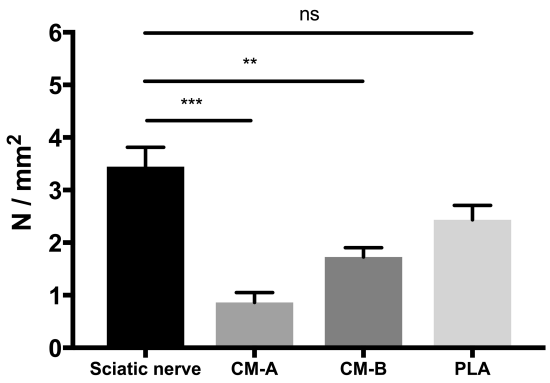

*Fig. 1: Ultimate tensile stress for sciatic nerve, CM-A, CM-B and PLA- based membranes. Data are means ± SEM, where n = 4. Statistical analysis was performed using one-way ANOVA, ns: non-significant, **p<0.01, ***p<0.001.*

DISCUSSION & CONCLUSIONS: The UTS of the collagen membranes were approximately 75% (CM-A) and 50% (CM-B) less than that of a sciatic nerve, suggesting they may not be suitable NGCs as a single sheet. Statistical analysis revealed significant differences between collagen-based membranes and sciatic nerve but no difference between the sciatic nerve and PLA-based membrane. Our data suggest that this particular PLA-membrane could be used as a potential NGC material for peripheral nerve repair. Future work would involve developing materials with similar properties to nerve.

REFERENCES: [1] Kehoe et al. (2012). Injury. 43(5), pp. 553-72. [2] Yao et al. (2010). Tissue Eng Part C; 16, pp. 1585-1596. [3] Ruiter et al. 2009. Neurosurgey Focus. 26 (2) E5 pp. 1-9.

Mechanosensitivity of neural cells on characterised RAFT-Stabilised collagen gradient gels.

C Kayal[1,3*], E Moeendarbary[1], RJ Shipley[1,3], JB Phillips[2,3]

[1]UCL Mechanical Engineering, London, UK [2]UCL School of Pharmacy, London, UK[3] UCL Centre for Nerve Engineering, London, UK

INTRODUCTION: Physical gradients play a major role in the regeneration of peripheral nerves [1, 2]. Collagen, the predominant structural protein in nerve extracellular matrix, is commonly used as a physical support for cells to make repair scaffolds [1]. To improve nerve repair approaches, it is useful to understand the mechanosensitivity of neurons and quantify the changes in behaviour induced by stiffness gradients [2]. However, little is known about the effect of gradients on neurite extension [3]. In this study, the stiffness of RAFT-stabilised Collagen gels (RsC) and RAFT-stabilised Collagen gradient gels (RsC_h) were characterised. The behaviour of NG108-15 neural cells were studied in response to these substrates.

METHODS: RsC gels were fabricated using rat tail collagen type I (First Link, UK). A standard protocol [4] was used to generate collagen gels within 3D printed moulds designed to generate collagen gradients (from 50 to 80 mg/ml). The gels were stabilised using RAFT™ absorbers (Lonza) to produce RsC and RsC_h. Atomic Force Microscopy (AFM)-based force spectroscopy was performed to map the stiffness profile across different regions of RsC and RsC_h [5].

NG108-15 cells were seeded onto the upper surface of RsC and RsC_h in serum-free DMEM. Cultures were maintained for 2 days in a humidified incubator. Neurite extension was observed using immunostaining and fluorescence microscopy and analysed using ImageJ.

RESULTS: AFM results showed an increase in stiffness correlated to the increase in collagen density from 0.3 to 10kPa for the RsC_h compared to the RsC with a uniform collagen density, 0.3 ±0.01kPa (Fig.1). On RsC 36±5% of cells expressed neurites versus 46±8% on RsC_h. On both substrates, there were 2±0.2 neurites per cells. Furthermore, on RsC_h, we observed 46.6±7% branches per neurites versus 24.4% ±7% on RsC.

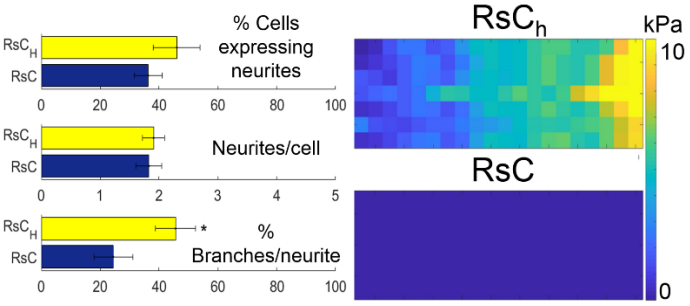

Fig. 1: NG108-15 cell behaviour on the top of RsC and RsC_h shown as mean± standard error (Left) * $p<0.05$. RsC and RsC_h stiffness map 1mm×2.5mm,(Right).

DISCUSSION & CONCLUSIONS: This study has revealed information about the mechanosensitivity of NG108-15 neurite growth in response to characterised stiffness gradients. Collagen gels were engineered to include well-defined density gradients for studying neural cell behaviour *in vitro.* Results indicated that neurite branching can potentially be altered in response to stiffness gradients (from 5-10kPa) within RsC_h gels *in vitro*. These data will inform a mathematical model to simulate how neurite extension might be enhanced and controlled, providing relevant information to aid in the design of scaffolds for peripheral nerve injury repair.

REFERENCES: [1] Carballo-Molina, O. A. and Velasco, *Front Cell Neurosci*, 2015. [2] G. Rosso et al, *Nanomedicine*, 2016.[3] Willits, R. K. and Skornia, S. L, *J Biomater Sci*, 2014. [4] JB Phillips et al, *Tissue Engineering*, 2005. [5] Moeendarbary, E et al. *Nature Communications* 8, 2017.

ACKNOWLEDGEMENTS: I would like to thank UCL for the award of a Dean's Prize and a PhD scholarship from UCL Mechanical Engineering. RJS would like to acknowledge funding of the EPSRC (EP—N033493—1).

Mesenchymal Stem Cell delivery within a Thermally Triggered Hydrogel Regenerates Nucleus Pulposus Matrix Following Injection into Degenerate Nucleus Pulposus Tissue.

AA Thorpe[1], SW Partridge[1], L Vickers[1], F Charlton[1], A Cole[2], N Chiverton[2], C Sammon[1], C L Le Maitre[1]

[1]Sheffield Hallam University, UK, [2]Sheffield Teaching Hospitals UK.

INTRODUCTION: Intervertebral disc (IVD) degeneration is a major cause of low back pain (LBP). We have reported an injectable hydrogel (NPgel)[1,2], which following injection into bovine NP explants, integrates with NP tissue and promotes NP cell differentiation of delivered mesenchymal stem cells (MSCs) without growth factors. Here, we investigated the injection of NPgel+MSCs into bovine NP explants under degenerate culture conditions. In addition the survival and differentiation capacities of hMSCs delivered via NPgel into degenerate human NP explants was also performed to ascertain the future clinical success of this therapy.

METHODS: hMSCs were incorporated within liquid NPgel and injected into bovine NP explants alongside controls. Explants were cultured for 6 weeks under hypoxia (5%) ± calcium 5.0mM $CaCl_2$ or IL-1β individually or in combination to mimic the degenerate microenvironment. hMSCs were incorporated within NPgel and also injected into naturally degenerate human NP explants cultured for 6 weeks under hypoxia (5%). Histological and immunohistochemical analysis was performed to investigate altered matrix synthesis and matrix degrading enzyme expression. In addition immunohistochemistry analysis of IL-1β and IL-1R1 was performed to investigate the catabolic phenotype of native NP cells following NPgel+MSC injection.

RESULTS: The NPgel integrated with bovine and human degenerate NP tissue and hMSCs produced matrix components: aggrecan, collagen type II and chondroitin sulphate in standard and degenerate culture conditions. Significantly increased cellular immunopositivty for aggrecan was observed within native NP cells surrounding the site where NPgel+MSCs were injected, cultured under degenerate conditions within bovine explants and within human degenerate NP explants (Fig 1), compared to media injected control tissues (P≤0.05). In bovine NP explants a significant decrease in the number of immunopositive cells for IL-1R1 was observed where NPgel+MSCs was injected in comparison to controls under standard culture conditions and when treated with $CaCl_2$ (P≤0.05). In degenerate human NP explants significantly decreased cellular immunopositivity for MMP3 expression was observed where NPgel+MSCs were injected in comparison to media injected controls (P≤0.05) (Fig 1).

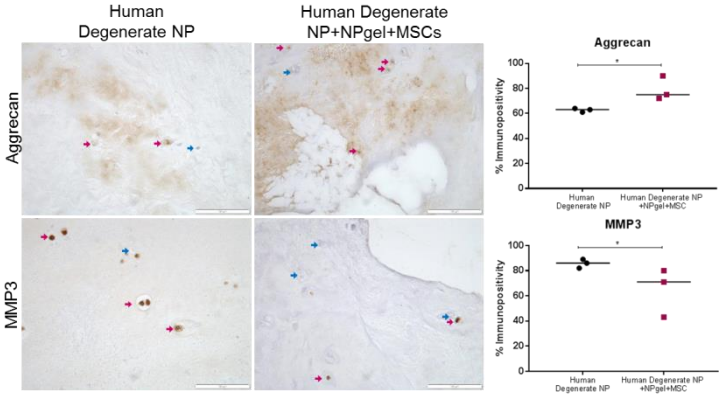

Figure 1: Aggrecan and MMP3 immunohistochemistry in human degenerate NP explants injected with media (Human Degenerate NP) or injected with NPgel + MSCs (Human Degenerate NP+NPgel+MSCs) cultured for 6 weeks 5% O_2 in standard cell culture media. (+) cells indicated by pink arrows and (-) cells indicated by blue arrows. *Scale bar 100μm*. Native NP cells surrounding injection site were counted and % immunopositivity calculated (P≤0.05).

DISCUSSION & CONCLUSIONS: In agreement with our previous findings[2] NPgel was sufficient alone to induce NP cell differentiation of MSCs following injection into NP tissue explants under standard culture conditions without the need for additional growth factors. Here, we have shown that viability and NP cell differentiation of MSCs incorporated within NPgel and injected into bovine NP tissue explants was unaffected by degenerate culture conditions which more closely mimic the *in vivo* environment of the degenerate IVD. In addition we have shown that the injection of NPgel with MSCs also increases aggrecan expression and reduces MMP3 and IL-1R1 expression by native NP cells. The NPgel with incorporated MSCs has the potential to regenerate the NP and provide mechanical support, whilst reducing the catabolic phenotype of degenerate NP cells, as a treatment strategy for IVD degeneration.

REFERENCES:

(1) Thorpe AA et al., (2016). Acta Biomater. 36:99-111.

(2) Thorpe AA et al., (2017). Acta Biomater. 54:212-226.

Mesenchymal stem-cell derived extracellular vesicles as therapeutic agents in Juvenile Idiopathic Arthritis.

M Hyland[1], C Mennan[1], K Wright[1], E Wilson[2], O Kehoe[1]

[1]*Institute for Science and Technology in Medicine (ISTM), Keele University at RJAH Orthopaedic Hospital.* [2]*Institute of Biomedical Science, University of Chester*

INTRODUCTION

Juvenile Idiopathic Arthritis (JIA) is an autoimmune disease affecting 1 in 1000 children in the UK. Treatments focus on the use of disease modifying anti-rheumatic drugs to reduce inflammation but approximately 50% of patients do not respond effectively. Alternative treatments, such as the use of mesenchymal stromal cells (MSCs), offer a potential alternative treatment to modulate the immune system. Pre-clinical and clinical studies of autoimmune diseases have shown the ability of MSCs to suppress immune responses and reduce inflammation. MSCs are thought to exert their therapeutic benefits mainly through paracrine signaling by releasing anti-inflammatory cytokines, growth factors and extracellular vesicles (EVs)[1]. EVs are small membrane vesicles secreted by cells and function as cell signaling molecules. They contain protein, RNA, miRNA and lipids in their 'cargo' which can be released into target cells and thereby change the function of the cell[1]. Therefore, research using MSCs-EVs may be beneficial towards the treatment of autoimmune diseases. Research on how to therapeutically exploit EVs could open new avenues for the treatment of inflammation in JIA.

METHODS

Bone marrow aspirate was ethically sourced from Lonza (Lonza, Maryland). MSCs were isolated from the bone marrow (BM-MSCs) as described previously[2-3]. BM-MSCs were cultured in normoxic (21% O_2) and hypoxic conditions (2% O_2). Umbilical cords (UCs) were collected (with ethical approval) and MSCs were isolated as previously described[2]. Cells were culture expanded in a Quantum® bioreactor (Terumo BCT) in normoxia (21% O_2). UC-MSCs were serum starved at 80% confluence for 48hrs and conditioned media was collected. EVs were isolated by differential ultracentrifugation. Flow cytometry assessed MSC surface markers (according to the International Society of Cell Therapy (ISCT) definition of MSCs). Population Doubling Time (PDT) assessed the proliferation of MSCs *in vitro.* Colony-forming units (CFU-f) assay was used to assess the clonogenic potential of isolated UC-MSCs at passage 5.

RESULTS

Both BM-MSCs and UC-MSCs fit the cell surface marker profile for MSCs according to the ISCT criteria. However, UC-MSCs showed a 23.6% expression of CD146. UC-MSCs are highly proliferative with an average PDT of 2.11 days and CFU-f value of 76 (±18 SD). BM-MSCs grown in normoxic conditions had a PDT of 24.46 days and 5.05 days in hypoxia.

DISCUSSIONS & CONCLUSIONS

All MSCs were in accordance with the ISCT criteria for MSCs due to their morphology, plastic adherence and expression of surface markers. However the presence of CD146 on UC-MSCs indicates that there may be a subpopulation of pericytes present[4]. BM-MSCs proliferated faster in in hypoxic conditions compared to those grown in normoxia. This may be due to the hypoxic conditions resembling the *in vivo* environment more closely as the oxygen level in human bone marrow is thought to be between 2-8%.

Future work will focus on isolating EVs from MSCs primed with pro-inflammatory cytokines (IFN-γ, TNF-α, IL-1β, to mimic the inflamed joint environment) and grown in EV-depleted FBS to avoid serum starvation. EVs will be analysed according to their surface markers, size, concentration, protein and miRNA contents. EVs, with potential immunosuppressive properties will be cultured *in vitro* with T-cells from patients with JIA to assess their effect on activated T-cell differentiation and proliferation.

REFERENCES

[1]S.R. Baglio, D.M. Pegtel, N. Baldini (2012) *Front. Physiol.* **3:** 1-11. [2]C. Mennan, K. Wright, A. Bhattacharjee, B. Balain, J. Richardson, S. Roberts (2013) *BioMed Res. Int.*1-8. [3]R. Agrawal, T. Dale, M. Al-Zubaidi, P. Malgulwar, N. Forsyth, R. Kulshreshtha (2016). *PLoS One* **11:**10, 1-20. [4]B Gokcinar-Yagci. O. Ozyuncu, B. Celebi-Saltik (2016) *Cell Tissue Bank.* **17**:345–352.

ACKKNOWLEDGEMENTS

This work is supported by the Orthopaedic Institute Ltd, ACORN fund at Keele University and the RJAH Orthopaedic Hospital Charity.

Modulating scar coherence by cultivating injured nervous tissue on surface-engineered coralline scaffolds

Orly Eva Weiss[1], Roni Mina Hendler[1], Eyal Aviv Canji[1], Tzachy Morad[1], Danny Baranes[1]

[1] *Department of Molecular Biology, Ariel University, Israel*

INTRODUCTION: Biological scaffolds provide a supportive environment for tissue generation and may be strong candidates for repairing damage in the nervous system[1]. Scaffolds made of coral skeletons promote bone regeneration and provide nutritional support for neurons *in vitro*[2]. This study characterizes the structural reaction of an injured nerve tissue to contact with coralline scaffolds of distinct topologies, as a prerequisite test of its usage for nervous tissue repair *in vivo*.

METHODS: Hippocampal slices from postnatal rats were cultivated on two distinct shaped of coralline scaffolds: 1. Micro-rough surface, porous, complex 3D architecture - made of intact skeleton pieces (ISP); 2. Macro-rough surface, non-porous, planar - a powder-like scaffold made of grained skeleton (GS). Visualization of the samples was done by scanning electron microscope to identify tissue-scaffold interactions and confocal-fluorescent microscope to test cellular responses after performing immunofluorescence staining to specific neural markers. Characterization of the scaffold's topology and analysis of tissue micrographs were done using ImageJ software.

RESULTS: Slices strongly adhered to the surface on both scaffolds. On ISP, slices deformed into complex 3D structures by engulfing the outer surface of the scaffold without penetrating the pores, yet, preserving their coherence. By contrast, on GS, slices were planar but broken into interconnected small segments of tissue, depending on the grains' size and density (Fig. 1). Both scaffolds induced formation of reactive astrocytes however, whereas on GS these cells tightened into a single thin stripe at the slice's periphery, on ISP, they dispersed globally, forming meshes having inter-cell distances spanning up to dozens of microns (Fig. 2).

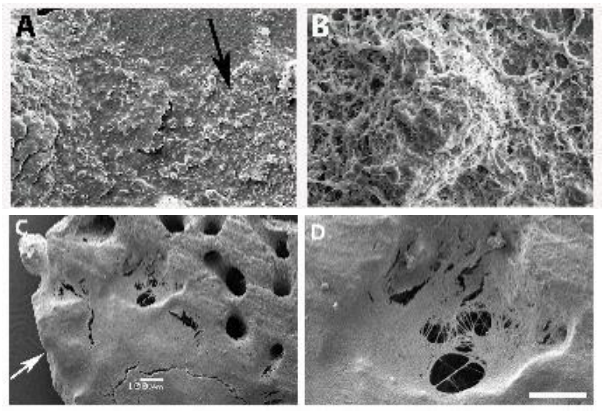

Figure 1: Hippocampal slices interact with GS/ISP in a scaffold surface-dependent manner. Scanning electron micrographs of nervous tissues interacting with GS (small grains-arrow) **(A)** and large grains **(B)**. **(C)** A scanning electron micrograph of a tissue (arrow) engulfing ISP. **(D)** Higher magnification of an area in (C) showing a flat layer of tissue crossing a pore. **Scale:** A - 200mm; B - 25mm; C – 0.5mm ; D - 50mm.

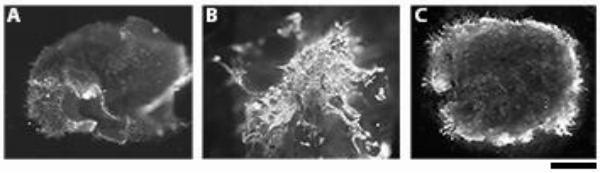

Figure 2: ISP and GS induce distinct patterns of GFAP expression level. Fluorescent imaging of GFAP in hippocampal slices cultivated on ISP and GS. **(A)** GFAP staining in non-cultivated slices. **(B)** A slice cultivated on ISP. **(C)** A slice cultivated on GS. **Scale:** A-C - 0.5mm.

DISCUSSION & CONCLUSIONS: The results demonstrate that implantation of scaffolds of pre-designed roughness and porosity can provide a control over the coherence and shape of nerve and scar tissues in the site of injury, opening a route for cell invasion, thus assisting in damage repair following brain wounds.

REFERENCES:

1. Pettikiriarachchi, J. T. S., Parish, C. L., Shoichet, M. S., Forsythe, J. S. & Nisbet, D. R. Biomaterials for Brain Tissue Engineering. *Aust. J. Chem.* **63,** 1143–1154 (2010).
2. Shany, B., Vago, R. & Baranes, D. Growth of primary hippocampal neuronal tissue on an aragonite crystalline biomatrix. *Tissue Eng.* **11,** 585–596 (2005).

Nanotopographies induce changes to mesenchymal stem cell metabolism and promote multipotency – linking adhesion to metabolism and function

EA Ross[1], LA Turner[1], A Saeed[2], PM Reynolds[2], J Mountford[3], KEV Burgess[4], RD Meek[1,5], N Gadegaard[2], ROC Oreffo[6], MJ Dalby[1]

[1] Centre for the Cellular Microenvironment, IMCSB, University of Glasgow, Glasgow, UK. [2] School of Engineering, University of Glasgow, UK. [3] Scottish National Blood Transfusion Service, Edinburgh, UK.

[4]Scottish Polyomics Facility, University of Glasgow, Glasgow, UK. [5] Department of Trauma and Orthopaedics, Queen Elizabeth University Hospital, Glasgow, UK. [6] Centre for Human Development, Stem Cells and Regeneration, Faculty of Medicine, University of Southampton, Southampton, UK.

INTRODUCTION: Naïve, multipotent mesenchymal stem cells (MSC) are a key cell product for patient therapy; their ability to regulate immune responses, haematopoiesis as well as their proven potential in tissue regeneration mean they have become a fundamental reagent for cell-based therapies. However, the quality of the naïve MSC is crucial to its therapeutic function. Over time in culture MSCs differentiate into mature stromal populations, losing their immunomodulatory properties. We have previously demonstrated that growing MSCs on nanotopographical surfaces consisting of a square pattern of nanopits maintains their naïve phenotype, with increased expression of multipotency markers and delayed differentiation into mature stromal cells [1]. In this study we explore the therapeutic potential of these nanotopography 'educated' MSC, revealing a new link between adhesion and cellular respiration which promotes naïve MSC functionality.

METHODS: MSCs were cultured in normoxia on nanotopographies with a SQ or NSQ pattern of nanopits or flat control (Flat) for 14 days (Fig 1). Changes to cellular respiration were measured by tracing metabolomic conversion of heavy labelled glucose. Co-culture of MSCs and CFSE labelled PBMCs allowed assessment of immunosuppression by flow cytometry. Inhibitors of mitochondrial function were used to model adhesion dependant changes to cellular respiration.

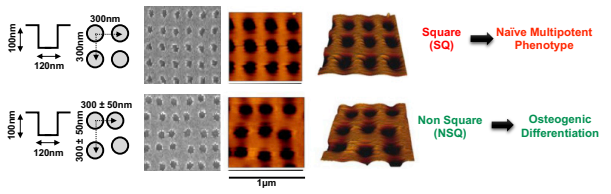

Fig. 1: Polycarbonate nanotopographical surfaces used to control MSC physiology.

RESULTS: Binding to the SQ nanotopography resulted in changes to MSC metabolism, with an increase in aerobic glycolysis as revealed by metabolomic analysis (Fig. 2A). Binding to the SQ topography resulted in significantly increased glucose uptake and generation of pyruvate and lactate metabolites compared to Flat and NSQ surfaces. These observations were also confirmed at the protein level in vitro. SQ educated MSCs maintained their immunomodulatory capacity in culture (Fig. 2B) and had higher expression of naïve multipotency markers compared to cells exposed to Flat or NSQ surfaces. To confirm that increased glycolysis correlated to MSCs multipotency and immunosuppression, mitochondrial inhibitors were used to reduce oxidative phosphorylation and promote aerobic glycolysis. Inhibitors recapitulated the SQ surface phenotype, maintaining MSCs immunosuppressive activity and upregulating multipotency markers.

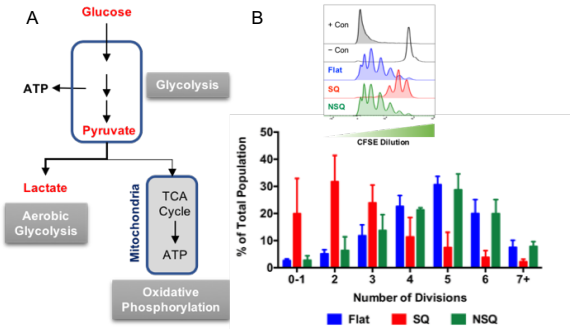

Fig. 2: A) Increased aerobic glycolysis metabolites (red) in MSCs cultured on SQ topographies compared to NSQ and Flat. B) Co-culture of MSCs with CFSE labelled PBMCs reveals their immunosuppressive properties by flow cytometry.

DISCUSSION & CONCLUSIONS: Interaction of MSCs with specific nanotopographical surfaces alters cellular respiration to promote a naïve, immunosuppressive phenotype. This model reveals the importance of metabolism as well as mechano-transduction signals in order to generate quality naïve, multipotent immunosuppressive MSCs for cell therapy.

REFERENCES: [1] R. McMurray et al (2011) *Nat Materials* **10**:637-644.

ACKNOWLEDGEMENTS: This work was supported by BBSRC (BB/N018419/1) funding.

New 3D polyglycolic acid scaffolds by $scCO_2$ for bone repair

Jiapeng Zhang[1, 2], Zhenhao Xi[1], Lian Cen[1], Ling Zhao[1], Ying Yang[2]

[1] *Shanghai Key Laboratory of Multiphase Materials Chemical Engineering, East China University of Science and Technology, China*

[2] *Institute of Science and Technology in Medicine, University of Keele, Stoke-on-Trent, UK*

INTRODUCTION: As a highly crystalline but fast biodegradable polymer, polyglycolic acid (PGA) has been applied to numerous scientific research and clinical devices. However, due to the high crystallinity of PGA, this polymer can only be processed into end using format, fiber, by one technique, melt-spinning. Loosen fibrous meshes have been used as 3D scaffolds in tissue engineering field previously but they have low mechanical strength. A new efficient technique, supercritical carbon dioxide ($scCO_2$) foaming, has been developed to produce porous PGA scaffolds.[1] It is found that the $scCO_2$ technique can induce surface topography of pores during the foaming process, allowing micro-/nano-meter features on pores. In this study, PGA scaffolds made from $scCO_2$ foaming and melt-spinning fiber have been assessed for their osteogenesis capacity on bone marrow stem cells (BMSCs) in comparison to PLGA porous scaffolds.

METHODS: PGA granules (Corbion, 1.4dL/g) were fabricated into porous scaffolds following the method in Figure 1.[1] PGA fiber was from China Textile Academy. PLGA (90:10) porous scaffolds were produced by salt-leach method.[2] Scaffolds were seeded with rat BMSCs at a density of 150,000 cells/scaffold. The constructs were incubated at 37°C for 4 weeks in proliferation media and cultured for 4 weeks under osteogenic media. The scaffolds' integrity and the Alizarin red staining were examined.

RESULTS: After total 8 weeks' culture, both types of PGA scaffolds became dispersed particles or short fibers. PLGA scaffolds remained integrity. The intensity of Alizarin red staining depended on the morphology and degradation rate of scaffolds. The PGA foams degraded fastest and showed the strongest staining, and PLGA showed the least staining.

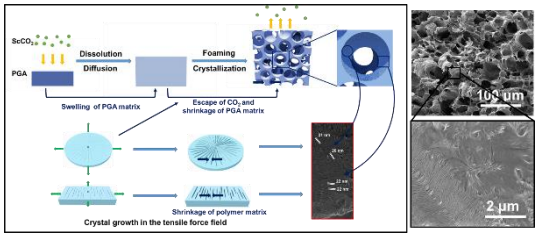

Fig. 1 Schematic illustration of the generation of micro-/nano-features on $scCO_2$ foamed scaffolds.

Uniquely Alizarin red staining showed strong staining on PGA foam after 1 week's osteogenesis induction.

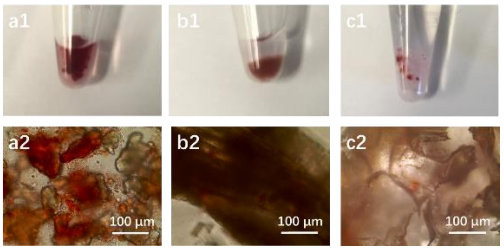

Fig. 2 Alizarin red staining images of BMSC osteogenesis on PGA foams scaffolds (a); PGA fibrous scaffolds (b) and PLGA scaffolds (c) after 1 week osteogenic induction.

DISCUSSION & CONCLUSIONS:

The higher osteogenetic capacity of $scCO_2$ formed scaffolds might be due to the fast degradation rate and unique surface topography in comparison to fibrous PGA and PLGA scaffolds. Controlling of the morphology of scaffolds and their degradation rate can be an effective way to control differentiation of stem cells.

REFERENCES: [1] Zhang JP et al (2018) *ACS Biomater. Sci. Eng.*, 4, 694–706. [2] Bardsley K, Wimpenny I, Yang Y and El Haj AJ (2016) *RSC Adv.*, 6, 44364-370.

Optimisation of extracellular matrix mimicry on a polymer based highly porous 3D pancreatic cancer organoid model

S Totti[1], MC Allenby[2], SB Dos Santos[2], A Mantalaris[2], EG Velliou[1]

[1] *Bioprocess and Biochemical Engineering group (BioProChem), Department of Chemical and Process Engineering, University of Surrey, Guildford.* [2] *Biological Systems Engineering Laboratory (BSEL), Department of Chemical Engineering, Imperial College, London*

INTRODUCTION: Pancreatic cancer is a lethal disease, the 5-year survival rate of which is at 8% [1]. The disease is characterised by a rather complex tumour microenvironment (TME) which consists of intense extracellular matrix (ECM) presence that partly contributes to the disease's progression and the inhibition of apoptotic pathways. Therefore, ECM mimicry is of great importance when modelling this malignancy *in vitro* [2-4]. More specifically, optimisation of the ECM mimicry provides better cell-cell and cell-matrix interactions, ECM secretion by the cells and cellular spatial distribution, consequently affecting tumour evolution. In this work, we modified our previously developed 3D polymer based pancreatic cancer model to mimic features of the structure and the extracellular matrix composition of pancreatic tumours.

METHODS: PANC-1 pancreatic cancer cells were seeded in polymeric highly porous scaffolds whose surface was modified with different extracellular matrix proteins dominant in pancreatic cancers' TME, i.e. fibronectin, laminin, collagen-I and RGD (Arg-Gly-Asp). The viability of the cells for all the conditions under study was monitored *in situ* with MTS viability assay as well as through live/dead staining and confocal laser scanning microscopy (CLSM) imaging of scaffold sections. Additionally, *in situ* sectioning, fluorescent staining and imaging with CLSM enabled the spatial determination of environmental gradients (oxidative, nutrient stress) and extracellular matrix production within the 3D model. Furthermore, quantitative assessment of the overall extracellular matrix secretion took place through measurement of the proteins in the cell culture supernatants.

RESULTS: Pancreatic cancer cells retained high viability in the 3D polymeric organoid model for all conditions under study for more than 29 days. Among all the ECM coatings, the fibronectin (FN) coated model exhibited a significant increase in cellular viability at the culture endpoint. Additionally, CLSM imaging of multiple scaffold sections revealed that cellular growth and spatial organisation is influenced by the type of ECM. For example, cells within the FN coated scaffolds formed bigger aggregates and expressed significantly higher amounts of collagen-I than scaffold coated with collagen type I. Furthermore, the amount and type of extracellular matrix detected in the spent medium varied between the different coatings and as compared to uncoated scaffolds.

DISCUSSION & CONCLUSIONS: Overall, in this study we evaluated different ECM coatings and further optimised the ECM mimicry on our previously developed 3D pancreatic cancer model[3,4]. Overall, ECM coated scaffolds could (i) increase pancreatic cell viability at the culture endpoint, (ii) allow the formation of bigger cellular aggregates, (iii) enhance the ECM production from the pancreatic cells, as compared to uncoated scaffolds. Furthermore, heterogeneous hypoxic regions were detected within the scaffolds. Similar trends have been reported *in vivo*, indicating the great potential of the developed model for pancreatic cancer studies.

REFERENCES: [1] R.L. Siegel, K.D. Miller, and A. Jemal. (2018) *CA Cancer J Clin* **68**:7-30. [2] S. Totti, S.I. Vernardis, L. Meira, et al (2017) *Drug Discov Today* **22**, 690-701. [3] S. Totti, M. Allenby, S B. Dos Santos, et al (2017) *Eur Cells Mater* **33** (Suppl. 2), 0249, [4] S. Totti, S B. Dos Santos, M. Allenby, et al (2016) *Eur Cells Mater* **31**(Suppl. 1), P441.

ACKNOWLEDGEMENTS: This work was supported by University of Surrey as well as an Impact Acceleration Grant (IAA-KN9149C) of the University of Surrey, an IAA–EPSRC Grant (RN0281J) and the Royal Society.

Optimisation of microparticle formulations for cytokine delivery for macrophage modulation in spinal cord injury

JZ Stening[1], FRAJ Rose[1], LJ White[1]

[1]*Regenerative Medicine and Cellular Therapies, School of Pharmacy, University of Nottingham, UK*

INTRODUCTION: Currently spinal cord injury (SCI) lacks treatment capable of restoring limb function and sensation. Current strategies focus on alleviating the triggered high inflammatory environment using pharmaceuticals. Understanding macrophage behavior and the roles of their sub phenotypes in SCI has suggested a method for controlling inflammation by modulation towards a pro-immunoregulatory subgroup (M2) using cytokine IL-4. Microparticles are widely reported as drug delivery methods for controlled and sustained release in pharmaceutical strategies. We aim to determine suitable release profiles for cytokine delivery.

METHODS: Particles were manufactured using a double emulsion method [1,2] with 50:50 or 85:15 (lactide:glycolide ratio) PLGA (52kDa). Release kinetics were tailored by: (i) incorporation of a PLGA-PEG-PLGA triblock modifier (TB) [1] and (ii) changing the total polymer (TP) percentage. Different surface thickness particles were manufactured using 10%, 15% and 20% TP using 500mg, 750mg, and 1g PLGA dissolved in 5ml DCM respectively. Total protein loaded was 10mg/ml for 1g polymer and 5mg/ml for 500mg polymer. Protein release kinetics were analysed using lysozyme as a model protein. Release results were reported as µg protein/ mg particles with a maximum of 10 µg/mg encapsulated. Particles were characterised using scanning electron microscopy and laser diffraction for size distribution. Protein encapsulation efficiencies and release were analysed over 20 days using a micro BCA assay to detect total protein content.

RESULTS: Microparticles fabricated were 20-50µm in size and had a smooth morphology. In a comparison of surface thickness the fastest release was observed for 10% TP 85:15 PLGA with a burst release of 2.5 µg/mg on day 1. Less burst release was seen for 15% TP 50:50 PLGA. The slowest release occurred for 10% TP 50:50 PLGA with 1 µg/mg released by day 20. Total polymer 10% and 15% particles showed release too fast and unsustained for this application. In a comparison of triblock percentages for 20% TP 50:50 PLGA, 30% TB showed the fastest release with 10 µg/mg released by day 20. The slowest release was seen for 0% and 20% TB showing a small burst release of 1 µg/mg at day 1 and only reaching 1.5 µg/mg and 3 µg/mg respectively by day 20. 10% TB showed a burst release of 3 µg/mg at day 1 as for 30% TB but showed a promising sustained and continuous release to 6 µg/mg over 20 days.

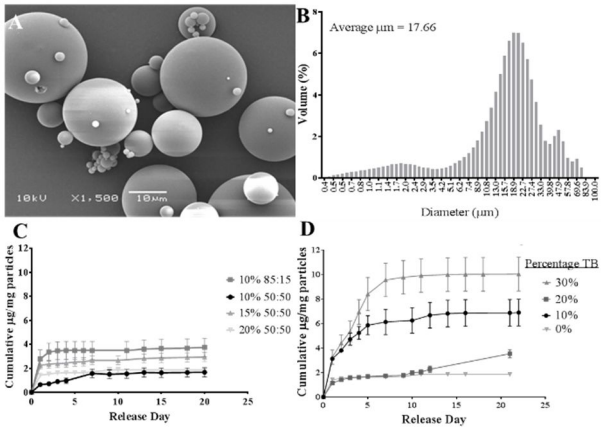

Fig. 1: SEM image (x1500) and size distribution 20% TP, 50:50 PLGA, 20% TB particles. Cumulative protein release (µg/mg) for different TP percentages (A) and percentage TB (B).

DISCUSSION & CONCLUSIONS: Particles prepared from 10% or 15% total polymer displayed protein release unsuitable for controlled release with a fast burst release followed by minimal daily release. Particles manufactured from 50:50 PLGA and 85:15 PLGA alone displayed release too slow for IL-4 delivery. Addition of a PLGA-PEG-PLGA triblock enabled release to be controlled with less initial burst release and accelerated overall release. Microparticles fabricated from 20%TP, 50:50 PLGA with 10% TB showed a release profile most suited to 14 days of controlled release.

REFERENCES: [1] White LJ, *et al.* (2013) Accelerating protein release from microparticles for regenerative medicine applications. *Mater Sci Eng C* **33**(5):2578–83. [2]Abu-Awwad HADM, *et al.* (2017) Controlled release of GAG-binding enhanced transduction (GET) peptides for sustained and highly efficient intracellular delivery. *Acta Biomater* **57**:225–37.

ACKNOWLEDGEMENTS: Supported by the International Foundation for Research in Paraplegia, Switzerland 'Combining stem cell and drug delivery to modulate macrophage phenotype toward M2 in spinal cord injury', grant no. P155.

Osteogenesis of embryonic stem cells by nanoscale mechanotransduction

Mathew Hollingworth[1], Morgan Alexander[2], Matthew Dalby[3], Lee Buttery[1]

[1]*Regenerative Medicine & Cellular Therapies, University of Nottingham* [2]*Advanced Materials & Healthcare Technologies, University of Nottingham* [3]*Centre for Cell Engineering, University of Glasgow*

INTRODUCTION: *In vitro* differentiation of embryonic stem cells (ESCs) to the osteoblast lineage is well established, typically using culture medium supplements (ascorbic acid, dexamethasone etc) to promote osteogenesis[1]. However stimulation by nanoscale mechanotransduction using the 'Nanokick' bioreactor has been shown to promote osteogenesis of human mesenchymal stem cells[2]. We show the application of nanovibrations also promotes osteogenesis of embryonic stem cells without need for traditional osteogenic medium supplements.

METHODS: mESCs and calvarial osteoblasts (extracted from 1-3 day old neonatal CD-1 pups) were cultured in osteogenic culture medium containing ascorbic acid, dexamethasone and β-glycerophosphatse (OCM) or stimulated by nanovibrations at 1000Hz, 30nm displacements (1000Hz) for up to 35 days. Bone nodules assessed by alizarin red staining and Raman spectroscopy (Renishaw inVIA). FAK assessed by immunocytochemical staining and quantified using infrared secondary antibody measurement (LiCor).

RESULTS:

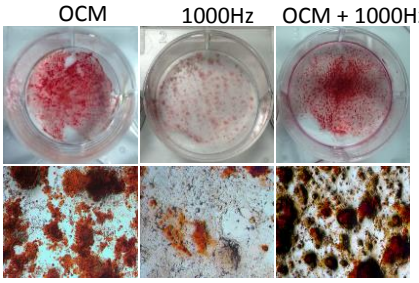

Fig.1: Morphology of mESC bone nodules formed following osteogenic culture.

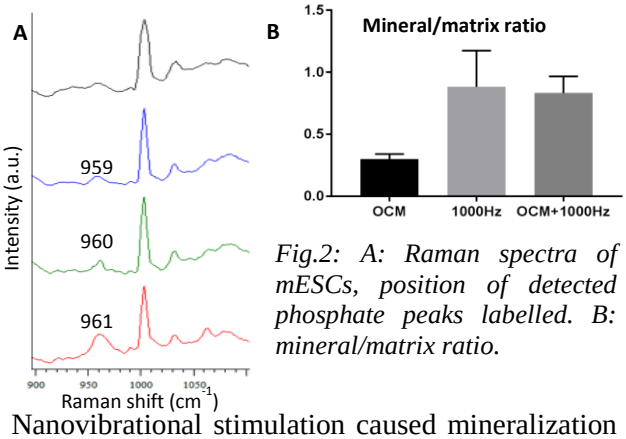

Fig.2: A: Raman spectra of mESCs, position of detected phosphate peaks labelled. B: mineral/matrix ratio.

Nanovibrational stimulation caused mineralization and expression of osteogenic markers RUNX2, osteocalcin and ALP in mESCs, at levels similar to calvarial osteoblasts (used as control). Interestingly the addition of nanovibration caused ESCs to form more numerous bone nodules with distinct morphology compared to those produced by osteogenic medium alone (fig 1). Raman spectroscopy revealed phosphate species under all conditions (except control), however the addition of nanovibration produced more prominent peaks and increased mineral to matrix ratio (Fig.2).

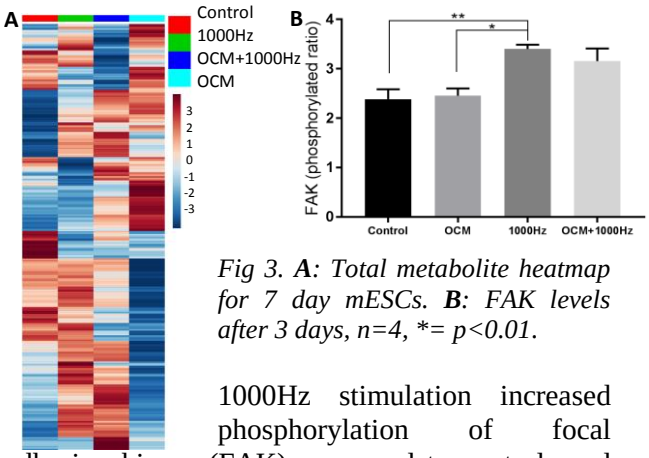

*Fig 3. **A**: Total metabolite heatmap for 7 day mESCs. **B**: FAK levels after 3 days, n=4, *= p<0.01.*

1000Hz stimulation increased phosphorylation of focal adhesion kinase (FAK) compared to controls and OCM suggesting nanovibration promotes osteogenesis by formation of more extensive focal adhesion complexes typical of mature osteoblasts. Metabolite populations were noticeably different following 1000Hz stimulation (Fig. 3A) whilst Ingenuity pathway analysis confirmed nanovibration stimulated activation of FAK signaling pathway as well as ERK1/2 and RUNX2.

DISCUSSION & CONCLUSIONS:

Nanovibrational stimulation promotes osteogenesis of mESCs *in vitro*, with notable differences in mineral morphology/content. These differences are likely due to induction of osteogenesis by FAK activation, not observed in OCM samples. These results highlight the influence of nanoscale mechanical stimulation, information that will aid the development of regenerative therapies for bone disorders. The 'Nanokick' bioreactor provides a scalable platform for simple, reproducible osteoblast culture without the need for expensive growth factors and supplements.

REFERENCES: [1] Buttery LDK, Bourne S, Xynos JD, et al. *Tissue Eng*. 2001;7(1):89-99. [2] I Nikukar H, Reid S, Tsimbouri PM, Riehle MO, Curtis ASG, Dalby MJ. *ACS Nano*. 2013;7(3):2758-2767.

ACKNOWLEDGEMENTS: Research funded by EPSRC. Nanovibrational bioreactor supplied by Nanokick technologies.

Peptide-graphene oxide hydrogel nanocomposites for intervertebral disc repair

C Ligorio[1,2], M Zhou[2], A Vijayaraghavan[1], J.A. Hoyland[3], A Saiani[1,2]

[1] School of Materials, The University of Manchester, Manchester, UK [2]Manchester Institute of Biotechnology, The University of Manchester, Manchester, UK , [3]Division of Cell Matrix Biology and Regenerative Medicine, School of Biological Sciences, The University of Manchester, UK

INTRODUCTION: Low back pain associated with intervertebral disc degeneration (IVDD) has been classified as a major contributor of global disability, affecting 84% of population and costing the healthcare over £12 billion/year in UK only[1]. Current treatments for IVD degeneration rely on disc replacements, which are highly invasive and poorly efficient in the long-term. Novel minimally invasive cell-based therapies allow delivery of cells or cell-seeded biomaterials at the injury site to repopulate damaged tissue and promote repair/regeneration. Among injectable biomaterials, self-assembling peptide hydrogels (SAPHs) represent potential candidates as 3D cell carriers, since they can mimic the native tissue supporting cell viability and differentiation[2,3]. Moreover, the advent of graphene-related materials as nanofillers has made the fabrication of graphene-hydrogel nanocomposites appealing, in which filler properties can be further exploited to direct cellular fate[4]. Here, we incorporated graphene oxide (GO) within a SAPH to develop a novel biocompatible peptide-GO nanocomposite as a potential cell carrier for IVD repair applications.

METHODS: Peptide hydrogels were prepared by dissolving 10, 15 and 20 mg/ml of FEFKFEFK (F8) powder in double distilled water and further titrated with 0.5M NaOH to a final pH of ~4. Solutions were mixed with an aqueous solution of GO (mean flake size of 4.79±2.13µm) to form peptide-GO hybrid hydrogels with GO final concentration of 0.5 mg/ml. Hydrogel microstructure was observed with atomic force and transmission electron microscopy (AFM and TEM), while mechanical performance was assessed via oscillatory rheology. Bovine nucleus pulposus cells (BNPCs) were then encapsulated in formed hydrogels and cultured in 3D for 7 days. Cell viability was assessed 1, 4 and 7 days after encapsulation using Live/Dead assay.

RESULTS: GO flakes were homogenously dispersed in F8 samples, showing different levels of interactions with the peptide-based nanofibrillar network (Fig. 1). The incorporation of GO enhanced the mechanical properties of peptide hydrogels, achieving average storage moduli (G'~12.8 kPa) comparable with human NP tissue (G'~10 kPa). Moreover, GO-containing F8 hydrogel were biocompatible, preserving rounded morphology and high viability of encapsulated NP cells over the entire period of observation (Fig. 2).

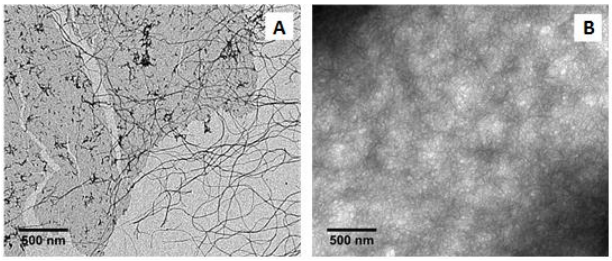

Fig. 1: TEM images of peptide at A) 15 and B) 20 mg/ml mixed with GO flakes.

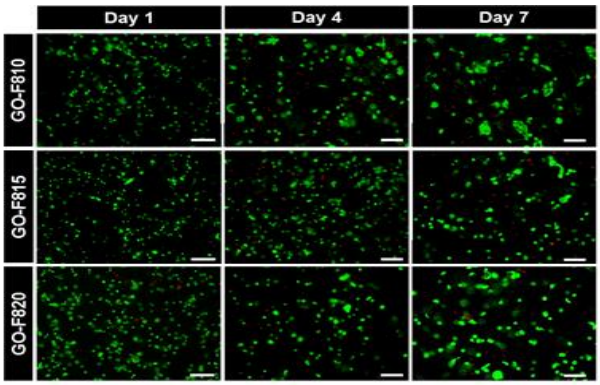

Fig. 2: Live/Dead assay of BNPCs (green=live, red=dead) in hybrid hydrogels with increasing peptide concentrations. Scale bar=100µm

DISCUSSION & CONCLUSIONS: The results showed that GO can be added to SAPHs to create mechanically-reinforced scaffolds which are biocompatible for 3D culture of NP cells resulting appealing as cell carrier in for IVD repair.

REFERENCES: [1]S. Richardson *et al.* (2013) *The Intervertebral Disc*, pp.177-200. [2]A. Mujeeb *et al.* (2013) *Acta Biomaterialia* **9**(1), pp.4609-4617. [3]L. Castillo Diaz *et al.* (2016) *Journal of Tissue Engineering*, **7**:1-15 [4]L. Kenry *et al.* (2018) *Biomaterials*, **155**: pp.236-250.

ACKNOWLEDGEMENTS: The authors thank EPSRC & MRC (EP/L014904/1 & EP/K016210/1) for their financial support and the University of Manchester BioAFM facility for their technical support during nanotopographical characterisation.

Physiologic oxygen levels and Rock inhibitor as a media supplement improve epithelial cell recovery from porcine lung tissue cultures

EL Borg D'Anastasi[1], TP Dale[1], NR Forsyth[1]

[1] *Guy Hilton Research Centre, Institute for Science and Technology in Medicine, Keele University, Stoke-on-Trent.*

INTRODUCTION: Respiratory disorders such as asthma and chronic obstructive pulmonary disease (COPD) represent a large proportion of worldwide morbidity and mortality, with approximately 10,000 new cases diagnosed each week in the UK[1]. Despite the prevalence of these disorders, therapies have mainly focused on improving symptoms rather than looking to effective treatments. This makes the lung an attractive target for regenerative medicine, with the need for well-defined methods to isolate and expand lung epithelial cells in culture. In this case, porcine lung was used as a biologically similar alternative to human lung. Rock inhibitor has been shown to enhance epithelial cell proliferation in airway cultures[2]; its effect on lung parenchyma cell recovery was examined alongside the effects of incubation in more physiologically relevant oxygen levels.

METHODS: Lung parenchyma was dissected from porcine lungs, minced and washed with antibiotics before being digested overnight in a pronase buffer (1 mg/mL protease XIV, 0.005% trypsin and 10 ng/mL DNAse I) at 4°C on a rocker. The resulting digest was then passed through sterile gauze to remove the tissue and collect the cells, followed by a 70µm cell strainer. The digest was centrifuged at 400xg for 20 minutes and the supernatant was removed. Where necessary the cells were treated with red blood cell lysis buffer. The cells were then resuspended in HBSS and viability established using Trypan blue.

Cells were seeded in collagen coated tissue culture flasks at a density of 100,000/cm^2 in one of three different epithelial media formulations; A (10% FBS), B (4% FBS) or C (serum free, commercial and small airway specific), either with or without the addition of a Rock Inhibitor (RI) Y27632. These were then incubated in either ambient (21%) or physiologic (2%) oxygen. Conditions were set up in triplicate and cell numbers were counted prior to confluence.

RESULTS: Cells were successfully recovered in medium A and B, and were predominantly of an epithelial morphology. In every instance reduced oxygen improved recovery, significantly so in A+RI ($p \leq 0.001$) and B-RI ($p \leq 0.0001$). In medium where cells recovered successfully, the presence of RI resulted in a large significant increase in cell numbers ($p \leq 0.01$-$p \leq 0.0001$). Medium formulation C resulted in very few cells, irrespective of oxygen level or the presence of Rock Inhibitor.

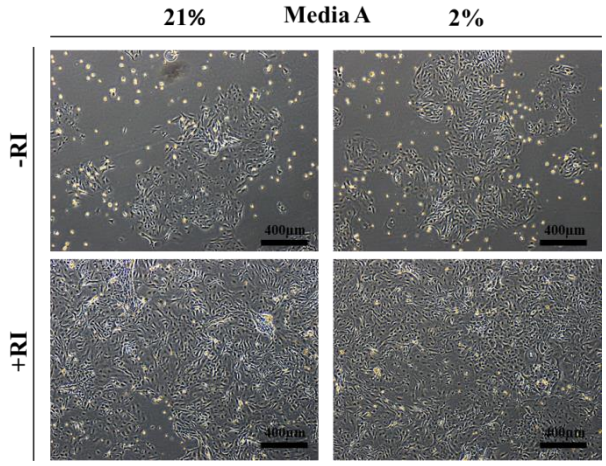

Fig. 1: Phase contrast image of porcine epithelial cells recovered in media formulation A with or without Rock Inhibitor, incubated in 21% or 2% oxygen.

DISCUSSION & CONCLUSIONS: Media formulation and oxygen level both influence lung epithelial cell recovery, with the addition of RI as a supplement significantly improving the initial yield. These optimised culture conditions for the isolation and expansion of lung cells may prove particularly crucial for work with human samples; where the tissue offered for cell isolation may be considerably smaller such as with biopsies.

REFERENCES: [1] Statistics.blf.org.uk. (2018) Lung disease in the UK. *British Lung Foundation*. https://statistics.blf.org.uk/ [2] Horani, A., Nath, A., Wasserman, M., Huang, T. and Brody, S. (2013). Rho-Associated protein kinase inhibition enhances airway epithelial Basal-cell proliferation and lentivirus transduction. American Journal of Respiratory Cell and Molecular Biology, 49(3), pp.341-347.

ACKNOWLEDGEMENTS: We would like to thank the North Staffordshire medical institute and UHNM Charity for funding our work in this field.

Placental mesenchymal stem cells for the treatment of bronchopulmonary dysplasia

Jessica Bratt[1], Pensee Wu[2], Nicholas Forsyth[1], Alicia El Haj[1]

[1]ISTM, Guy Hilton Research Centre, Keele University, Stoke-on-Trent, UK

[2]Univeristy Hospital of North Midlands, Stoke-on-Trent, UK

INTRODUCTION: Bronchopulmonary Dysplasia (BPD) is a neonatal disease affecting the lungs of premature infants. The disease interferes with alveolar maturation and vascularisation. There are currently no treatment options but only supportive (oxygen ventilation and surfactant treatment) and prevention measures (Costeloe KL *et al.* 2012). Mesenchymal stem cells (MSCs) are the focus of regenerative medicine and have the potential to offer a promising therapeutic tool for the treatment of BPD (Ahn SY *et al.* 2015). As shown in hyperoxia induced rodent and murine models. Placental derived MSCs (pMSCs) are associated with fewer ethical concerns, easy attainability and a high capacity for differentiation (Pasquinelli G *et al.* 2007). The study currently focuses of developing an *in vitro* model (fig. 1) to assess the suitability of pMSCs for the treatment of BPD.

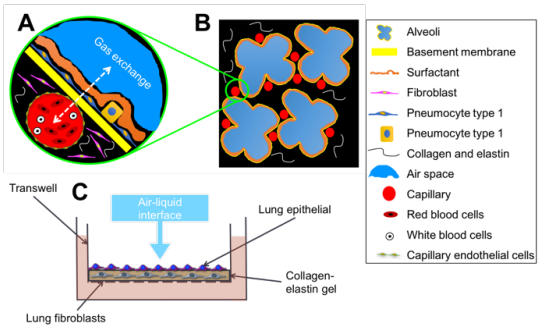

Fig. 1: The development of an in vitro model to represent the BPD lung alveoli. A representative image of the alveoli wall (A) which resides with the lung interstitium tissue (B). An in vitro model (C) has been developed to represent the lung alveoli.

METHODS: 3.5mg/ml collagen and elastin hydrogel constructs were made using type I rat-tail collagen (BD Bioscience) using a previously described protocol. Human adult lung fibroblasts 35FL were seeded in monolayer or within the gels and human epithelial cell line A549 were seeded on the gel surface. The constructs were incubated for 20 days at either 21% O_2 or 40% O_2. The contraction of hydrogels was measured using optical coherence tomography (OCT). DNA quantification was achieved on day 0 and day 20 using the PicoGreen dsDNA quantification assay (Invitrogen). Gene expression was examined using qPCR. The equivalent experiments were conducted with cells extracted form endotracheal suctioning of neonates on ventilation in the NICU (NL cells).

RESULTS: An increase in cell number was observed in all samples except adult lung fibroblasts 35FL cultured at 40% O_2. NL cell seeded hydrogels did not contract at 40% O_2.

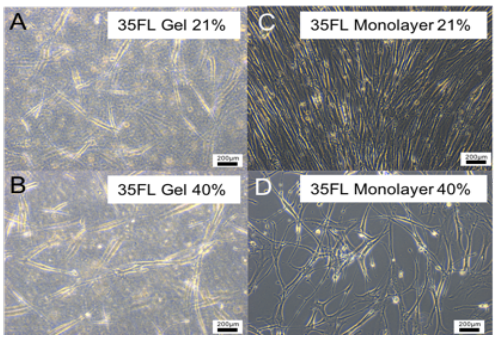

Fig. 2: Phase contrast images of the cells within the hydrogels (A,B) or in monolayer (C,D).

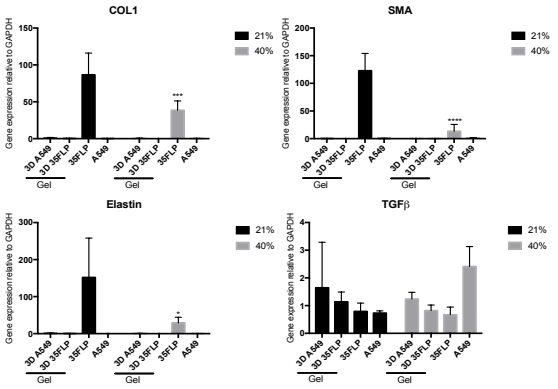

Fig 3: qPCR analysis looking at BPD associated genes. Collagen, smooth muscle actin and elastin are all downregulated at 40% O_2 culture.

DISCUSSION & CONCLUSIONS: In this work we have developed an *in vitro model* to represent the human lung alveoli and BPD. The air-liquid interface allows us to model the high O_2 ventilation BPD patients are exposed to. Current results show that culture at 40% O_2 has a significant effect on adult lung fibroblast proliferation, contraction and gene expression. So far, we have not seen the same effect in NL cells.

ACKNOWLEDGEMENTS: The authors would like to thank the CDT Regenerative Medicine for funding. This template was modified with kind permission from eCM Journal.

Primary cilia mediated mechanotransduction in differentiating osteoblasts

LA Boyle[1], GC Reilly[1]

[1] *INSIGNEO Institute for in silico Medicine, Department of Materials Science and Engineering, University of Sheffield, UK*

INTRODUCTION: Primary cilia are non-motile, hair-like protrusions that emanate from the cell body of most mammalian cells. They play a wide range of roles in our body from the light receptors in our retinas to mechanosensory roles in multiple tissue types. It is believed that the deflection of primary cilia caused by fluid flow loading triggers a cellular mechanoresponse in bone cells [1, 2]. One of the ways cilia control their mechanosensitivity is through controlling their length, shortening in response to continuous loading. Further understanding of how the structure of the cilium and how subsequent cellular responses can be manipulated could prove to be a useful tool in the treatment of ciliopathies, osteoporosis and osteoarthritis, as well as improving tissue engineered bone constructs.

METHODS: Human embryonic stem-cell-derived mesenchymal progenitor cells were subjected to oscillatory, low magnitude (0.05 Pa) fluid shear generated by a rocking platform. Primary cilia were elongated with 1 mM lithium chloride (LiCl) [3] to assess if elongating cilia increases mechanosensitivity. This concentration was selected as it is the blood serum concentration that is aimed for when treating medical disorders and it did not have an osteogenic effect in static conditions. Osteogenic markers prostaglandin E2 (PGE2), alkaline phosphatase (ALP) activity and total calcium production were evaluated on day 7, 14 and 21 respectively (Figure 1).

RESULTS: 1 mM LiCl treatment did not affect the number of ciliated cells but enhanced mean cilia length by almost 50% (3.5 μm to 5 μm) after 24 hours of exposure. PGE2 levels increased when cells were treated with LiCl, likely through the GSK3β/β-catenin signalling pathway. LiCl treated cells subjected to rocking showed no further increase in PGE2 production. Rocking alone did not affect ALP activity but did increase matrix calcium production. There was evidence of increased mechanosensitivity induced by LiCl treatment as rocked cells treated with 1 mM LiCl demonstrated higher ALP activity than static cultures. Additionally, increased mechanosensitivity was confirmed by the higher quantity of calcified matirx produced by the cells subjected to both rocking and LiCl.

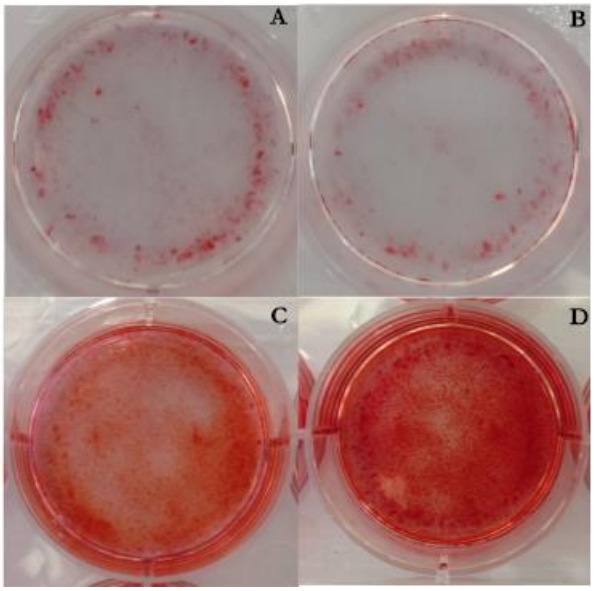

Fig. 1: Day 21 ARS staining. (A) static 0 mM, (B) static 1 mM, (C) rocked 0 mM, (D) rocked 1 mM

DISCUSSION & CONCLUSIONS: Elongation of primary cilia resulted in enhanced responses to mechanical loading compared to mechanically stimulated cells without elongated cilia. Increases were seen in both early osteogenic markers (ALP activity) and in mineralized matrix production. This tool could therefore be beneficial in tissue engineering to create bone constructs in vitro in a quicker more efficient manner. These results also suggest that the mechanotransduction mechanism of cells can be beneficially altered to increase mechanically induced cellular responses. Manipulation of the primary cilia may therefore be beneficial in the treatment of some ciliopathies where defects in cilia length occur.

REFERENCES: [1] R. Delaine-Smith A. Sittichokechaiwut and G.C Reilly (2014) FASEB Journal **28**:430-9 [2] R. Kwon et al. (2010) FASEB Journal **24**:2859-68 [3] C. Thompson et al. (2016) FASEB Journal **30**:716-26

ACKNOWLEDGEMENTS: We are grateful to the EPSRC (UK) for the funding.

Response of Endothelial Cells to hypoxia on hybrid protein electrospun scaffolds

JA Reid, A Callanan
The Institute for Bioengineering, School of Engineering, The University of Edinburgh, UK

INTRODUCTION: Oxygen deficiency (hypoxia) has been shown to lead to several vascular pathologies in endothelial cells [1]. Alongside this, the addition of decellularized extracellular matrix (ECM) to a polymer scaffold has been shown to drastically alter cellular gene expression [2]. In this study, we propose combining the effects of hypoxia with that of vascular based ECM/Polycaprolactone (PCL) bioscaffold to see how the performance of human umbilical vein endothelial cells (HUVECs) is affected.

METHODS: Briefly, pieces of bovine aorta were perfusion decellularized (0.5% sodium dodecyl sulfate), lyophilized and milled into a pulp. This ECM pulp was added at a concentration of 0.25% w/v to an 8% w/v PCL/HFIP solution. The solution was electrospun into randomly orientated fibres. Electrospun PCL was used as a control. Scaffolds were punched out (diameter = 10mm) and seeded with HUVECs at 110,000 cells/cm^2. All scaffolds were left in incubator conditions (18.6% O_2) [3] for 2h to allow cells to bind to the scaffold. After 2h, half of the scaffolds were moved into hypoxic conditions (2% O_2), and the other half were left in normoxic conditions. Various biochemical quantification methods were performed, including DNA quantification, PCR and cell viability. Scanning electron microscopy was performed, along with immunohistochemistry looking at the collagen I and elastin content of the scaffolds.

RESULTS:

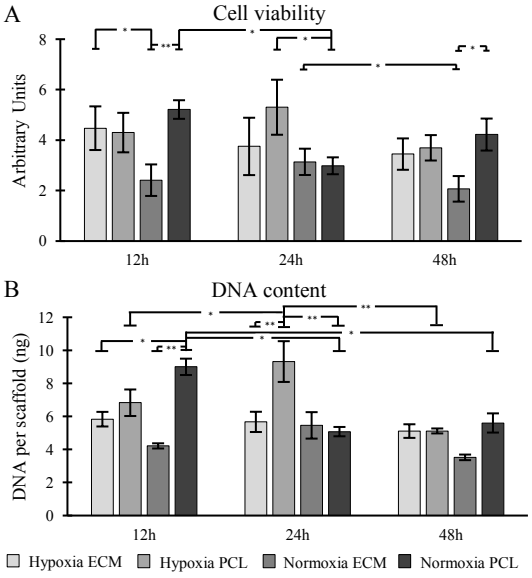

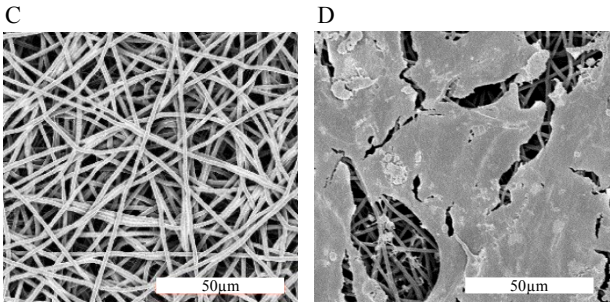

*Fig. 1: A) Cell viability on each scaffold. N=4, error bars = SE, one-way ANOVA with Fishers' post hoc performed *p<0.05, **p<0.01. B) DNA quantification C) Representative SEM image of electrospun ECM bioscaffold. D) SEM image of HUVEC monolayer on the electrospun ECM bioscaffold.*

Overall, HUVECs showed higher cell viability and DNA content at all timepoints when grown on the ECM scaffolds in hypoxia rather than normoxia. However, no real trends were noted between the PCL scaffold and ECM scaffold. Representative SEM images of the HUVEC monolayer show good cell adhesion and growth across the scaffold.

DISCUSSION & CONCLUSIONS: This systematic study has shown that aorta ECM bioscaffolds are capable of accommodating the attachment and growth of HUVECs under hypoxic and normoxic conditions. Results show the great potential of the scaffolds and their possible applications in tissue engineering and/or drug testing platforms.

REFERENCES: [1]C. Michiels, T. Arnould, J. Remacle (2000) *Biochimica et biophysica Acta*: 1-10. [2] R. Grant, D.C. Hay, A. Callanan (2017) *Tissue Eng: Part A* **23**:650-662. [3]R.H. Wenger, *et al* (2015) *Hypoxia* **3**:35-43.

ACKNOWLEDGEMENTS: ESPRC no. EP/N509644/1. MRC grant MR/L012766/1.

Self-assembling peptide nanofiber hydrogel for cardiac tissue engineering

KA Burgess[1], D Oceandy[2], A Saiani[1]

[1] School of Materials & Manchester Institute for Biotechnology , University of Manchester, Manchester, UK; [2] Institute of Cardiovascular Sciences, University of Manchester, Manchester, UK.

INTRODUCTION: Stem cells reside in complex microenvironments, from which they interpret both mechanical and biochemical cues.[1] Only by moving towards 3D cell culture can we effectively mimic the regulation of stem cell behaviour in vivo. Of interest are hydrogels; water-swollen polymeric networks which are thought to closely resemble the native extracellular matrix.[2] In particular, our focus is on β-sheet forming, self-assembling peptide hydrogels (SAPHs) developed by Zhang's group; based on the alternating pattern of hydrophilic/ hydrophobic residues.[3] These SAPHs provide a suitable platform for the construction of a defined, controlled microenvironment for stem cell culture and differentiation.

METHODS: Human induced pluripotent stem cells (hiPSCs) were cultured on Geltrex and maintained in Essential 8 medium. Once confluent, cells were treated with Accutase to obtain a single-cell suspension; before subsequent encapsulation within FEFKFEFK (F8) peptide hydrogels. Hydrogels were prepared at different concentrations (10, 15 and 20 mM); yielding hydrogels with different mechanical properties (storage moduli of 2.7, 6.6 and 10.1 kPa). Cells were assessed in terms of viability, morphology and gene expression; during short-term culture (3-4 days).

Following expansion, the media was replaced with RPMI 1640 plus B27 without insulin between day 0 and 8, and in RPMI 1640 plus B27 thereafter. To induce cardiomyocyte differentiation, the media was supplemented with the following small molecules: CHIR99021, for days 0–2; and Wnt-C59 for days 2–4. Gene expression profiles were mapped overtime to assess markers of successful differentiation.

RESULTS: All concentrations of F8 hydrogel supported the in vitro culture of hiPSCs: which progressed from loose, disorganised cell clusters, typically 50 μm in diameter; to smooth spheroid aggregates around 250-300 μm in size. Encapsulated cells continued to express typical markers of pluripotency (Oct-4, Nanog and Sox-2); regardless of differences in the bulk mechanical properties. Following induction of cardiomyocyte differentiation, encapsulated hiPSCs up-regulated specific markers of mesoderm commitment; indicative that the cells are responding to biochemical cues and ultimately, successful 3D generation of iPSC-cardiomyocytes.

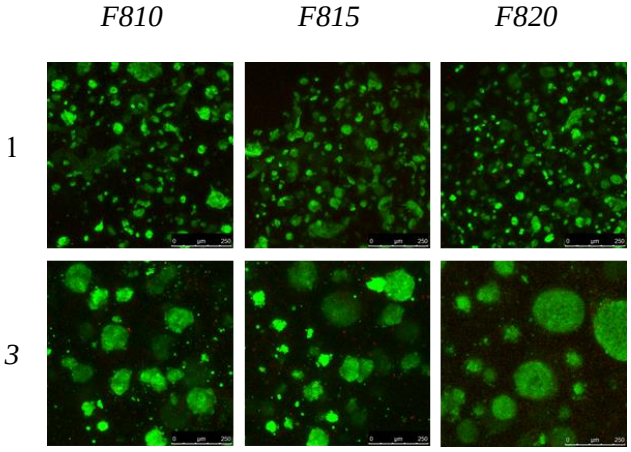

Fig. 1: Images of hiPSCs encapsulated in F8 hydrogels (10, 15 and 20 mM) after 1 or 3 days in culture. Live cells are stained with calcein (Green) and dead cells with ethidium homodimer-2 (Red). Scale bar – 250 μm.

DISCUSSION & CONCLUSIONS: SAPHs provide a biocompatible matrix for 3D stem cell culture and differentiation. These SAPHs are tuneable and can be easily functionalised; thereby, providing a fully-defined scaffold which can be tailored for the efficient differentiation of hiPSCs. These materials have great potential for applications in tissue engineering.

REFERENCES: [1] M.P. Lutolf, P.M. Gilbert and H.M. Blau (2009) *Nature* **462**:433-441. [2] Y. Fan, J. Wu, P. Ashok et al (2015) *Stem Cell Reviews* **11**:96-109.[3] S. Zhang, T. Holmes, C. Lockshin et al (1993) Proc Natl Acad Sci USA **90**:3334-3338.

ACKNOWLEDGEMENTS: The authors acknowledge an EPSRC Fellowship (EP/K016210/1) and the joint grant from the MRC and EPSRC (CDT in Regenerative Medicine) for providing financial support to this project.

Self-assembling peptides with chondroitin sulfate to replenish cartilage proteoglycans in order to restore biomechanics

K Bostock[1], L Jennings[1], H Fermor[1]

[1] *Institute of Medical and Biological Engineering, University of Leeds, LS2 9JT.*

INTRODUCTION: Post-traumatic arthritis occurs in up to 50% of patients who experience joint trauma, and this accounts for 12% of patients with osteoarthritis.

This trauma causes cartilage swelling, collagen rupture, cell necrosis and glycosaminoglycan (GAG) loss from within the injury site. This leads to a cartilage lesion forming which cannot heal and degenerates over time [1].

The functional role of GAGs in cartilage is to provide compressive stiffness. Repair of cartilage damage at any stage of severity should restore tissue biomechanics. We aim to restore the compressive stiffness of cartilage by replenishing GAGs using a self-assembling peptide hydrogel combined with chondroitin sulphate. This will be employed in two ways (1) direct injection to repair early cartilage lesions and (2) to improve the biomechanical properties of decellularised scaffolds for later stage cartilage lesion regeneration. By restoring tissue biomechanical function we aim to prevent the progressive degeneration of cartilage lesions to osteoarthritis.

RESEARCH AIMS: The main aims for this research are to restore the biomechanics of cartilage offering a range of treatments for different stages of cartilage damage.

METHODS: Osteochondral scaffolds will be decellularised using SDS to generate an immunocompatible natural tissue scaffold. This bioprocess removes proteoglycans from the scaffold reducing the compressive stiffness of the cartilage. Using histological and biochemical methods we will assess the replenishment of scaffold GAGs using self-assembling peptide hydrogels. This will also be assessed in in vitro models of early cartilage lesions.

The peptides are assembled with chondroitin sulphate and delivered into the cartilage. Any leaching of the peptides will be monitored, as they must be maintained within the cartilage to provide mechanical strength.

The deformation and friction characteristics of peptide enhanced osteochondral scaffolds and restored model lesions will be assessed using indentation, pin on plate testing and whole natural joint simulation methods.

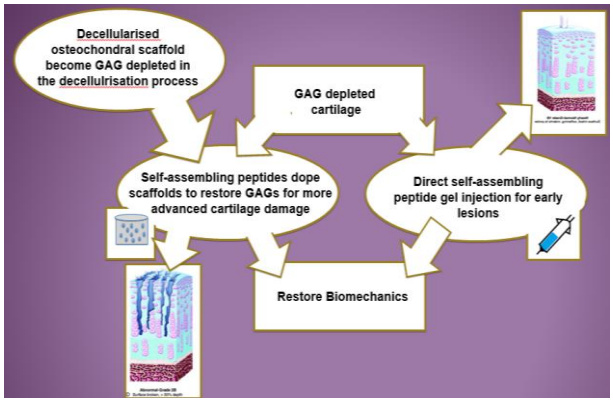

Fig. 1: Flow diagram showing the process restoring biomechanics in both early cartilage lesions and decellularised osteochondral scaffolds by restoring the GAG content

EXPECTED OUTCOMES: An injectable self-assembling peptide chondroitin sulphate treatment will be developed which will treat early cartilage lesions (grade I) and prevent the degeneration towards osteoarthritis.

A biomechanically competent regenerative osteochondral scaffold for effective functional repair of grade II-IV cartilage lesions.

BENEFICIARIES: Patients will have a more rapid recovery and be able to be weight bearing sooner due to improved biomechanics

Clinicians will have a new treatment option, this could be game changing as there is no "off the shelf" treatment option for cartilage lesions

REFERENCES: [1]. Punzi L, Galozzi P, Luisetto R, Favero M, Ramonda R, Oliviero F, and Scanu A. (2016). Post-traumatic arthritis: overview on pathogenic mechanisms and role of inflammation. RMD Open. 2(2). e000279

ACKNOWLEDGEMENTS: EPSRC CDT TERM funding

This template was modified with kind permission from eCM Journal.

Studying osteoclast activity *in vitro*

R Owen[1], GC Reilly[1]

[1] *INSIGNEO Institute for In Silico Medicine, Department of Materials Science and Engineering, University of Sheffield, UK*

INTRODUCTION: *In vivo*, mature osteoclasts tightly attach to the bone surface and degrade the osteoid through secretion of acids and enzymes. To classify an osteoclast as mature, it must be multinucleated, tartrate-resistant acid phosphatase 5b (TRAP) positive, and capable of resorbing bone. When generating osteoclasts *in vitro*, it is relatively straightforward to verify the first two requirements; however, confirming resorption is much more difficult. Historically, natural tissues such as bone, dentine, or ivory would be used as culture surfaces for pit-formation assays [1]. However, the required processing and preparation steps are time consuming and expensive.

This led to the production of bone-like culture surfaces, such as the BD BioCoat™ Osteologic™ and Corning® Osteo Assay. However, these only mimic the organic component of bone by providing a sub-micron film of calcium phosphate. Therefore, resorption on these surface does not mimic *in vivo* where osteoclasts predominantly resorb a highly mineralised collagen extracellular matrix (ECM).

METHODS: IDG-SW3 osteoblast-osteocytes were cultured for 21 days to allow sufficient mineralised ECM to be deposited before adding RAW264.7 monocyte macrophages and co-culturing for ten days. TRAP activity was assessed and resorption quantified by comparing total calcium by Alizarin Red S (ARS) staining before and after osteoclast addition. To create mineralised substrates more quickly, MLO-A5 osteoblasts were cultured for 7 days before decellularising. Freeze/thaw, enzymatic and chemical processes were compared by caclium, collagen and nuclei staining to assess efficacy and impact on the ECM.

RESULTS: The ability of RAW264.7 to resorb ECM deposited by IDG-SW3 was highly seeding density dependent. The highest TRAP activities and greatest resorption occurred when seeded at 2,500 precursors per cm^2, with 50% lower TRAP activities and no resorption occurring at the highest seeding densities (10,000/cm^2) (Fig. 1). MLO-A5 deposited a greatly mineralised collagenous ECM within one week, three times faster than IDG-SW3. Decellularisation by overnight incubation in 1% Triton X-100 and 1% ammonium hydroxide was found to be superior to the use of trypsin and sodium dodecyl sulfate.

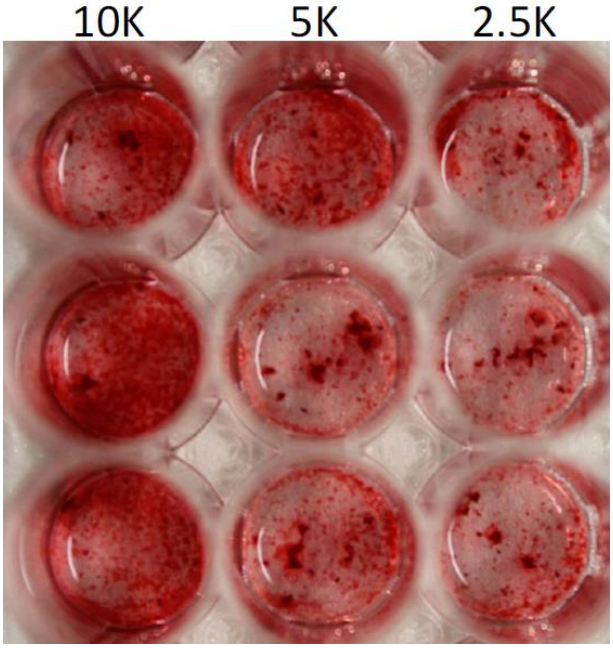

Fig. 1: Remaining mineral after ten days of RAW264.7 culture by ARS staining. The greatest resorption was observed at the lowest seeding density (2.5k).

DISCUSSION & CONCLUSIONS: The culture of osteoblasts *in vitro* is a quick and simple method of depositing a bone-like ECM onto tissue culture plastic and scaffolds. This matrix is resorbable by osteoclasts, cheaper and simpler than processing natural tissues, and more physiologically relevant than commercially available systems. Before this approach to analysing osteoclast activity *in vitro* can become established, further work needs to focus on reproducibility of matrix deposition, determination of how long surfaces can be stored for after decellularisation, and confirmation that both organic and inorganic resorption is occurring through the use of additional resorption assays such as CTX collagen peptide ELISAs.

REFERENCES: [1] Bradley E.W., Oursler M.J. (2008) Osteoclast Culture and Resorption Assays. In: Westendorf J.J. (eds) Osteoporosis. Methods In Molecular Biology™, vol 455. Humana Press

ACKNOWLEDGEMENTS: Funding from the EPSRC (EP/N509735/1)

Suitability of Optimized PVA Electrospun Scaffolds for ACL Replacement

Elisa Roldán[1], Neil D. Reeves[2], Glen Cooper[3], Kirstie Andrews[1]

[1] School of Engineering, Faculty of Science & Engineering, Manchester Metropolitan University, Manchester, UK. [2] School of Healthcare Science, Faculty of Science & Engineering, Manchester Metropolitan University, Manchester, UK. [3] School of Mechanical, Aerospace & Civil Engineering, University of Manchester, Manchester, UK

INTRODUCTION: PVA is an inexpensive, highly hydrophilic, biodegradable, nontoxic and biocompatible polymer. These properties make the PVA a promising polymer from which to create nanofibrous electrospun scaffolds for tissue engineering applications. However, its use for the manufacturing of electrospun ligament implants has not been investigated. The aim of this work was to evaluate the suitability of optimized PVA electrospun scaffolds to be used as ACL replacements, with comparable mechanical behaviour [1, 2], topography and morphology to the native ligament in order to promote tissue ingrowth and be mechanically functional.

METHODS: After a systematic electrospun optimization varying process and solution parameters, 2D optimized electrospun scaffolds were manufactured using 12% w/v of PVA (Sigma Aldrich, UK) dissolved in distilled water (Table 1). Fibre diameter and interfibre separation were determined though scanning electron microscopy images (SEM) and AxioVision image analysis software, measuring 20 fibres per sample (18 samples). The effect of crosslinking with 25% glutaraldehyde vapour for 24 hours was investigated using the following samples (0.5 x 0.5 cm): 2 non-crosslinked samples; 2 crosslinked samples; 2 crosslinked samples, rinsed in PBS for 30 seconds and dried under a fume hood for 24 hours; and 12 crosslinked samples placed into an incubator at 37°C and 5% CO_2 for 1, 5, 7, 14, 21 and 28 days in 10xPBS (phosphate buffered saline) and then dried-air 24 hours into a fume hood. Average roughness was measured using 6 white light interferometry images per sample (18 samples). A total of 28 non-crosslinked and crosslinked optimized samples were mechanically characterized longitudinally and transversally. The samples were removed with a dog-bone cutting die (25 x 4 mm, test length x width) and tensile tested with a 100 N load cell and 1 mm/min test speed in order to determine the mechanical properties (Young's modulus, tensile strength and strain at break). Mean and standard error of the mean (Std. Error) were calculated for each structural and mechanical property.

RESULTS: This work revealed that an optimum electrospinning setup (Table 1) could create 2D PVA electrospun scaffolds with a tensile strength of 30 ± 1 MPa statistically comparable to the natural ligament (38 MPa [3]) and superior to maximum values reported during high impact activities [2].

Table 1: Optimum process and solution parameters.

Concentration	Voltage (kV)	Flow rate (ml/h)	Distance (mm)	rpm	Needle	Time
12%	20	1	80	2000	18 G	2 h

The topography of the optimized scaffolds remained unaltered after being exposed to 25% GTA and immersed in PBS for 28 days (Fig.1).

The scaffolds showed values of fibre diameter between 120 and 140 nm comparable to the values of the collagen fibrils in the extracellular matrix [4].

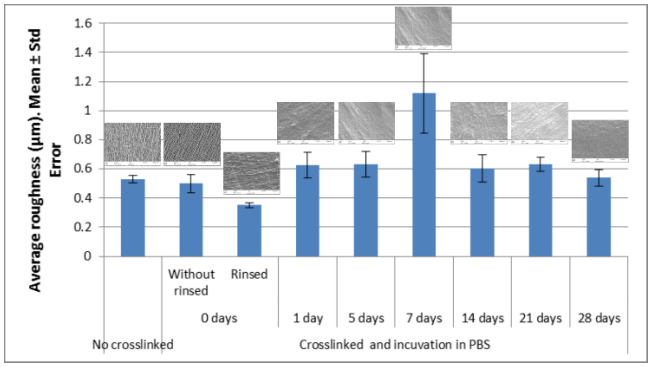

Fig. 1: Average roughness and degradation assay for samples exposed to 25% GTA (5kX SEM)

DISCUSSION & CONCLUSIONS: It was shown that 2D PVA electrospun scaffolds exhibited excellent mechanical morphological and topographical properties suitable for use in the manufacturing of ACL implants, and show potential for investigation as 3D PVA electrospun structures.

REFERENCES: [1] Roldán E. et al. *Procedia CIRP* 49, 133–138, 2016; [2] Roldán E. et al. *Gait Posture* 58, 201–207, 2017; [3] Noyes FR, Grood ES. *J.Bone & Joint Surg. Am.* 58, 1074–1082, 1976. [4] Shino K. et al. *Am. J. Sports Med.*, 23, 203–208, 1995.

ACKNOWLEDGEMENTS: This research was funded by the Faculty of Science & Engineering, Manchester Metropolitan University.

Testing emulsion templates as platforms for kidney tissue engineering

W Shanahan, A Callanan

Institute of Bioengineering, School of Engineering, University of Edinburgh, UK

INTRODUCTION: Chronic Kidney Disease (CKD) has a global prevalence of 10.6-13.4%[1]. Management options for those requiring renal replacement therapy are restricted to dialysis or organ transplantation; economically costly and resource limited treatments[2]. While promising strides have been made in the field of kidney tissue engineering to develop alternative therapies, there is much progress yet to be made[3]. Polymerised high internal phase emulsions (polyHIPEs) offer a hierarchically porous platform for the growth of cells and have recently been described as potential strategies for bone tissue engineering[4]. Herein we assess the use of variably porous polyHIPEs as a platform for renal tissue regeneration.

METHODS: The organic phase of the emulsion comprised of the monomer, 2-ethylhexyl acrylate (EHA); crosslinker, trimethylopropane triacrylate (TMPTA); surfactant, hypermer B246-SO-(MV); and photoinitiator, (2,4,6-trimethylbenzoyl)-phosphine oxide/2-hydroxy-2-methylpropiopheno ne , 50/50. Deionized water comprised the aqueous phase. Three different pore sizes were achieved by adding the aqueous phase dropwise to the organic phase under either low shear (medium pores, large pores), or high shear (small pores), at room temperature (small pores, medium pores) or 50°C (large pores). The emulsions were cured in petri dishes using a 3W UV lamp, and 10mm scaffolds punched out. These were sterilized in ethanol, seeded with rat primary renal cells and cultured over 9 days. Cell viability assay, DNA quantification, and fluorescence imaging were assessed at days three and nine.

RESULTS: Scanning electron microscopy (SEM) imaging was used to confirm pore sizes. Representative samples may be seen in figure 1 (A – C). Cell viability was highest at day 9 in the large pore scaffold as may be seen from the graph in figure 2. This scaffold also showed most DNA retention. Deepest cell penetration was however achieved in the medium sized pore scaffold, achieving a depth of approximately 120µm.

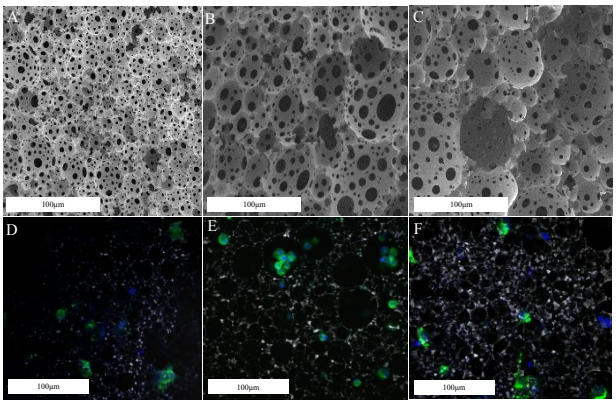

Fig. 1: SEM images of (A) Small pores, (B) Medium pores, (C) Large pores. (D), (E) & (F) show fluorescent images of cells within respective scaffolds stained with DAPI & phalloidin.

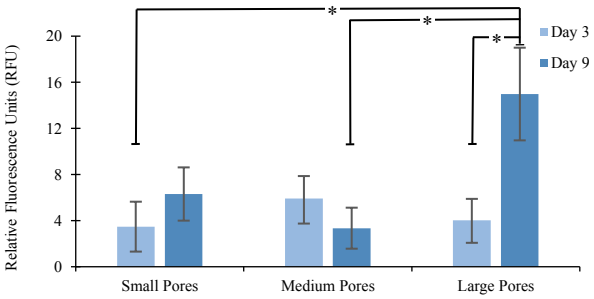

*Fig. 2: Cell viability results for scaffolds seeded with rat primary kidney cells. N=5. One way ANOVA with post hoc Tukey test, *P<0.05. Error bars indicate standard error of the mean.*

DISCUSSION & CONCLUSIONS: This work shows that polyHIPEs offer a viable platform for the growth of renal tissue *ex vivo*. Its success warrants further investigation into the use of polyHIPEs as scaffolds for kidney cells.

REFERENCES: [1]NR Hill, ST Fatoba, JL Oke et al (2016) *PLoS One* **11**:e0158765 [2] T Liyanage, T Nimomiya, V Jha, et al (2015) *Lancet* **385**:1975-1982 [3] S Yamanaka and T Yokoo (2015) *Stem Cells Int.* 724047 [4] R Owen, C Sherborne, T Paterson et al (2016) *J Mech Behav Biomed Mater* **54**:159-172.

ACKNOWLEDGEMENTS: Fluorescence imaging was kindly performed by Dr Alison McDonald.

The effect of activity levels on the function of the human knee: preliminary examination of data collected as part of an ongoing cell therapy clinical trial.

T Hopkins[1,2], JB Richardson[*], JM Williams[1,2], B Linklater-Jones[2], J Wales[2], S Roberts[1,2], JH Kuiper[1,2].
[1] The University of Keele, Stoke-on-trent, Staffordshire, UK. [2] The Robert Jones and Agnes Hunt Orthopaedic Hospital NHS Trust, Oswestry, Shropshire, UK. [*] Deceased.

INTRODUCTION: The recovery of knee function, quantified by patient-reported outcome measures, varies widely between patients following surgical intervention. One factor thought to play a part in this variability is the patient's activity levels[1]. However, the precise effect of activity levels on the reported function of the knee, particularly post-surgery, remains largely uncharacterised. This poses a problem for the clinical evaluation of knee function, as currently available validated scoring systems do not accurately take activity levels into account and are therefore prone to unwanted variation on a short-term basis. Also, a particular concern is that more active patients may load their knee more, potentially evoking more symptoms and paradoxically resulting in a lower functional outcome. Therefore understanding the relationship between knee function and activity levels may enable the creation of improved knee function scoring systems with an appreciation for different levels and types of activity. Here we report a preliminary analysis of activity and knee function data collected in an extensive rehabilitation diary as part of an on-going clinical trial of cell therapy.

METHODS: Data was collected from 27 patients (15♂, 12♀; mean age: 40±9.9) who were at least 15 months post a surgical procedure on the knee. The Lysholm Knee Scoring Scale is a 7-item knee function scoring system which is widely used in the evaluation of condition severity and intervention success[2]. The Human Activity Profile (HAP) is a 94-item, self-reported measure of energy expenditure and physical fitness[3]. The average activity score (AAS) was calculated from the HAP score. Lysholm score for the operated knee was collected alongside AAS data at baseline, 12 month and 15 months post-surgery. Pearson's product-moment correlation was used to investigate the three time points individually. Subsequently, the AAS and Lysholm data for each patient, at the three time points, as well as the confidence intervals for both the slope and intercept of the resulting lines, were plotted. The AAS data was then centered by subtracting the overall mean. Through multi-level modelling, individual patient lines were adjusted to take into account the average relationship across all patients, as well as the confidence intervals. The resulting lines were plotted.

RESULTS: There was a strong, positive Pearson correlation (r) between AAS and Lysholm score at all three time points for all 27 patients (figure 1). Increasing AAS was associated with increasing Lysholm score.

Table 1. Pearson product-moment correlation.

Timepoint	r	p
Baseline	0.729	0.000*
12 Month	0.751	0.000*
15 Month	0.724	0.000*

Our mixed models showed that the relationship between the AAS and Lysholm score data had significant variation between individual patients ($p<0.01$; examples of patient 1-6 shown in fig. 1). The mean of the slope, across all patients was found to be 0.258 ± 0.160SD ($p<0.0001$). Given that 95% of patients fall within the range ±1.96SD, this suggests that most patients have a positive relationship between activity level and knee function. However, for some, the relationship will be negatively correlated.

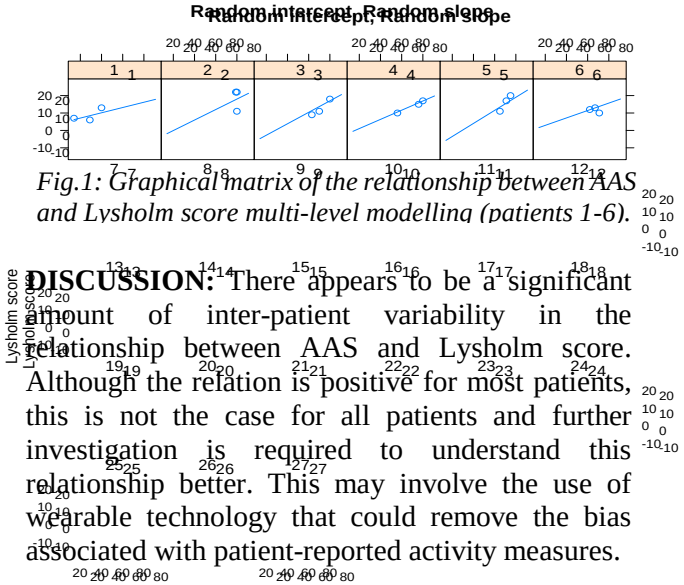

Fig.1: Graphical matrix of the relationship between AAS and Lysholm score multi-level modelling (patients 1-6).

DISCUSSION: There appears to be a significant amount of inter-patient variability in the relationship between AAS and Lysholm score. Although the relation is positive for most patients, this is not the case for all patients and further investigation is required to understand this relationship better. This may involve the use of wearable technology that could remove the bias associated with patient-reported activity measures.

REFERENCES: [1.] Urquart, D., Tobing, J., Hanna, F., Berry, P., Wluka, A., Ding, C. and Cicuttini, F. (2011). What Is the Effect of Physical Activity on the Knee Joint? *Medicine & Science in Sports & Exercise*, 43(3), pp.432-442.[2.] Collins, N., Misra, D., Felson, D., Crossley, K. and Roos, E. (2011). Measures of knee function. *Arthritis Care & Research*, 63(S11), pp.S208-S228.[3.] Davidson, M. and de Morton, N. (2007). A systematic review of the Human Activity Profile. *Clinical Rehabilitation*, 21(2), pp.151-162.

The effect of electrospun polycaprolactone fibre morphology on the function and behaviour of hepG2 cells

TSR Bate[1], SJ Forbes[2], A Callanan[1]

[1]*Institute for Bioengineering, School of Engineering, The University of Edinburgh, UK*
[2]*MRC Centre for Regenerative Medicine, The University of Edinburgh, Edinburgh BioQuarter, UK*

INTRODUCTION: Electrospinning techniques enable the fabrication of promising 3D polymer scaffolds for liver tissue engineering[1]. Highly tailorable nano-micro fibrous structures can be created that mimic the native extracellular matrix (ECM) microenvironment[2]. Electrospun fibre architecture has been shown to direct and influence cell growth and behaviour for neural, vascular and renal cell types but there is a current lack of similar published research concerning hepatic cell types[2–4]. This study is intended to highlight the effects of electrospun fibre morphology on the function and behaviour of hepatocytes and how scaffold architecture can be utilised in liver tissue engineering.

METHODS: Using previously described methods**,** scaffolds were fabricated from polycaprolactone (PCL) using electrospinning apparatus (IME Technologies) under various conditions to obtain small and large fibre diameters with differing architectures[2]. Briefly, randomly oriented fibres and aligned fibres were obtained by altering the mandrel rotation speed, 250RPM for random and 1800RPM for aligned. A cryogenic mandrel filled with dry ice (-70°C) was used to produce a highly porous fibre architecture via the deposition of ice crystals on the mandrel surface. Each architecture was fabricated for both small and large fibre diameters using 7w/v% PCL in HFIP for small fibres and 19w/v% PCL in Chloroform:Methanol (5:1) for large fibres. Scaffold architectures were characterised using Scanning Electron Microscopy (SEM), 2D FFT Image Analysis (MATLAB) and Tensile Testing (Instron 3367). HepG2 cells were cultured on scaffolds for 7 and 14 days and subsequently assessed for viability and function using biochemical, histological and gene expression analyses.

RESULTS: Mechanical characterisation shows variances in fibre diameter and young's modulus between scaffold groups. Cells are shown to proliferate over 7 and 14 days and trends in cell viability and DNA quantitation have been noted between groups. Moreover, histology shows details of cell attachment, morphology and distribution.

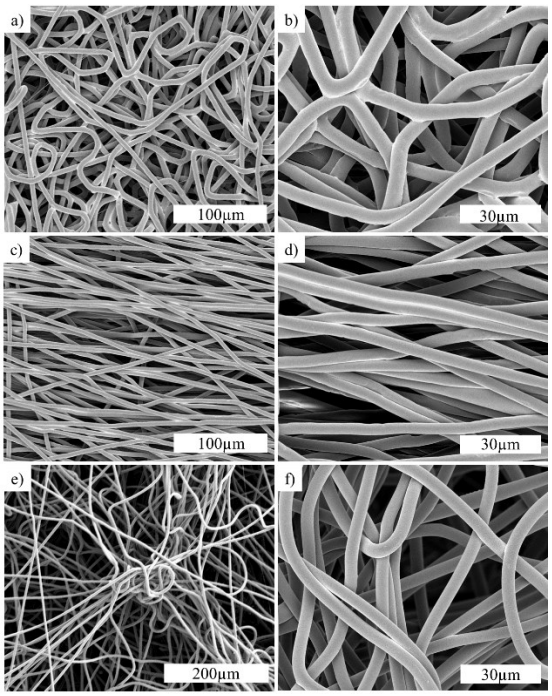

Fig. 1: SEM Images of scaffold morphologies: a)-b) Random fibre orientation, c)-d) Aligned fibre orientation, e)-f) Porous cryogenic fibres.

	Random	Aligned	Cryogenic
Fibre Diameter (µm)	5.40 ± 0.46	4.48 ± 0.27	4.70 ± 0.37
Young's Modulus (MPa)	6.33 ± 0.68	20.97 ± 0.83	1.15 ± 0.06

Table 1. Large fibre diameter and Young's modulus for each architecture at 0-10% Strain. N ≥ 5 presented as mean ± standard deviation.

DISCUSSION & CONCLUSIONS: Results show that PCL scaffold morphology influences hepG2 function and behaviour. These initial studies provide motivation for further investigation into electrospun fibre morphology and how it can be optimised to provide a niche environment for hepatocytes.

REFERENCES: [1]Grant, R., Hay, D. C. & Callanan, A. *Tissue Eng.* Part A **23**, 650–662 (2017). [2]Burton, T. P., Corcoran, A. & Callanan, A. *Biomed. Mater.* **13**, 15006 (2017). [3]Gupta, D. et al. *Acta Biomater.* **5**, 2560–2569 (2009). [4]Whited, B. M. & Rylander, M. N. *Biotechnol. Bioeng.* **111**, 184–195 (2014).

ACKNOWLEDGEMENTS: EPSRC grant EP/N509644/1 and MRC grant MR/L012766/1.

The effect of hypoxia on olfactory ensheathing cell cultures: implications for spinal cord repair

Bartlett RD[1,2,3*], Burley S[1,3*], Choi D[2,3], Phillips JB[3,4]

[1] *Biomaterials & Tissue Engineering, Eastman Dental Institute, UCL, England.* [2] *Brain Repair & Rehabilitation, Institute of Neurology, UCL, England.* [3] *Centre for Nerve Engineering, UCL.* [4] *Department of Pharmacology, School of Pharmacy, UCL, England. * indicates where authors contributed equally.*

INTRODUCTION: Olfactory ensheathing cells (OECs) represent a promising strategy to repair the damaged spinal cord [1]. However, following trauma, vasculature in the spinal cord becomes damaged, leading to local hypoxia. Hypoxia has been found to have a substantial effect on a number of other cell types used in regenerative medicine [2], yet the effect of low O_2 conditions on OECs remains poorly understood. This study investigated the effect of low oxygen conditions on OECs *in vitro*.

METHODS: Bulb OECs were extracted from Sprague-Dawley rats and cultured for 14 days. Cells were then incubated in either 1%, 5% or standard incubator O_2 conditions. The viability of cells was assessed using Syto 9 and propidium iodide live-dead staining, and morphological analysis was performed following immunostaining for $p75^{NTR}$ in monolayer culture.

RESULTS: Ambient O_2 levels as low as 1% did not significantly affect the survival of mixed OEC cultures up to 72 hours. Likewise, culturing OECs in low oxygen conditions did not appear to alter the composition of cultures, as the proportion of cells expressing $p75^{NTR}$ remained unchanged. However, quantitative analysis of $p75^{NTR}$ immunopositive cells revealed marked differences in cell morphology. Specifically, when cultured in low oxygen environments, $p75^{NTR}$ positive OECs had significantly smaller cell areas and perimeters than OECs cultured in standard incubator conditions. In 1% O_2, the density of filopodia extending from the cell membrane was also reduced to approximately half that found in standard incubator conditions.

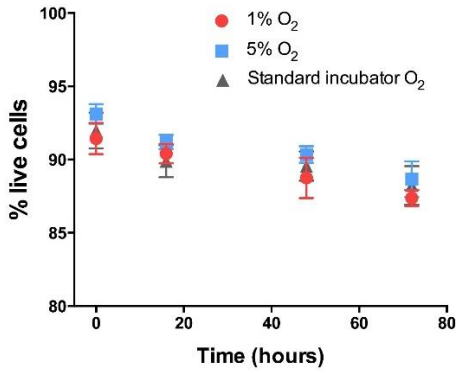

Fig. 1: Survival of OECs up to 72 hours in low oxygen environments. Mean ± SEM (n = 3, 3 and 6 for 1% O_2, 5% O_2 and standard incubator conditions, respectively). No significant differences between conditions at any time point as assessed by Kruskal-Wallis.

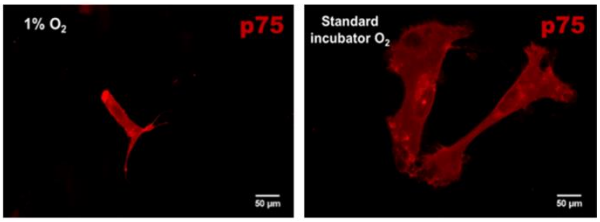

Fig. 2: Morphological differences between OECs cultured in 1% O_2 and standard incubator conditions at 72 hours.

DISCUSSION & CONCLUSIONS: The survival and proportion of OECs within mixed cultures does not appear to be significantly affected by low oxygen environments. However, the gross morphology of $p75^{NTR}$ cells was markedly altered and this corresponded to substantial differences in filopodia density. These data suggest that whilst OECs are likely to survive transplantation into hypoxic milieu, the ability of $p75^{NTR}$ positive cells to extend fine cellular processes may be significantly reduced in low oxygen environments. This could have important implications for the ability of OECs to direct neurite growth and guidance at the hypoxic spinal cord injury site.

REFERENCES: [1] R. Watzlawick et al. (2016) Olfactory ensheathing cell transplantation in experimental spinal cord injury: effect size and reporting bias of 62 experimental treatments: a systematic review and meta-analysis *PLoS Biol* **14**(5): e1002468. [2] E Blande et al (2013) Overcoming hypoxia to improve tissue-engineering approaches to regenerative medicine *J Tissue Eng Regen Med* **7**(7):505-14.

ACKNOWLEDGEMENTS: This work was kindly funded by the UCL MB/PhD programme, the Sackler Fund and the Wellcome Trust.

The effect of increasing dosage of atmospheric dielectric barrier plasma discharge (DBD) on the mechanical properties, surface chemistry and topography on electrically conductive electrospun PLCL/PANI biomaterials

GC Menagh[1], D Dixon[1], G Burke[1]

[1] *NIBEC, Ulster University, Belfast, Northern Ireland.*

INTRODUCTION: Plasma surface treatments such as DBD are routinely used to enhance cellular attachment and differentiation in tissue engineering.[1-3] Electrically conductive polymers have become increasingly important as a method of promoting cellular response and monitoring real-time cell culture in vitro.[4] Here we investigate the effects of increasing DBD plasma processing on the surface physical, mechanical and chemical properties of electrospun PLCL/PANi an electrically conductive polymer.

METHODS: Electrically conductive PLCL/PANi (4:1) composite polymer was manufactured from 10% w/w PLCL and 0.3% w/w PANi in chloroform/DMF solvent. Polymers were electrospun at 12 cm distance and 20kV to produce a randomly aligned 50µm disc. This was exposed to increasing dosages of DBD plasma up to 20 J/cm^2 under atmospheric conditions. After a 48-hour resting period, the samples were characterised using wettability analysis, SEM, Tensile Testing AFM, FTiR and XPS.

RESULTS: Randomly aligned, electroconductive electrospun PLCL/PANi matrices 50µm of thickness, with an average fibre diameter of 1.75µm were manufactured. The effect of the increasing DBD treatment caused a dose dependent statistically significant enhancement in their wettability until the point where surface melting was observed. SEM revealed a dose dependent beneficial change in fibre morphology and topography at low DBD dosages up to 10 J/cm^2. However, higher dosages above this caused polymer fibre fractures and surface melting changes to be observed. FTiR analysis following DBD plasma treatment showed no chemical changes to the bulk properties of the polymer. AFM showed alterations in the topography of the individual surface fibres (*Fig 1*). Chemical XPS analysis showed an increase in surface oxygenation in plasma treated samples a desirable quality in a cell culture biomaterial. Tensile testing was used in this study to firstly assess the effect of adding PANi to PLCL. Adding PANi causes a significant increase in Young's modulus and strength ($P < 0.05$) with no significant difference between the maximum load potentials between the two groups. Increasing plasma dosages on PLCL/PANi was also mechanically tested. A significant decrease Young's modulus and strength was noted on all DBD treated samples ($P < 0.05$), the samples also showed an increased maximal extension following DBD treatment.

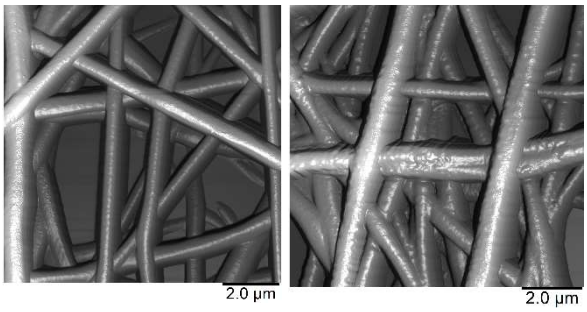

Fig. 1: AFM images of PLCL/PANi (L) and PLCL/PANi (R) DBD treated with 10 J/cm^2.

DISCUSSION & CONCLUSIONS: Electrically conductive polymers have many applications in tissue engineering. The problems associated with synthetic medical polymers are their inherent hydrophobicity and poor surface chemistry. The research presented here clearly shows that atmospheric DBD plasma treatment alters the surface topography to improve surface wettability. The addition of PANi to PLCL leads to the formation of stronger, stiffer fibre scaffolds with a similar maximum load potential. Despite DBD being a cold plasma technology thermal damage to the individual fibres was observed at higher DBD dosages. DBD treatment causes PLCL/PANi fibres to become more pliable at the cost of overall fibre strength. 10 J/cm^2 DBD treatment is the optimal DBD dosage to surface modify electrospun PLCL/PANi matrices balancing the need for improved surface wettability against polymer thermal degradation.

REFERENCES [1].Sorkio A, Porter PJ et al (2015) *Tissue Engineering Part A* 21:2301-14. [2]. D'Sa RA (2015) *J Mater Sci Mater Med* 26:260. [3] Wang M, Favi P, Cheng X, et al (2016) *Acta Biomater* 46:256-65. [4] Balint R, Cartmell SH. (2014). *Acta Biomater* 10:2341-53.

ACKNOWLEDGEMENTS: PhD Funding from Department for the Economy (DfE) Studentship (Northern Ireland)

The role of circadian clock genes in regulating the chondrogenic potential of human pluripotent stem cells

M.A Naven[1] QJ Meng[1] S.J Kimber[1]

[1] *Division of Cell Matrix Biology & Regenerative Medicine, University of Manchester, Manchester, M13 9PT, UK*

INTRODUCTION: Osteoarthritis (OA) is a common joint disease causing severe pain, joint deformity and loss of mobility. A common feature of OA is the loss of articular cartilage and chondrocytes. A future regenerative therapy for OA treatment may involve the transplantation of chondrogenic cells derived from differentiation of human embryonic stem cells (hESCs). In murine cartilage the cell autonomous circadian molecular clock has been implicated in cartilage homeostasis [(1)]. hESC appear to lack this circadian rhythm and it is still largely unknown how it is first activated [(2)]. The timing of this activation and the genes activated during chondrogenic differentiation may provide novel niche factors for differentiation and inform potential future OA chronotherapies.

METHODS: Human embryonic stem cells were directed towards a chondrogenic linage *in vitro* using a combination of growth factors and small molecules [(3)]. These cells were further cultured in 3D pellet culture yielding an extracellular matrix structure with histological features associated with cartilage (Figure 1). Bioluminescent image analysis using the reporter Per2::Luciferase was used to investigate the activation of cell intrinsic circadian rhythm.

RESULTS: Pilot data suggests that during chondrogenic directed differentiation of human embryonic stem cells that cell intrinsic circadian rhythm may be activated. Rhythm was found after 14 days 2D differentiation and 28 days of 3D differentiation.

DISCUSSION & CONCLUSIONS: The emergence of cell intrinsic molecular clocks during chondrogenic differentiation suggests that this model may be used to investigate the mechanisms leading to the emergence of circadian rhythm. In addition, the affects of modulation of circadian rhythm on the extracellular structure may be used to investigate potential OA chronotherapies.

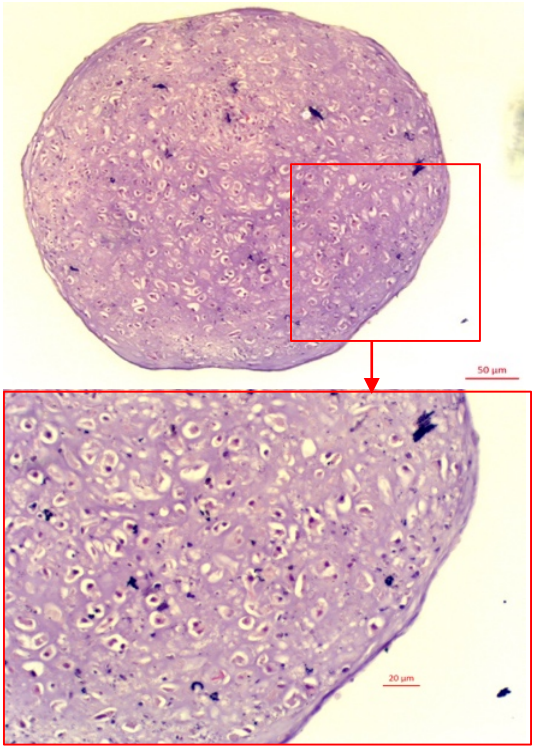

Fig. 1: Histological analysis using Haematoxylin and Eosin staining of a 3D chondrogenic pellet.

REFERENCES: **(1)** Gossan N, Zeef L, Hensman J, Hughes A, Bateman JF, Rowley L, Little, CB, Piggins HD, Rattray M, Boot-Handford RP, Meng QJ (2013). The circadian clock in chondrocytes regulates genes controlling key aspects of cartilage homeostasis. Arthritis and Rheumatism; Epub ahead of print. **(2)** P. Dierickx, M.W. Vermunt, M.J. Muraro, M.P. Creyghton, P.A. Doevendans, A. van Oudenaarden, N. Geijsen, L.W. Van Laake. (2017) Circadian networks in human embryonic stem cell-derived cardiomyocytes EMBO Rep., 18 (2017), pp. 1199-1212 **(3)** Cheng A, Kapacee Z, Peng J. Lucas R, Lu S, Lucas R, Hardingham TE & Kimber SJ (2014) Cartilage Repair Using Human Embryonic Stem Cell-derived Chondroprogenitors. Stem cell Translational Medicine (Oct). (2014). Cartilage Repair Using Human Embryonic Stem Cell-derived Chondroprogenitors. Stem Cells Translational Medicine. 3, 1287-1294.

ACKNOWLEDGEMENTS: Thank you to Kazuhiro Yagita for kindly providing the bioluminescent reporter construct.

Tissue-derived ECM hydrogels for peripheral nerve repair

S C Kellaway[1,2], J B Phillips[1], L J White[2]

[1]*UCL Centre for Nerve Engineering, UCL School of Pharmacy, London, England.* [2]*Division of Regenerative Medicine and Cellular Therapies, University of Nottingham, Nottingham, England.*

INTRODUCTION: Injury to peripheral nerves can be debilitating and poses a challenging problem. The current gold standard for repair of a large gap is a nerve autograft; a procedure that can cause donor site morbidity and is of limited availability. Engineered neural tissue (EngNT) can promote axonal regeneration across critical sized defects [1], however, as the conduit uses collagen I for its base material, the regenerative capacity may be improved with the use of a decellularized matrix. Decellularized scaffolds have been reviewed extensively [2]. We hypothesise that biologic scaffolds, with their potential to be immunomodulatory, will provide a pro-regenerative environment when implemented in EngNT. Herein we provide a portfolio of five biochemically and mechanically characterized ECM candidates to be screened for their suitability for use in EngNT.

METHODS:

Decellularization was confirmed via dsDNA quantification of known sample weights using a Quant-iT™ PicoGreen dsDNA assay (Invitrogen, Paisley, UK). Total glycosaminoglycan (GAG) content was measured using a dimethylmethylene blue assay.

Rheological characterization was carried out using a parallel plate rheometer (Anthon Paar, Hertford, UK). Gelation kinetic profiles for 8 $mgml^{-1}$ were produced by bringing pre-gel solutions to physiological pH and temperature and measuring the storage and loss modulus over time at a constant frequency and amplitude.

RESULTS: Bone ECM (B-ECM) had the lowest dsDNA content whereas the small intestinal submucosa ECM (SIS-ECM) had the highest (Figure 1A). Similarly, B-ECM also had the lowest GAG content (Figure 2) whereas SIS-ECM had the highest.

Gelation kinetics were measured using a parallel plate rheometer, inducing gelation and measuring storage and loss moduli over time (Figure 2). The B-ECM hydrogel took the least time to show solid-like behaviour and was the only material to exhibit a sigmoidal gelation profile. The liver ECM (LIV-ECM) gel was the stiffest, whilst the urinary bladder ECM (UBM-ECM) was the softest hydrogel.

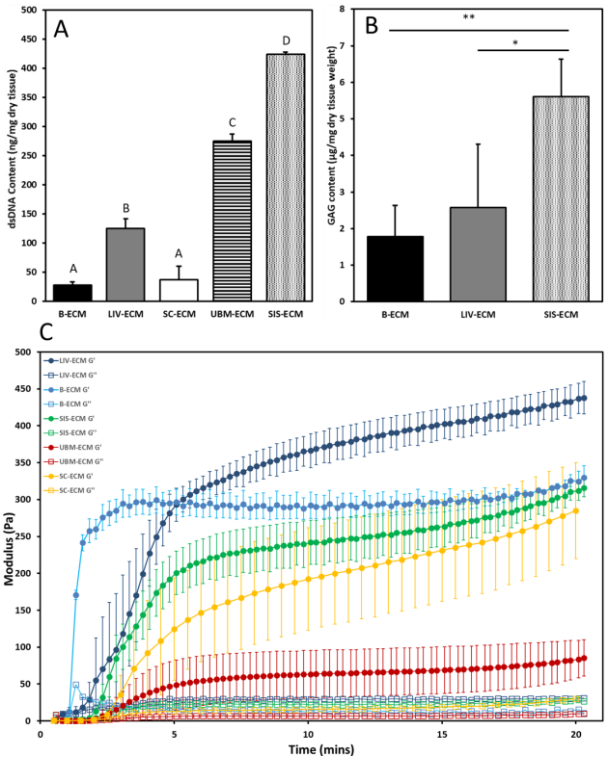

Fig. 1: dsDNA content [A], total GAG content [B] and gelation kinetics for 8mg/ml ECM gels [C]

DISCUSSION & CONCLUSIONS: We have created a portfolio of biochemically and mechanically characterized decellularized ECM that can be explored for nerve tissue engineering.

It is essential to achieve a balance in removal of antigens and the retention of biologically active soluble factors; although B-ECM has the lowest dsDNA content, it also possesses a lower GAG content. The biochemical and mechanical properties differ between the materials, providing a means to influence cellular behavior, both of implanted cells and those in the surrounding tissue. The characterization performed in this study will underpin future work to screen ECM hydrogels for their potential to be used in EngNT.

REFERENCES: [1] M. Georgiou et al. (2013) Engineered neural tissue for peripheral nerve repair, *Biomaterials*, **34**(30): 7335-7343. [2] P.M.Crapo, T.W. Gilbert and S. F. Badylak (2011) An overview of tissue and whole organ decellularization, *Biomaterials*, **32**(12): 3233–3243.

ACKNOWLEDGEMENTS: The EPSRC funded this research. Project code: EP/L01646X

Tissue-engineered blood vessels with user-defined geometries

S Pashneh-Tala[1], C Sherborne[1], R Owen[2], F Claeyssens[1]

[1] Kroto Research Institute, Materials Science and Engineering Department, The University of Sheffield, UK. [2] INSIGNEO Institute for In Silico Medicine, Materials Science and Engineering Department, The University of Sheffield, UK

INTRODUCTION: A great need exists for blood vessels for use as vascular grafts in the treatment of cardiovascular disease. Autologous vessels are of limited availability and quality and their harvest is invasive. Synthetic vascular grafts are prone to thrombosis and infection. A tissue-engineered blood vessel, able to grow, remodel and repair in vivo, offers an attractive solution to vascular grafting. Additionally, natural vasculature is composed of complex geometries (tapers and bifurcations) and it is known that the geometry of the vascular constructs created during surgery has a strong influence on their performance. The ability to generate tissue-engineered blood vessels with varied geometries would therefore be of great potential benefit. The aim of this research was to develop a tissue-engineered blood vessel that may be produced in various geometries relevant to natural vasculature.

METHODS: A photocurable polymer, poly(glycerol sebacate) methacrylate (PGS-M) was developed for use as a scaffold material to support the growth of the tissue-engineered blood vessels. PGS-M is highly elastic, degrades rapidly and displays excellent cytocompatibility [1]. Porous PGS M scaffolds of various geometries, including tapers, bends and bifurcations, were produced. These scaffolds were seeded with vascular smooth muscle cells and cultured in a bespoke, pulsatile flow, bioreactor which provided mechanical stimulation to the developing constructs.

RESULTS: The porous PGS-M scaffolds displayed significant cell penetration (~300 µm) following seeding. Bioreactor culture generated vessels with cellular organisation similar to natural vasculature and an extracellular matrix of collagen and elastin. Dynamic culture under pulsatile flow increased vessel elastin content, compared to static culture, after only 7 days.

DISCUSSION & CONCLUSIONS: Porous PGS-M scaffolds, of various geometries, seeded with vascular smooth muscle cells and cultured under dynamic conditions produce blood vessel tissue *in vitro*. Dynamic culture enhanced ECM deposition, as seen in previous reports [2-3]. This method may be used to produce tissue-engineered vascular grafts of various sizes and shapes for stratified applications or with user defined geometries for tailored clinical solutions.

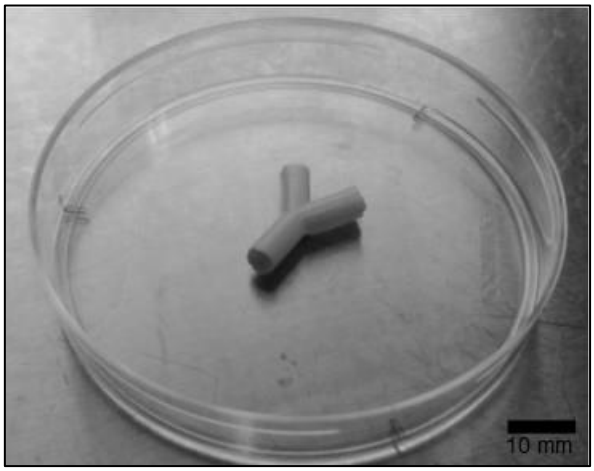

Fig. 1: Bifurcated tissue-engineered blood vessel.

REFERENCES: [1] S. Pashneh-Tala, R. Owen, H. Bahmaee, et al (2018*) Front Phys* **6**: 41. [2] K. Lee, D.B. Stolz, and Y. Wang (2011) *Proc. Natl. Acad. Sci.* **108**: 2705-2710. [3] L. Niklason, J. Gao, W.M. Abbott, et al (1999) Science **284**: 489-493.

ACKNOWLEDGEMENTS: We are grateful to the EPSRC and MRC for supporting this research.

Towards a mathematical model to predict the influence of therapeutic cell distribution on VEGF gradients for the promotion of vasculogenesis *in vitro*

GF Al-Badri[1,2], JB Phillips[2,3], RJ Shipley[2,4], NC Ovenden[1,2]

[1] Department of Mathematics, UCL, UK [2] Centre for Nerve Engineering, UCL, UK [3] Department of Pharmacology, UCL School of Pharmacy, UK [4] Department of Mechanical Engineering, UCL, UK

INTRODUCTION: Accelerated vascularisation of clinically-viable engineered tissues is essential for the survival and function of vital therapeutic cells once implanted *in vivo*, which may otherwise lack sufficient oxygen and nutrients [1]. Pre-vascularisation by the inclusion of endothelial cells (ECs) that form capillary-like structures *in vitro* is one such promising method [1]. Here, we use mathematical and computational modelling to investigate interactions between VEGF-producing therapeutic cells, in this case Schwann cells (SCs) for peripheral nerve repair, and endothelial cells during *in vitro* culture, with a focus on resulting VEGF gradients which guide EC migration and promote vascular network formation [2, 3].

METHODS: Coupled partial differential equations (PDEs) were used to describe the time and spatial development of the Schwann cell density, endothelial cell density, and VEGF concentration. Interaction terms include uptake and production of VEGF by ECs and SCs respectively, and chemotaxis, whereby ECs migrate towards a positive VEGF gradient. The model was parameterised using existing values from literature including cellular and VEGF diffusion, and VEGF degradation [4], alongside parameters determined by previously obtained experimental data for the production of VEGF by SCs.

The equations were discretised on 200x200 grid representing a 2.5x2.5mm square, and were solved using second order finite differences in Python, considering a timescale of 48h (scaled to t=1). We apply no flux boundary conditions representative of *in vitro* culture in a dish or mould, and consider an initially uniform distribution of ECs and VEGF.

RESULTS: Computational simulation results demonstrate VEGF gradients resulting from co-culture of ECs with VEGF-producing therapeutic cells. We further demonstrate dependence of these gradients on the initial Schwann cell density distribution as well as key parameters in the model, which can be utilised to influence the resulting EC distribution. Figures 1c and 1d demonstrate the effect such gradients may have on EC connectivity, illustrated by cluster size, which can lead to more effective vascularisation.

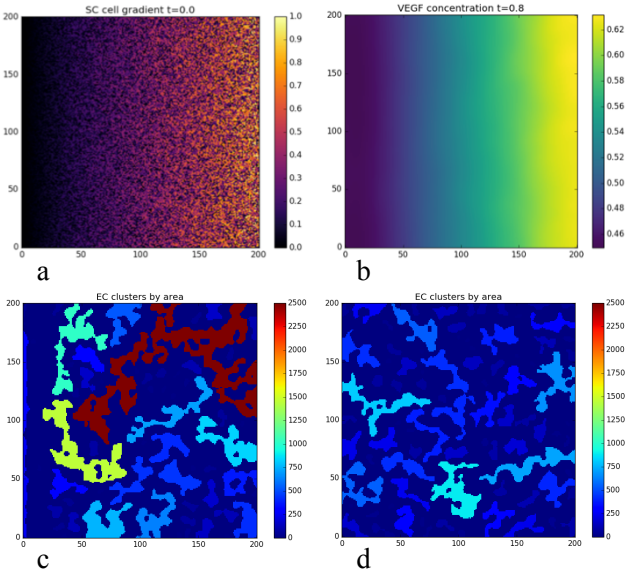

Fig. 1: a) Initial Schwann cell distribution used in plots (b) and (c), b) VEGF gradient at t=0.8, c) Clusters in EC distribution at t=0.8 labelled by cluster area (total no. of grid points), d) Clusters in EC distribution at t=0.8 when a uniform initial Schwann cell distribution is used.

DISCUSSION & CONCLUSIONS: Further development of the PDE model will allow us to consider optimum co-culture densities and cell distributions for effective pre-vascularisation of engineered tissue constructs. This model is easily adapted to other therapeutic cells, with few parameters to be determined particular to each cell type by a short experiment set.

REFERENCES: [1] J. Rouwkema and A. Khademhosseini (2016) *Trends in Biotechnology* **34**(9):733–745. [2] I. Barkefors et al (2008) *Journal of Biological Chemistry* **283**(20):13905-13912. [3] J.E. Leslie-Barbick et al (2009) *Journal of Biomaterials Science* **20**(12): 1763-1779. [4] M.J. Holmes and B. D. Sleeman (2000) *Journal of theoretical biology* **202**(2):95-112.

ACKNOWLEDGEMENTS: This work was supported by an EPSRC studentship EP/R512400/1 to GFAB. RJS gratefully acknowledges funding from EPSRC (EP/R004463/1, EP/N033493/1).

Transient immobilisation and release of nerve growth factor in a modified heparin / allylamine surface to promote neurite outgrowth

AM Sandoval-Castellanos[1], JW Haycock[1]

[1] *Department of Materials Science and Engineering. The University of Sheffield, U.K.*

INTRODUCTION: Peripheral nerve injury is a major cause of disability, which impacts on the quality life of 1 in 1000 patients every year. Nerve autografts remain the gold standard, but this approach has major limitations, with implantable conduits a potential alternative. However, current devices do not support sufficient regeneration in practice. Modifications to the nerve guide biomaterial can address this, where surface functionalization is a promising approach to stimulate neurite growth. The aim of the present study considered an allylamine surface modification to bind a heparin layer, which could be used to bind nerve growth factor (NGF) for stimulating neurite formation upon contact.

METHODS: Surfaces were modified by allylamine plasma deposition and then exposed to heparin binding. Contact angle was performed to characterise the modified surface of allylamine and heparin. Concentrations of 5, 10, 20 and 40 ng/mL NFG were passively bound to the surface and NG108-15 neuronal cells cultured on active surfaces for 3 and 5 days in serum free medium. β-III tubulin immunolabeling was performed to identify neuronal cells. Differentiation was assessed by measuring the length and proportion of neuron bearing neurites. Metabolic activity was evaluated by a Resorcinol assay.

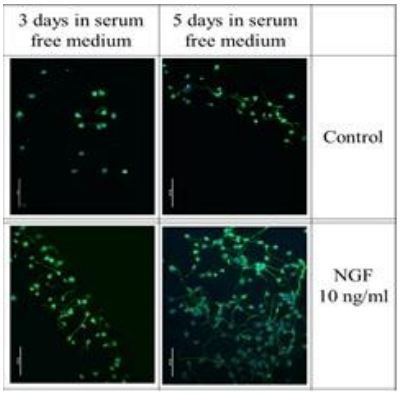

Fig. 1: Development of neurites in NG108-15 neuronal cells with no NGF and NGF 10 ng/mL. Scale bar 50 µm.

RESULTS: At day 3, surfaces with NGF 10 ng/mL and NGF 20 ng/mL supported 19.9 µm (17% of neurons bearing neurites) and 23.3 µm (22% neuron bearing neurites). NGF 40 ng/mL supported neuronal neurite lengths of 35.0µm, representing 26% of neurons bearing neurites. However, at day 5 neurite length was of 63.7 µm, 67.7 µm and 51.7 µm respectively. The percentage of neurons bearing neurites was 62%, 81% and 36%. Moreover, metabolic activity showed that by day 5 NGF 10 ng/mL was highest. Figure 1 shows the comparison of developing neurites of NG108-15 neuronal cells with no NGF and NGF 10 ng/mL in 3 and 5 days in serum free media.

DISCUSSION & CONCLUSIONS: The results suggested that NGF used between 10 ng/mL and 20 ng/mL could promote the rapid assembly of microtubules as assessed by neurite length and proportion *in vitro.* This can be extrapolated to stimulating neurite growth for reconnecting target neurons following injury. Moreover, the metabolic activity indicated that the NGF concentrations used increased cell viability up to limited concentration and seeding time. This work will be extended to rodent PC12 cells and then primary neurons for exploring the response to surface activation of biomaterial scaffolds. The results obtained from this project are encouraging for applying this technology to nerve guide conduit development.

REFERENCES: [1]X. Gu, F. Ding, Y. Yang and J. Liu, "Construction of tissue engineered nerve grafts and their application in peripheral nerve regeneration," *Progress in Neurobiology,* vol. 93, no. 2, pp. 204-230, 2011. [2]S. Bhang, T. Lee, H. Yang, W. La, A. Han, Y. Kwon and B. Kim, "Enhanced nerve growth factor efficiency in neural cell culture by immobilization on the culture substrate," *Biochemical and Biophysical Research Communications,* vol. 382, no. 2, pp. 315-320, 2009. [3]Crawford-Corrie A, Buttle DJ & Haycock JW. (2017) Medical Implant. WO2017017425A1.

ACKNOWLEDGEMENTS: The authors would like to thank to CONACYT for their financial support to develop this project.

Using adipose-derived stromal cells and tissue to induce vascularization and soft tissue wound healing

A. Penuelas Alvarez[1], J. Shepherd [2], V. Hearnden[1]

[1] *Department of Material Science and Engineering, The University of Sheffield, United Kingdom.*

[2] *School of Clinical Dentistry, The University of Sheffield, United Kingdom*

INTRODUCTION: Although different skin engineering strategies have been developed to help wound healing, crucial obstacles such as vascularization have yet to be overcome. Fat-derived stromal cells have been shown to aid in wound healing through their ability to drive angiogenesis, increase protein production, and reduce inflammation. In addition, there are theories that suggest that the regenerative potential from adipose tissue and its stromal cells come from their derived secreted products. In this work, we tested and compared the vascularization properties of human adipose tissue, cultured adipose-derived stromal cells as well as conditioned media from adipose tissue and adipose derived stromal cells.

METHODS: Adipose-derived stromal cells (ADSC) were isolated using enzymatic digestion and adherence culture. In order to test the effect of secreted factors from adipose tissue and ADSC, condition media was used. Conditioned media from adipose tissue and cultured ADSC were obtained after 3 days of culture. Chicken Embryo Chorioallantoic Membrane assay (CAM assay) was performed to observe at new blood vessel formation from adipose tissue, its stem cells, and their conditioned media in an *in vivo* model. The chick aortic ring assay was used to study tubular structure formation promoted by conditioned media from adipose tissue and ADSC.

RESULTS AND DISCUSION: Conditioned media from ADSC showed a small but non-significant increase in blood vessel formation on the CAM assay (Fig 1). In contrast the conditioned media from adipose tissue showed no increase in vessel formation compared to media alone. In the aortic ring assay there was no clear trend seen between the three conditions (Fig 2). After analysing CAM and aortic ring assay results, the number of ADSCs cultured and the volume of fat used for conditioned media will be adjusted to further test the angiogenic capacity of secreted factors from adipose products.

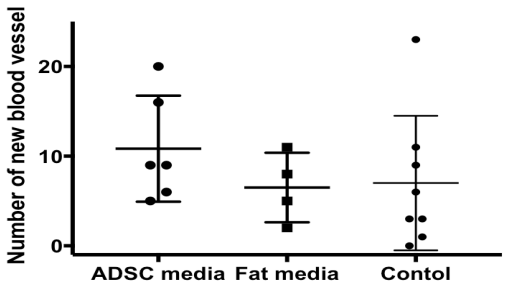

Fig. 1 Number of new blood vessels on CAM assay between day 7 and 10 using conditioned media from ADSC and adipose tissue.

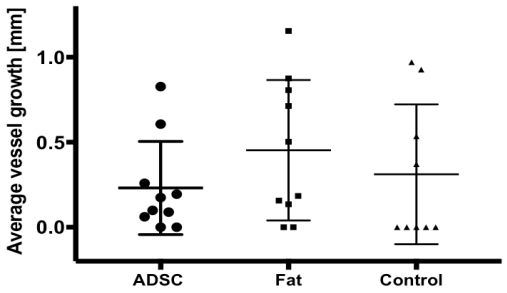

Fig. 2. Average length of vessels sprouting on aortic ring assay following treatment with ADSC and fat conditioned media.

CONCLUSIONS: ADSCs have previously been shown to be a promising tool for regenerative medicine since they enhance wound healing however there are relatively few *in vitro* studies investigating whole fat. While no significant differences have been observed to date the CAM and aortic ring assays were found to be suitable assays to study angiogenesis in a biologically relevant way.

ACKNOWLEDGEMENTS: This work is supported by Consejo Nacional de Ciencia y Tecnología (CONACYT) and the University of Sheffield.

Using advanced 3D engineered cell cultures to investigate drug synergy in promoting peripheral nerve regeneration.

MLD Rayner[1, 2], J Healy[1, 2] and JB Phillips[1, 2].

[1] *School of Pharmacy, UCL, London, UK.* [2], *Centre for Nerve Engineering, UCL, London, UK.*

INTRODUCTION: Peripheral nerve injuries (PNI) are associated with unsatisfactory clinical recovery due to the poor regeneration capacity of neurons *(1)*. Currently the gold standard treatment options are microsurgical with no drug therapies available. In recent years advancements have been made in the identification of small molecules which target the complex cascade of signalling pathways that are activated following injury. There has been particular focus on the inhibitory Rho/ROCK signalling pathway, as its activation blocks neuron outgrowth. Therefore, drug candidates that inhibit this pathway are potential novel therapies for PNI as they act to promote neuron outgrowth.

Drug synergy aims to increase the total drug efficacy eliciting a greater effect than if either drug was given alone. Combination therapies have shown some promise in PNI, however, this needs to be explored further before moving therapies towards clinical translation *(2, 3)*.

Engineered neural tissue (EngNT) supports the regeneration of neurons within an aligned 3D Schwann cell-seeded collagen gel environment. The aim of this study was to use this model to explore the synergy effects of small molecules targeting the Rho/ROCK pathway on neuron regeneration.

METHODS: Small molecules targeting the Rho/ROCK pathway were identified using cheminformatics and screened using an *in vitro* PNI model. This model was a 3D EngNT co-culture prepared by tethering 1 mL of solution containing; 80% Type I rat tail collagen, 10% 10x MEM, 5.8% neutralising solution and 4.2% Schwann cell suspension, within rectangular moulds to facilitate cellular self-alignment. After 24h incubation at 37 °C, the aligned cellular gels were stabilised using plastic compression and PC12 neurons were seeded onto the surface. Co-cultures were subjected to drug treatments for 72h before fixing. Neurites were visualised using βIII-Tubulin immunoreactivity and fluorescence microscopy. Neurite growth was quantified by measuring neurite length using ImageJ software.

RESULTS: Drug synergism was tested by combining ibuprofen (NSAID/PPAR-γ agonist) and fasudil (ROCK inhibitor), selected due to their different mechanisms of action on the Rho/ROCK pathway. It was found that the drugs in combination elicited a greater increase in neurite growth (71.1%) *c.f.* either drug given alone (ibuprofen: 52.2%, fasudil: 27.2%) or with no drug treatment (Figure 1).

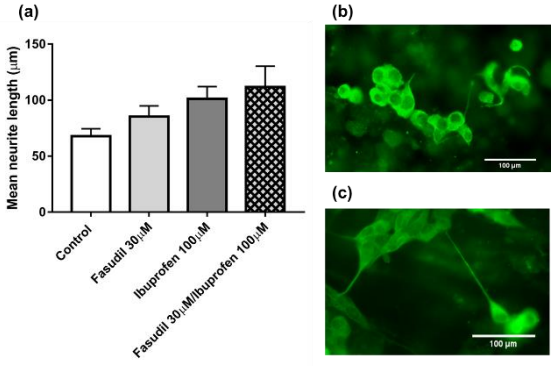

Figure 1: Dual treatment with 100 μM ibuprofen and 30 μM fasudil *elicited a synergistic effect on neurite growth in the 3D EngNT co-culture* (a). *Fluorescence micrographs with no drug treatment (b) and with dual treatment of* ibuprofen and fasudil *(c). N=6 of co-culture gels, mean ± SEM.*

DISCUSSION & CONCLUSIONS: The dual treatment of fasudil and ibuprofen resulted in a substantial increase of neurite length compared to either drug given alone. This echoed the result previously published by *Hou et al., (2015)* in which fasudil and celecoxib improved recovery following a spinal cord injury. Drug synergy provides an exciting new area for drug development, as the combination therapy could treat multiple aspects of PNI such as neural viability, nerve regeneration and neuropathic pain.

REFERENCES: 1. Hoke A, Brushart T. Introduction to special issue: Challenges and opportunities for regeneration in the peripheral nervous system. Experimental neurology. 2010;223(1):1-4. **2**. Duan W, Que L, Lv X, Li Q, Yin H, Zhang L. Tolerance of neurite outgrowth to Rho kinase inhibitors decreased by cyclooxygenase-2 inhibitor. Neural regeneration research. 2012;7(34):2705-12. **3**. Hou XL, Chen Y, Yin H, Duan WG. Combination of fasudil and celecoxib promotes the recovery of injured spinal cord in rats better than celecoxib or fasudil alone. Neural regeneration research. 2015;10(11):1836-40.

ACKNOWLEDGEMENTS: This research was made possible through the support and funding of the EPSRC (Grant EP/L01646X).

Using electrospun bilayer scaffolds to tissue engineer the annulus fibrosis

A.H. Shamsah[1], S.M. Richardson[2], S.H. Cartmell[1], L.A. Bosworth[1,3]

[1]School of Materials, Faculty of Science and Engineering, University of Manchester; [2]School of Biological Science, Faculty of Biology, Medicine and Health, University of Manchester; [3]Institute of Ageing and Chronic Disease, University of Liverpool

INTRODUCTION: Regeneration of the Annulus Fibrosis (AF) could provide a new treatment for degenerate intervertebral discs. However, it is a challenging task because of the remarkable complexity of AF tissue and tissue-engineered constructs must ensure they mimic the cellular and structural features of native AF tissue[1]. The AF is principally composed of collagen fibre lamellae with orientated fibres alternating ±30° to the sagittal plane. This structural arrangement is crucial for their mechanical function[1]. Our previous work demonstrated aligned, bilayer electrospun fibrous scaffolds (±30°) prepared from a 50:50 blend of polycaprolactone (PCL) and poly L-lactic acid (PLLA) closely mimicked the architecture and mechanical properties of AF tissue. In this study, we investigated the effect of bovine AF cells seeded on ±30° bilayer fibre scaffolds in terms of morphology and mechanical properties.

METHODS: A 50:50 solution of PCL:PLLA was electrospun as previously described[1]. Bovine AF cells were seeded (1x10^5 cells/cm^2) on scaffolds with fibres orientated 30° relative to the vertical and cultured at 37°C, 5%CO_2 for 5 days. Cell-seeded sheets were then assembled to create bilayer scaffolds, where cells were in direct contact with each other and fibre orientation was ±30° relative to the vertical. Bilayer scaffolds were subsequently cultured for 14 days. Confocal imaging determined cell morphology (phalloidin) and fibre orientation (rhodamine) (n=2). Tensile testing (5N load cell, 0.1% strain rate) with comparison to acellular bilayer scaffolds was performed under wet conditions (n=5). Statistical analysis using one-way Anova with Tukey's multiple comparison tests and 95% confidence level was applied.

RESULTS: Confocal microscopy clearly demonstrated the ±30° fibre orientations in bilayer scaffolds (Fig.1a). Cells were evident within the bilayer scaffold and exhibited alignment in both ±30° fibre directions after 7 days (Fig.1b). Cell-seeded bilayer scaffolds had a positive effect on tensile properties, becoming significantly stiffer (85±7MPa) and stronger (8±0.6MPa) over time when compared to acellular constructs (Fig.1C).

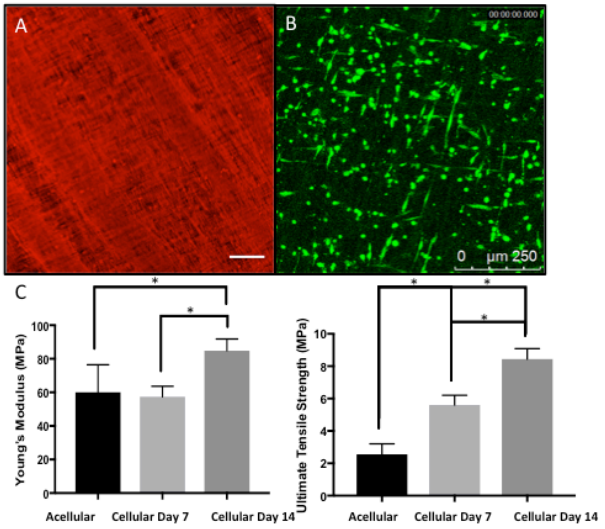

*Fig. 1: Confocal images of (A) rhodamine stained bilayer scaffolds with ±30° fibre directions (scale = 50µm), (B) alignment of phalloidin stained annulus fibrosis cells after 7 days (scale = 250µm), (C) Young's Modulus and tensile strength data for bilayer cellular and acellular scaffolds. Data expressed as mean ± SD (*p<0.05).*

DISCUSSION & CONCLUSIONS: Electrospun fibres are known to infer contact guidance cues to cells and influence their alignment[2]. Our results demonstrate the ability of producing bilayer electrospun scaffolds with ±30° fibre orientation that continue to influence and guide alignment of AF cells. Furthermore, culture of AF cells within bilayer scaffolds over a two-week period resulted in significant improvements in mechanical properties, which are within the range for human AF lamella[3] (Modulus: 59-136MPa and tensile strength: 4-10MPa). This study presents a step closer towards successful tissue engineering and regeneration of the annulus fibrosis.

REFERENCES:[1]Shamsah, A., et al. Mimicking the annulus fibrosus with electrospun nanofibre scaffolds. European Cells and Materials, **32,** 2262, 2016. [2]Nerurkar, N.L., et al. Mechanics of oriented electrospun nanofibrous scaffolds for annulus fibrosus tissue engineering. *J. Orthop. Res.* **25,** 1018–1028, 2007. [3]Skaggs, D.L., et al. Regional variation in tensile properties and biochemical composition of the human lumbar anulus fibrosus. *Spine.* **19,** 1310–1319, 1994.

ACKNOWLEDGEMENTS: The scholarship institution in Kuwait for their funds.

Using *in vitro*, bioengineered models of skeletal muscle to investigate treatment modalities for OA

K Aguilar-Agon[1], MP Lewis[1], A Capel[1], N Martin[1], D Player[2]

[1]School of Sport, Exercise and Health Sciences, Loughborough University, Loughborough [2] Institute of Orthopaedics and Musculoskeletal Science, University of College London, Stanmore.

INTRODUCTION: *In vitro* tissue engineered skeletal muscle resembles some of the characteristics of native skeletal muscles function and structure, allowing myogenic cells to proliferate, fuse, arrange in 3-dimensions (3D) and differentiate into functional myotubes. Therefore, providing highly accurate models of myogenesis and testing therapies for muscle wasting diseases. The model described emulates *in vivo* like native human skeletal muscle, using C2C12 myoblasts, embedded within a collagen matrix. Therefore, the model will be used to develop the most hypertrophic mechanical overload regime possible. Thereafter, this regime will be used to try to reverse myotube atrophy *in vitro*.

METHODS: The protocol for the construction of C2C12 populated collagen constructs was based upon previously published protocols [1-2]. Following 14 days of culture, constructs floated in differentiation media were mechanically loaded using a mechanical stimulation bioreactor (MSB), programmed to apply mechanical strain to several constructs, using a floatation bar attached to two pins mounted to a stepper motor (Parker, USA). The mechanical stimulus was varied by altering the amount of strain applied to each construct.
Biological repeats of each ramp load protocol using the 50µl constructs were carried out where constructs were either subject to no load (control (CON)) (n=3), 10% (n=2), 15% (n=2) and 20% (n=3) ramp mechanical load for 60 minutes, followed by a 2 hour static stretch at the desired stretch length (%). Additionally, biological repeats of each ramp load protocol described above, using also the 50µl constructs were also carried out, whereby constructs were either sampled immediately (n=2), 21 (n=2) or 45 hours(n=3) following experimentation for RNA extraction.

RESULTS: Immediately following ramp loading, 10 % and 15% stretch significantly increased IGF-1 mRNA compared to CON. MMP-2 mRNA significantly increased in both 10% and 15% strain compared to CON ($p<0.05$), whilst MMP-9 mRNA increased at both 10% and 15% stretch compared to CON, it was not significant ($p=0.1$). No significant changes were observed when looking specifically at the atrophic genes MAFbx and MuRF-1 following ramp load. Significant increases in IGF-1, MMP-2 were observed immediately, 21 and 45 hours following 15% ramp stretch over 60 minutes followed by a 2-hour static stretch compared to CON ($p<0.005$), peaking at 21 hours post stretch. MMP-9 and MuRF-1 mRNA expression were left unchanged. However, significant changes in MAFbx mRNA expression levels were observed following a period of 45 hours post ramp load.

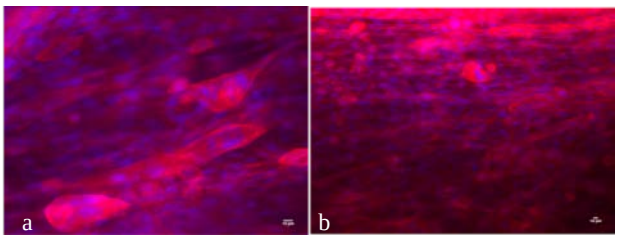

Fig. 1:. *DAPI (blue) and Phalloidin immunostaining (red) in constructs with (a) 20x and (b)40x magnification, displaying myotubes and nuclei present. Scale bar represents 10 µm.*

DISCUSSION & CONCLUSIONS: The current investigation demonstrates the acute and chronic hypertrophic transcriptional response following ramp mechanical load. The scaled *in vitro* model provides an effective system for time-efficient, controlled mechanical stimulation of tissue engineered skeletal muscle. Allowing the stimulation of more than one construct, proposing several benefits over mechanical stimulation devices only capable of stimulating single constructs.

REFERENCES: [1] Cheema, U., Yang, S., Mudera, V., Goldspink, G. G., & Brown, R. A. (2003). 3-D In Vitro Model of Early Skeletal Muscle Development, 226–236. [2] Smith, A. S. T., Passey, S., Greensmith, L., Mudera, V., & Lewis, M. P. (2012). Characterization and optimization of a simple, repeatable system for the long term in vitro culture of aligned myotubes in 3D. *Journal of Cellular Biochemistry*, *113*(3), 1044–1053.

ACKNOWLEDGEMENTS: Mark Lewis lab and all my supervisors.

Vascular Tissue Engineering: Incorporating ECM into polymer scaffolds

JA Reid, A Callanan
The Institute for Bioengineering, School of Engineering, The University of Edinburgh, UK

INTRODUCTION: Cardiovascular disease killed an estimated 15.6 million people worldwide in 2010, accounting for 29.6% of all deaths [1]. Tissue engineering scaffolds for cardiovascular regeneration provide an alternative to existing treatments. Combining extracellular matrix (ECM) with a polymer to create a hybrid scaffold has shown improved cellular performance when using meniscus and cartilage [2,3]. By combining myocardium and aorta ECM with polycaprolactone (PCL), the aim is to improve the performance of PCL as a platform for the attachment and growth of HUVECs.

METHODS: Bovine myocardium and aorta were perfusion decellularization with 0.5% sodium dodecyl sulfate. Decellularized tissue was lyophilized and milled. The resulting ECM powder was added at a 0.25% concentration to an 8% PCL and HFIP solution, which was electrospun into randomly orientated fibres. Scaffolds were seeded with human umbilical vein endothelial cells (HUVECs) at 35,000 cells/cm^2. Various biochemical quantification methods were performed at timepoints of 24 hours, 5 days and 10 days, including DNA quantification, RT-qPCR and cell viability. Biomechanical properties were assessed and scanning electron microscopy (SEM) was performed at 10 days and on unseeded scaffolds. Fluorescence images taken at 24 hours and 10 days. Immunohistochemistry was performed on all scaffolds to look at collagen I and elastin content.

RESULTS: Functional electrospun hybrid scaffolds were successfully fabricated. Overall, HUVECs showed positive responses to all three hybrid scaffolds. Original cell attachment was improved by the addition of aorta ECM, with the heart ECM scaffold showing comparatively poor initial cell adhesion. Notably, cell viability after 10 days increased across all three scaffolds, with the aorta ECM scaffold performing best. The DNA content increased across all scaffolds after 10 days. Fluorescence and SEM images show living cells attached to all three scaffolds. Furthermore, gene expression trends were observed between the scaffolds and timepoints.

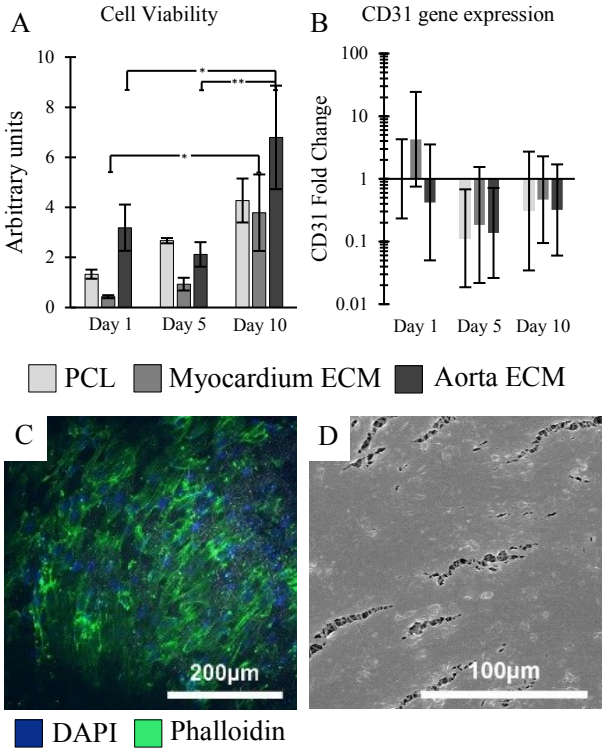

*Fig 1: A) Cell viability on each scaffold. N=4, error bars = SE, one-way ANOVA with Fishers' post hoc performed *p<0.05, **p<0.01. B) CD31 gene expression. N=5, error bars = 95% CI. C) and D) Representative fluorescence and SEM images of HUVEC monolayer on the aorta ECM scaffold at 10 days.*

DISCUSSION & CONCLUSIONS: This methodical study has shown that incorporating aorta ECM with electrospun PCL improves the performance of the scaffold for HUVEC attachment. The components of aorta ECM provide a hospitable environment for the growth of HUVECs and promote improved attachment. These results warrant a long term study to test the full potential of these ECM hybrid scaffolds.

REFERENCES: [1]N. Townsend, *et al* (2015) *Eur. Heart J.* **36**: 2696-2705. [2]S. Gao, *et al* (2017) *J Mater Chem B* **5**: 2273-2285. [3]N.W. Garrigues, *et al* (2014) *J Biomed Mater Res A* **102**: 3998-4008

ACKNOWLEDGEMENTS: ESPRC no. EP/N509644/1. MRC grant MR/L012766/1. Many thanks to Dr Alison McDonald for fluorescent imaging.

Vitamin E incorporated electrospun scaffolds protect mesenchymal stem cells against hydrogen peroxide induced oxidative stress

N. Munir, A. Callanan

Institute for Bioengineering, *School of Engineering, University of Edinburgh, United Kingdom*

INTRODUCTION: The use of mesenchymal stem cells (MSC) to repair cartilage defects is a promising avenue, as cartilage lacks self-healing properties[1]. However, concerns including hypertrophy and production of fibrocartilage need to be addressed[1]. Recently, the accumulation of reactive oxidative species (ROS), including hydrogen peroxide, has been linked to cartilage deterioration and the pathogenesis of osteoarthritis[2-3]. ROS has also been shown to restrict the repair potential of MSCs. Vitamin E, an antioxidant which provides protection against ROS, is known for its chondroprotective effects when supplemented into culture media[4-5]. The potential of vitamin E in tissue engineering applications is not known. This study incorporated vitamin E into PCL scaffolds and investigated the effects of these scaffolds against hydrogen peroxide induced oxidative stress.

METHODS: Vitamin E scaffolds were fabricated, using electrospinning, at two concentrations 200µM vitamin E in 8% polycaprolactone (PCL) w/v in HFIP and 500µM vitamin E in 10% PCL w/v in HFIP. PCL scaffolds (10% w/v PCL in HFIP) were used as controls. The antioxidant capacity of scaffolds was determined using a hydrogen peroxide detection assay. Moreover, scaffolds were stained with vitamin E antibody to show the incorporation of vitamin E into the PCL fibres. Scaffolds were seeded with isolated primary rat MSC and were allowed to attach to scaffolds for 24hrs before the addition of chondrogenic media supplemented with hydrogen peroxide. Various biochemical and oxidative stress assessments were carried out at 24 hours, 3 and 5 day time points. Scanning electron microscopy (SEM) was used to assess scaffold morphology and cell attachment.

RESULTS: All scaffolds display a fibrous architecture which allowed MSC attachment (Fig 1). Vitamin E scaffolds exhibited antioxidant capabilities which were noted through the reduction of hydrogen peroxide in the culture media after 24 hours. These scaffolds also allowed for cell attachment and viability. Moreover, trends in the expression of key genes and DNA quantification were also noted.

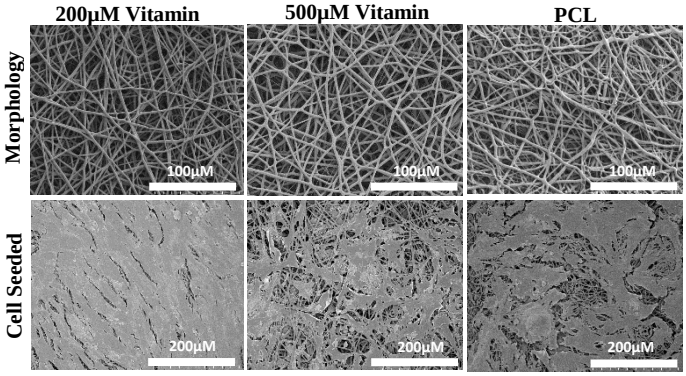

Fig. 1: SEM images of scaffolds and MSC seeded scaffolds.

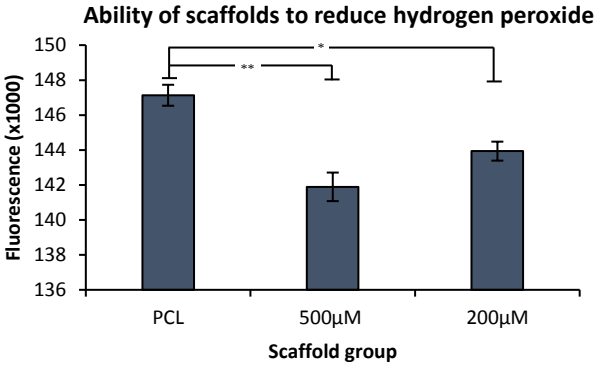

*Fig. 2: The effects of vitamin E scaffolds on media hydrogen peroxide levels after 24 hours. Error bars=SE, n=4. *p<0.05, **p<0.01; one-way ANOVA.*

DISCUSSION & CONCLUSIONS: Vitamin E scaffolds which displayed antioxidant capabilities were successfully fabricated. The addition of vitamin E allowed cell attachment and viability, as well as modulation of markers of oxidative stress, highlighting the potential of these scaffolds in cartilage regeneration.

REFERENCES: [1] W. Y. Lee and B. Wang (2017). *Journal of Orthopaedic Translation*. **9**: 76-88. [2] K. Yudoh et al (2005) *Arthritis Research & Therapy.* **7**: 380-391. [3] S. Vyas et al (2015) *International Journal of Scientific and Research Publications.* **5**: 1-4. [4] A. Graeser et al. 2010. *Molecules.* **15**: 27-39. [5] F. Bhatti et al. (2013) *Inflammation Research.* **62**: 781-789.

ACKNOWLEDGEMENTS:

EPSRC and MRC grant MR/L012766/1.

WNT polymer bandages as a stem cell niche for MSC proliferation and differentiation

MT Shephard[1], K Bardsley[1], Y Okuchi[2], SJ Habib[2], Y Yang[1], AJ El Haj[1]

[1]*Institute for Science and Technology in Medicine, Keele University, UK.*

[2]*Centre for Stem Cells & Regenerative Medicine, King's College London, UK.*

INTRODUCTION: The timing, location and levels of WNT signalling are tightly regulated during early embryonic development and further involved in the maintenance of adult tissues. WNT signalling has been shown to play a key role in establishing and maintaining the stem cell niche, the microenvironment that regulates adult stem cell fate. Further to this, WNT signalling is important in the osteogenic differentiation and regulation of hMSCs. Consequently, the ability to recapitulate developmental processes *in vitro* relies on developing systems that provide a defined and directed source of WNT proteins [1]. MSCs are therefore an attractive proposition in the production of stem cell-seeded polymer "bandages" with applications in orthopedic medicine.

METHODS: Poly(lactic-co-glycolic acid) (PLGA) and polycaprolactone (PCL) polymer surfaces were chemically grafted with WNT proteins (or WNT-DTT control). TCF-LEF reporter cell lines were then used to validate WNT surface grafting through increases in eGFP. 1.5mm full thickness punch defects were formed in the parietal bone on either side of the sagittal suture of mouse crania. The defect was then filled with a pre-set collagen gel and the polymer film was placed on top of the defect. To monitor the real-time degradation of the polymer bandages rhodamine was grafted onto polymer surfaces to monitor fluorescent degradation rates over the course of bone remodeling *in vivo*.

RESULTS: Immobilised WNT proteins can be successfully grafted onto the surface of PLGA polymers and activate the WNT signaling pathway providing a stem cell niche for hMSCs (Figure 1). This hMSC maintaining niche can be transplanted into an *ex vivo* mouse cranium defect model with a view to assess bone repair potential through an increase in defect site mineralization as assessed by µCT in WNT3A grafted polymers (Figure 2). Cell response, migration and differentiation will be further assessed based on WNT concentration gradients. Fluorescent polymers were implanted subcutaneously into mice over 21 days to define a degradation curve that showed a 50% reduction in fluorescence intensity and area size (Figure 3).

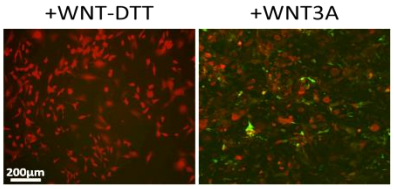

Fig. 1: *WNT3A grafting to PLGA polymer surfaces. Increase in GFP+ cells in TCF-LEF reporter cells compared to WNT-DTT controls.*

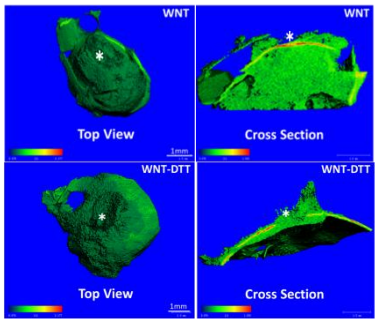

Fig. 2: *µCT of mouse cranium defect sites (*) after 28 days of culture.* ***(A)*** *WNT-DTT grafted polymer bandage.* ***(B)*** *WNT3A grafted polymer bandage showing increased density in defect repair site.*

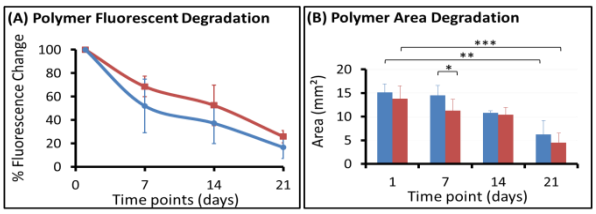

Fig. 3: ***(A)*** *Fluorescence of cellular (red) vs. acellular (blue) rhodamine modified subcutaneous scaffolds.* ***(B)*** *Total area of polymers.*

DISCUSSION & CONCLUSIONS: The ability to recapitulate the stem cell-maintaining niche capable of differentiation to repair bone has been assessed through the use of an *ex vivo* cranial defect model. Methods to relate mineralisation with polymer degradation have been further assessed. Work now concerns *in vivo* studies to monitor cranial defect repair using the fluorescent-WNT3A grafted polymers.

REFERENCES: [1]Lowndes et al. (2016) Immobilized WNT Proteins Act as a Stem Cell Niche for Tissue Engineering. Stem Cell Reports. **7:** 126-137.

ACKNOWLEDGEMENTS: This project is funded by the MRC Niche Hub Grant.